Spring 5-3-2024

Exploration of Liquid-infused Urinary Catheters: Fabrication, Functionality, and Liquid Loss

Chun Ki Fong
University of Maine, chun.fong@maine.edu

EXPLORATION OF LIQUID-INFUSED URINARY CATHETERS: FABRICATION, FUNCTIONALITY, AND LIQUID LOSS

By

Chun Ki Fong

B.S. Hong Kong University of Science and Technology, 2017

M.Phil. Hong Kong University of Science and Technology, 2019

A DISSERTATION

Submitted in Partial Fulfillment of the

Requirements for the Degree of

Doctor of Philosophy

(in Biomedical Science and Engineering)

The Graduate School of Biomedical Science and Engineering

The University of Maine

May 2024

Advisory Committee:

Caitlin Howell, Associate Professor of Biomedical Engineering, Advisor

David Neivandt, Professor of Biomedical Engineering

Ling Cao, Professor of Biomedical Sciences

Robert Wheeler, Associate Professor of Microbiology

William Gramlich, Associate Professor of Chemistry

UNIVERSITY OF MAINE GRADUATE SCHOOL LAND ACKNOWLEDGMENT

The University of Maine recognizes that it is located on Marsh Island in the homeland of Penobscot people, where issues of water and territorial rights, and encroachment upon sacred sites, are ongoing. Penobscot homeland is connected to the other Wabanaki Tribal Nations— the Passamaquoddy, Maliseet, and Micmac—through kinship, alliances, and diplomacy. The University also recognizes that the Penobscot Nation and the other Wabanaki Tribal Nations are distinct, sovereign, legal and political entities with their own powers of self-governance and self-determination.

EXPLORATION OF LIQUID-INFUSED URINARY CATHETER: FABRICATION, FUNCTIONALITY AND LIQUID LOSS

By Chun Ki Fong

Dissertation Advisor: Dr. Caitlin Howell

An Abstract of the Dissertation Presented
in Partial Fulfillment of the Requirements for the
Degree of Doctor of Philosophy
in Biomedical Science and Engineering
May 2024

Catheter-associated urinary tract infection (CAUTI) stands out as one of the most prevalent hospital-acquired infections, the long-term presence of urinary catheters in patients elevates the risk of contracting CAUTI by 80-100%. Despite the widespread use of antibiotics, the current standard of care, effective treatment is still challenging due to formation of biofilms by uropathogens on catheter surfaces, which shield the pathogens from both antibiotics and the immune system. Silicone urinary catheters infused with silicone oil have emerged as a promising alternative, diminishing microbial adhesion to catheter surfaces, bladder colonization, and systemic spread. In this dissertation, we provided a comprehensive account of the development of these catheters, detailing their physical properties throughout the infusion process, such as length, inner, and outer diameter. We demonstrated that these parameters are dependent on infusion duration, with full infusion resulting in a significant increase in these properties. This highlights the crucial role of manufacturing controls, as catheters must be customized in size for each patient's needs. While fully infused catheters have proven effective in repelling pathogen adhesions in mouse models, the potential leakage of silicone oil into the host system is undesirable. Therefore,

we fabricated liquid-infused catheters devoid of a free liquid layer, achieved by either removing excess silicone oil from fully infused samples through absorption or through partial infusion. We demonstrated the efficacy of our methods in reducing the amount of free liquid layer on infused catheters through confocal microscopy. Our analysis revealed a significant decrease in the thickness of the liquid layer from approximately 60 μm to <1 μm. Additionally, by reducing the infusion time, we were able to produce catheters infused with varying percentages, resulting in different quantities of silicone liquid incorporated into the polymer matrix. Furthermore, we investigate their efficacy in repelling protein and bacterial adhesion. Our findings reveal that fully infused catheters, with the free liquid removed, exhibit equal efficacy in reducing host protein fibrinogen and the common uropathogen *E. faecalis* adhesion when compared to fully infused catheters with free liquid. Additionally, they demonstrate a substantial ~64% decrease in liquid loss into the environment. Partially infused catheters also show reduced liquid loss as the total liquid content decreases, with samples infused to 70-80% of their maximum capacity displaying an impressive ~85% reduction in liquid loss compared to fully infused controls. Moreover, samples infused above 70% exhibit no significant increase in fibrinogen or *E. faecalis* adhesion. Together, our findings suggest that eliminating the free liquid layer, either mechanically or through partial infusion, holds promise in reducing liquid loss from liquid-infused catheters while maintaining functionality.

DEDICATION

To my mother and father, who have taught me to always do my best and persevere through hardships.

To my significant other, who has never stopped believing in me.

ACKNOWLEDGEMENTS

I am incredibly fortunate to have always had people willing to cultivate my talent around me. Without them, I would not have been able to accomplish the work I have done today.

At the beginning of my scientific research journey, I would never have even started without my undergraduate capstone project mentor, who later became my MPhil supervisor, Dr. Andrew L. Miller and Dr. Sarah E. Webb. Thank you for giving me the opportunity to start my first research project and for all your advice and teaching during one of the most stressful periods of my life as I transitioned from graduation. I will forever remember and appreciate the opportunity and how it shaped my career path.

Equally important, I would like to express my gratitude to Dr. Caitlin Howell for giving me the opportunity to work in her lab on one of the most meaningful projects. Working and living in a foreign country is stressful, but she was very welcoming and always strove to create a comfortable environment for students to voice their thoughts. Her enthusiasm for science is infectious, and it is what made me fall in love with my project and feel that every hardship is worthwhile. As an introverted and anxious person, it is never easy to voice my thoughts, but working in her laboratory changed me to be a more confident person. I have taken on challenges and spoken up, which I would never have done if I had not joined her team. I would also like to thank Dr. Daniel P. Regan, who trained me in laboratory techniques when I first started and gave me advice on my scientific journey. Thank you to all the other students in the Howell lab for always being supportive, helpful, and welcoming. It is not easy to find a working environment that feels like home.

Finally, I would like to thank my advisory committee for always providing me with helpful scientific advice and equipping me with the skills to see things from different perspectives. Thank

you to Dr. Ana Flores-Mireles and Dr. Marissa Andersen for being so welcoming and helpful during my laboratory trip to the University of Notre Dame. Thank you to Dr. Emma Perry for assisting with technical difficulties in microscopic instruments, and to Dr. Bill Halteman for his patience and advice on statistics.

TABLE OF CONTENTS

LIST OF FIGURES

CHAPTER 1
INTRODUCTION

1.1 Catheter Associated Urinary Tract Infection

1.1.1 Medical Usage of Catheters

The urinary system (Figure 1) plays a crucial role in maintaining homeostasis in the human body. The system begins with the kidneys, which serve as filters, selectively extracting waste and excess fluids from the bloodstream to produce urine (Di Benedetto *et al*., 2013; Haraldsson & Sörensson, 2004; Tryggvason & Wartiovaara, 2005). Subsequently, the ureters transport the urine generated by the kidneys to the bladder (Hashitani & Lang, 2019; Sergeant *et al*., 2019). The internal and external sphincter muscles of the urethra work together to uphold continence until prompted by brain signals to urinate (Brading, 1999). The presence of both sphincters serves to prevent incontinence and allows conscious control over the release of urine (Aharony et al., 2017; Rother *et al*., 1996). Upon receiving the signal, the muscular wall of the bladder contracts, and the sphincter muscles relax, leading to the expulsion of urine through the urethra.

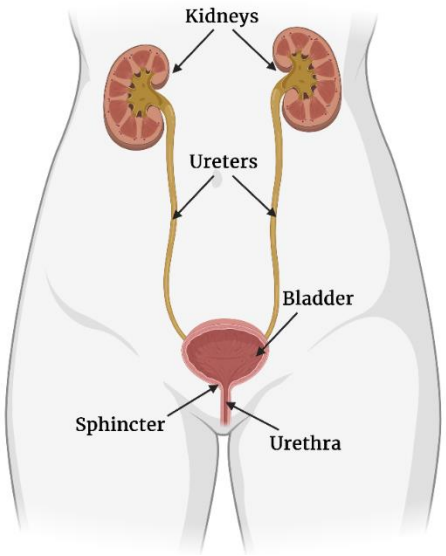

Figure 1. Urinary System.

Urine undergoes filtration in the kidneys, travels through the ureters to reach the bladder for collection. Sphincter muscles enable the maintenance of continence until the brain signals the need to urinate. In cases where patients are unable to execute this process, a catheter may be necessary, usually inserted through the urethra into the bladder, as seen with Foley catheters. (Figure made via BioRender)

Numerous medical conditions can disrupt normal bladder function. Individuals with neurological disorders such as spinal cord injuries and multiple sclerosis often experience difficulties in bladder

control due to impaired communication between the brain and the bladder, leading to the inability to void urine or other complications (Hardy *et al.,* 2022; Al Taweel & Seyam, 2015). The management of urinary retention in such cases often necessitates the use of urinary catheters, facilitating proper drainage. Another group facing urinary challenges comprises individuals with cognitive impairment, such as those with dementia or Alzheimer's disease. Patients with these conditions may struggle to control their bladder function and may face difficulties in communication or adhering to regular toileting schedules (Feneley *et al*., 2015). In such scenarios, the use of urinary catheters becomes a practical solution for continuous urine drainage. Furthermore, individuals undergoing surgery, especially procedures involving the urological or reproductive systems, may require temporary catheters to aid in post-operative recovery and prevent complications associated with urine retention (Eriksen et al., 2019; Webb and Neal, 1990).

1.1.2 Types of Catheters

As a crucial medical tool for managing various medical conditions, urinary catheters are available in diverse designs tailored to meet the specific needs of patients. Among the most prevalent designs is the clean intermittent self-catheterization system (Figure 2A), specifically designed for

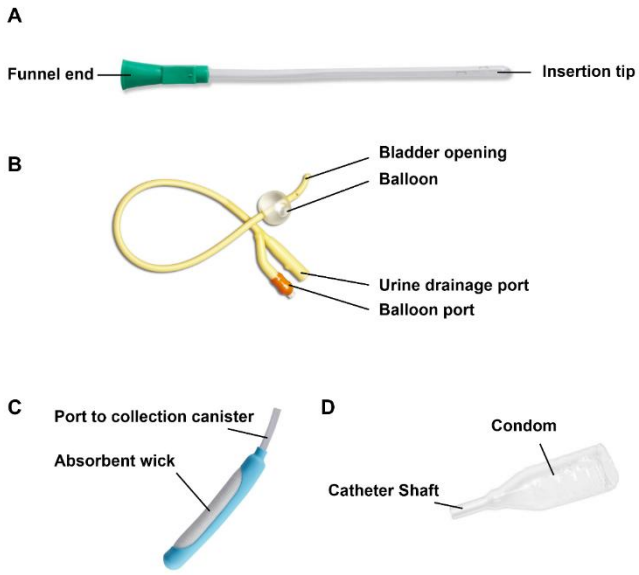

Figure 2. Types of Catheters.

Catering to diverse medical needs, patients can choose from different types of catheters, including **(A)** Intermittent catheter; **(B)** Indwelling catheter (commonly known as Foley catheters); and external options such as **(C)** the female PureWick catheter and **(D)** the Condom catheter designed for male use. Photo credit: (A) Bard, Clean-Cath Female Length Catheter; (B) Dover, Foley Catheters; (C) PureWick, Female External Catheter; (D) Bard, Ultraflex- Self Adhering Condom Catheter

individuals with impaired bladder function who can actively participate in the catheterization process (Prieto *et al*., 2021). This catheter design emulates normal bladder function by allowing periodic filling and complete emptying of urine (DiCarlo-Meacham *et al*., 2022). In this system, patients autonomously insert the catheter through the urethra, facilitating the direct drainage of urine into the toilet or a container. While the process may initially be uncomfortable, with sufficient practice, self-catheterization can become manageable and plays a crucial role in ensuring proper bladder function for individuals with impaired bladder control.

For individuals unable to perform self-catheterization, the use of indwelling catheters (Figure 2B), such as the commonly employed Foley catheter, can be beneficial. Indwelling catheters are designed with two channels: one for urine passage and the other equipped with a balloon at the end, which inflates to secure the catheter in place within the bladder (DiCarlo-Meacham *et al*., 2022). The tip of the catheter features an opening known as the drainage eye, which facilitates urine passage and enhances the flow of urine. Bladder drainage through indwelling catheters can be achieved by inserting the catheter via the urethra, a process termed transurethral catheterization. Alternatively, drainage can also be accomplished through suprapubic catheterization, involving the creation of an artificial pathway between the lower abdominal wall and the bladder (Gibson *et al*., 2019; Belfield, 1988). Catheter sizes are often expressed in French gauge (Figure 3), allowing patients use (or healthcare providers to select) the most suitable size without unnecessary discomfort, thus facilitating a smoother catheterization process (Bagley & Severud, 2021).

An alternative catheter design catering to patients with urinary incontinence is the external catheter (Rose & Pyle-Eilola, 2021; Warren *et al.,* 2020; Zavodnick et al., 2020; Golji, 1981; Figure 2C). These catheters collect urine through tubing into a container or bag, employing either gravity or suction through a receptacle. A notable example for male patients is the condom catheter (DiCarlo-

Meacham *et al.,* 2022; Figure 2D). The sheath of the condom catheter fits over the penis, and a tube at the tip transports urine into a collection bag secured to the leg. While this method is non-invasive, making it more appealing than some other catheter designs, the condom catheter comes with several drawbacks. Up to 40% of patients using this type may develop urinary tract infections (UTIs), and approximately 15% may experience skin issues such as skin erosion (Flores-Mireles *et al*., 2019; Sinha *et al*., 2018; Ouslander *et al*., 1987). Additionally, there is a risk of detachment that could result in urine leakage.

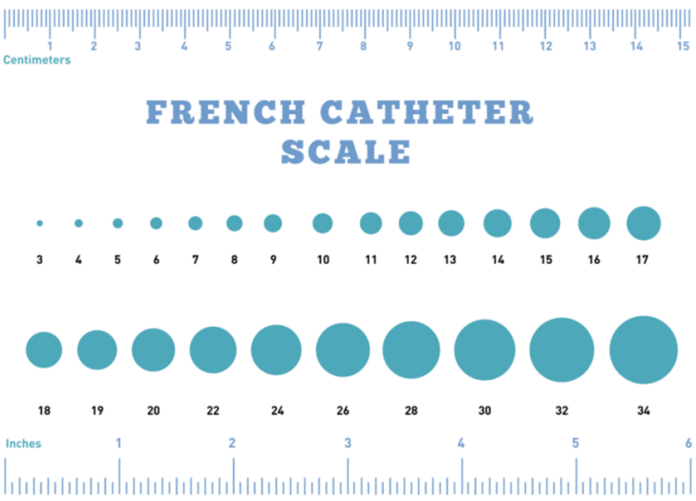

Figure 3. French Gauge for Catheter Size.

French sizes for both intermittent and indwelling catheters provide an approximate measure of the catheter's circumference, with 1 French (Fr) equivalent to 0.33 mm (0.013 inches). Typically, the average catheter size for adult males falls within the range of 14Fr to 16Fr, whereas for adult females, it is typically between 10Fr and 12Fr. Photo Credit: CompactCath

Urinary catheters play a pivotal role in the care provided within hospitals and nursing homes, aiding patients in maintaining proper bladder function. The diverse designs of urinary catheters are tailored to address a spectrum of patient needs. Continuous progress in the materials used for catheters and ongoing research into antimicrobial solutions for these devices are crucial for improving patient health and safety.

1.1.3 Catheter Materials

A diverse array of catheter materials is available in the market, where conventional options like latex, polyvinyl chloride, and silicone coexist with emerging alternatives like polyolefin-based elastomers (Hosseinpour *et al*., 2014; Gould *et al.,* 2009; Ruutu *et al*., 1985). The selection of an

appropriate catheter material is crucial for ensuring the well-being of patients. Individual considerations may include concerns related to allergies, microbial resistance, and comfort levels. Among the various materials, silicone emerges as a particularly optimal choice for its versatile properties and suitability across a range of requirements (Andersen & Flores-Mireles, 2019; Gould *et al*., 2009; O'Brien *et al*., 2016).

For individuals considering catheterization, the presence of issues such as allergies and comfort levels poses significant concerns. Silicone, being a non-allergenic material, stands out as an excellent choice for those who have experienced latex allergies. In contrast to latex, silicone is not only non-allergenic but also biocompatible. Studies have demonstrated that silicone does not adversely affect the viability and metabolic activity of human cells (Villanueva *et al.,* 2011; Drewa *et al.,* 2004; Pariente *et al.,* 2000). Furthermore, the United States Centers for Disease Control and Prevention (CDC) recommends silicone as a preferred catheter material for individuals prone to frequent obstructions. In comparison to latex, silicone exhibits higher resistance to kinking, enhancing both patient comfort and catheter efficiency (Andersen & Flores-Mireles, 2019; O'Brien *et al*., 2016). This combination of non-allergenicity, biocompatibility, and resistance to obstructions and kinking makes silicone a compelling option for individuals seeking a reliable and comfortable catheterization experience (O'Brien *et al*., 2016; Gould *et al*., 2009). In addition, silicone also proves to be compatible with liquid infusion techniques in biomedical engineering research. This compatibility facilitates the development of antifouling surfaces, effectively reducing pathogen colonization—a topic that will be explored in greater detail in subsequent sections.

1.1.4 Significance, Symptoms and Diagnosis of CAUTI

While catheters play a crucial role in supporting patients with compromised bladder functioning, a significant drawback exists in the form of catheter-associated urinary tract infection (CAUTI). This infection occurs when bacteria colonize the urinary tract through the catheter, often leading to medical complications that can impact the well-being and even mortality rates of patients (Andersen *et al*., 2022; Rubi *et al*., 2022; Andersen & Flores-Mireles, 2019; Tambyah and Oon, 2012; Johnson *et al.,* 2006; Trautner & Darouiche, 2004; Tambyah *et al.,* 2002; Tambyah and Maki, 2000; Warren, 1997). The amount of time the catheter remains in the urinary system directly correlates with an increased risk of bacterial colonization and subsequent infection. Given the gravity of this issue (further discussed in Section 1.1.4.1), preventive strategies become paramount for patient well-being. Strict hygiene practices and continuous monitoring are essential components of such preventative measures. Additionally, there is a pressing need to explore antimicrobial materials or techniques that can be applied to catheters, with the goal of hindering bacterial colonization. Such initiatives are crucial for the long-term improvement of overall safety and effectiveness in catheter use.

1.1.4.1 Significance of CAUTI

CAUTI represents a significant challenge in healthcare environments and stands as one of the most prevalent hospital-acquired infections (HAIs) (National Healthcare Safety Network, 2024; Feneley et al., 2015; Reed & Kemmerly, 2009). Data from the CDC reveal that CAUTI constitutes nearly 40% of all HAIs, establishing it as a widespread concern in hospitals and nursing homes (National Healthcare Safety Network, 2024; Feneley et al., 2015; Reed & Kemmerly, 2009). Annually, out of the 2 million patients affected by HAIs in the United States, and approximately 100,000 died to these infections (Schallom et al., 2020). The financial burden of these infections is estimated to be

as much as 4.5 billion USD (Schallom et al., 2020). This issue is exacerbated by the extensive use of urinary catheters in healthcare facilities, with approximately 100 million catheters being inserted worldwide each year (Nasr, 2010; Saint *et al*., 2000).

The consequences of CAUTI are severe, particularly impacting patient mortality rates. Residents in nursing homes who are equipped with catheters experience a significantly elevated level of mortality and are more likely to die within a year when compared to residents with similar medical histories but without catheters (Parker *et al.,* 2009). This heightened mortality is directly attributed to the presence of a catheter, where pathogens colonizing the catheter can lead to infections and complications. Short-term catheterization with a duration of 14 or less days significantly increases the risk of developing CAUTI and other complications, with the risk of these infections reaching as high as 80% (CDC, 2022; Margaret *et al.,* 2009; Maki & Tambyah, 2001). For long-term catheterization of 30 days or more, the risk escalates to 100% (CDC, 2022; Margaret *et al.,* 2009; Maki & Tambyah, 2001). There is an urgent need to address this issue given the indispensability of catheters as a crucial medical instrument for patients.

Beyond its direct clinical consequences, CAUTI also plays a role in contributing to antibiotic resistance, thereby adding an additional layer of complexity to public health challenges. According to the CDC's 2022 report, pathogens associated with CAUTI, such as *Enterococcus spp.* and *Pseudomonas aeruginosa*, are specifically categorized as threats to public health due to their development of antibiotic resistance (Trautner & Darouiche, 2004b). The report highlights a notable increase in infections resistant to treatment, particularly following the extended hospitalizations associated with the COVID-19 pandemic. In the report, the need for prolonged surveillance and the importance of ongoing research to develop approaches that effectively counter the escalating problem of antibiotic resistance posed by these pathogens were emphasized.

Addressing CAUTI not only has direct implications for patient health but also holds significance in the broader context of preserving the effectiveness of antibiotics and combating the challenges of microbial resistance in the public health domain.

The conventional use of antibiotic treatments for CAUTI is not effective due to the formation of biofilms on catheter surfaces (Feneley *et al*., 2015; Sharma *et al*., 2019). A biofilm refers to a collection of microbial cells that are irreversibly attached to a surface, enveloped within a polysaccharide matrix (Rodney, 2002). Biofilms act as protective shields for pathogens, significantly limiting the efficacy of antibiotics. Furthermore, the overuse of antibiotics in CAUTI exacerbates the broader issue of antibiotic resistance, making it more severe. In light of these challenges, ongoing research efforts in catheter technologies and the exploration of novel approaches to prevent pathogen colonization on catheters are important. Developing strategies that address pathogen adhesion on catheter materials and enhance the effectiveness of treatments without contributing to antibiotic resistance is critical in improving the management and outcomes of CAUTI.

1.1.4.2 Symptoms of UTIs

UTIs can manifest through a spectrum of symptoms that serve as indicators of the infection. Individuals affected by UTIs commonly experience an urgent and frequent need to urinate, disrupting their daily routines (Burkett *et al*., 2019; Gadalla *et al*., 2019; Kumar *et al*., 2013). This persistent urge to urinate is often accompanied by discomfort, a burning sensation, or pain during urination—an indication of inflammation or irritation in the urinary tract. Additionally, patients with UTI may notice changes in the color or odor of their urine (Dutta *et al*., 2022). Cloudiness, a strong, unpleasant smell, and the presence of blood (hematuria) in the urine suggest the presence of pathogens in the urinary system (Burkett *et al*., 2019; Kumar *et al*., 2013). Urine color can range

from pink to red or even purple (Figure 4), reflecting the involvement of infectious agents (Dutta *et al*., 2022; Kaur & Kaur, 2021; Popoola & Hillier, 2022).

Inflammation or infection within the bladder or other components of the urinary system may also lead to lower abdominal pain or discomfort (Piljić *et al*., 2010). As the infection progresses, more severe symptoms such as fever or chills may occur, particularly when UTI complications, like pyelonephritis (kidney infection), arise (Johnson and Russo, 2018; Ramakrishnan, 2005; Steward *et al*., 1985). Recognizing these symptoms is crucial for patients to seek timely medical assistance for CAUTI, ensuring prompt intervention to address the infection and prevent the development of further complications.

Figure 4. Purple Urine Bag Syndrome.

Discolored urine is detected in the collection bags of nursing home patients with CAUTI. This discoloration is attributed to the pathogen's digestion of the amino acid tryptophan. In the metabolic process, the production of indirubin and indigo occurs, imparting a red and blue coloration, respectively, to the urine. Photo Credit: Lin *et al*., 2008

1.1.4.3 Diagnosis of CAUTI

Diagnosing CAUTI presents challenges due to ongoing debates surrounding the effectiveness of common UTI indicators such as pyuria (white blood cells in urine) and bacteriuria (bacteria in urine) (Hooton *et al*., 2010; Steward *et al*., 1985). Differing guidelines propose varied thresholds, with bacterial content cutoffs ranging from 10^3 to 10^5 colony-forming units (CFU)/mL (National Healthcare Safety Network, 2024; Bonkat *et al.,* 2017; Cortes-Penfield *et al*., 2017; Hooton *et al*., 2010; Gribble *et al*., 1988). The lack of consensus is evident, with the National Institute on Disability

and Rehabilitative Research suggesting a cutoff of 10^2 CFU/mL, while others advocate for 10^3 or even 10^5 CFU/mL, depending on laboratory feasibility and equipment sensitivity (National Healthcare Safety Network, 2024; Bonkat *et al.,* 2017; Cortes-Penfield *et al*., 2017; Hooton et al., 2010; Gribble *et al*., 1988).

Complicating matters further, some catheterized patients may exhibit UTI or bacteriuria without symptoms, adding complexity to the diagnosis process. While asymptomatic bacteriuria is generally considered benign, hospitals often prescribe antibiotics without clear symptomatic justification (Hooton *et al*., 2010). Technical issues, such as failing to ensure urine collection before antibiotic prescription and potential contamination, further hinder the diagnostic process when relying solely on bacterial counts in urine samples. For patients with long-term indwelling urinary catheters, the recommended method for urine sample collection involves replacing the old catheter and obtaining samples from the newly inserted catheter. This recommendation stems from observations that urine culture results may not accurately reflect bladder status if there is biofilm on the catheter surface (Tractenberg *et al*., 2021; Grahn *et al*.,1985; Bergqvist *et al.,* 1980).

Traditional symptoms like urgency and pain during urination hold limited diagnostic significance, as catheterized individuals cannot urinate independently, and the impact of a catheter might affect the comfort level of urination (National Institute on Disability and Rehabilitation Research, 1992). Moreover, these symptoms may not be detectable in patients with critical or spinal cord injuries, increasing the risk of overdiagnosis (Skelton-Dudley *et al*., 2019; Saran *et al*., 2018; Steward *et al.,* 1985). Observations of cloudy or odorous urine, once considered differentiators between CAUTI and asymptomatic bacteriuria, have proven inconsistent in guiding diagnostic and treatment decisions (Schwartz & Barone, 2006; Tenney and Warren, 1988).

In response to diagnostic challenges, ongoing research has explored alternative approaches. Urinary symptom questionnaires filled out by patients and detection of biomarkers show promise in enhancing diagnostic precision (Gadalla *et al*., 2019). Examples of biomarkers include procalcitonin, a peptide precursor that escalates in response to bacterial infection (Levine *et al*., 2018); interleukins, small proteins released by white blood cells serving as markers for inflammation (Mazaheri, 2021); and urinary cell-free DNA, derived from dying microbes or host cells (Burham *et al.*, 2018). Current limitations for the speed and accuracy of infection diagnosis may be improved in the future by integrating artificial intelligence and machine learning. Further research and innovative approaches are crucial for accurately assessing the infection status of patients with CAUTI. However, research efforts toward preventing CAUTI from initially occurring would be significantly more beneficial for public health.

1.1.5 Host Factors

CAUTI is influenced by a multitude of factors, with host elements, the catheter material itself and pathogens frequently interacting, thereby introducing complexity to our full comprehension of the CAUTI infection process.

1.1.5.1 Gender, Age, and Behaviors

UTIs have long been recognized as predominantly affecting women, with over 50% experiencing UTIs at some point in their lives (McLellan & Hunstad, 2016; O'Brien *et al*., 2016; Flores-Mireles *et al*., 2015). However, susceptibility to UTIs varies across age groups.

In infancy, vulnerability is particularly high, primarily due to the underdeveloped immune systems of infants (Becknell *et al*., 2015; Bonadio and Maida, 2014). Studies reveal that within the first 3-6 months after birth, male infants experience a higher incidence of UTIs compared to females

(Becknell *et al*., 2015; Bonadio and Maida, 2014). Among infants, the highest rates occur in uncircumcised males under three months and females under twelve months, with lower birth weights correlating to an increased risk of UTIs (Bonadio and Maida, 2014; Nader *et al*., 2008).

As individuals reach adulthood, women become more prone to UTIs than men. Anatomical differences, such as the proximity of the urethral opening to the anus and the shorter length of the female urethra, contribute to increased susceptibility (Gyftopoulos, 2018). Hormones, such as estrogen, may also play a role. Research on estrogen's impact on UTIs presents conflicting results: some studies indicates that estrogen could promote bacterial invasion, and others suggesting a protective role through antimicrobial peptide production, e.g. psoriasin and human beta-defensin (Sen *et al*., 2019; Lüthje *et al.,* 2013; Wang *et al.,* 2013; Han *et al*., 2010; Perrotta *et al*., 2008; Curran *et al*., 2007). Moreover, the highest UTI susceptibility is observed in young adult women expressing elevated estrogen levels, but postmenopausal females, with lower estrogen levels, also exhibit heightened susceptibility (Sonnex, 1998). In clinical trials, estrogen supplementation yields varying results as well (Sonnex, 1998).

In the elderly, UTI occurrence significantly rises in males due to prostatic hypertrophy, promoting urinary retention and increasing infection risks (Jin and Seung, 2021; Tolani *et al*., 2020). Moreover, consequences of UTIs are more severe in males, leading to higher morbidity, mortality rates, and an elevated risk of hypertension and end-stage renal diseases (Calderon-Margalit *et al*., 2018; Foxman, 2010; Efstathiou *et al.,* 2003; Foxman *et al*., 2003; Nicolle *et al*., 1996). Androgen levels in males may play a role in the severity of UTI in males: it was suggested that higher androgen levels may contribute to renal scarring and fibrosis, suppressing innate responses to UTIs and exacerbating the severity of consequences, as shown in murine models (Humphreys, 2018;

Scalerandi *et al*., 2018; Flum *et al*., 2017; Olson *et al*., 2016; Hannan *et al*., 2012a, 2012b). This suggests that UTIs are not solely a female issue, they are also a significant concern for males.

Behavioral factors, such as increased sexual activity and the use of spermicides, contribute to recurring UTIs (Lin et al., 2022). Studies indicate that women engaging in frequent intercourse or using spermicides face an elevated risk of recurrent UTIs. Regarding catheterization, gender differences diminish, with males now accounting for 30-40% of cases, which is largely due to the presence of catheters (Kakaria *et al*., 2018; Flores-Mireles *et al*., 2015; Daniels *et al*., 2014).

1.1.5.2 Host protein

In both murine models and human patients, catheterization induces the release of fibrinogen (Fb) into the bladder, triggered by mechanical damage to the urothelial lining (Flores-Mireles *et al*., 2014; Clarke and Hammonds, 1989). Once Fb is released, it attaches to catheter surfaces, coating the catheter and serving as a docking site for bacteria (Flores-Mireles *et al*., 2014; Jennewein *et al*., 2011; Clarke and Hammonds, 1989). This process allows bacteria to colonize the catheter surface and form biofilms. Remarkably, the attachment of Fb onto catheter surfaces can occur as early as one-hour post-catheterization (Flores-Mireles *et al*., 2016). This creates an environment conducive to pathogen invasion, leading to infection. Several pathogens commonly associated with healthcare infections, some of which have been identified as threats to human health by the CDC, have demonstrated an affinity for binding to Fb (Andersen *et al*., 2022; Walker *et al*., 2017; Flores-Mireles *et al*., 2014, 2016). This binding serves as an initial step in the establishment and progression of diseases.

1.1.6 Pathogens in CAUTI

CAUTI can lead to numerous follow-on medical complications due to the involvement of a diverse range of pathogens causing the infection. A review by the National Healthcare Safety Network highlights the vast variety of pathogens associated with CAUTI (Weiner *et al*., 2016; Figure 5). The most prevalent pathogen causing CAUTI is uropathogenic *Escherichia coli* (UPEC), contributing to 23.9% of CAUTI cases (Weiner *et al*., 2016; Foxman, 2014,2010). *Candida spp.* also play a significant role, contributing to 17.8% of CAUTIs, emphasizing the importance of considering fungal agents in CAUTI prevention strategies. *Enterococcus spp.* contribute to 13.8% of CAUTI cases, followed by *Pseudomonas aeruginosa* (*P. aeruginosa*) at 10.3%, *Klebsiella spp.* at 10.1%, and *Proteus spp*. at 4%. Although less common, pathogens such as *Enterobacter spp.*, coagulase-negative *Staphylococci*, and *Staphylococcus aureus* (*S. aureus*), contributing 3.7%, 2.4%, and 1.6%, respectively, can still lead to medical complications. *Bacteroides spp.*, contributing less than 0.1% to CAUTI, warrant attention due to the potential involvement of anaerobic bacteria.

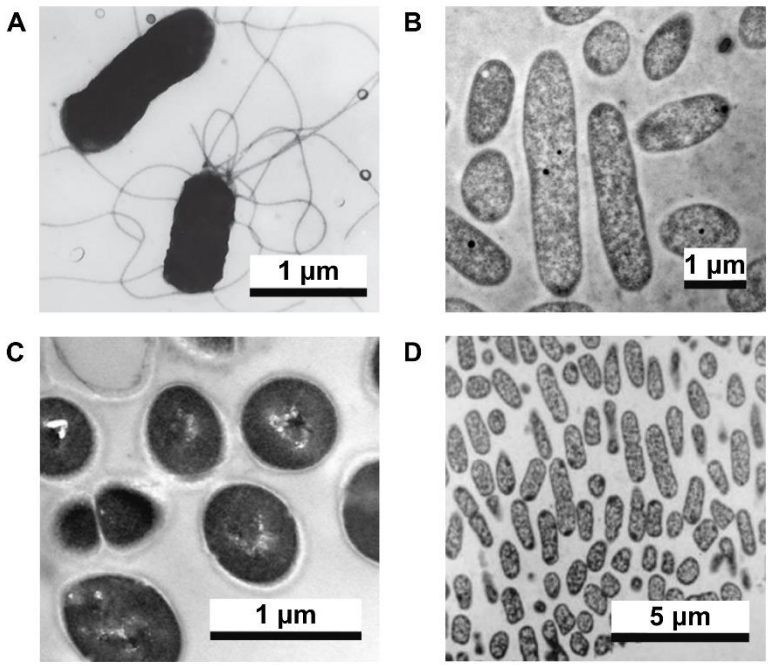

Figure 5. Pathogens associated with CAUTI.

Transmission microscopy images of **(A)** *E.coli* (Modified from: Eisenbach, 2001); **(B)** *P. aeruginosa* (Modified from: Gerstel *et al*., 2018); **(C)** *E. faecalis* (Modified from: She *et al*., 2021), and **(D)** *K. pneumoniae* (Modified from: Zahller and Stewart, 2002).

This quantitative information shows the extensive distribution of pathogen types in CAUTI, highlighting the diverse and intricate nature of CAUTI infections. In cases of prolonged catheterization, UPEC, *Enterococcus spp*., and *P. aeruginosa* are commonly known to establish colonization on catheter surfaces (Gaston *et al*., 2020).

1.1.6.1 Uropathogenic *E. coli*

E. coli, a facultative anaerobe in the *Enterobacteriaceae* family, attracts researchers' interest due to its dual nature—it can exist as a benign commensal bacterium or a pathogenic one. In its commensal form, *E. coli* peacefully coexists with the host, but the pathogenic version, known as UPEC, has evolved to efficiently colonize tissues and cause infections (Schreiber *et al.,* 2017; Jacobsen *et al*., 2008; Hacker and Kaper, 2000; Johnson *et al*., 1998; Nataro and Kaper, 1998; Foxman *et al*., 1995). UPEC adapts and colonizes through the expression of virulence factors, such as uropathogenic-specific fimbriae—finger-like projections that aid in traveling and recognizing tissues for colonization (Spurbeck *et* al., 2011; Kanamaru *et al.,* 2003; Hacker and Kaper, 2000; Mobley *et al*., 1987). UPEC is responsible for over 70% of community-acquired UTIs and up to 50% of hospital-acquired UTIs, making it the most prevalent organism in CAUTI (Kucheria *et al*., 2005).

E. coli strains can be categorized into phylogenetic clades (A, B1, B2, and D) based on genetic similarities and further classified into different pathotypes based on their disease-inducing capacity (Ejrnæs *et al*., 2011; Skjøt-Rasmussen *et al.,* 2011; Piatti *et al*., 2008; Starčič Erjavec *et al*., 2007; Nowrouzian *et al*., 2006; Rijavec *et al.*, 2006). However, distinguishing uropathogenic-prone strains from commensal strains is challenging due to the lack of clear genomic uniqueness (Schreiber *et al*., 2017; Vejborg *et al*., 2011). In the United States and Europe, the majority of

UPEC strains in the B2 clade dominate. In patients with CAUTI, *E. coli* tends to be multidrug-resistant and belongs to the ST131 lineage (Schreiber *et al*., 2017; Vejborg *et al*., 2011).

Although genetic differences might not easily distinguish UPEC, its distinctive protein expression pattern during CAUTI provides insights. For instance, in CAUTI, UPEC exhibits high expression of type 1 fimbriae, allowing it to persist and travel through catheterized urinary tracts *(Mobley et al*., 1987). UPEC also produces virulent factors such as P-fimbriae, K-antigens, and hemolysin, potentially leading to pyelonephritis (kidney infection). Notably, over half of the strains identified in CAUTI are not typically found in uncomplicated UTIs, showcasing the uniqueness of UPEC in the context of CAUTI (Benton *et al.,* 1992).

1.1.6.2 Enterococcus spp.

Enterococcus spp., such as *Enterococcus faecalis* (*E. faecalis*), are commonly found in the human gut microbiome and play a significant role in various infections, including wound infections, bloodstream infections, and CAUTI (Tien *et al*., 2017; Hidron *et al.,* 2015; Gilmore *et al.,* 2014; Gjødsbøl *et al*., 2006; Wisplinghoff *et al*., 2004; Maki & Tambyah, 2001). In UTI patients within ICU units, *E. faecalis* ranks as the second most common microorganism causing infections. Instances of *E. faecalis* causing UTIs are more prevalent in hospital settings, potentially linked to increased urethral catheterization during extended hospitalization periods, particularly amid the COVID-19 pandemic (Díaz Pollán *et al*., 2022).

In the context of CAUTI, the presence of a catheter plays a pivotal role in facilitating the colonization of *E. faecalis* in the bladder. The catheter allows *E. faecalis* to ascend along the urinary tract, potentially reaching the kidneys and causing pyelonephritis (inflammation of the kidneys), thereby elevating the risk of mortality (Warren *et al.,* 1988). Studies indicate that *E. faecalis* can cause minimal inflammation and can be cleared from bladders in the absence of

catheters (Guiton *et al.,* 2013; Warren *et al.,* 1988). Murine models have demonstrated that when artificial inflammation is introduced without catheters, *E. faecalis* fails to promote infection, underscoring the crucial role of catheters in promoting CAUTI (Warren *et al.,* 1988).

Rather than causing infections in isolation, *E. faecalis* actively participates in polymicrobial communities during CAUTI, influencing the antibiotic resistance of co-infecting organisms such as *P. aeruginosa* and *Proteus mirabilis* (Tien *et al*., 2017; Flores-Mireles *et al*., 2015; Croxall *et al*., 2011; Tsuchimori *et al*., 1994). *E. faecalis* secretions can enhance the pathogenicity of *P. mirabilis* in CAUTI by stimulating urease activity and increasing amino acid production, providing additional nutrient resources for pathogens (Hunt *et al*., 2023). In CAUTI models, these pathogens have been observed to co-localize in biofilm communities, reinforcing their persistence and protection against the host's immune system and antibiotics (Hunt *et al*., 2023; Gaston *et al*., 2020). Interestingly, *E. faecalis* has also been noted to facilitate infections by non-pathogenic *E. coli* and modulate the host response to promote infection (Tien et al., 2017). This polymicrobial synergy can induce mixed infections, contributing to the development of more severe pyelonephritis. Despite a tendency to dismiss *E. faecalis* as a cultural contaminant in urine testing for CAUTI diagnosis, its significance should not be overlooked due to its ability to enhance the pathogenic potential of other bacteria (Kline & Lewis, 2016; Hooton, 2012).

1.1.6.3 P. aeruginosa

P. aeruginosa employs various virulence factors and adaptive mechanisms to enhance infection in CAUTI, including the use of quorum sensing systems—a chemical signaling network that gauges cell density and regulates the expression of virulence factors (Flores-Mireles *et al.,* 2019). *P. aeruginosa* possesses two quorum sensing systems, namely the *las* and *rhl* systems, which coordinate the expression of virulence factors by generating signaling molecules like N-(3-

oxododecanoyl)-homoserine lactone (OdDHL) and N-butanoylhomoserine lactone (BHL) (Mittal *et al*, 2009; Ochsner & Reiser, 1995; Pearson *et al*., 1994, 1995; Winson *et al*., 1995; Gambello & Iglewski,1991). These systems play a crucial role in transitioning *P. aeruginosa* from a planktonic state (free-swimming) to a biofilm-producing state, although in CAUTI, the quorum sensing systems are not essential for biofilm formation (Cole *et al*., 2018, 2014; Davies *et al.,* 1998).

P. aeruginosa has been observed to produce robust biofilms, particularly on catheter surfaces (Cole *et al*., 2014; Mittal *et al*., 2009). Thick biofilms on indwelling catheters significantly contribute to the persistence and recurrence of infections, providing higher resistance to antibiotics and the host's immune defenses (Mittal *et al.,* 2008; Boles *et al*., 2004; Kurosaka *et al.,* 2001; Costerton *et al*., 1981). Despite the host's production of macrophages and neutrophils for defense, *P. aeruginosa* can exploit secretory products of macrophages to fuel its own growth and enhance virulence (Mittal *et al.,* 2006).

Virulence factors produced by *P. aeruginosa*, such as alginate, lipopolysaccharide, pilus, and proteases, are known to enhance infections in wounds and respiratory tracts (Michalska & Wolf, 2015; Vance *et al*., 2005; Lyczak *et al*., 2000; Woods *et al.,* 1997; Woods *et al*., 1986). However, the specific roles of these factors in CAUTI are not fully understood. Bacteriocin genes like pyocins S4, R, and S2 are frequently detected in *P. aeruginosa* strains associated with CAUTI and are considered potential contributors to its virulence (Snopkova *et al*., 2020).

Compared to UTIs, *P. aeruginosa* strains found in CAUTI exhibit higher resistance rates against antibiotics (D'Incau *et al*., 2023). This resistance poses a challenge for effective treatment strategies, emphasizing the need for ongoing research to explore alternative treatment or preventive methods for CAUTI that do not solely rely on antibiotics.

1.1.7 Infection Process of CAUTI

1.1.7.1 Pathogen Invasion

UTIs typically initiate when pathogens reach the urinary meatus, the entry point of the urethra (Klein and Hulgren, 2020; Flores-Mireles *et al*., 2015, 2019). Factors such as sexual intercourse and improper hygiene practices, like wiping genitals from back to front after urination in females, can contribute to this event (Nicolle, 2014). Urine retention, resulting from catheter use or medical conditions affecting proper bladder voiding, can create an environment conducive to pathogen proliferation (Levison and Kaye, 2013; Lichtenberger and Hooton, 2008).

Once pathogens reach the urethral entry point, they can ascend the urethra using appendages like flagella and pili, reaching the bladder or, more severely, the kidneys (Flores-Mireles et al., 2015; Armbruster & Mobley, 2012; Morgenstein & Rather, 2012; Nielubowicz & Mobley, 2010; Jacobsen et al., 2008). The translocation or migration mechanisms of *E. faecalis*, a flagella-lacking bacterium, remain largely unexplored. However, one study has proposed that *E. faecalis* uses the glycopolymer expressed on its cell surface to facilitate translocation, and enabling semisolid penetration (Ramos *et al.,* 2019). In the case of CAUTI, both extraluminal and intraluminal infections can occur. Extraluminal infection happens when pathogens colonize the external surface of catheters due to the aforementioned factors (Assadi, 2018; Eto et al., 2007; A. L. Flores-Mireles et al., 2015; Guiton et al., 2012; Lee, 2011; Zhou et al., 2001). In contrast, intraluminal infection may occur when pathogens ascend from the urine collection bag into the bladder during urine reflux in the catheter system (Assadi, 2018). Pathogens contributing to such infections are usually exogenous, potentially originating from environmental cross-contamination or personnel handling the catheter (Assadi, 2018).

After reaching urinary tissues, pathogens can directly bind to them. For instance, UPEC attaches to bladder epithelium through type 1 pili, recognizing and binding to uroplakins—a major protein component of bladder epithelial cell membranes used for protecting the bladder from harmful substances in urine (Flores-Mireles *et al*., 2019, 2015; Guiton *et al*., 2012; Lee, 2011; Khandelwal *et al*., 2009; Eto *et al*., 2007; Zhou *et al*., 2001). UPEC recognizes mannose, a type of sugar that is expressed on uroplakins, for attachment, allows it to cause both uncomplicated and complicated UTIs, such as in the case of CAUTI (Flores-Mireles *et al*., 2019, 2015; Zhou *et al*., 2001). Unlike UPEC, *E. faecalis* and *P. aeruginosa* primarily cause complicated UTIs, especially in the presence of catheters (Flores-Mireles *et al*., 2019, 2015).

Catheterization induces mechanical stress, releasing Fb in the bladder. Fb coats the catheter surface, providing binding sites for pathogen colonization and inducing CAUTI, damaging nearby tissues which further escalating Fb release (Andersen *et al*., 2022; Flores-Mireles *et al*., 2014). *E. faecalis* uses endocarditis- and biofilm-associated (Ebp) pili to recognize Fb for adhesion, allowing attachment, migration, and biofilm formation (Nielsen *et al*., 2013). The use of antibodies to block Ebp sites in CAUTI mouse models has been shown to prevent catheter colonization by *E. faecalis*, highlighting the crucial role of Fb in this process (Flores-Mireles *et al*., 2014; Nielsen *et al*., 2013; Figure 6). Fb on the catheter also serves as a nutrient source: *E. faecalis* release proteases like SprE and GelE to digest Fb (Xu *et al*., 2017). Less is known about the mechanism used by *P. aeruginosa* in CAUTI, but it is suggested that they use Fb as a docking site as well (Andersen *et al*., 2022). Virulence factors like bis-(3′-5′) cyclic dimeric GMP (c-di-GMP) influence *P. aeruginosa* biofilm

formation during CAUTI, and microcolonies may form through the production of rhamnolipids, allowing migration along the urinary tract via modifying bacterial cell surface hydrophobicity (Newman *et al*., 2017; Cole & Lee, 2016; Pamp & Tolker-Nielsen, 2007).

1.1.7.2 Infection, Survival and Propagation

Once pathogens use the catheter surface to ascend into bladder tissues, the initiation of infection begins. If they progress further into the kidneys, it can lead to pyelonephritis, escalating the severity of the medical condition (Flores-Mireles *et al*., 2019, 2015).

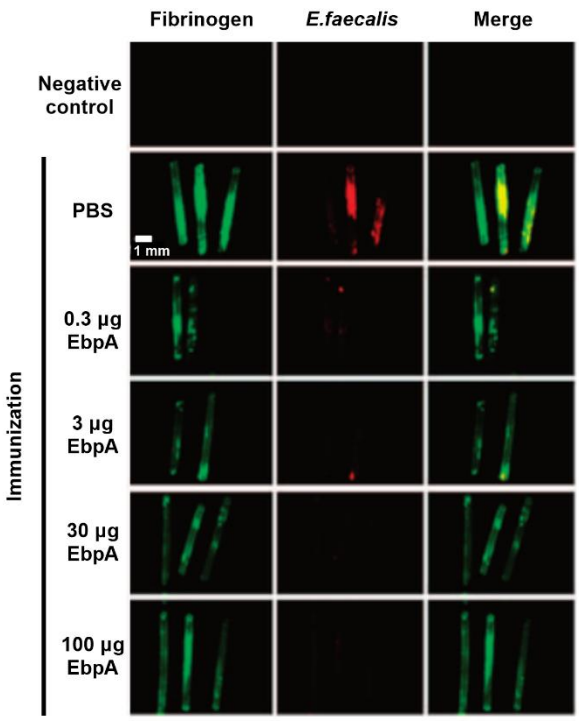

Figure 6. *E.faecalis* Adhesion on Catheters with EbpA Immunization.

Fluorescent image showing adhesion level of fibrinogen (left column) and *E.faecalis* (middle column) on silicone mouse catheters. Different dosages ranging from 0.3 µg to 100 µg of anti-EbpA vaccines were administered to the mouse models during catheterization. Scale Bar = 1mm. (Modified from Flores-Mireles *et al*., 2014)

Normally, epithelial cells in the bladder possess defense mechanisms that can expel pathogens and halt infection through intracellular signaling pathways (Flores-Mireles *et al*., 2019, 2015). However, some pathogens, like UPEC, have mechanisms that remain unidentified, allowing them to access the cell cytoplasm. The known pathway used by UPEC involves the binding of type 1 pili to mannose-expressing uroplakins of the bladder epithelial cells, initiating bacterial internalization (Flores-Mireles *et al*., 2019, 2015; Thumbikat *et* al., 2009; Wang *et al*., 2009). Once inside the cell, UPEC rapidly multiplies, forming intracellular bacterial communities with biofilm-like properties that obstruct the access of host immune cells (Hannan *et al*., 2010; Anderson *et al.,* 2003). Matured colonies can detach, flux out of infected cells, and invade other nearby healthy

cells (Flores-Mireles *et al*., 2019, 2015; Kostakioti *et al*., 2013; Hannan *et al*., 2010; Anderson *et al.,* 2003). UPEC can also transition to a filamentous state, resisting engulfment by white blood cells. The development of an intracellular reservoir enables UPEC to remain viable for months, leading to recurrent and antibiotic resistant UTIs (Flores-Mireles *et al*., 2019, 2015; Hannan *et al*., 2012).

In addition to using Fb as a food source and a docking site, the SprE protease released by *E. faecalis* promotes bacterial dissemination in the kidneys (Flores-Mireles *et al*., 2014). To counteract *E. faecalis*, the host limits manganese availability to starve pathogens. However, *E. faecalis* can use multiple manganese transporters, enhancing its ability to survive in a manganese-limited environment and continue infecting and spreading to other healthy areas (Colomer-Winter *et al*., 2018).

P. aeruginosa promotes survival by modifying cell surface hydrophobicity and enhancing microcolony formation, a strategy similar to UPEC (Newman *et al*., 2017; Pamp & Tolker-Nielsen, 2007). To maximize nutrient acquisition, *P. aeruginosa* expresses siderophores (iron-chelating compounds) to scavenge iron for nutritional resources (Podschun & Ullmann, 1998). To initiate UTI, *P. aeruginosa* produces enzymes like elastases, exoenzyme S, and hemolytic phospholipase C (Mittal *et al*, 2008, 2006) Elastases promote tissue destruction, releasing iron from damaged cells for *P. aeruginosa* growth; exoenzyme S inhibits white blood cell function and impacts host cell morphology by affecting cytoskeletal protein formation; phospholipase C is a toxin that hydrolyzes host cell membranes, weakening cell integrity and promoting tissue damage (Cathcart *et al*., 2011; Wargo *et al*., 2011; Rocha *et al*., 2003; Meyers *et al*., 1992; Berka & Vasil, 1982).

In summary, pathogen invasion, survival, and propagation in CAUTIs are multifaceted and influenced by a range of factors. Catheterization exacerbates the situation by offering surfaces that

facilitates protein adhesion and subsequent pathogen colonization. Thus, comprehending the interaction among pathogens, materials, and host tissues is important in devising successful preventive and therapeutic approaches against CAUTIs.

1.1.8 Existing Prevention Strategies for CAUTI

1.1.8.1 Catheterization Techniques and Timing

The risk of developing UTI increases by 3-7% per day a patient has a catheter, and for long-term catheterized patients with an average catheter duration of 30 days, the likelihood of UTI can reach 100% (Nicolle, 2014). Therefore, the most effective preventive measure is to minimize catheter use and remove the catheter as soon as possible, although this may not always be feasible depending on the patient's medical condition (Gould et al., 2019; Saint et al., 2016; Nicolle, 2014).

As described earlier, catheter placement in the urinary system can lead to infection as pathogens ascend using pili or appendages, using the catheter as a docking site. Hence, practicing good hand hygiene before and after catheterization is crucial, involving thorough handwashing with soap and water (Nicolle, 2014). Catheterization should only be performed by trained personnel familiar with aseptic techniques to minimize contamination risks (Tenke *et al*., 2008). In case of any leakage or disconnection during the catheterization process, immediate replacement of the catheter is necessary, and reusing catheters should be avoided to maintain sterility in a closed system (Saint *et al*., 2016; Hooton *et al*., 2010; Tenke *et al*., 2008).

Research indicates that the position of catheter tubing can also impact the risk of infection. Placing the catheter tubing above the bladder or below the level of the urine collection bag poses the highest infection risk (Maki & Tambyah, 2001). Best practices involve placing the urine collection bag below the bladder and connection tubing, above the floor, at all times to prevent contamination

or reflux of urine back into the catheter tubing (Saint *et al*., 2016). Securing the catheter to the patient's thigh can aid in proper placement and prevent urine flow obstruction (Assadi, 2018). Regular emptying of urine from the collection bag is essential to lower the chances of urine reflux, facilitating pathogen ascension (Saint *et al*., 2016).

As mentioned earlier, the adhesion of pathogens is facilitated by Fb, which is released in response to mechanical friction caused by catheterization, and deposits on the catheter surface, creating docking sites (Andersen *et al*., 2022; Flores-Mireles *et al*., 2014a, 2014b, 2015, 2019). Additionally, wounds caused by mechanical friction during catheterization can weaken the tissue structure, compromising its ability to defend against pathogens. Therefore, it is important to ensure adequate lubrication of catheters to ensure smooth catheterization, and to select an appropriate French size for each individual, in order to minimize friction and trauma to the tissue (Maki & Tambyah, 2001).

In common practice, catheters are typically removed and replaced monthly, with no specific guidelines for the optimal replacement time (Tenke *et al*., 2008). Existing guidelines recommend removal and replacement when infection occurs, when there is obstruction, or when the system is no longer a closed system (e.g., leakage) (Gould *et al.,* 2010). Future studies may address this issue to determine an optimal time based on risk of infection for catheter or patient specific factors such as immune status, moving beyond the current monthly practice.

1.1.8.2 Surface Modification Approaches

Extensive research has been conducted on surface coatings for urinary catheters as a preventive measure against CAUTI. An in-depth review conducted by Andersen et al. has offered valuable insights and a comprehensive summary (Andersen & Flores-Mireles, 2019). The overarching

concept behind these coatings is either to hinder the adhesion and growth of pathogens or to impede the formation of biofilms, for example, via the release of antibiotics or metal ions.

1.1.8.2.1 Polymer Coatings

Polytetrafluoroethylene (PTFE), commonly known as "Teflon," is a fluoropolymer known for its smooth and low-friction properties. Coating urinary catheters with this polymer creates a low surface energy, smooth environment that theoretically inhibits pathogen adhesion, thereby preventing colonization (Wang *et al*., 2019). However, when compared to silicone material in preventing blockage, PTFE performs less effectively. Studies support the use of silicone catheters, particularly for patients experiencing blockage in long-term catheterization situations (Kunin *et al.,* 1987). Catheter blockage and encrustation predominantly arise from bacterial activity (Gibney, 2016), bacterial breakdown of urea can alkalize urine, leading to crystallization (Stickler and Morgan, 2008). These crystals tend to aggregate within the catheter lumen and drainage eye, especially on rough or irregular surfaces, causing blockage (Stickler *et al*., 2003; Tunney and Gorman, 2002). Silicone catheters exhibiting superior performance in reducing blockage is potentially due to their smoother surfaces observed under electron microscopes compared to materials such as PTFE, hydrogel, or latex (Lawrence and Turner, 2006a), thus minimizing salt aggregation. Additionally, silicone catheters also feature larger lumen which promotes better drainage (Lawrence and Turner, 2006b; Figure 7).

Furthermore, a comparative study between Teflon-coated catheters and hydrogel-coated catheters revealed that hydrogel outperforms PTFE (Murakami *et al*., 1993). Hydrogel-coated catheters exhibit the lowest bacterial adhesion and the least irritation to urinary tissue compared to PTFE. As a result, the study recommends the use of hydrogel-coated catheters over Teflon-coated urinary catheters.

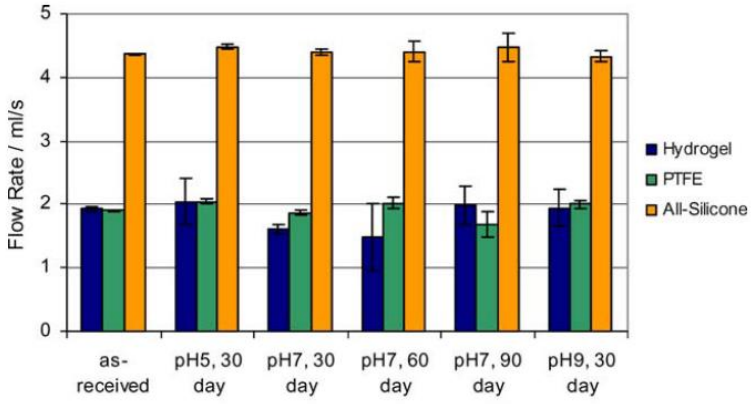

Figure 7. Flow Rate of Different Catheter Materials.

Flow rate of 14Fr sized catheters made of hydrogel-coated latex, PTFE-coated latex, and all-silicone latex under distilled water of different pH level. Average flow rate in 30, 60, or 90 days are plotted. (Modified from Lawrence and Turner, 2006a)

Hydrogel coatings have demonstrated superior performance compared to Teflon-coated urinary catheters in reducing bacterial adhesion in studies (Murakami *et al*., 1993). The polymer network structure of hydrogel allows it to retain a significant amount of water and can achieve close to 99% water content (McCloskey *et al*., 2014). The attraction of hydrogel comes from the ability to incorporate and release various agents and antimicrobial chemicals. For instance, hyaluronic acid can be integrated into hydrogels to mitigate protein adhesion (Beek *et al.*, 2008). Studies suggest that hyaluronic acid functions similarly to polyethylene glycol (PEG) by inhibiting protein absorption through the creation of a repulsive hydration layer or by obstructing protein adsorption sites (Beek *et al*., 2008). Furthermore, this hydration layer may serve as a physical barrier, preventing bacterial adhesion (Dai *et al*., 2023).

However, the performance of hydrogels as a coating for urinary catheters are subjected to conflicting findings. Some studies have shown no significant difference between hydrogel-coated urinary catheters and silicone catheters in terms of reducing CAUTI (Chene *et al*., 1990). Full silicone catheters were found to induce the lowest degree of inflammation in the urethra compared to hydrogel-coated latex catheters (Talja and Järvi, 1990). Some researchers argue that there is insufficient evidence to support the idea that hydrogel coatings provide better protection than non-

coated catheters (Thibon *et al.,* 2000). The effectiveness of hydrogel-coated catheters in preventing blockage also varies between studies. While some suggest that hydrogel-coated catheters perform better in preventing blockage than silicone, some suggested that catheter blockage may be caused by the hydrogel layer's potential to increase the aggregation of planktonic pathogens (Kazmierska *et al*., 2010, Talja and Järvi, 1990). Due to biofilm formation, hydrogel-coated catheters may lead to faster catheter blockage compared to silicone catheters (Kazmierska et al., 2010).

PEG coating is also being explored as a potential candidate for preventing CAUTI. This material has demonstrated its ability to repel proteins and does not trigger immune response, making it a promising option for urinary catheters (Alcantar *et al*., 2000). In tests against bacteria such as *S. aureus* and *E. coli*, PEG coating exhibited antibacterial and antifouling properties when combined with antibacterial cations (Yang *et al*., 2014). The coating also proved to be stable under simulations of blood flow (Yang *et al*., 2014). Atomic force microscopy measurements, assessing the force of interaction between *E. coli* and PEG-coated materials, suggested that the coating could block long-range attractive forces, and introduce repulsive effects between the pathogen and the coated substrate (Razatos *et al*., 2000). However, it is important to note that pathogens like *Staphylococcus epidermidis* could still attach to the material surface (Park *et al*., 1998). Park *et al*. suggested that this variance arises from differences in surface chemistry among pathogens. For instance, *E. coli* exhibits notably higher hydrophilicity compared to *S. epidermidis*. (Gilbert *et al*., 1991). Additionally, the evaluation of these studies was conducted in laboratory media and not urine, which may not fully mimic the environment for pathogen growth in CAUTI settings (Colomer-Winter *et al.,* 2019; Xu *et al.,* 2017; Flores-Mireles *et al*., 2014, Figure 8). As a result, the effectiveness of this coating *in vivo* remains uncertain despite its success in *in vitro* settings.

1.1.8.2.2 Metal Coatings

The concept behind silver-coated catheters is based on the idea that the toxicity of silver can damage bacterial membranes and proteins, inhibiting the growth of pathogens (Singha *et al*., 2017). While silver-coated catheters have been studied both *in vitro* and *in vivo*, similar to polymer coatings, their results in clinical trials are often inconsistent, leading to uncertainty regarding their ability to prevent CAUTI.

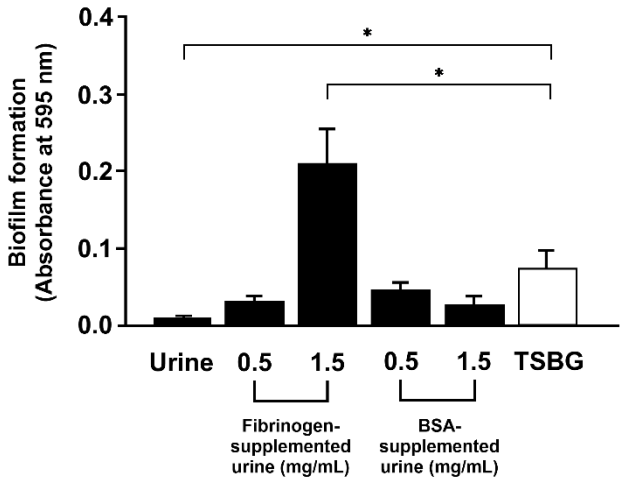

Figure 8. *E.faecalis* Biofilm Formation in Different Media.

Biofilm formation of *E.faecalis* in standard 96-well polystyrene plate is plotted for *E. faecalis* growing in human urine, human urine supplemented with fibrinogen or BSA, and TSBG. BSA = bovine serum albumin; TSBG = tryptic soy broth media supplemented with 0.25% glucose (standard laboratory growth medium). Statistical significance between the groups was assessed using ANOVA, the error bars represent the standard error of the mean. * = $P < 0.05$. (Modified from Flores-Mireles *et al*., 2015)

In a randomized crossover study involving hospitalized patients, it was demonstrated that the use of silver-coated urinary catheters reduced the risk of infection by 20-35% (Karchmer *et al.,* 2000). Another study focused on silver-alloy hydrogel catheters reported a close to 50% reduction in CAUTI occurrence rates among a population of acute care hospital patients using Foley catheters (Lederer *et al*., 2014). However, contrasting findings exist, with several studies indicating that silver-coated urinary catheters may not effectively prevent CAUTI. Blind prospective studies with hydrogel-silver coated catheters in intensive healthcare units showed no statistical significance in CAUTI reduction (Bologna *et al*., 1999). Additionally, catheters coated with hydrogel and silver salts did not exhibit significant differences in performance compared to non-coated catheters (Thibon *et al*., 2000). Clinical trials also suggested that silver alloy-coated catheters are unlikely to be cost-effective in preventing

CAUTI (Kilonzo *et al*., 2014). Considering the mixed results, the potential toxicity of silver ions to the host, and the poor cost-effectiveness, silver-coated catheters appear to be a less attractive candidate in the fight against CAUTI.

1.1.8.2.3 Antibiotic Coatings

Antibiotics such as nitrofurazone, gentamicin, and fluoroquinolones have been considered for coating urinary catheters to aid in preventing CAUTI. However, due to concerns about antibiotic resistance, mixed results in clinical settings, and high costs, this approach has its challenges and is not considered the most favorable option.

Nitrofurazone inhibits pathogen DNA replication, preventing their proliferation and biofilm formation (Zhu *et al.,* 2018). In *in vitro* studies, CAUTI-causing pathogens like UPEC and *S. aureus* were inhibited (Johnson *et al*., 1993). However, translating this antibiotic coating to *in vivo* settings has not been successful. Clinical trials comparing nitrofurazone-coated catheters with non-coated silicone catheters showed no significant differences, and there were more frequent side effects with the antibiotic-coated catheters (Menezes *et al.,* 2018; Lee *et al*., 2004). Patients also reported more discomfort and pain with nitrofurazone-coated catheters (Lam *et al.,* 2014). Moreover, nitrofurazone is considered carcinogenic, causing mammary and ovarian tumors, and has been banned by the US Food and Drug Administration for use in food-producing animals (Hiraku *et al*., 2004). Although catheters are not included in this ban, the potential toxicity and carcinogenicity of nitrofurazone have made it less attractive for researchers.

Gentamicin inhibits bacterial protein synthesis, preventing bacterial growth and biofilm formation (Krause *et al*., 2016; Tangy *et al*., 1985; Hahn and Sarre, 1969). Given its antibacterial properties, scientists are exploring its potential application as a coating for catheters. Gentamicin-releasing

catheters have shown promise in rabbit models, reducing bacteriuria occurrence and decreasing bacterial colonization on catheter surfaces (Cho *et al.,* 2002). Gentamicin-coated catheters have also demonstrated antibacterial efficacy against pathogens such as *S. aureus*, *S. epidermidis,* and *Proteus vulgaris* for a duration of one week (Cho *et al.,* 2012). The release of gentamicin depends on the molecular weight of coating agent used, with results suggesting release periods of up to 12 days (Rafienia *et al*., 2013). However, further clinical trials examining gentamicin-coated catheters are ongoing.

Fluoroquinolones, including norfloxacin, ciprofloxacin, and sparfloxacin, have been used to coat urinary catheters for CAUTI studies. These antibiotics prevent DNA replication in pathogens by binding to bacterial enzymes that support DNA formation (Mohr, 2016). Studies have shown that ciprofloxacin and norfloxacin can destroy *P. aeruginosa* biofilms and significantly reduce the number of bacteria attached to the coated material (Reid *et al*., 1994). These antibiotics can be released for up to a month, maintaining antimicrobial efficacy (Saini *et al*., 2016). However, the effectiveness of these antibiotics has not been thoroughly evaluated in clinical studies.

1.1.8.2.4 Nanoparticles Coatings

Copper nanoparticles have demonstrated the ability to destroy bacterial membranes by inhibiting enzyme activity and degrading DNA, leading to apoptosis (programmed cell death) (Rtimi *et al*., 2016). *In vitro* studies have indicated that copper nanoparticles effectively reduce the viability of *E. coli* on material surfaces within five minutes, with comparable performance across different coating thicknesses (Mihut *et al.*, 2019). Moreover, copper ions incorporated into fabrics have exhibited the ability to combat antibiotic-resistant bacteria, such as methicillin-resistant *S. aureus* and vancomycin-resistant *Enterococci* (Borkow and Gabbay, 2004). Beyond the necessity for additional research into the efficacy and potential toxicity of copper nanoparticles in *in vivo*

settings, recent studies have uncovered that metal ions, including iron and copper, can chelate antibiotics like ciprofloxacin and doxycycline, leading to a reduction in their bioactivity (Sutradhar et al., 2023). This interference contributes to the increase of antibiotic resistance in *E. coli* over time. Therefore, the incorporation of copper nanoparticles may not be the optimal strategy in catheters for addressing CAUTI.

Silver nanoparticles have been explored as an alternative to address the toxicity associated with silver-coated materials while retaining their antibacterial functionality. Although the precise mechanism of action is not fully understood, it is suggested that silver nanoparticles can attach to the cell surface, causing structural or functional damage. Additionally, free silver ions can lead to the production of reactive oxygen species, contributing to cellular damage (Akter *et al*., 2018; Zheng *et al*., 2018l Durán *et al*., 2016). Their nanoscale size allows for effective dispersion in the environment, avoiding aggregation (Guan *et al*., 2019). In *in vivo* studies, catheters coated with silver nanoparticles demonstrated significant prevention of biofilm formation by pathogens such as UPEC, *Enterococcus spp*., *S. aureus*, *P. aeruginosa*, and *C. albicans* (Roe *et al*., 2008). The antibacterial activity of silver nanoparticles outperformed hydrogel coatings against these pathogens (Alshehri *et al*., 2016). However, the potential inflammation and toxicity of such coatings in the bladder environment remain untested, necessitating further research to understand their health impact.

Gold nanoparticles function by inhibiting enzyme activity to reduce ATP levels, and disrupting membrane potential in bacteria (Cui *et al*., 2012). *In vitro* experiments have shown their ability to inhibit the growth of bacteria such as *P. aeruginosa* and *E. faecalis* (Okkeh *et al*., 2021). However, concerns arise as bacterial growth is still present after two days of gold nanoparticle treatment *in vitro*, raising questions about their efficiency, especially when translated to *in vivo* settings.

1.1.8.3 Other CAUTI Prevention Strategies

Modification of the topography of urinary catheter surfaces is a promising avenue of research, inspired by nature's designs to prevent biofilm formation. Micro and nanoscale patterns on material surfaces have been shown to inhibit the formation of biofilms by pathogens such as *E. coli* and *Pseudomonas fluorescens* (Hsu *et al.,* 2013). Pathogens exhibit a preference for maximal contact area with surfaces and align themselves based on the topographic details of the surfaces (Figure 9), adjusting the expression of their appendages accordingly (Hsu *et al.,* 2013). Microscale surface patterns inspired by shark skin on silicone have successfully reduced *E. coli* attachment without the need for biocidal agents (Carman *et al.,* 2005). Similarly, nanoscale protrusions on black silicon, inspired by dragonfly wings, exhibited high bactericidal activity against *P. aeruginosa* and *S. aureus* (Ivanova et al., 2013). While these techniques have yet to undergo *in vivo* testing or be specifically evaluated in urinary catheter settings, their efficacy may only extend to the short term when deployed in medical environments. This limitation arises because molecules such as proteins and bacterial secretions (e.g. exopolysaccharides), have the capacity to alter surface topography by masking and filling surface patterns, which render the proposed strategies ineffective (Wu *et al*., 2018).

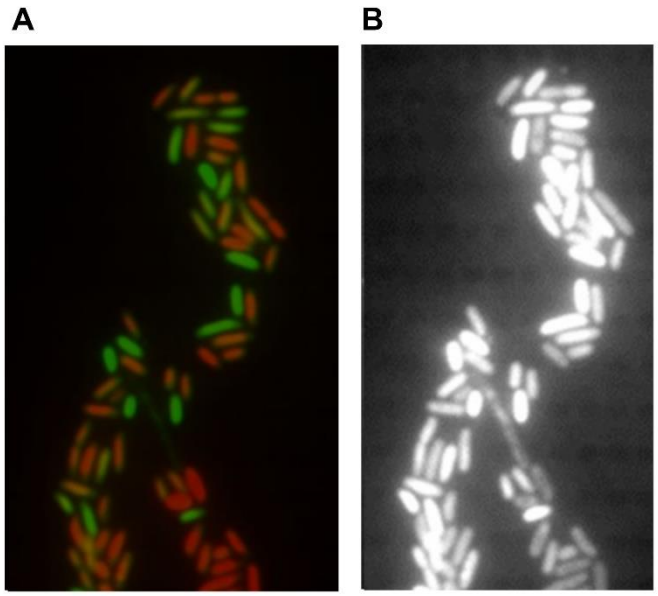

Figure 9. *E.coli* Attachment on Patterned Silica Material.

(A) Fluorescent image showing attachment of *E.coli* on silica with thin wells (500 nm diameter; 200 nm inter-well spacing), areas inside the wells were avoided by *E.coli*. Red = dead cells; Green = live cells. **(B)** Same image in black and white to accentuate topographical details of the material. (Modified from Hsu *et al*., 2013).

Bacterial interference is another intriguing technique involving the use of host-native pathogens to compete with incoming pathogens, creating a healthier and competitive environment (Darouiche & Hull, 2012). Lower-virulence pathogens can be artificially introduced into the bladder to establish this competitive environment against CAUTI causing pathogens (Darouiche & Hull, 2012). However, clinical studies have yielded mixed results. Some studies demonstrated that catheters pre-treated with *E. coli* could lower UTI rates in catheterized patients (Prasad *et al*., 2009). Conversely, other studies showed that precoating catheters with *E. coli* did not lower UTI cases and even led to overgrowth of pathogens (Horwitz *et al*., 2015). This technique poses the potential risk of non-pathogenic pathogens colonizing the bladder if not properly controlled: further research is needed to refine and understand the effectiveness and potential risks associated with bacterial interference.

1.1.8.3.1 Cranberries and Probiotics

Cranberry juice has gained popularity as a home remedy for UTI patients, with its proposed mechanism involving proanthocyanins inhibiting the P pilus-mediated attachment of pathogens to bladder or vagina epithelial cells (Gupta *et al*., 2007). Additionally, fructose, another abundant component in cranberries, has been shown to inhibit *E. coli* attachment to urinary tract epithelial cells (Zafriri *et al*., 1989; Schaeffer *et al*., 1980). Despite these promising attributes, clinical trials have produced conflicting results. Some studies indicate that daily cranberry consumption could reduce the pathogen colony count in urine by half (Thomas *et al*., 2017). In contrast, other research suggests no significant benefit associated with consuming cranberry juice concentrate to prevent CAUTI occurrence (Gunnarsson *et al*., 2017). Discrepancies in these findings may be attributed to variations in cranberry ingredient contents, such as sugar levels, or the different forms of consumption, whether in juice or as whole fruits. Currently, there is limited information and

research on the effectiveness of cranberry in combatting CAUTI, necessitating further investigation.

Lactobacillus spp, a type of probiotic, has become a subject of research interest in several studies. However, akin to cranberry consumption, clinical trials have produced diverse outcomes. For instance, in trials involving spinal cord injured patients with indwelling catheters, no significant difference was observed between those who consumed probiotics and the control group (Toh *et al*., 2019). Conversely, another study revealed a noteworthy alteration in microbial communities within catheter biofilms when probiotics were administered to patients (Bossa *et al*., 2017). This potential form of bacterial interference in combating CAUTI and other harmful pathogens, though temporary, warrants attention (Bossa *et al*., 2017). Despite these findings, a comprehensive understanding of the mechanisms and outcomes of probiotics administration is still in its infancy. Further studies are imperative to elucidate the potential role of probiotics in treating CAUTI, possibly in conjunction with other preventive measures.

1.1.8.3.2 Prophylactic Antibiotics

Oral antibiotics are frequently prescribed both during catheterization and post-urethral catheter removal as a prophylactic measure (preventive measure in medical terms), aimed at preventing potential infections. A survey conducted in the United Kingdom revealed that more than 50% of practitioners adhere to this practice (Wazait *et al*., 2004). Typically, the approach to treating CAUTI involves a three-day antibiotic course for women under 65 years of age following catheter removal. For others, a prescription spanning five to seven days is standard, with the possibility of extending it to two weeks in the absence of prompt clinical improvement (Hooton *et al*., 2010; Inge, 2010; Pfefferkorn *et al*., 2009).

Despite its prevalence, the use of prophylactic antibiotics raises concerns. This practice contributes to the alarming issue of antibiotic resistance, a problem exacerbated by the aftermath of the COVID pandemic, wherein the U.S. witnesses at least 2.8 million cases of antimicrobial-resistant infections annually (D'Incau *et al.,* 2023; CDC, 2019). Moreover, the efficacy of prophylactic antibiotics is questionable, as demonstrated in a study involving over 40 patients treated with ciprofloxacin, where a two-day antibiotic regimen failed to prevent UTIs in the subsequent weeks (Wazait *et al.,* 2004a, 2004b). A potential cause of this result is that the effectiveness of antibiotics can be compromised by the formation of biofilm on catheter surfaces, shielding pathogens from antibiotic action (Feneley *et al*., 2015; Jarrel *et al.,* 2015; Tenke *et al.,* 2014; Niël-Weise *et al.,* 2012; Hooton *et al*., 2010; Darouiche *et al*., 2008; Ha & Cho, 2006; Thomas *et al.,* 2004; J. R. Johnson *et al*., 1993). The biofilm environment also intensifies antimicrobial resistance, fostering rapid sharing of genetic material among pathogens and accelerating the spread of antibiotic-resistant genes (Hooton *et al*., 2010).

The CDC discourages the use of prophylactic antibiotics in catheterized patients unless there are clear indications of bacteriuria or infection symptoms (Gould *et al.,* 2009). Notably, there are no guidelines for the use of prophylactic antibiotics at the time of catheter removal. Attempts to mitigate contamination, such as adding antibiotics to urine collection bags or employing periodic catheter irrigation, have proven ineffective (Hooton *et al*., 2010). For instance, the use of a neomycin-polymyxin B sulfate irrigation system did not yield significant benefits compared to non-irrigated catheters, and uropathogens in irrigated catheters demonstrated increased resistance to the irrigation system's antibiotics (Warren *et al.,* 1978). Similarly, bladder irrigation with neomycin-polymyxin showed no discernible difference from the control group (Waites *et al*., 2006).

1.1.8.3.3 Vaccinations

The effectiveness of vaccination strategies against CAUTI remains uncertain; however, ongoing research has identified several promising candidates for vaccination. Against uncomplicated UTIs, clinical trials have explored MV-140 and OM-89 vaccines:

MV-140, a sublingual (administered under the tongue) spray composed of inactivated cell lysates from common uropathogens such as *E. coli*, *E. faecalis*, and *K. pneumonia*, demonstrated positive outcomes in a study where patients with recurrent UTIs received the vaccine for three months (Yang and Foley, 2017; Lorenzo-Gómez *et al*., 2015). More than 50% of the study group remained free of recurring UTIs in the subsequent year, though one patient experienced a rash reaction necessitating treatment cessation (Yang and Foley, 2017). Other clinical studies also revealed a higher UTI-free rate for MV-140-treated patients compared to placebo controls in the following nine months, albeit with five reported adverse reactions among the testing groups (Nickel *et al*., 2021).

On the other hand, the OM-89 vaccine, administered orally for 30 days, is a lyophilized (freeze-dry) formulation containing 18 different *E. coli* strain membrane proteins. Meta-analysis on five different clinical trials involving over 1000 patients with recurrent infections and acute UTI indicate a significant reduction in the average occurrence of UTIs compared to placebo treatment (Naber *et al*., 2009). Other vaccines incorporating multi-strain cell lysates are still in development, with no available clinical trial data (Magistro and Stief, 2019).

In the specific context of combatting CAUTI, a noteworthy study identified the EbpA tip of *Enterococcus spp.* as a potential vaccination candidate (Flores-Mireles *et al*., 2014). EbpA, a component of the endocarditis and biofilm-associated pilus in *E.faecalis*, is an adhesin (cell surface

proteins that allows adhesion to other cells or surfaces) that facilitates attachment to host Fb released during catheterization (Flores-Mireles *et al*., 2014). Immunization against the N-terminal domain of EbpA protected mouse models against CAUTI by blocking the attachment of *E. faecalis* to Fb-coated catheters (Flores-Mireles *et al*., 2014). This strategy showed promise not only against *E. faecalis* but also *E. gallinarum*, *E. faecium*, and vancomycin-resistant *Enterococci* (Flores-Mireles *et al*., 2014). This discovery is particularly intriguing due to the prevalent occurrence of gram-positive pathogens and fungal adhesion to Fb (Andersen *et al*., 2022; Flores-Mireles *et al*., 2016). The revelation that hindering Fb deposition on catheter material can also impede the colonization of such pathogens highlights the potential efficacy of blocking the adhesion proteins presented by these pathogens as a promising strategy for infection prevention (Andersen *et al*., 2022).

Similarly, the FimCH vaccine, targeting the FimH, adhesin of type 1 pilus in pathogens, demonstrated effectiveness in preventing colonization in cynomolgus monkey and murine models (Langermann *et al*., 2000; Langermann *et al.,* 1997). FimH recognizes uroplakins (a type of cell membrane protein) and integrins (a type of cell receptor) on bladder cells, facilitating pathogen internalization. Vaccination allows the generation of antibodies that block FimH, preventing the binding of pathogens on bladder cells and hence protecting against pathogen colonization. However, this vaccine has only completed phase 1 of clinical trials, further results are necessary to assess its effectiveness (Eldridge *et al*., 2021).

Vaccination presents an exciting alternative to antibiotics for preventing pathogen colonization in the bladder or catheter material, though ongoing research is essential to validate their efficacy and safety. Moreover, certain constraints on vaccination may diminish its effectiveness in addressing CAUTI. For instance, the protection of vaccines like MV-140 and OM-89 did not protect against

all CAUTI-causing pathogens, as only prevalent uropathogens were targeted (Yang and Foley, 2017; Lorenzo-Gómez *et al*., 2015; Naber *et al*., 2009). Moreover, rare adverse reactions, such as those observed in some patients treated with MV-140 (Nickel *et al*., 2021), render this intervention unsuitable for all, particularly individuals with compromised immune systems. Additionally, public skepticism towards vaccines, fueled by misinformation, could further dampen public willingness to undergo vaccination, as evidenced during the COVID pandemic (Skafle *et al*., 2022).

1.1.9 Limitations of Existing Prevention Strategies

CAUTI poses a substantial challenge in healthcare, and the herein methods discussed to address it can have significant limitations. While minimizing catheter usage and early removal is crucial, it might not be feasible for patients with complex medical conditions requiring long-term catheterization. Although emphasizing good hand hygiene and aseptic techniques is important, human errors and challenges in continuous protocol monitoring in healthcare settings can limit their effectiveness. Even with appropriate catheter size selection and lubrication during catheterization, tissue damage can still occur, weakening the tissue's defense against pathogens and leading to increased Fb release, which subsequently deposits on the catheter surface, providing a docking site for pathogens. Coating catheters with materials like polymers, antibiotics, and nanoparticles has shown inconsistent results, and the translation from successful *in vitro* outcomes to *in vivo* scenarios varies, limiting their widespread use. Antibiotics, commonly used for CAUTI prevention, are associated with antibiotic resistance, and their prophylactic overuse raises concerns in the healthcare sector. Moreover, their effectiveness is compromised by biofilm formation on catheters, shielding pathogens from antibiotic action. While vaccination strategies show promise in murine models, further research is needed to validate their efficacy and safety in human patients.

Natural remedies, such as cranberry consumption and probiotics, lack conclusive evidence in preventing CAUTI, with conflicting results in clinical trials raising concerns about their reliability.

In conclusion, existing preventive measures are either not entirely effective or lack consistent results, prompting the need for a novel, reliable approach. An ideal preventive measure should (1) effectively counter pathogen fouling of catheters or eliminate pathogens, (2) be cost-effective, (3) not compromise patient comfort, and (4) avoid side effects on patient health.

1.2 Liquid Infused Materials

Placing medical instruments within the human body presents numerous challenges due to the inevitable exposure of medical materials to various contaminants such as bodily fluids, proteins, and mucus. This exposure can lead to contamination and the colonization of pathogens. Urinary catheters are no exception: as previously discussed in detail, the deposition of Fb on the material surface significantly amplifies pathogen attachment, resulting in infections (Flores-Mireles *et al*., 2014; Jennewein *et al*., 2011; Goble *et al.,* 1989)

Nature has already devised inherent mechanisms to prevent adhesion of foreign substances to surfaces. A variety of substrates in the natural world are usually enveloped in fluid as a defense strategy. In the human body, several interfaces are similarly lined with liquid, such as our eyes, joints, and intestines. The tear film in our eyes, for instance, not only maintains moisture but also houses enzymes that combat bacteria and function as natural pain relievers (Akkurt Arslan *et al*., 2023; Figure 10A). The synovial fluid enveloping our joints prevents bone friction during daily activities, while the mucus layers in our intestines are physical barriers to bacteria (Herath *et al*., 2020; Tamer, 2013; Figure 10B).

The inspiration from natural design has led researchers to delve into integrating liquid linings across a broad range of substrates (Howell *et al*., 2018; Manna *et al*., 2015). This approach has demonstrated its versatility by extending to various solid substrates commonly encountered in medical settings, including polyvinyl chloride (Wylie *et al*., 2020; Leslie *et al*., 2014), polypropylene (Brown and Bhushan, 2017; Leslie *et al*., 2014), polystyrene (Abdulkareem *et al.,* 2022; Leslie *et al*., 2014), and silicone (Abdulkareem *et al.,* 2022; Andersen *et al*., 2022; Leslie *et al*., 2014). Moreover, liquid infusion goes beyond polymer medical materials, finding applications on surfaces such as glass (Togasawa *et al*., 2018; Wang *et al*., 2017; Sunny *et al*., 2016), fabric (Damle *et al*., 2015; Shilling *et al*., 2013), paper (Regan *et al*., 2019; Glavan *et al*., 2014), metals (R. Liu *et al*., 2020; Togasawa *et al*., 2018; Doll *et al*., 2017; Kim *et al*., 2012), other polymers of daily use (Yong *et al*., 2018), or even biological tissue such as enamel (Yin *et al*., 2016).

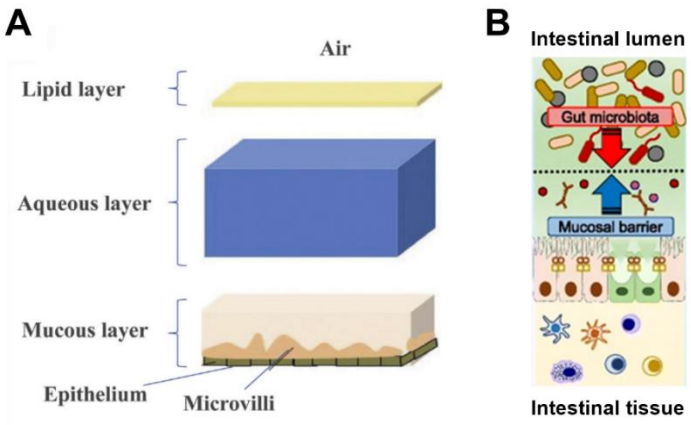

Figure 10. Natural Tissue Enveloped in Liquid.

(A) Schematic of the tear film found in eyes. (Willcox, 2019); **(B)** Schematic of intestinal tissue. (Modified from Okumura and Takeda, 2018).

Methods for applying a liquid layer onto solids include liquid-infused surfaces and infused polymers. While both techniques yield a liquid layer that covers the substrate, they exhibit fundamental distinctions. Liquid-infused surfaces feature a liquid covering the material's surface (R. Liu *et al*., 2020; Doll *et al*., 2017; Sunny *et al*., 2016), whereas for infused polymers, the liquid

not only coats the surface but also penetrates the polymer matrix (Fong *et al*., 2023; Andersen *et al.,* 2022, MacCallum *et al*., 2015).

1.2.1 Liquid Infused Surfaces

Creating a liquid-infused surface requires a solid to support the liquid layer, and a liquid that has a higher affinity for the solid than a contaminant (Howell *et al*., 2018; Bohn & Federle, 2004). Once submerged or in contact with the infusing liquid, the liquid adheres to the solid through van der Waals force and capillary force (if the solid surface is rough) (Quéré, 2005). When the infusing liquid is immiscible with potential foulants, it becomes less energetically favorable for foulants to penetrate the liquid layer and contact the solid below, rendering the infused surface antifouling—where foulants simply slide off the surface (T.-S. Wong *et al*., 2011). The solid being infused can possess varying degrees of roughness, but the essential criterion is that the infusing liquid must share a chemical nature that matches the solid's surface chemistry. While surface roughness is not indispensable, a textured solid can enhance liquid retention compared to planar materials (Liu *et al*., 2020; Huang and Guo, 2019; Howell *et al*., 2018; Wen *et al*., 2017; Bohn & Federle, 2004).

To construct liquid infused surfaces, several methods can be employed to enhance the affinity between the liquid and the solid underneath: Artificial enhancement of liquid affinity with the infusing material can be accomplished through chemical functionalization of the surface. Liquid phase deposition, a method involving the immersion of materials in a solution for chemical reactions to take place, offers a means of achieving this. For instance, perfluorocarbon lubricants can be deposited onto surfaces containing fluorous elements. The robust intermolecular interaction between the fluorinated lubricant and the fluorosilane layer ensures the retention of the liquid layer, resulting in a stable coating (Badv *et al*., 2017). Chemical vapor deposition can overcome certain drawbacks of liquid phase such as solvent wastage, and potential exposure of the substrate to by-

products during chemical reactions (Badv *et al*., 2017; Hang *et al*., 2017). In this widely adopted technique, substrates undergo treatment with plasma, while the infusing liquid is supplied in a gaseous form (Badv *et al*., 2017; Hang *et al*., 2017). Chemical reactions then occur on the substrate surface, facilitating the formation of liquid coatings. Examples include reactions between halosilanes and surface hydroxyl groups, and silanization (Howell *et al*., 2018).

Achieving surface roughness to further increase liquid affinity to the solid can be realized by adding a textured layer through various methods such as chemical vapor deposition, liquid phase deposition, or electrochemical deposition. Layer-by-layer or self-assembly techniques have also been explored in research (Kasapgil *et al*., 2022; Zhou *et al*., 2018; Zhu *et al*., 2018; Badv *et al*., 2017; Sunny *et al*., 2016; Manabe *et al*., 2015; Tesler *et al*., 2015). Porous coatings on materials can be created through the deposition of charged polymers and particles via layer-by-layer deposition, while surface textures can result from the use of porogenic solvents to create porous surfaces (Manabe *et al*., 2015; Manna and Lynn, 2015; Sunny *et al*., 2014; Li *et al*., 2013; Levkin *et al*., 2009). Nanostructures have been employed for this purpose as well (Lv *et al*., 2022; Boveri *et al*., 2021; Cai *et al*., 2021, 2020; Huang and Guo, 2019). Alternatively, surface roughness can be achieved by removing a portion of the surface, employing methods like laser ablation, etching, or lithography (Yan *et al*., 2023; Fang *et al*., 2022; Zhang *et al*., 2022; Atthi *et al*., 2021; M. Liu *et al*., 2020; R. Liu *et al*., 2020; Yu *et al*., 2020; Yong *et al*., 2018; Yin *et al*., 2016; Kim *et al*., 2012). Large-area textured surfaces can even be produced by evaporating water off polyphenylene oxide surfaces (Zhang *et al*., 2015). These methods typically generate random surface topography, but ordered surface patterns can also be achieved through colloidal self-assembly (Vogel *et al*., 2013).

1.2.2 Infused Polymers

In the case of infused polymers, the underlying principle resembles that of liquid-infused surfaces. However, instead of the liquid layer remaining solely on the surface of the substrate, in infused polymers, the infusing liquid penetrates the polymer matrix. As long as the liquid demonstrates a higher affinity for the solid material than contaminants, it can effectively repel them, much like in liquid-infused surfaces (Howell *et al*., 2018; Bohn & Federle, 2004). Similarly, a crucial requirement is that the infusing liquid must share a chemical nature that aligns with the surface chemistry of the polymer, facilitating its infusion into the polymer matrix. This compatibility is easily achieved by pairing the solid material with a corresponding infusing liquid. For instance, silicone material can be effectively paired with silicone oil. (Fong *et al.,* 2023; Andersen *et al*., 2022; MacCallum *et al*., 2015).

While not an absolute prerequisite for infusion, the introduction of surface roughness onto the infusing polymer can also enhance stability through capillary forces. For instance, the incorporation of small pore sizes in substrates can generate high capillary pressure, facilitating the retention of the lubricant within the substrate (Lv et al., 2022; Boveri et al., 2021; Cai et al., 2021, 2020; Huang and Guo, 2019). Similarly, highly porous substrates increase the surface contact area between the liquid layer and foulants, thereby enhancing antifouling effects. Although both liquid infused surfaces and infused polymers are capable of creating a liquid-repellent surface, they are different from the construction of superhydrophobic surfaces, which is typically achieved through the use of surface structures to deter contaminants (Figure 11). An iconic example in nature inspiring the development of superhydrophobic surfaces is the lotus leaf, exhibiting what is commonly known as the lotus effect (Barthlott & Neinhuis, 1997). This natural mechanism involves micro-scaled pillars distributed across the lotus leaf. When a water droplet contacts this

superhydrophobic surface, it avoids penetration into the spaces between the pillars (Yao *et al*., 2022; Sotiri *et al*., 2016). Instead, the droplets remain suspended on the elevated edges of the surface, supported by air pockets—a condition known as the Cassie-Baxter State (Figure 11A). This unique state enables water to effortlessly roll off the surface because it is not pinned down and in full contact with the material (as in the Wenzel State; Figure 11A).

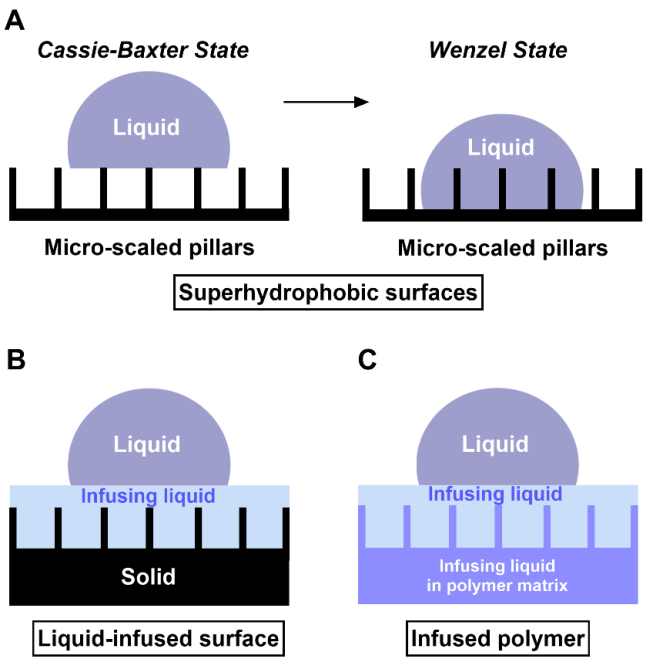

Figure 11. Different Liquid-repellent Surfaces

(A) Schematic superhydrophobic surfaces, where fouling liquid transitioned from Cassie-Baxter to Wenzel state; **(B)** Schematic of liquid infused surface; **(C)** Schematic of infused polymer.

In contrast to superhydrophobic surfaces that trap air pockets in their textured structure, the liquid infusion technique involves introducing liquid between the structures (Figure 11B and 11C). This distinction allows liquid infusion to overcome certain limitations associated with superhydrophobic surfaces. For instance, under high pressure, the air pockets in superhydrophobic surfaces may fail to support liquids, causing them to be compressed and pinned onto the material (Figure 11A) (Bocquet & Lauga, 2011). Additionally, superhydrophobic surfaces may struggle to effectively repel liquids with low surface tension (Yao *et al*., 2022). Furthermore, the longevity of superhydrophobic surfaces may be compromised when subjected to physical damage (Bocquet & Lauga, 2011). Conversely, liquid infusion retains liquid within the textured structure rather than air pockets. The resulting liquid layer proves highly stable, capable of withstanding high pressures and physiological shear rates (Wong *et al*., 2011; Howell *et al*., 2015).

This stability ensures the effectiveness of liquid-infused substrates in repelling foulants, as long as the foulant is immiscible with the infused liquid. Additionally, owing to the liquid nature of the infusing liquid, the liquid layer is capable of self-healing by flowing and filling any damaged sites (Xiao *et al*., 2013; Epstein *et al*., 2012; Kim *et al*., 2012).

1.2.3 Liquid Choices for Medical Applications

While a diverse range of liquids has been employed for generating liquid-infused materials, only a select few exhibit biocompatibilities or have been used in medical applications. Identifying infusing liquids suitable for medical use can be a formidable task, necessitating regulatory approvals and sterilization methods prior to implementation. Nonetheless, certain infusing liquids are anticipated to be biocompatible and hold potential for use in infusing medical instruments. Examples include edible oils such as almond, coconut, and canola oil (Manna *et al*., 2015; Manabe *et al*., 2015). Infusion is made possible by employing polymers containing azlactone groups and treating the polymers with amine containing molecules (Manna *et al*., 2015; Manabe *et al*., 2015). Additionally, medical-grade perfluorocarbons like perfluorodecaline and perfluoroperhydrophenanethene could be employed in infusion owing to their fluorinated groups. Fluorous molecules can be physically adsorbed onto surfaces containing fluorous elements, allowing a variety of substrates to be infused with the mentioned perfluorocarbons (Horváth, 2012; Harris and Chess, 2003). FDA-approved and used as blood substitutes and ocular tamponades respectively, these perfluorocarbons make promising candidates for infusing medical instruments (Badv et al., 2017) (Castro *et al.,* 2010; Kertes *et al.,* 1997). Silicone oil, widely used as ocular tamponades and in cosmetics, is also a favorable candidate due to its biocompatibility (Pavlidis, 2015; Narins and Beer, 2006). Its application as a lubricant in existing urinary catheters (e.g. CompactCath) further highlights its potential for medical instrument infusion.

1.2.4 Characterizing Liquid Infused Materials

To develop an effective system, researchers must possess a comprehensive understanding of the system's parameters and properties. In the context of liquid-infused systems, researchers typically measure the distribution, thickness, and stability of the liquid layer. However, obtaining such measurements can sometimes be challenging due to the minute volume of the liquid layer on the material, necessitating the use of specialized instruments that may not be readily available in all research laboratories.

1.2.4.1 Thickness and Distribution

Microscopic methods represent a direct and valuable approach for visualizing liquid layers, with confocal microscopy standing out for its capability to generate 3D reconstructions from image stacks (Elliott, 2020). When employing fluorescently labeled infusing liquids in liquid infusion, this method allows visualization of the thickness of the liquid layer on a flat surface (Song & Rutledge, 2023; Peppou-Chapman *et al*., 2020; Howell *et al*., 2015). However, confocal microscopy has limitations: it cannot quantify liquid layers with a thickness below 500 nm, and issues such as poor matching of index of refraction between infusing liquid and the substrate may lead to significant scattering (Song & Rutledge, 2023; Peppou-Chapman *et al*., 2020, Cox and Sheppard, 2003). The lateral resolution of this method is also limited to a maximum of 250 nm (Cox and Sheppard, 2003).

To enhance resolution, researchers can use scanning electron microscopy, which offers insights into the behavior of droplets on liquid-infused surfaces. While this method facilitates the visualization of liquid distribution, directly quantifying thickness may prove challenging without additional treatments such as cryogenic processing of the samples. (Smith *et al*., 2013). Atomic force microscopy (AFM) has proven more successful in estimating and quantifying liquid layer

thickness. By employing contact mode force spectroscopy, researchers can use AFM probe's tip to determine the location of the top and bottom layers of the liquid (Peppou-Chapman *et al*., 2020). However, limitations include dependence on the microscope's hardware, where the radius of the tip determines image resolution, and the slow process compared to other microscopy techniques.

Alternatively, thickness estimation can be calculated by knowing the mass before and after infusion and the surface area being infused, assuming a uniform liquid layer on the surface (Goodband *et al*., 2020). This method is not universally applicable to all experimental substrates and may be influenced by the sensitivity of the balance used. Ultra-violet visible spectrophotometry has been used to indirectly measure the amount of oil in liquid-infused materials, where liquid quantity can be estimated via a standard curve after dissolving all infused liquid in the material with extraction solvents (Wu *et al*., 2021). Similarly, a fluorimeter can be employed if the infusing liquid is fluorescent, providing information about the amount of liquid left in the material (Ware *et al*., 2018). These methods however lack spatial information and are destructive to the samples.

Characterizing liquid layers poses a significant challenge, primarily attributed to the minimal volume of liquid on infused surfaces and constraints imposed by analysis protocols. Nevertheless, overcoming these challenges might be feasible through the synergistic application of various characterization methods in research studies, offering a more comprehensive and nuanced understanding of the liquid layer.

1.2.4.2 Damage and Aging

Liquid-infused materials serve as effective systems in preventing fouling and contamination. However, concerns arise regarding the depletion and aging of these materials, given that their

antifouling property is contingent on the presence of a functional liquid layer. Researchers have devised multiple methods to assess the depletion of this liquid layer.

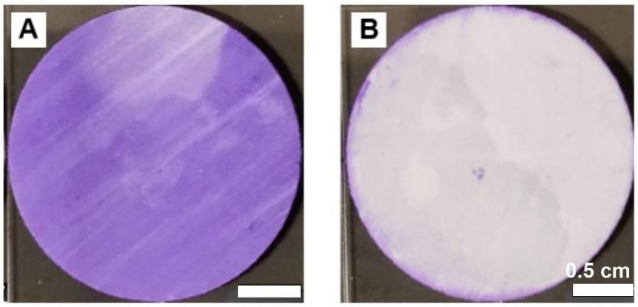

Figure 12. Stained Membrane With and Without Liquid Infusion.

Crystal violet treated **(A)** bare membrane; and **(B)** membrane infused with commercial Krytox oil with low viscosity (K103). Membranes show here are made of poly(vinylidenefluoride). (Modified from Shah *et al*., 2022).

Visual detection of liquid presence can be achieved through dye staining (Shah *et al*., 2022; Figure 12). By using a dye with different hydrophobicity than the infusing liquid, researchers can qualitatively reveal areas of substrates lacking the lubricant, as the dye is immiscible with the infusing liquid (Shah *et al*., 2022). Another simple yet effective method is the paper stain test, where intentional damage to the liquid layer is followed by pressing the sample on paper to detect stains, indicating the presence of the liquid layer (Cai & Pham, 2022).

The sliding angle test measures the critical angle at which a water droplet, of specific volume, initiates sliding down an inclined plate of the infused material. This angle serves as a crucial parameter for assessing the hydrophobic characteristics and fluid repellency of surfaces (Nongnual *et al*., 2022; Miwa *et al*., 2000). Previous research has established that surface roughness contributes to the resistance encountered by water droplets during sliding (Bikerman, 1950). A smaller sliding angle is therefore indicative of a smoother and more slippery surface, suggesting that the liquid layer is likely intact and not damaged. Additionally, if the substrate is placed at a fixed angle, the volume of liquid required to make the droplet start rolling off from the surface also indirectly measures the slipperiness and smoothness, indicating potential damage to the liquid layer (Cai & Pham, 2022). Monitoring the damage or aging of the liquid layer can also be

accomplished through periodic measurements of wetting properties. Researchers also assess the contact angle of a water droplet on infused surfaces before and after aging treatments (Goodband *et al*., 2020; Sotiri *et al*., 2018). The contact angle is the angle at which a liquid droplet forms when in contact with the infusing substrate. A decrease in the contact angle suggests increased wetting of the substrate by the fouling droplet, potentially indicating damage to the infused material. However, this testing method cannot accurately be used to assess liquid-infused materials. This limitation arises from the presence of infusing liquid on the surface of materials, which can interact with the liquid droplet applied for testing (Semprebon *et al*., 2017). For instance, factors such as the volume of infusing liquid in the infused material, the contact time of the liquid droplet applied on the infused material, viscosity of the infusing liquid, and the wetting ridge formed by the infusing liquid around the testing droplet can significantly influence the observed contact angle in the test (Cai *et al.,* 2021; Wong *et* al., 2020; Semprebon *et al*., 2017; Figure 13).

While various methods exist to detect liquid layer damage, a lack of standardization in depleting or damaging liquid-infused surfaces complicates direct comparisons between different studies and surfaces in the current literature.

1.2.5 Interaction of Infused Material with the Environment

Liquid-infused materials have garnered attention for their potential applications in biomedical settings, primarily owing to their remarkable antifouling properties. This is

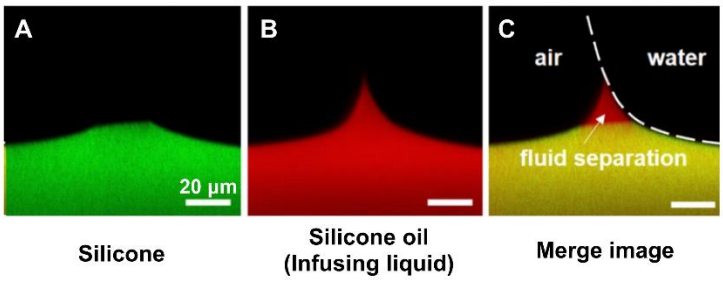

Figure 13. Confocal Images of Infused Silicone Polymer With Water Droplet Deposited on Surface.

Confocal images were captured following the application of a water droplet on an infused silicone polymer. The images depict **(A)** the silicone polymer, **(B)** the infusing liquid, and **(C)** the merged image. In **(C)**, the infusing liquid is highlighted in red, whereas areas where silicone and the infusing liquid co-localize appear in yellow. (Modified from Cai *et al.,* 2021).

significant as attachment of pathogens, biofilms or other biological foulants on medical devices can lead to device failure or even infections. For example, as discussed in Section 1.1.8.2, numerous surface modifications, including polymer coatings and substrate-releasing coatings like those incorporating antibiotics and nanoparticles, often fail to transition effectively to *in vivo* settings due to issues related to biofilm contamination.

1.2.5.1 Biological Fluids

Preventing contamination by biological fluids on medical devices presents a formidable challenge due to the diverse composition and protein/biomolecule content of fluids such as blood, mucus, and urine. An effective antifouling medical device must be able to repel these fouling proteins and biomolecule content, each with distinct surface attachment properties.

Researchers have achieved success in preventing biological fluid contamination through liquid-infused materials, with many studies revolving around the prevention of blood fouling. Liquid infused surfaces such as slippery tungsten oxide coatings on medical-grade steel devices effectively repel blood (Tesler *et al*., 2015). Infusing sesame oil on endoscopes prevents blood coagulation, ensuring clear visualization of murine stomachs (Nishioka *et al*., 2016). Liquid-infused endoscopes can also maintain their antifouling properties over a hundred blood-dipping cycles (Sunny et al., 2016). Investigating biocompatible liquids like almond oil for antifouling biodevices, researchers have also found that blood does not coagulate on edible oil coated surfaces (Manabe *et al.*, 2015). Coating surfaces with liquid perfluorodecalin, an artificial blood substitutes, prevents fibrin and blood platelet attachment; these types of liquid layers have also been shown to remain stable under physiological relevant flow rate (Leslie *et al*., 2014). Perfluorocarbon-coated and fluorine-based organosilane-coated catheters have also demonstrated lower thrombogenicity than uncoated counterparts, with blood-repelling properties lasting up to 8 hours without

anticoagulants- values comparable to coagulant-based coatings (Badv *et al*., 2017; Leslie *et al*., 2014). In addition, liquid infusion can also transform cotton coatings, preventing permeation of water and blood (Sasaki *et al*., 2016). These findings are of significant interest as implants or wound dressings often encounter various biological fluids, and fouling or contaminant accumulation can lead to implant failure or infections.

Beyond blood fouling, liquid-infused materials can be further functionalized by incorporating molecules into the infusion liquid (Applebee and Howell, 2024). For instance, liquid infusion incorporated into vascular grafts prevents coagulation while promoting endothelial cell adhesion by adding antibodies as a coupling agent (Badv *et al*., 2019). This infused material can selectively capture endothelial cells while preventing other proteins and cells.

Silicone oil-infused urinary catheters (infused polymer) have recently demonstrated excellent fouling resistance in the bladder or urinary environment against Fb adhesion *in vivo* in murine models (Andersen *et al.*, 2022). The complex bladder environment, involving periodic filling and voiding of liquid, as well as protein secretions in case of catheter-induced wounds, makes the success of liquid infusion *in vivo* promising for creating antifouling medical devices that can effectively combat contaminations and infections. Further elaboration on liquid infused urinary catheter will be provided in Section 1.2.6.

1.2.5.2 Cells and Pathogens

To better be able to take advantage of liquid-infused materials in medical settings, researchers aim to enhance understanding of the interaction between liquid-infused surfaces and cells or pathogens. Achieving a delicate balance between repelling pathogen or biological foulant adhesion and avoiding immune responses is crucial for materials implanted or placed in the human body. Various

factors, including cell signaling, protein or pathogen adhesion properties, and the potential influence of the liquid on the infused surface, must be considered to achieve this balance.

In vitro studies have demonstrated the ability of liquid infused surfaces to transport cells. Hydrophobic liquid barriers on infused surfaces allow researchers to control the adhesion and migration of eukaryotic cells, confining them within liquid barriers with minimal cell toxicity (Ueda and Levkin, 2013). Similarly, preparing mouse cell suspensions in a solution that can gel into a bead on liquid-infused surfaces enables the encapsulation of cells, while maintaining viability and healthy growth (Schlaich *et al.,* 2018). Additionally, mesenchymal stem cells were able to proliferate on silicone oil-infused silicone surfaces coated with fibronectin. Notably, the resulting cell sheet could detach from the infused substrate while maintaining viability. (Juthani *et al.,* 2016). These findings highlight the capability of liquid-infused surfaces to prevent mammalian cell adhesion without compromising viability, demonstrating the promise of liquid-infused surface for applications in medical devices.

1.2.5.3 Environmental Damage

The durability of the liquid layer on infused materials is a crucial aspect of research, as it could impact the functionality of the infused material. Remarkably, infused materials subjected to various forms of mechanical damage have exhibited robust stability and functionality. For instance, silicone oil infused materials have demonstrated resilience against challenging conditions, including icing and deicing cycles, frosting and defrosting cycles, exposure to liquid nitrogen and water cycles, submersion under ice, and contact with acidic or basic solutions (Jamil *et al*., 2020). Furthermore, these materials have proven their resistance to mechanical damage such as pressing, sandpaper abrasions, touching, and knife cuts, all while maintaining their slippery performance (Jamil *et al*., 2020, Yu *et al*., 2020). Similarly, perfluoropolyether infused nanofibers

have displayed enduring slippery properties, with the lubricant layer remaining stable even during long-term storage in harsh temperature environments ranging from -10°C to 70°C, water immersion, and exposure to ultraviolet radiation (Yu *et al*., 2020).

The liquid nature of the lubricant layer plays a crucial role in this resilience, allowing self-healing of external damage to restore functionality. Additionally, the affinity of the liquid layer to the infused solid also contributes to the overall stability of liquid-infused materials (Howell *et al*., 2018). The versatility of liquid-infused materials is noteworthy, as they can be applied in a wide range of settings. The stability and durability against damage can be further enhanced by increasing the surface roughness of the infusing substrate and the viscosity of the infusing liquid of the coating (Bazyar *et al*., 2018; Bjelobrk *et al*., 2016; Colosqui *et al*., 2016). This highlights the potential for tailoring liquid-infused materials to meet specific requirements in diverse environments.

1.2.6 Using Liquid Infusion to Combat CAUTI

As discussed in Section 1.1.9, despite the exploration of various coatings for urinary catheter materials, such as hydrogel and antibiotic-releasing coatings, a common challenge is the difficulty in translating their efficacy from *in vitro* to *in vivo* environments. Moreover, the undesirable consequences of antibiotic resistance and the ineffectiveness of substance-releasing coatings in CAUTI due to biofilm formation have led to the search for alternative solutions (Hunt *et al*., 2023; Gaston *et al*., 2020). Given that deposition of Fb on catheters has been identified as the primary cause of the persistence of pathogens and subsequent biofilm formation on catheter surfaces (as elaborated in Section 1.1.5.2; Figure 14), efforts aimed at reducing the availability of pathogen binding sites by lowering Fb adhesion could effectively reduce microbial colonization. Recent

collaborative work in our labs has shown that liquid-infused silicone catheters offer a promising solution in this regard, as they are straightforward to manufacture, exhibit greater stability, and prove more cost-effective compared to alternative antifouling polymer modifications (Andersen and Flores-Mireles, 2019). To prepare liquid-infused mouse catheters for *in vivo* testing, we submerged silicone mouse catheters in silicone oil until reaching saturation, as determined by the absence of further weight gain. The polymer matrix of the resulting mouse catheters had been fully saturated with silicone oil, in contrast to liquid-infused surfaces where the infusing liquid merely coats the surface without liquid penetration.

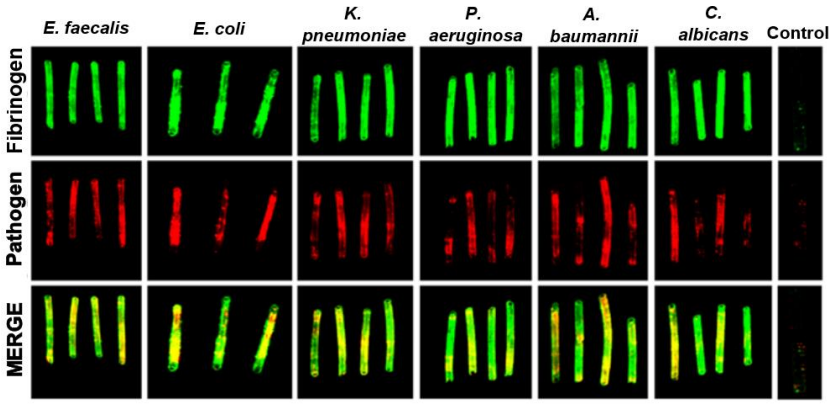

Figure 14. Interaction Between Uropathogens and Fibrinogen *in vivo*.
Urinary catheters that were implanted in mice were stained with immunofluorescence to show location of fibrinogen (green) and pathogens (red). Unimplanted catheters were used as controls. n=3-4.

Following catheterization of mice with either unmodified or liquid-infused mouse catheters, the mice were subsequently infected with uropathogens for a duration of 24 hours. Our results showed a significant reduction in microbial colonization in the bladder and on the catheter surface among mice catheterized with liquid-infused mouse catheters, irrespective of the infecting pathogen (Figure 15). Additionally, deposition of other host-secreted proteins such as serum albumin was notably diminished. Furthermore, hematoxylin and eosin analysis revealed that catheterization with liquid-infused catheters did not exacerbate bladder inflammation, regardless of the presence of infection. Our study is significant as it shows that the liquid infused technique can be applied to

urinary catheters and most importantly, proved to function effectively in *in vivo* environment. This differs from other antifouling coatings, as they frequently struggle to maintain efficacy when transitioning from *in vitro* to *in vivo* environments (as described in Section 1.1.8.2). Nevertheless, gaining a deeper understanding of the impact of silicone oil on the immune system or host tissue will be essential for ensuring the safe and successful translation of this technique into the market.

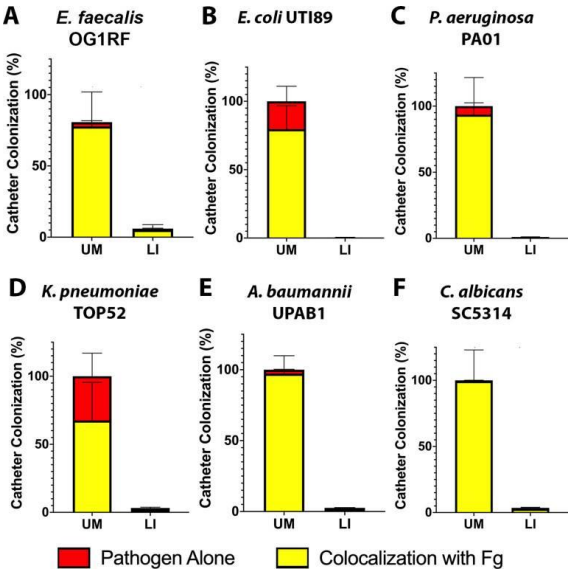

Figure 15. Colocalization of Fibrinogen and Pathogen on Liquid Infused Catheters or Unmodified Catheters.

Quantification of colocalization of fibrinogen and uropathogens on unmodified (UM)- and liquid infused catheters (LI) from catheterized mice infected with **(A)** *E. faecalis*, **(B)** *E.coli*, **(C)** *P. aeruginosa*, **(D)** *K. pneumoniae*, **(E)** *A. baumannii*, **(F)** *C. albicans*.

1.2.6.1 Acknowledgement

Section 1.2.6 is based on work previously published in eLife, doi: 10.7554/eLife.75798; authors: Marissa Jeme Andersen, **ChunKi Fong**, Alyssa Ann La Bella, Jonathan Jesus Molina, Alex Molesan, Matthew M Champion, Caitlin Howell, and Ana L Flores-Mireles.

1.2.7 Potential Health Impact of Silicone Oil

While silicone oil boasts excellent biocompatibility and has garnered FDA approval as a catheter lubricant in current market catheter products, concerns persist regarding its potential to cause health impacts to the host system. Addressing this concern, researchers have conducted toxicity tests on silicone oil, revealing that while silicone oil infused surfaces can repel adhesions and prevent biofilm formation by various microorganisms, and it does not induce suffocation of cells in *Botrycoccus braunii*—a type of algae heavily reliant on gases for photosynthesis (Howell *et al.*,

2014). This biocompatibility extends to mammalian cells, as evidenced by the growth of mouse mesenchymal stem cells on silicone oil-infused coatings, where no toxicity is observed, and cell coverage mirrors that on plain glass (Sunny *et al*., 2016). Additionally, mesenchymal stem cells can grow on silicone oil-infused surfaces, where they remained viable and exhibited continued growth and proliferation after being transferred from these surfaces. (Juthani *et al*., 2016). While these studies indicate that cytotoxicity or loss of cell functionality does not occur in algae and mammalian cells, it does not necessarily imply complete safety for human use, given the inherent differences between these experimental systems and the human body. For example, high concentrations of silicone oil, at ~5.4 mg/mL, have been associated with potential protein structural alterations and the potential initiation of antibody responses (Krayukhina *et al.,* 2019; Chisholm *et al*., 2015).

Silicone oil is widely used in medical devices, such as syringe lubricants and ocular tamponades. The precise threshold of free silicone oil required to trigger an immune response however remains poorly understood and likely varies among individuals. It has been estimated that the volume of silicone liquid coating clinically used prefilled siliconized syringes can range from 0.6 to 1 mg/mL, with around 0.11±0.03 mg/mL of this volume typically released into the bloodstream (Chisholm *et al*., 2015). This suggests that the host system can tolerate a limited exposure of free silicone oil. Previous studies on ocular tamponades and connective tissue have also suggested adverse effects of silicone liquid leakage, including heightened inflammatory cell response and antibody production (Melo *et al*., 2021; Cheng *et al*., 2020; Krayukhina *et al*., 2019; Chisholm *et al*., 2015). It is believed that the immune response is linked to the formation of protein aggregates around silicone liquid droplets. *In vivo* studies have indicated elevated concentrations of antidrug antibodies in the presence of silicone liquid-protein complexes (Cheng *et al*., 2020; Krayukhina *et*

al., 2019; Chisholm *et al*., 2015). Recent findings also suggest that liquid silicone droplets can trigger the formation of adherent cell masses similar to granuloma formation (Cheng *et al*., 2020).

Previous studies have demonstrated that repeated exposure to an air/water interface is an effective method for removing the free liquid layer from infused systems, as the lower-surface-energy liquid will spontaneously move to cover the higher-surface-energy water interface and be carried away into the environment (Sotiri *et al*., 2018; Howell *et al*., 2015). In urinary catheters, the intermittent flow of urine over the surface of the catheter is very likely to result in the loss of free silicone liquid from liquid-infused surfaces. At the same time, repeated contact of the exterior surface of the catheter with urethral and bladder tissue is likely to physically remove free liquid present there (Veronesi et al., 2021). It is therefore critical to understand the potential for surface liquid loss in liquid infused catheters and explore methods of reducing such loss while continuing to preserve their antifouling capabilities.

1.3 Dissertation: Rationale, Scope, and Contribution

In this dissertation, we explore the development of liquid-infused urinary catheters, focusing on controlling protein and pathogen deposition, and improving the safety of liquid-infused urinary catheters. The comprehensive approach involved three key aspects:

(1) Fabricating and characterizing the infused material: One notable advantage of producing silicone oil-infused silicone urinary catheters is their compatibility with existing commercial silicone catheters (Andersen *et al*., 2023), obviating the need to produce catheters from the ground up. Understanding how the infusion process affects the infused material is crucial for manufacturing. Our investigation delved into parameter alterations of silicone catheters during the infusion process, encompassing changes in length, outer diameter, inner diameter, and the quantity of silicone oil intake. Additionally, we explored various fabrication methods

for liquid-infused catheters aimed at minimizing the quantity of silicone oil within the catheter material to enhance safety.

(2) Assessing the functionality of the infused catheters in terms of protein and pathogen adhesion: Following the fabrication of liquid-infused catheters with reduced quantities of silicone oil, our investigation focused on assessing whether these catheters maintained their ability to repel protein and pathogen adhesion. Preserving this crucial functionality is essential for combating CAUTI, making it a critical aspect to evaluate.

(3) Investigating the impact of removing the free liquid layer from infused catheter on liquid loss into the environment. Another crucial aspect to investigate is whether these methods aimed to reduce free liquid layer from infused catheters also minimize the release of silicone oil into the environment into the host bladder. Gaining insight into the potential quantity of silicone oil lost could facilitate further testing to ascertain the safety levels associated with using liquid-infused urinary catheters as a medical instrument.

In conclusion, the primary objective of this dissertation was to advance the safe use of liquid-infused catheters in combating CAUTI, as this technique has shown to be successful in *in vivo* settings (Andersen *et al*., 2023). This holds significance as it represents one of the rare instances where a surface modification approach has effectively transitioned from *in vitro* to *in vivo* applications, notably without resorting to antibiotics, thus mitigating the risk of contributing to antibiotic resistance. Given the indispensable role of urinary catheters in the care of a diverse range of patients, we aspire for this study to offer an alternative in the future, enabling patients to mitigate infections without facing repercussions for a crucial medical treatment they require.

CHAPTER 2
LIQUID INFUSED SILICONE CATHETERS IN MOUSE MODELS

2.1 Introduction

Recent findings in mouse and human urinary catheterization have unveiled the importance of the host clotting factor 1, fibrinogen (Fg), for surface adhesion and subsequent establishment of biofilms and persistence of CAUTIs in *Enterococcus faecalis* and *Staphylococcus aureus* infections (Flores-Mireles *et al*., 2019; Flores-Mireles *et al*., 2014; Flores-Mireles *et al*., 2016a; Flores-Mireles *et al*., 2016b; Gaston *et al*., 2020; Klein and Hultgren, 2020). Fg is continuously released into the bladder lumen in response to mechanical damage to the urothelial lining caused by catheterization (Flores-Mireles *et al*., 2019; Flores-Mireles *et al*., 2014; Flores-Mireles *et al*., 2016a; Klein and Hultgren, 2020). Once in the lumen, Fg is deposited on the catheter, providing a scaffold for these incoming uropathogens to bind and establish infection in human and mouse CAUTI. When blocking the interaction between Fg and *E. faecalis* using antibodies, the pathogen is not able to effectively colonize the bladder (Di Venanzio *et al*., 2019; Flores-Mireles *et al*., 2014; Flores-Mireles *et al*., 2016a; Gaston *et al*., 2020; Walker *et al*., 2017).

Thus, we hypothesized that reducing availability of binding scaffolds, in this case Fg, would decrease microbial colonization in a catheterized bladder. To test our hypothesis, we used a mouse model of CAUTI and a diverse panel of uropathogens, including *E. faecalis*, *C. albicans*, uropathogenic *Escherichia coli*, *Pseudomonas aeruginosa*, *A. baumannii*, and *Klebsiella pneumonia*, which we found all bind more extensively to catheters with Fg present. To resolve the deposition of Fg, we focus on antifouling modifications, specifically, liquid-infused silicone (LIS). LIS is simpler to make, more stable, and more cost effective than other antifouling polymer modifications (Andersen and Flores-Mireles, 2019; Campoccia *et al*., 2013; Homeyer *et al*., 2019; Howell *et al*., 2018; Chamy, 2013; Singha *et al*., 2017; Sotiri *et al*., 2018; Villegas *et al*., 2019).

Additionally, LIS has been shown to reduce clotting in central lines and infection in skin implants (Chen *et al*., 2017; Leslie *et al*., 2014). We show that our LIS-catheters reduced Fg deposition and microbial binding not only *in vitro* but also *in vivo*. Furthermore, LIS-catheters significantly decrease host-protein deposition when compared to unmodified (UM)-catheters as well as reducing catheter-induced inflammation. These findings suggest that targeting host-protein deposition on catheter surfaces and the use of LIS-catheters are plausible strategies for reducing instances of CAUTI.

2.1.1 Special Introduction

This chapter is based on work previously published in eLife, doi: 10.7554/eLife.75798; authors: Marissa Jeme Andersen, **ChunKi Fong**, Alyssa Ann La Bella, Jonathan Jesus Molina, Alex Molesan, Matthew M Champion, Caitlin Howell, and Ana L Flores-Mireles. This published paper is the collaboration work between University of Maine and University of Notre Dame, we have contributed to paper review, and the following experimental sections: infused tube fabrication and infused tube parameter characterization.

2.2 Materials and Methods

2.2.1 Mouse infection models

Mice used in this study were ~6-week-old female wild-type C57BL/6 mice purchased from Jackson Laboratory and The National Institute of Cancer Research. Mice were subjected to transurethral implantation and inoculated as previously described (Conover *et al*., 2015). Briefly, mice were anesthetized by inhalation of isoflurane and implanted with a 6-mm-long UM-silicone or LIS-catheter. Mice were infected immediately following catheter implantation with 50 µl of ~2 × 107 CFU/ml in phosphate-buffered saline (PBS) introduced into the bladder lumen by

transurethral inoculation. To harvest the catheters and organs, mice were sacrificed at 24 hpi by cervical dislocation after anesthesia inhalation; the silicone catheter, bladder, kidneys, heart, and spleen were aseptically harvested. Catheters were either subjected to sonication (Branson, Ultrasonic Bath) for CFU enumeration analysis, fixed for imaging via standard IF described below, or sent for proteomic analysis as described below using nonimplanted catheters as controls for all assays. Bladders for IF and histology were fixed and processed as described below. Kidneys, spleens, and hearts were all used for CFU analysis. The University of Notre Dame Institutional Animal Care and Use Committee approved all mouse infections and procedures as part of protocol number 18-08-4792MD. All animal care was consistent with the Guide for the Care and Use of Laboratory Animals from the National Research Council.

2.2.2 Bladder Immunohistochemistry (IHC) and H&E staining of mouse bladders

Mouse bladders were fixed in 10% neutralized formalin (Leica) overnight, before being processed and sectioned by ND CORE. Staining was done as previously described (Walker *et al*., 2017). Briefly, bladder sections were deparaffinized, rehydrated, and rinsed with water. Antigen retrieval was accomplished by boiling the samples in Na-citrate, washing in water, and then incubating in PBS three times. Sections were then blocked (1× PBS, 1.5% BSA, 0.1% sodium azide), washed in PBS, and incubated with appropriate primary antibodies overnight at 4°C. Next, sections were washed with PBS, incubated with secondary antibodies for 2 hr at RT, and washed once more in PBS prior to Hoechst dye staining. H&E stain for light microscopy was done by the CORE facilities at the University of Notre Dame (ND CORE). All imaging was done using a Zeiss inverted light microscope (Carl Zeiss, Axio Observer). Zen Pro (Carl Zeiss, Thornwood, NY) and ImageJ software were used to analyze the images.

2.2.3 Quantifying catheter colonization and Fg deposition

As previously described (Colomer-Winter *et al.*, 2019). Briefly, catheters were fixed with 10% neutralized formalin, blocked, and stained using Goat anti-Fg primary antibody (Sigma) (1:1000) and Rabbit anti-pathogen followed by Donkey anti-Goat IRD800 antibody (Invitrogen) (1:5000) and Donkey anti-Rabbit IRD680 antibody (Invitrogen) (1:5000) secondary. The catheters were then dried over night at 4°C and imaged on an Odyssey Imaging System (LI-COR Biosciences) to examine the infrared signal. Images of the signals (Fg in green and pathogens in red) were analyzed in ImageJ using Pixel color counter (Gaston *et al*., 2020).

2.2.4 Human urine collection

Human urine was collected and pooled from at least two healthy female donors between 20 and 40 years of age. Donors had no history of kidney disease, diabetes, or recent antibiotic treatment. Urine was sterilized using a 0.22 μm filter (Sigma-Aldrich) and pH adjusted to 6.0–6.5. When supplemented with BSA (VWR Lifesciences), urine was filter sterilized again following BSA addition. All participants signed an informed consent form and protocols were approved by the local Internal Review Board at the University of Notre Dame under study #19-04-5273.

2.2.5 Microbial growth conditions in supplemented urine

E. faecalis and *C. albicans* were grown static for ~5 hr in 5 ml of respective media (Supplementary file 1) followed by static overnight culture in human urine supplemented with 20 mg/ml BSA (urine BSA20). *E. coli, K. pneumoniae, P. mirabilis, A. baumanii*, and *P. aeruginosa* were grown 5 hr shaking at 37°C in LB then static in fresh urine BSA for 24 hr then, supplemented into fresh urine BSA for an additional 24 hr static (2 × 24 hr) in urine BSA20. All cultures were washed in PBS (Sigma) three times and resuspended in assay appropriate media.

2.2.6 Silicone disk preparation

Disks of UM-silicone (Nalgene 50 silicone tubing, Brand Products) or LIS were cut using an 8 mm leather hole punch. UM disks were washed three times in PBS and air dried. LIS disks were stored in filter sterilized silicone oil at RT. Disks were skewered onto needles (BD) to hold them in place and put in 5 ml glass tubes (Thermo Scientific) or placed on the bottom of 96-well plate wells (Fisher Scientific) (UM-silicone only). Plates and glass tubes were UV sterilized for >30 min prior to use.

2.2.7 Protein-binding assays

Human Fg free from plasminogen and von Willebrand factor (Enzyme Research Laboratory #FB3) was diluted to 150 µg/ml in PBS. 500 µL of 150 µg/ml Fg was added to each disk in glass tubes, sealed, and left over night at 4°C. Disks were then processed according to standard IF procedure as described above (Colomer-Winter *et al*., 2019). Briefly, disks were washed three times in PBS, fixed with 10% neutralized formalin (Leica), blocked, and stained using Goat anti-Fg primary antibody (Sigma) (1:1000) and Donkey anti-Goat IRD800 secondary antibody (Invitrogen) (1:5000). Disks were then dried over night at 4°C and imaged on an Odyssey Imaging System (LI-COR Biosciences) to examine the infrared signal. Intensities for each catheter piece were normalized against a negative control and then made relative to the pieces coated with Fg which was assigned to 100%. Images were processed using Image Studio Software (LI-COR, Lincoln, NE) Microsoft Excel and graphed on GraphPad Prism (GraphPad Software, San Diego, CA).

2.2.8 Microbial-binding assays

For assessing the effect of protein deposition on microbial binding, 100 µl of 150 µg/ml Human Fg, 100 µl of 150 µg/ml BSA, or 100 µl of PBS were incubated on UM-silicone disks in 96-well

plates overnight at 4°C. The following day disks were washed three times with PBS followed by a 2-hr RT incubation in 100 µl of urine containing microbes at a concentration of ~108 CFU/ml.

For assessing microbial binding to UM-silicone vs LIS, 500 µl of microbe containing media was added to prepared disks in glass tubes. Standard IF procedure was then followed as described above using goat anti-Fg and rabbit anti-microbe primary antibodies (1:1000) (see Supplementary file 1 for details). Secondary antibodies used were Donkey anti-Goat IRD800 and Donkey anti-Rabbit IRD680 (1:5000). Quantification of binding was done using ImageStudio Software (LI-COR). Intensities for each catheter piece were normalized against a negative control and then made relative to the pieces coated with Fg which was assigned to 100%.

2.2.9 Silicone and Tygon tube infusion

Five samples of 20-cm Tygon tube (14-171-219, Saint-Gobain Tygon S3 TM 3603 Flexible Tubings, Fisher Scientific, USA) or silicone tube (8060-0030, NalgeneTM 50 Platinum-cured Silicone Tubing, Thermo Scientific, USA) were utilized in weight measurement. Weight of the tubes prior to infusion were measured with an analytical balance (AL204, Analytical Balance, Mettler Toledo, Germany). After the measurement of the initial weights, the tubes were submerged in silicone oil (DMS-T15, polydimethylsiloxane, trimethylsiloxy, 50 cSt, GelestSInc, USA) and weighed at designated time points. For each time point, tubes were removed from the oil with forceps and held vertically for 30 s for the excess silicone oil to flow out of the tube. The bottoms of the tubes were then gently dabbed with Kimwipes (Kimwipe, Kimberly-Clark Corp., USA). After measurement, the tubes were again submerged in silicone oil until the next time point. Tubes were measured every 3 hr for the first 2 days; every 6 hr from days 3 to 6; and every 24 hr from day 6 and onwards. Measurements were taken until data showed no significant increase, and that the plateau trendline consisted of at least three data points. Based on these data, for all the protein-

and microbial-binding assays, silicone catheters were submerged in silicone oil for 5 days prior to use to ensure full infusion.

2.2.10 Mouse catheter infusion

Five samples of 20-cm mouse catheter (SIL 025, RenaSil Silicone Rubber Tubing, Braintree Scientific, Inc, USA) were utilized in weight measurement. Weight of the tubes prior to infusion were measured with an analytical balance. After the measurement of the initial weights, the tubes were submerged in silicone oil for different time points. For each time point, catheters were removed from the oil with forceps and a Kimwipes was immediately pressed against the bottom of the catheters to remove the excess silicone oil via capillary action. After the excess oil was drained, catheters were weighed and placed back into silicone oil to continue with the infusion until the next time point. Catheters were measured every 1 min for the first 5 min of the experiment; every 2 min from 5 to 15 min; and every 5 min from 15 min and onwards. Measurements were taken until weight showed no significant increase, and that the plateau trendline consisted of at least three data points. Silicone catheters modified and used in mouse infections were submerged in silicone oil for at least 30 min prior to use.

2.2.11 Parameter measurement of silicone tube before and after infusion

The length, inner diameter, and outer diameter of silicone tubes were measured before silicone oil infusion and following complete infusion (after incubating with silicone oil for >5 days). All parameters were measured using a digital caliper (06-664-16, Fisherbrand Traceable Digital Calipers, Fisher Scientific, USA). For mouse catheters, length was measured using a digital caliper. For inner and outer diameter measurement, photos of the tube openings of the catheters and a scale

of known length were taken and estimated using ImageJ. Percentage weight change of Tygon tube, silicone tube, and mouse catheters were calculated based on the formula below:

$$\frac{Weight\ of\ the\ tube\ after\ infusion - Initial\ weight\ of\ the\ tube}{Initial\ weight\ of\ the\ tube} * 100\%$$

2.2.12 Proteomic analysis of mouse catheters

Five mice catheterized with a LIS-catheter and four mice were catheterized with an UM-catheter were sacrificed after 24 hr of infection with *E. faecalis* OG1RF. Catheters were harvested and put into 100 µl of sodium dodecyl sulfate (SDS buffer (100 mM Tris–HCl, pH 8.8, 10 mM Dithiothreitol (DTT), and 2% SDS)), then vortexed for 30 s, heated for 5 min at 90°C, sonicated for 30 min and the process repeated once more. Samples were sent to the Mass Spectrometry and Proteomics Facility at Notre Dame (MSPF) for proteomic analysis. Proteins were further reduced in DTT, alkylated and digested with trypsin using Suspension Trap and protocols (Zougman *et al*., 2014). nLC–MS–MS/MS was performed essentially as described in Sanchez et al., 2020 on a Q-Exactive instrument (Thermo). Proteins were identified and quantified using MaxLFQ (Label Free Quantification) within MaxQuant and cutoff at a 1% FDR (Cox and Mann, 2008). This generated a total of eight data records from UM-catheters and 10 from LIS-catheters. Data reduction was performed by removing contaminants proteins. Protein abundance for each catheter type was then calculated by summing the LFQ intensity of proteins which comprised 95% of the total abundance on the catheters. Strict filtering criteria of at least two replicates with technical duplication from the UM-catheters and three replicates with technical duplication from the LIS-catheters were required to keep an identification. Abundance of the reduced proteins was plotted using GraphPad Prism. Statistical significance was tested using Mann–Whitney U. A volcano plot was created

using the ranked mean difference for each protein and −log of calculated p values with alpha = 0.05.

2.2.13 Statistical analysis

Unless otherwise stated, data from at least three experiments were pooled for each assay. Significance of experimental results was assessed by Mann–Whitney U test using GraphPad Prism, version 7.03 (GraphPad Software, San Diego, CA). Significance values on graphs are *p ≤ 0.05, **p ≤ 0.01, ***p ≤ 0.0001, and ****p ≤ .00001.

2.3 Results

2.3.1 Uropathogens interact with Fg during CAUTI

Due to the understood interaction between Fg and some uropathogens and Fg accumulation on catheters over time in human and mice, we assessed potential interaction of *E. faecalis* OG1RF,

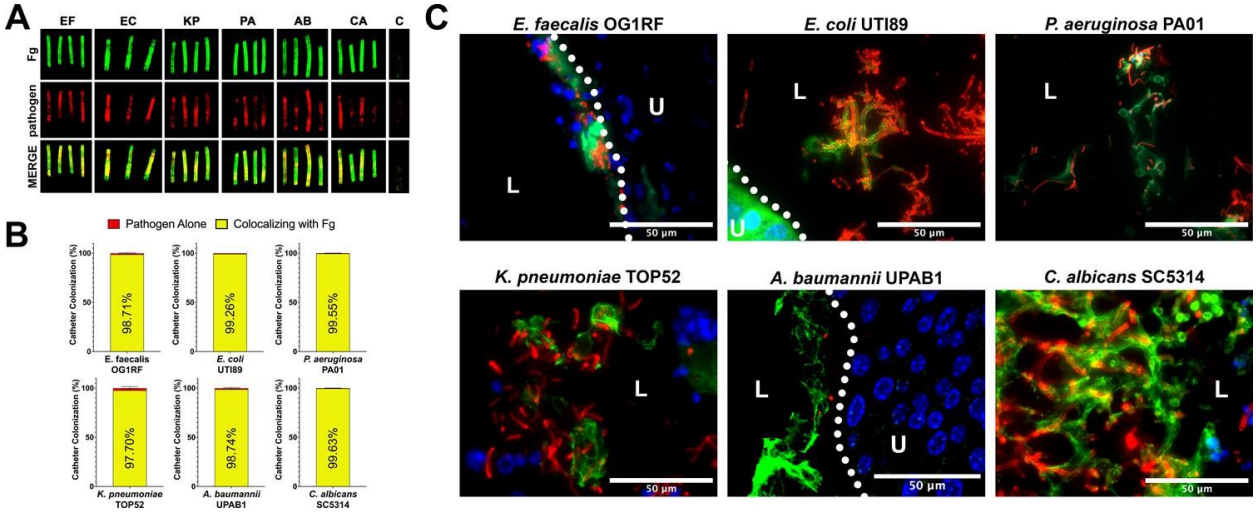

Figure 16. Uropathogens interact with fibrinogen (Fg) in vivo.

(A) Urinary catheters stained with immunofluorescence (IF) for Fg deposition (Fg; green) and microbe binding (respective pathogen; red). Unimplanted catheters were used as controls for autofluorescence, n = 3–4. **(B)** Quantification of uropathogen–Fg colocalization on catheters from panel A. **(C)** Representative images from a single bladder illustrating the interaction of uropathogens (red), Fg (green), and nuclei (blue) on the bladder urothelium (U) and in the lumen (L). Scale bar, 50 nm. For all graphs error bars show the standard error of the mean (SEM). Between 3 and 5 replicates of n = 4–12 each were performed for each pathogen and condition.

uropathogenic *E. coli* UTI89, *P. aeruginosa* PAO1, *K. pneumoniae* TOP52, *A. baumannii* UPAB1, and *C. albicans* SC5314 with Fg in vivo, using a CAUTI mouse model, which recapitulates human CAUTI pathophysiology (Flores-Mireles *et al*., 2019; Flores-Mireles *et al*., 2014; Flores-Mireles *et al*., 2016a; Flores-Mireles *et al*., 2016b). Mice catheterized and infected with the respective uropathogen were sacrificed at 24 hours post infection (hpi). Catheters and bladders were harvested, stained, and imaged. Visual and quantitative analysis of the catheters showed all uropathogens colocalizing strongly with Fg deposits exhibiting preference for Fg (Figure 16A, B) and robust Fg deposition on catheters, validating previous studies on human catheters (Flores-Mireles *et al*., 2019; Flores-Mireles *et al*., 2014; Flores-Mireles *et al*., 2016a; Flores-Mireles *et al*., 2016b). Importantly, immunofluorescence (IF) analysis of bladder sections showed that all uropathogens interact with Fg on the bladder urothelium or in the lumen during CAUTI (Figure 16C). Although we show interaction between the pathogens and Fg, further studies are needed to characterize each pathogen–Fg interaction mechanism, as previously done with E. faecalis and S. aureus (Flores-Mireles *et al*., 2014; Flores-Mireles *et al*., 2016b; Walker *et al*., 2017).

2.3.2 Fg on urinary catheter material enhances microbial binding

Based on our in vivo findings, we assessed whether Fg could promote initial binding of the uropathogens to silicone catheters as previously seen for *E. faecalis* (Flores-Mireles *et al*., 2014). In addition to Fg, bovine serum albumin (BSA) was tested since serum albumin is one of the most abundant proteins on human and mouse urinary catheters (Molina *et al*., 2024). We compared uropathogen binding to Fg-, BSA-, and uncoated silicone, finding that Fg significantly enhanced the binding to the catheter for all uropathogens when compared with uncoated and BSA-coated silicone catheters (Figure 17). Interestingly, *P. aeruginosa* and *A. baumannii* binding to BSA-coated silicone was ~14% and ~10% higher than uncoated controls, respectively (Figure 17C, E),

alluding to a role for other host-secreted proteins during infection. However, these values were still significantly lower than the increase in binding observed on Fg-coated silicone (Figure 17C, E). Taken together, these data suggest that uropathogen interaction with host proteins deposited on silicone surfaces, particularly Fg, increases the ability of uropathogens to colonize urinary catheters.

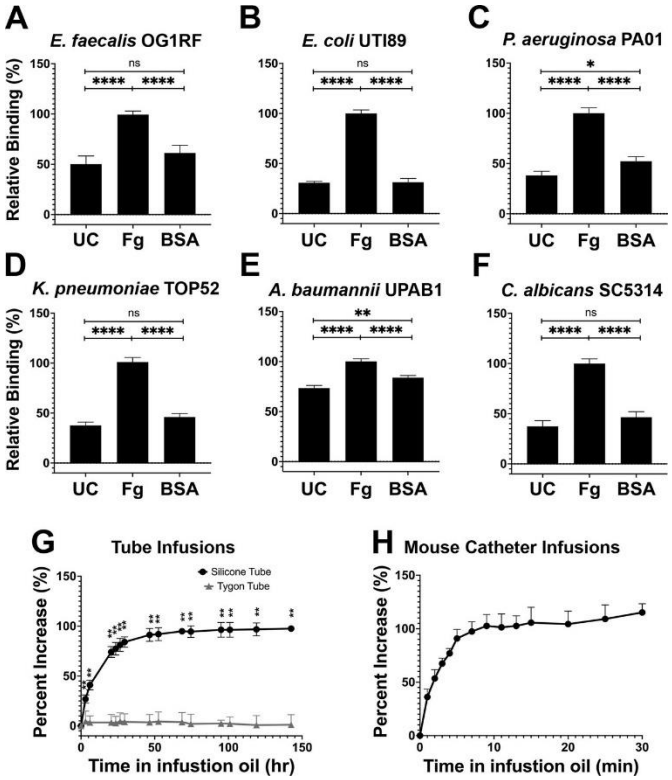

Figure 17. Silicone infusion and fibrinogen (Fg) enhancement of microbial surface binding.

(**A–F**) Uropathogens were tested for their ability to bind to protein coated and uncoated (UC) silicone catheters. For all graphs, error bars show the standard error of the mean (SEM). Between 3 and 5 replicates of $n = 4–12$ each were performed for each pathogen and condition. (**G**) Kinetics of silicone oil infusion on silicone and Tygon tubes, as well as (**H**) mouse silicone catheters. Differences between groups were tested for significance using the Mann-Whitney U test. *, $P < 0.05$; **, $P < 0.005$; and ****, $P < 0.0001$.

2.3.3 Characterization of liquid-infused catheters to prevent host-protein deposition

Based on the exploitative interaction of uropathogens with deposited Fg, we hypothesized that development of a material to prevent protein deposition would also reduce microbial colonization. Recent work with liquid-infused surfaces has demonstrated resistance to protein and bacterial fouling (Goudie *et al*., 2017; Howell *et al*., 2018; Leslie *et al*., 2014; Sotiri *et al*., 2018). This prompted us to develop a LIS material by modifying medical-grade silicone using inert trimethyl-terminated polydimethylsiloxane fluid (silicone oil) (Goudie *et al*., 2017). Infusion was completed by submerging silicone into

medical-grade silicone oil, the oil was then naturally taken up by the silicone tube creating a fully infused silicone tube with a slippery surface. Analysis of the oil's infusion rate showed a significant increase in silicone weight during the first 3 days of infusion then a gradual decrease in infusion until a plateau was reached after ~50 hr (Figure 17G). Plastic Tygon tubes (non-silicone) were used as negative controls (Figure 17G). Full infusion of mouse silicone catheters was achieved by 10 min of infusion (Figure 17H).

2.3.4 LIS modification reduces Fg deposition and microbial-binding in vitro

The ability of the LIS-catheters to reduce Fg deposition in vitro was tested for infused medical-grade silicone material and two commercially available urinary catheters, Dover and Bardex with UM versions of each used as controls. The UM- and LIS-catheters were incubated with Fg overnight and assessment of Fg deposition by IF. We found that Fg deposition was reduced in all LIS-catheters, showing ~90% decrease on Dover and ~100% on the Bardex and medical-grade silicone tubing when compared with the corresponding UM controls (Figure 18A, B).

Based on previous reports of the biofouling ability of liquid-infused surfaces and our LIS's success in reducing Fg deposition, we tested its ability to prevent microbial surface binding (Howell *et al*., 2018). Our six uropathogens were grown in urine supplemented with BSA at 37°C (Supplementary file 1), cultures were normalized in urine, added to UM control and LIS-catheters, incubated under static conditions and quantified via IF. Binding analysis by each of the uropathogens showed that all were able to bind in significantly higher densities to the UM-catheters than to the LIS-catheters (Figure 18C). These results further demonstrate the capability of silicone LIS-catheters to reduce not only protein deposition but to also impede microbial colonization.

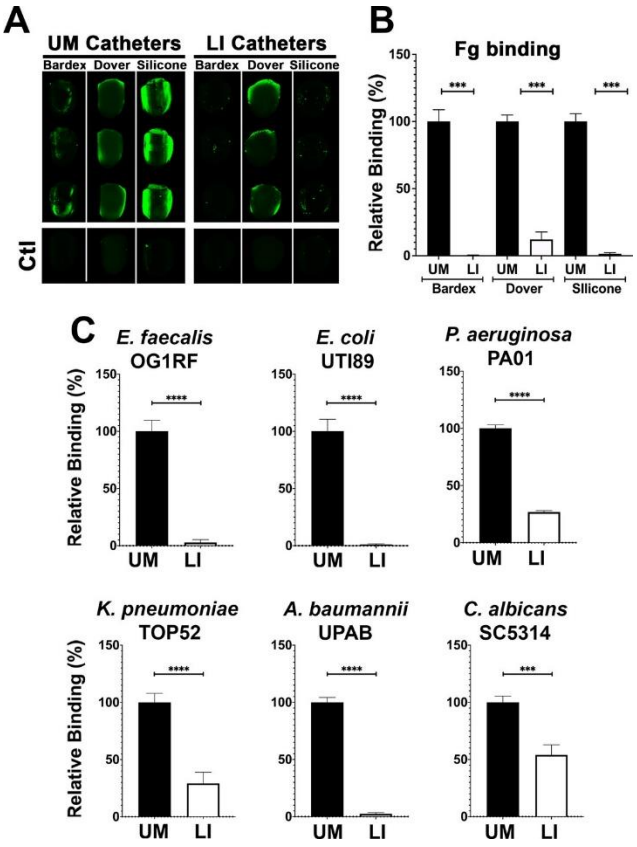

Figure 18. Liquid-infused silicone (LIS) modification reduces fibrinogen (Fg) deposition and microbial-binding in vitro.

(A) Visualization and (B) quantification of Fg (green) deposition on unmodified (UM)-catheter material (black bars) and LIS-catheter materials (white bars) by immunofluorescence (IF) staining. Three replicates with n = 2–3 each. (C) Microbial binding on UM and LIS. For all graphs, error bars show the standard error of the mean (SEM) and each condition had 3 replicates with n = 3 each. Differences between groups were tested for significance using the Mann-Whitney U test. ***, $P < 0.0005$; and ****, $P < 0.0001$*.

2.3.5 Fg deposition and microbial biofilms on catheters was reduced by LIS

Mice were catheterized with either an UM- or LIS-catheter and infected with one of six uropathogens for 24 hr. Bladders and catheters were harvested and assessed for microbial burden by CFU enumeration or fixed for

staining. Kidneys, spleens, and hearts were collected to determine microbial burden. We found that mice with LIS-catheters significantly reduced microbial colonization in the bladder and on catheters when compared with UM-catheterized mice regardless of the infecting uropathogen (Figure 19). Additionally, colonization was significantly lower in LIS-catheterized mouse kidneys for *P. aeruginosa*, *A. baumannii*, and *E. coli* infections (Figure 19C, E, G) and LIS-catheterized mice infected with *E. coli* or *C. albicans* showed significantly less colonization of the spleen (Figure 19G, K). *K. pneumoniae* kidney and spleen colonization difference was not statistically

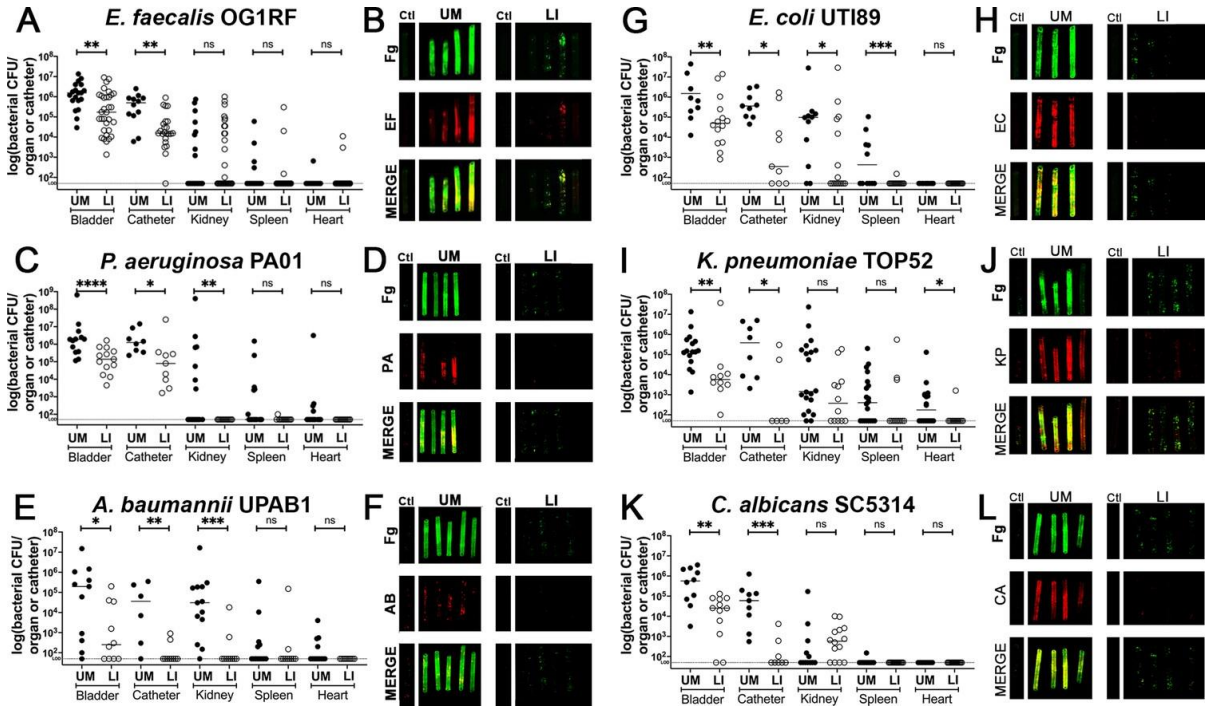

Figure 19. In vivo reduction of fibrinogen (Fg) deposition to restrict microbial burden.

Mice were catheterized and infected with one of six uropathogens. (A, C, E, G, I, K) Organ and catheter CFUs from mice with either an unmodified (UM)-catheter (closed circles) or liquid-infused silicone (LIS)-catheter (open circles) show the dissemination profile of the pathogen. (B, D, F, H,J,L) Imaging of catheters for Fg (green), respective uropathogen (red), and a merged image compare deposition on UM-catheters (left) with LIS-catheters (right); nonimplanted catheters as controls. Quantification of microbial colonization and colocalization on the catheters can be found in Figure 4—figure supplement 1. All animal studies for CFUs, catheter and bladder imaging had at least 10 animals per strain and catheter type. Differences between groups were tested for significance using the Mann-Whitney U test. *, $P < 0.05$; **, $P < 0.005$; ***, $P < 0.0005$; and ****, $P < 0.0001$.

significant, however they showed a trend of less colonization and there was significantly less colonization of the heart (Figure 19I). Furthermore, IF imaging and quantification of catheters confirmed decreased Fg deposition and microbial biofilms on LIS-catheters compared to UM (Figure 19B, D, F, H, J, I). These data demonstrate pathogens preferentially bind to Fg, and that the LIS modification successfully reduced Fg deposition (the microbes' binding platform), disrupts uropathogen biofilm formation on catheters, and colonization of the bladder *in vivo*. Importantly, hematoxylin and eosin (H&E) analysis shows the LI-catheter does not exacerbate bladder

inflammation regardless of the presence of infection or not (Figure 20A–G), an important factor to account for when developing a new medical device. In fact, for some pathogens, the LI-catheter results in less inflammation than bladders catheterized with an UM-catheter (Figure 20B, C, G). Furthermore, we examine Fg presence, uropathogen colonization, and neutrophil recruitment in UM- and LIS-catheterized and infected bladders by IF microscopy. This analysis revealed a reduction of microbial colonization as well as decreased neutrophil recruitment (Figure 20H–M).

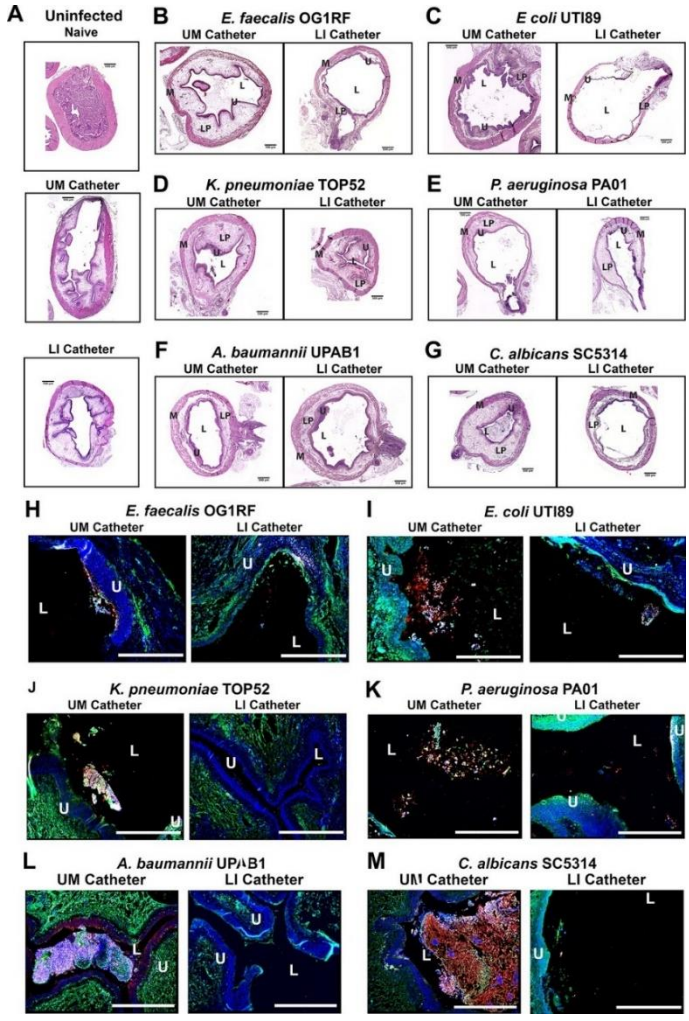

Figure 20. Liquid-infused silicone (LIS)-catheters reduce bladder colonization and inflammation.

Mice were catheterized and inoculated one of six strains. (A) Naive or bladders catheterized with an unmodified (UM)- or LIS-catheter were uninfected controls. (B–G) Bladder sections were stained with hematoxylin and eosin (H&E) to compare inflammation from UM-catheters (left) and LIS-catheters (right). (C–M) ×20 images of immunofluorescence (IF) stained bladders catheterized with an UM-catheter (left panels) or a LIS-catheter (right panels). Bladders stained for nuclei (blue), fibrinogen (Fg; green), respective uropathogens (red), and neutrophils (white). The urothelial/lumen boundaries are outlined in white dotted lines and labeled U (urothelium) and L (lumen) and all scale bars are 500 μm.

2.3.6 LIS modification reduces protein deposition on catheters in CAUTI mouse model of *E. faecalis*

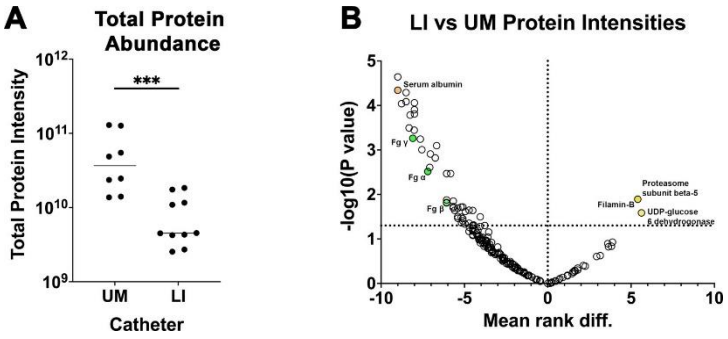

Figure 21. Liquid-infused silicone (LIS)-catheter reduces host-protein deposition in vivo.

A subset of unmodified (UM)- and LIS-catheters taken from mice 24 hpi with *E. faecalis* were assessed for protein deposition via mass spectrometry four UM-catheters and five LIS-catheters were used. (**A**) Intensities of the 95% most abundant proteins were summed in a total proteome approach and compared between the UM- and LIS-catheter groups. (**B**) A volcano plot for a subset of proteins. Negative mean rank difference indicates less protein on the LIS-catheter then on the UM-catheter and a significant difference is a −log10(p value) over 1.3. The fibrinogen (Fg) chains (α, β, and γ) are highlighted in green, serum albumin in orange, UDP-glucose 6-dehydrogenase, filamin-B, and proteasome subunit beta type-5 in yellow. Differences between groups were tested for significance using the Mann-Whitney U test. ***, $P < 0.0005$.

A quantitative-proteomics comparison was performed to identify proteins deposited on UM- and LIS-catheters retrieved 24 hpi with E. faecalis. Harvested catheters were prepared and protease digested with trypsin as in Zougman *et al*., 2014. nLC–MS/MS was performed in technical duplicate and label-free-proteomics (LFQ) processed as in Cox and Mann, 865 proteins were identified at a 1% False Discovery Rate (FDR) (Cox and Mann, 2008). Total abundance of protein was significantly reduced in LIS- vs UM-catheters (Figure 21A). Additionally, abundance of Fg and over 130 other proteins significantly decreased while only three proteins showed a significant increase (UDP-glucose 6-dehydrogenase, filamin-B, and proteasome subunit beta type-5) (Figure 21B). These data further demonstrate that the LIS modification not only reduced Fg deposition but also a wide variety of host proteins, which could play a role in microbial colonization and biofilm formation as demonstrated earlier with BSA (Figure 17).

2.4 Discussion

This is the first study to show a diverse set of uropathogens including gram-negative, gram-positive, and fungal species interact with Fg to more effectively bind to silicone urinary catheter surfaces. Furthermore, we found that by disrupting Fg deposition with LIS-catheters we reduced the ability of uropathogens to bind and colonize the catheter surface and bladder in an in vivo CAUTI mouse model. Moreover, LIS also reduced dissemination of *E. coli, P. aeruginosa*, and *A. baumannii* into the kidneys and other organs. Furthermore, LIS-catheters did not increase inflammation and for half of the pathogens inflammation was reduced. Finally, the deposition of other host-secreted proteins on LIS-catheters was around 6.5-fold less then UM-catheters. Together, these findings indicate that catheters made using LIS are a promising new antibiotic sparring approach for reducing or even preventing CAUTIs by interfering with protein deposition (Figure 22).

Pathogen–Fg interaction has been shown to be important for both *E. faecalis* and *S. aureus* during human and mouse CAUTI (Flores-Mireles *et al*., 2016b; Walker *et al*., 2017). Binding to Fg is critical for efficient bladder colonization and biofilm formation on the catheter via protein–protein interaction using EbpA and ClfB adhesins, respectively, and their disruption hinders colonization (Flores-Mireles *et al*., 2014; Walker *et al*., 2017). Gram-negative pathogens, *A. baumannii* and *P. mirabilis*, have shown colocalization with Fg during urinary catheterization (Gaston *et al*., 2020); however, the bacterial factors and any mode of interaction have not been described. While interaction of *E. coli* and *K. pneumoniae* with Fg during CAUTI has not been described previously, pathogenesis during urinary tract infection (UTI) (no catheterization) has been extensively studied. These studies show that type 1 pili, a chaperone–usher pathway (CUP) pili, allows them to colonize the bladder urothelium by binding to mannosylated receptors on the urothelial surface through the

tip adhesin FimH (Klein and Hultgren, 2020). Furthermore, other CUP pili including the P pili, important for pyelonephritis, and the Fml pilus, important for colonizing inflamed bladder urothelium, bind specifically to sugar residues Galα1–4Gal in glycolipids and Gal(β1–3)GalNAc in glycoproteins, respectively (Campoccia *et al*., 2013). Interestingly, Fg is highly glycosylated, containing a wide variety of sugar residues including mannose, N-acetyl glucosamine, fucose, galactose, and N-acetylneuraminic acid (Adamczyk *et al*., 2013). Therefore, the glycosylation in Fg may be recognized by CUP pili, allowing pathogens expressing CPU adhesins to become established and colonize the bladder. Furthermore, *A. baumannii* CUP1 and CUP2 pili are essential for CAUTI, this together with A. baumannii interactions with Fg *in vivo*, suggests that these pili may play a role in Fg interaction (Di Venanzio *et al*., 2019). Similarly, *P. aeruginosa* also encodes CUP pili, CupA, CupB, CupC, and CupD, which have shown to be important for biofilm formation (Mikkelsen *et al.,* 2013); however, their contribution during CAUTI has yet to be investigated.

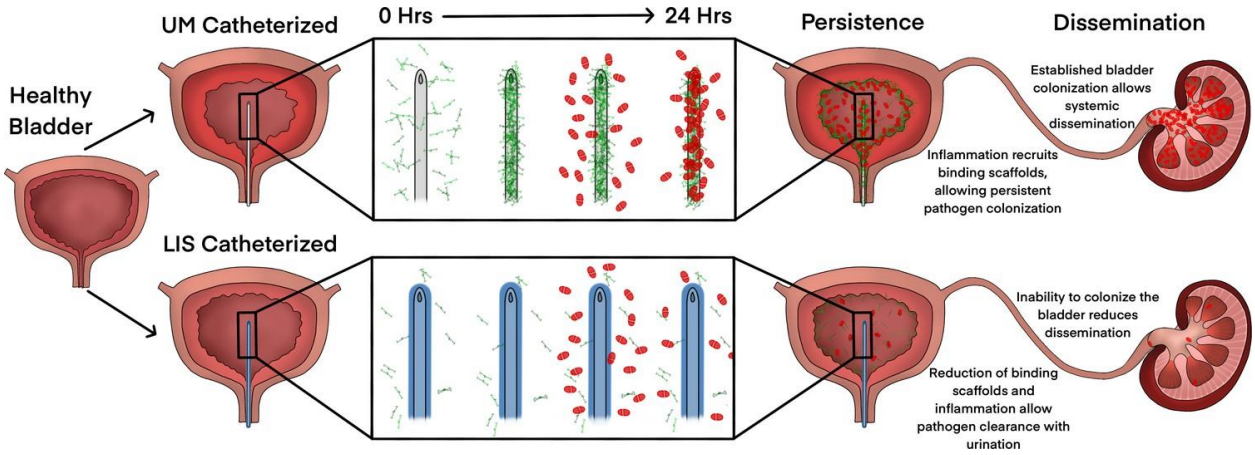

Figure 22. Liquid-infused silicone (LIS)-catheter reduces bladder inflammation, incidence of catheter-associated urinary tract infection (CAUTI), and dissemination.

Urinary catheter-induced inflammation promotes the release of fibrinogen (Fg) into the bladder to heal physical damage. Consequently, this Fg is deposited onto the catheter creating a scaffold for incoming pathogens to bind, establish infection, and promote systemic dissemination. However, catheterization with a LIS-catheter reduces Fg deposition onto its surface; thus, reducing the availability of a binding scaffolds for incoming pathogens. Consequently, overall bladder colonization and systemic dissemination are reduced making LIS-catheters a strong candidate for CAUTI prevention.

Furthermore, *C. albicans* has several adhesins, ALS1, ALS3, and ALS9, which have a conserved peptide-binding cavity shown to bind to Fg γ-chain (Hoyer and Cota, 2016).

Inhibition of initial uropathogen binding is crucial to reduce colonization and biofilm formation on urinary catheter surfaces and prevent subsequent CAUTI (Flores-Mireles *et al*., 2014; Flores-Mireles *et al*., 2016b). To prevent surface binding, a variety of modified surfaces impregnated with antimicrobial or bacteriostatic compounds have been generated and have proven to reduce microbial-binding in vitro but not in vivo (Andersen and Flores-Mireles, 2019; Singha *et al*., 2017). It is possible that in vitro studies do not efficiently mimic the complexities of the in vivo environment, for example; (1) Growth media: the majority of in vitro studies use laboratory rich or defined culture media, and it has been shown that laboratory media do not recapitulate the catheterized bladder environment that pathogens encounter (Colomer-Winter *et al*., 2019; Xu *et al*., 2017). Specifically, urine culture conditions have shown to activate different bacterial transcriptional profiles than when cultures are grown in defined media (Conover *et al*., 2016; Xu *et al*., 2017), which may affect microbial persistence and survival. (2) Host factors: host-secreted proteins are released into the bladder due to catheter-induced physical damage and subsequent inflammation. These proteins are deposited on the catheter surface and may hinder the release of antimicrobials or block interaction of antimicrobials with the pathogen if the antimicrobials are tethered to the surface. As has been observed with Fg deposition on human and mouse catheters, that host-protein deposition is not uniform, which may lead to antimicrobial release or pathogen–antimicrobial agent interaction at a subinhibitory concentrations (Di Venanzio *et al*., 2019; Flores-Mireles *et al*., 2014; Flores-Mireles *et al*., 2016a; Walker *et al*., 2017). Consequently, these interactions can contribute to the development of multidrug resistance among uropathogens (‘Antibiotic resistance threats in the Antibiotic resistance threats in the United States, 2019', 2019).

Based on the role of deposited host proteins in promoting microbial colonization and presence in human CAUTI (Flores-Mireles *et al*., 2016a; Flores-Mireles *et al.,* 2016b; Walker *et al.,* 2017), antifouling catheter coatings present a better approach to decreasing CAUTI prevalence rather than using biocidal or biostatic compounds, such as antibiotics, that promote resistance (Campoccia *et al.*, 2013; Singha *et al*., 2017). Antifouling coatings made from polymers have shown resistance to protein deposition (He *et al*., 2016); however, these coatings can become unstable over time and be difficult to produce requiring extensive wet chemistry (Singha *et al*., 2017). Most reports on the use of purely antifouling coatings to combat CAUTI have shown a successful reduction in bacterial colonization in vitro yet have not been successfully tested *in vivo* (Andersen and Flores-Mireles, 2019). This may be partly explained by the fact that many of the antifouling coatings are optimized to target bacterial adhesion, as it is understood that the first stage of biofilm development is bacterial attachment to a surface (Faustino *et al*., 2020). However, in a complex environment such as the *in vivo* bladder, the first change to the catheter surface is the adhesion of a complex set of host-generated proteins and biological molecules, generally referred to as a conditioning film, which can mask the surface (Faustino *et al*., 2020; Gaston *et al*., 2020; Scotland *et al*., 2020). Yet studies on catheter coatings to-date have rarely focused on the role of the host in infection establishment; namely, the host-secreted proteins. The data we present here suggest that this missing element may at least partly explain the differing results seen for most antifouling catheter treatments *in vitro* vs *in vivo*.

This study used clinically relevant silicone oil to create a simple to make LIS that was not only microbial resistant but also protein resistant, filling in the missing link between in vitro and in vivo work, the conditioning film. Interestingly, despite the increased weight, length, inner diameter, and outer diameter of the LIS mouse catheter by full silicone infusion, the LIS-catheters did not

exacerbated the inflammation response. This findings are consistent with previous *in vivo* work showing reduced fibrous capsule formation in implants coated with a liquid layer, suggesting that the use of a liquid surface may convey additional anti-inflammatory benefits (Chen *et al*., 2017).

Our mouse model of CAUTI has shown to faithfully recapitulate the pathophysiology of human CAUTI, showing urinary catheterization induces inflammation and contribution of Fg to biofilm formation on catheters recovered from humans suffering of CAUTI (Delnay *et al*., 1999; Flores-Mireles *et al.*, 2014; Flores-Mireles *et al*., 2016a; Flores-Mireles *et al*., 2016b; Glahn *et al*., 1988; Peychl and Zalud, 2008; Walker *et al*., 2017). This suggests that our findings have the potential to be translated for prevention and management of human CAUTI. However, for successful translation of this technology into humans, we need to further understand the effects of silicone oil on the immune response to infection as well as bladder tissue and better understand the impact the swelling of the material will have on manufacturing these catheters.

A deeper understanding of the pathogenesis of CAUTI is critical to moving beyond current developmental roadblocks and creating more efficient intervention strategies. Here, we have shown that that infusion of silicone with an immiscible liquid coating significantly decreases Fg deposition and microbial binding by using in vitro conditions that more thoroughly recapitulate the catheterized bladder environment. Importantly, our *in vitro* results were confirmed *in vivo* using our established mouse model of CAUTI. Our data showed that LIS-catheters are refractory to bacterial colonization without targeting microbial survival, which often leads to antimicrobial resistance. This study has found that protein deposition on urinary catheters is the Achilles heel of CAUTI pathogens, disrupting pathogen–Fg interaction represent a vulnerability that could be exploited. Thus, LIS-catheters hold tremendous potential for the development of lasting and

effective CAUTI treatments. These types of technologies are desperately needed to achieve better public health by decreasing healthcare-associated infections and promoting long-term wellness.

CHAPTER 3
LIQUID INFUSED SILICONE CATHETERS: FABRICATION AND CHARACTERIZATION

3.1 Introduction

Although liquid-infused silicone catheters have shown promise in repelling host proteins and bacterial adhesion *in vivo*, providing an alternative for combating CAUTI without the need for antibiotics (Andersen et al., 2023), transitioning to entirely new technologies can be challenging for patients requiring long-term catheter use. Fortunately, silicone oil infusion can be applied to commercially available silicone catheters, allowing patients to utilize pre-existing manufactured catheters without undergoing a significant transition process. This not only simplifies the adoption of the new technology but also maintains continuity of care for patients who rely on urinary catheters for their medical needs.

However, the infusion of pre-existing manufactured silicone catheters may lead to mechanical changes. The silicone material contains silicon-oxygen chain as the backbone, silicone oil consists of the same chemical units (Figure 23; Kashi *et al*., 2018). Previous research has indicated that laboratory-made silicone squares infused with silicone oil exhibit swelling, leading to infusion time-dependent increases in both mass and length of the silicone squares. (Sotiri *et al*., 2018). The extent of swelling in silicone was found to depend on both the viscosities of the silicone oil and the ratio of base to curing agents: silicone formulations with fewer crosslinking sites showed greater expansion and incorporation of silicone oil into the silicone matrix; lower viscosity silicone oil was found to be more readily incorporated into the silicone polymer. (Cai and Pham, 2022;

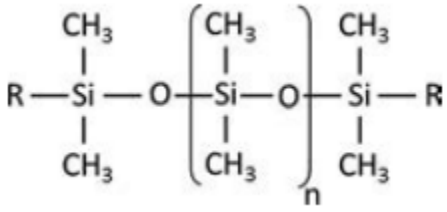

Figure 23. Chemical structure of silicone.

Silicone material chemical structure consisting of silicon-oxygen (siloxane) backbone (Figure from Kashi *et al*., 2018).

Sotiri *et al*., 2018). Moreover, research has demonstrated that infused silicone polymers can undergo a process called syneresis, in which unbound oligomers or silicone oil molecules slowly migrate to the surface of the material, re-forming a free liquid layer which is then available to be lost into the environment (Kolle et al., 2022; Lavielle et al., 2021; Wong et al., 2020). Oligomer here is defined as silicone polymers possessing identical chemical structure outlined in Figure 23. However, it is distinguished by its low molecular weight and comprises a smaller number of repeating siloxane units. However, this can be minimized by reducing the amount of free silicone oil in the system (Cai & Pham, 2022).

Understanding the fabrication of the material and characterizing the production process are crucial steps in ensuring the successful deployment of liquid-infused catheters in the market, this also offers an important tool for ongoing research and innovation in catheter technology. Due to the reported changes in material dimensions, it is important to analyze the impact of swelling on urinary catheters to ensure that the resulting material would remain suitable for use. This section demonstrates that liquid infusion can lead to significant changes in catheter length, outer and inner diameter, and that these changes can be controlled by adjusting the infusion duration. We hypothesized that by only partially infusing catheter samples, we could reduce the amount of free silicone oil that could be lost. We demonstrate in this section our success in reducing the amount of free liquid layer on liquid-infused catheters through mechanical removal, and by minimizing the infusion time of the material. These fabrication methods suggest potential future manufacturing techniques that could minimize the amount of silicone oil present in the material. Catheters infused using these techniques will also be utilized in subsequent sections for functionality testing.

3.2 Materials and Methods

The experimental protocol in this section involves characterizing the infusion of silicone catheter materials (Thermo Scientific, Silicone Tubing, 8060-0030) using various viscosities of silicone oil (Gelest, polydimethylsiloxane). All catheters used here were pre-cut into approximately 2-centimeter (cm) sections before the experiment, and the entire infusion process was conducted at room temperature.

3.2.1 Infusion Duration and Extent

The initial mass of catheters was measured using a digital analytical balance (Fisher Science Education, Analytical Balance, S72473) and recorded. Subsequently, the catheters were fully immersed in commercially available silicone oil with varying viscosities (3, 5, 10, 20, or 50 centistokes (cSt)) for the infusion process. At designated time intervals, catheters were removed from the oil using forceps and held vertically for 30 seconds (s) or until excess oil was drained off. Excess oil was then absorbed using a Kimwipe (Kimwipe, Kimberly-Clark Corp., USA), and the mass of the catheters was measured and recorded. Following this, the catheters were returned to the oil to continue the infusion process. This was repeated until the mass reached a plateau, indicating the complete infusion, where their mass was measured again. The quantity of silicone oil integrated into the catheters is determined by calculating the mass differences before and after the infusion process. To obtain volume of liquid per length of catheters, mass difference of the catheters between before and after infusion was divided by the measured catheter length. Non-silicone tubing (Saint-Gobain, Tygon tubing, E-3603; PVC-based tubing) was used as a control.

3.2.2 Length, inner and outer diameter measurements

The initial length, outer diameter, and inner diameter of the catheters were measured using a digital caliper (Fisher Scientific, Fisherbrand™ Traceable™ Digital Calipers, 14-648-17), and the values were recorded. The catheters were then infused and extracted from the oil as previously described in Section 3.2.1. The length, outer diameter, and inner diameter of the samples were measured and recorded. The samples were then returned to the oil to resume infusion. These steps were repeated until the catheters were fully infused (indicated by plateau in mass). For mouse catheters (SIL 025, RenaSil Silicone Rubber Tubing, Braintree Scientific, Inc, USA), a similar procedure was followed with a modification in the measurement process. Instead of using a digital caliper, photos of the mouse catheters were taken with a digital camera (EOS Rebel T5 Digital SLR Camera; Canon; USA). These images were then imported into ImageJ for parameter estimation due to the small size of mouse catheters.

3.2.3 Fabrication of Infused Catheters Without Free Liquid Layer

3.2.3.1 Physical Removal

The catheters were fully submerged in 20 cSt silicone oil, and any air bubbles in the catheter lumen were removed to ensure uniform infusion. Silicone oil of 20 cSt viscosity was chosen due to its use in recent *in vivo* CAUTI models (Andersen *et al*., 2022). The catheters were removed from the silicone oil after 5 days and excess liquid was allowed to flow out of the tube by holding the samples vertically for at least one minute or until all the excess liquid had dripped off the sample. These materials were then used as samples with intact liquid layer (LL); for the samples without intact liquid layer (ØLL), the catheters were gently blotted on both the exterior and interior surfaces using absorbent cellulose wipe (Kimwipe, Kimberly-Clark Corp., USA) to absorb the free liquid. Schematic representation of this fabrication method is shown in Figure 24.

3.2.3.2 Partial Infusion

The catheters underwent complete immersion in 20 cSt silicone oil and were removed at specified time intervals to achieve distinct infusion percentages. The mass of the catheters was measured both before and after infusion for the calculation of infusion percentage, as outlined in Section 3.1.2. Specifically, the catheters were removed from the silicone oil after 30 minutes, 6 hours and 30 minutes, 30 hours and 30 minutes, and beyond 5 days, respectively, resulting in catheters with varying infusion percentages. All infused samples were allowed to equilibrate for a minimum of 24 hours before undergoing additional testing. Schematic representation of this fabrication method is shown in Figure 24.

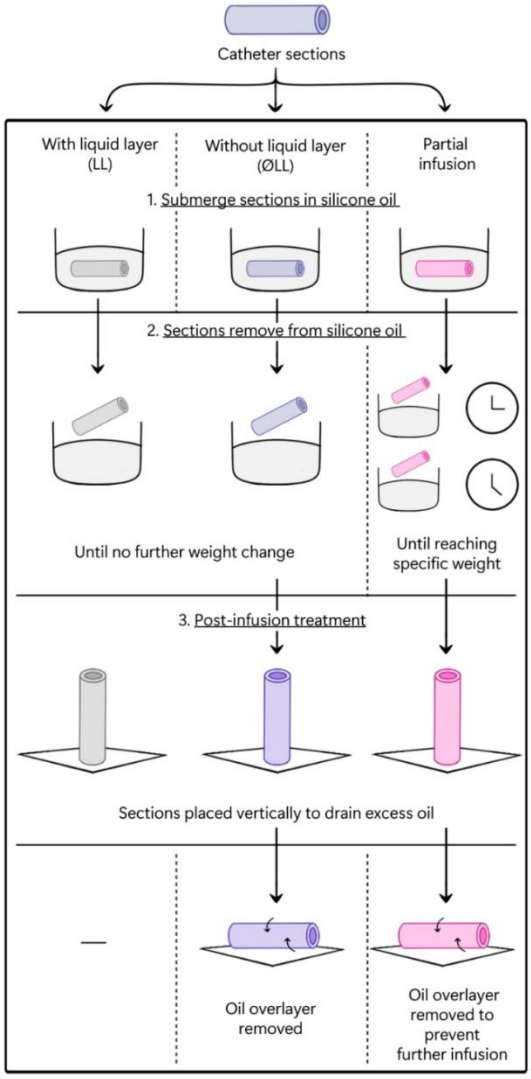

Figure 24. Infusion Methods to Fabricate Liquid-infused Catheters.

3.2.4 Confocal Imaging

Silicone squares crafted in the laboratory, along with dyed silicone oil, were employed for visualizing the liquid layer. The squares were used instead of silicone catheter material because silicone catheter material lacks fluorescent molecules, making it difficult to distinguish between solid and liquid silicone. To create fluorescent silicone squares, a mixture of 850 µg of BDP FL alkyne laser dye (D14B0, Lumiprobe, USA), 10 mL of dichloromethane, and 100g of silicone elastomer base (Dow SILGARDTM 184 Clear, Dow, USA) were combined in a planetary

centrifugal mixer (ARE-310, Thinky, USA) at 2000 rpm for 1 minute, followed by an additional mixing at 2200 rpm for 1 minute. The mixture was left in a desiccator overnight to remove any trapped gases. Next, 10 g of curing agent (Dow SILGARDTM 184 Clear, Dow, USA; in a 10:1 ratio) was added to the resulting solution, which was mixed again in the centrifugal mixer using the same settings. Aliquots of 0.9 mL were then transferred into the square depressions (2.0 cm x 2.0 cm x 0.5 cm) of a mold master and were degassed for 2 hours and cured overnight at 70ºC.

To prepare the dyed silicone liquid for infusion, approximately 9 mg of pyrromethene (05971, Pyrromethene 597-8C9, Exciton, USA) was added to every 100 mL of silicone liquid and thoroughly mixed. The solution was filtered through a 0.45 μm filter to remove any particulates. The silicone squares were fully submerged in the infusion liquid for over 5 days. LL samples were placed vertically to drain off excess liquid; ØLL samples were placed vertically to allow excess infusion solution to drain off then gently dabbed on a Kimwipe (Kimwipe, Kimberly-Clark Corp., USA). Finally, the samples were imaged using a Leica Stellaris confocal microscope equipped with a white light laser, using an HC PL APO CS2 20x/0.75 mm objective lens. False coloring was added to the image with Clip Studio Paint (Clip Studio Paint, Japan).

3.3 Results and Discussion

3.3.1 Infusion Duration and Extent

To understand the influence of infusing liquid viscosities on the infusion process on our silicone catheters, they were fully infused with varying

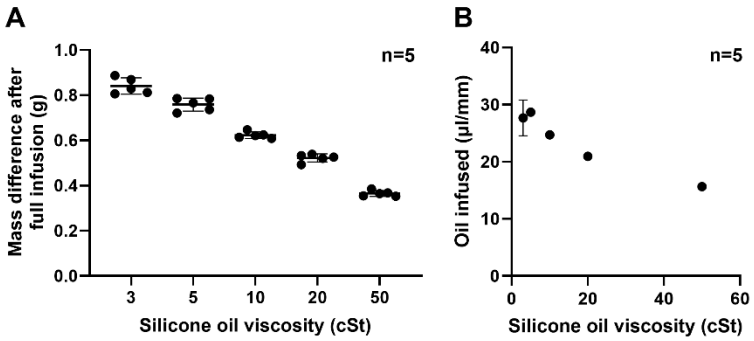

Figure 25. Silicone Oil Infused into the Catheter After Full Infusion.

(A) The mass difference between before and after infusion; **(B)** Amount of silicone oil infused into the catheters. In all graphs presented, the error bars represent the standard deviation.

viscosities of silicone oil. The viscosity of silicone oil is contingent upon the length of its polymer chains. Longer polymer chains, characterized by higher molecular weights, result in greater viscosity (Steel *et al*., 2021). As indicated in the manufacturer's datasheet (Gelest, Inc.), silicone oils exhibit a range of molecular weights corresponding to their viscosity levels. Specifically, the molecular weights for silicone oils with viscosities of 3 cSt, 5 cSt, 10 cSt, 20 cSt, and 50 cSt are reported as 550, 770, 1250, 2000, and 3780, respectively. The degree of polymerization varies accordingly, with values ranging from 3-7 for 3 cSt, 8 for 5 cSt, 15 for 10 cSt, 25 for 20 cSt, and 50 for 50 cSt viscosity of silicone oils (Mojsiewicz-Pieńkowska, 2012).

Upon complete infusion of catheters, the amount of oil incorporated into the material varied based on the viscosity of the silicone oil used for infusion, reflected by the mass gain after infusion (Figure 25A). Generally, a higher quantity of oil was infused when the infusing liquid had a lower viscosity, which aligned with previous literature (Sotiri *et al*., 2018). The specific amounts of oil infused into the catheters were 27.70 (±3.15) µL/mm, 28.68 (±0.68) µL/mm, 24.71 (±0.67) µL/mm, 20.96 (±0.47) µL/mm, and 15.64 (±0.14) µL/mm for viscosities of the infusing liquid at 3, 5, 10, 20, and 50 cSt, respectively (Figure 25B). This observation highlights the impact of viscosity on the infusion process, with lower viscosity oils demonstrating a higher capacity for incorporation into the catheters.

To investigate the influence of infusion duration on the extent of infusion, the mass change of silicone material over time during the infusion process was examined (Figure 26). The results

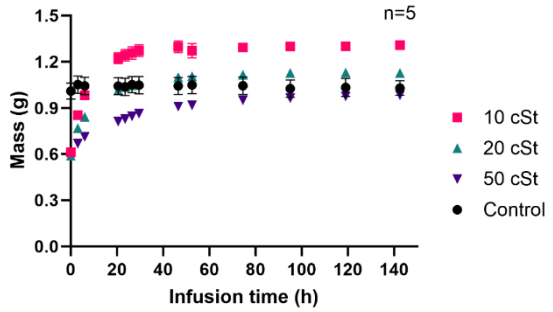

Figure 26. Catheter Mass Increase with Increasing Infusion Time.

Catheter mass infused with 10, 20 or 50 cSt of silicone oil is plotted against infusion time. Error bars represent the standard deviation.

indicated a consistent trend for all viscosities of silicone oil used in the infusion. There was a gradual increase in mass over time, indicating the uptake of silicone oil by the sample. This increase continued until reaching a plateau after approximately 100 hours of infusion. These data provide important insights into the duration of infusion required to achieve a specific percentage of material infusion for subsequent experiments.

The above results indicate that catheters infused with different viscosities of oil can incorporate varying amounts of oil when fully infused. Therefore, it is challenging to compare infusion extent between infused catheters based solely on mass difference. To address this, infusion percentages are standardized using the $Q\text{max}$ value, representing the maximum infusion ratio when the catheter is fully infused. It is calculated through the formula:

$$Q\text{max} = \frac{m_s}{m_d}$$

where m_s is the mass of fully infused catheter (measured at the last infusion time point); and m_d is the mass of non-infused catheter (Cai & Pham, 2022). The $Q\text{max}$ values for catheters infused with 3, 5, 10, 20, and 50 cSt silicone oil are ~2.56 ± 0.05, 2.39 ± 0.02, 2.17 ± 0.02, 1.95 ± 0.02, and 1.68 ± 0.01, respectively (Figure 27A).

With the $Q\text{max}$ values established, infusion percentages (I%) for catheters infused at different viscosities of infusing liquid or durations can be calculated once their degree of infusion (Q) is known.

The Q value can be calculated through the formula:

$$\text{Q} = \frac{m_i}{m_d}$$

where m_i is the mass after infusion; and m_d is the mass of non-infused catheter. The infusion percentage (I%) can then be calculated though the formula:

$$I\% = (\text{Q-1})/(\text{Qmax-1}) \times 100\%$$

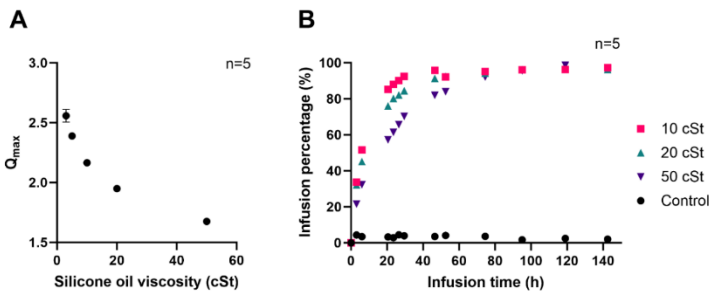

Figure 27. Development of Standardized Infusion Percentage.

(A) The Qmax value was experimentally determined through mass measurements taken after complete infusion. **(B)** Infusion percentages for catheters were calculated and plotted against infusion time. In all graphs presented, the error bars represent the standard deviation.

This approach yields infusion percentages ranging from 0–100%, despite the viscosities of infusing liquid used, facilitating straightforward comparisons between samples infused to different extents (Figure 27B). These data are crucial for subsequent characterization experiments as they provide information regarding the potential production time of infused catheter samples in a manufacturing process. For example, catheters infused to 50% of its maximum uptake (%I) requires approximately 6 hours of incubation when using 20 cSt silicone oil, but only around 5 hours with 50 cSt silicone oil.

The results obtained here align with previous literature, which indicate that infused materials typically undergo a progressive weight increase and swelling during the infusion process until reaching a state of saturation, commonly referred to as full infusion (Sotiri *et al*., 2016). Regardless, there is significance in independently characterizing the infusion process for our materials, as the size and shape of the infused material can necessitate varying infusion times and result in different degrees of swelling. For instance, we applied the same procedure to characterize mouse catheter materials for *in vivo* experiments, and the time required for complete infusion was found to be 30 minutes, contrasting with over 5 days for our catheters (Figure A1).

3.3.2 Physical Parameter Changes: Length, Inner and Outer Diameter

The infusion of liquid into catheters induces swelling, causing changes in physical parameters such as wall thickness and length. These alterations are critical in the context of catheter materials, where achieving an optimal fit with the patient's urethra is essential for enhancing comfort and minimizing friction during catheterization. As part of our study, we aimed to characterize these parameters, as it would be useful for the production process. This characterization serves as a foundation for technical transfer to industries, enabling the application of this innovative approach in the development and manufacturing of catheters.

To understand how liquid infusion alters the catheter's physical parameters, including length, inner diameter, and outer diameter, measurements were conducted throughout the infusion process. The results reveal significant differences in these parameters after complete infusion, depending on the viscosity of the silicone oil used. After full infusion, the length increases for catheters infused with 10, 20, and 50 cSt silicone oil was ~26%, ~25%, and ~17%, respectively. (Figure 28A*i*) The corresponding increases in inner diameter were ~33%, ~27%, and ~18% (Figure 28B*i*), and in outer diameter were ~35%, ~28%, and ~21% for the same viscosities of silicone oil (Figure 28C*i*).

Continuous measurements over time depicted a similar trend as observed in the mass change section, where length (Figure 28A*ii*), inner diameter (Figure 28B*ii*), and outer diameter (Figure 28C*ii*) increased gradually over time, eventually reaching a plateau. This trend indicates a progressive incorporation of infusing liquid, causing swelling and expansion of these parameters.

Furthermore, catheters infused with lower viscosities of oil demonstrated greater increases in these parameters, aligning with the observation that lower viscosity oils allow for higher amounts of silicone oil incorporation during infusion (Cai and Pham, 2022).

As of now, no specific models have been published for estimating forces resulting from 3D polymer network swelling (Metze et al., 2023). 3D polymer network swelling is defined as scenarios where the polymer network can freely swell from all directions, as observed in our liquid-infused catheters. This stands in contrast to situations where the polymer is attached to a solid surface and swells under physical constraints. However, the changes observed in the

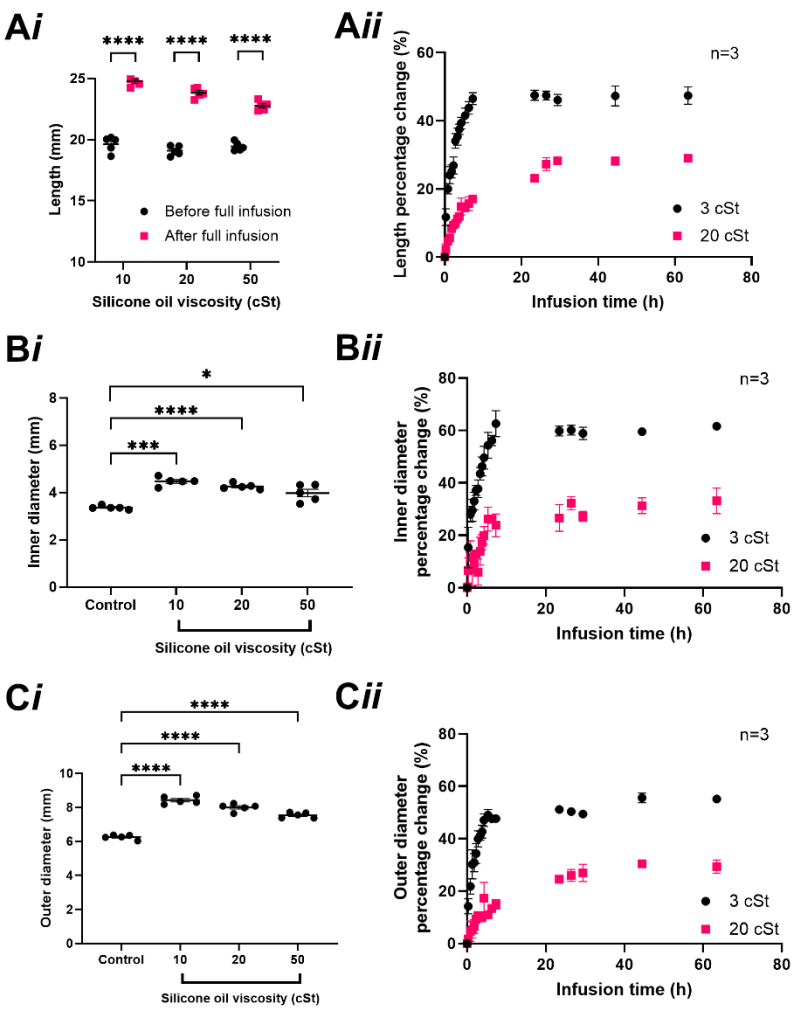

Figure 28. Parameter Changes of Catheters After Infusion.

The **(A)** length; **(B)** inner diameter; and **(C)** outer diameter change of catheters was measured under two conditions: ***(i)*** after complete infusion and ***(ii)*** during infusion in silicone oil. Statistical significance between the groups was assessed using ANOVA. * = P <0.05; *** = P ≤ 0.001; **** = P < 0.0001. In all graphs presented, the error bars represent the standard deviation.

properties of our catheters upon silicone oil infusion align with some of our current understanding of polymer material swelling:

According to the Flory-Rehner theory, polymer swelling induced by solvent uptake can be seen as a balance between the disorder (entropy) of polymer chains (where swelling is promoted) and the energy changes associated with the interaction between the polymer chains and the solvent (enthalpy; where swelling is prevented) (Flory, 1950; Flory and Rehner, 1943). In our case, the enthalpy change might not be substantial as silicone oil and silicone have closely matched chemical compositions (Sotiri *et al*., 2018). The observed differences in swelling when the catheters were infused with various viscosities of silicone oil likely stem from entropy. Higher viscosities of silicone oil correspond to higher molecular weights, resulting in fewer molecules per volume (Steel *et al*., 2021). Consequently, this reduction in molecular density diminishes the entropic driving force for swelling. This may explain why a lower amount of higher viscosity silicone oil was infused into the silicone catheter as observed in Figure 26. As the polymer chains elongate during their interaction with the infusing liquid, an elastic retractive force may arise within the polymer network, counteracting the continuous swelling (Toomey *et al*., 2003). The increase in swelling at the beginning of the infusion process gradually decreases the entropy as the polymer chains stretch with the incorporation of silicone oil, while simultaneously increasing the elastic retractive force. This process continues until both forces reach equilibrium, where no further infusing liquid enters the polymer matrix, reflected by the plateauing of mass (Figure 26; Sotiri *et al*., 2018).

Gedde et al. (1996) utilized Fick's second law of diffusion to describe the diffusivity of silicone liquids in silicone rubbers. They found that the rate of penetrant liquid into the polymer decreases with increasing molar mass, coinciding with our data showing that catheters incorporated higher

amounts of silicone oil into the polymer matrix when infused with decreasing viscosities of silicone oil (Figure 26). Additionally, the increase in length and diameter in response to the increasing oil content was more prominent with lower viscosity infusion (Figure 28A*ii*, 28B*ii* and 28 C*ii*).

Sotiri *et al.* (2018) demonstrated that the swelling of silicone material in silicone oil can also be described by poroelasticity theory and Darcy's law. They found that the diffusivity of the infusing liquid is linearly proportional to permeability, with higher cross-link density leading to lower permeability and a reduced rate of diffusion (Sotiri *et al*., 2018). Future research endeavors could involve measuring the crosslink density of proprietary catheter materials and further evaluating and modeling the infusion phenomenon in these commercially available catheters.

In clinical practice, literature suggests that both reduced catheter length and increased outer diameter exhibits faster drainage time, while catheter sizes exceeding 18 Fr (equivalent to 0.236 inches in outer diameter) do not significantly enhance drainage (Lee et al., 2017). In our infused catheters, dimensions such as length, inner, and outer diameter increase in a time-dependent manner during infusion. With complete infusion, all three parameters experience a roughly 20-30% increase. While the diameter increase may increase urine flow, further testing is necessary to confirm this effect. Commercially available urinary catheters come in various lengths and diameters, the initial catheter should be shorter in length and smaller in diameter to accommodate the anticipated swelling-induced changes adequately. As appropriate sizes can minimize friction with urinary tissue and enhance comfort in patients (Bagley & Severud, 2021), this will be an important consideration for the manufacturing of liquid infused catheters.

3.3.3 Removal of Free Liquid Layer

As mentioned in Section 1.3, the removal of infused liquid, specifically silicone oil in our context, into the host system raises health considerations (Melo *et a*l., 2021; Cheng *et al*., 2020; Krayukhina *et al*., 2019; Chisholm *et al*., 2015). We have therefore devised two methods to fabricate liquid infused catheters with minimal or no free liquid layer: (1) physical removal: fully infused catheters were wiped with cellulosic wipe; and (2) partial Infusion: catheters were not fully infused but were removed from infusing liquid at designated time points.

To better understand the role of the free liquid layer in a protein and bacterial adhesion system, we fabricated infused catheter samples by immersing them in 20 cSt silicone oil until complete saturation was achieved, indicated by a plateau in weight gain (Andersen *et al*., 2022; Sotiri *et al*., 2018). Silicone oil with a viscosity of 20 cSt was chosen because it has been documented to effectively repel protein and pathogens *in vivo* (Andersen *et al*., 2022). The catheters were then removed from the silicone oil and all excess oil was allowed to drain from the surface; these samples were considered to have an intact free liquid layer (LL). A subset of catheters was then subjected to removal of the free liquid layer (ØLL) via absorption of the liquid from both interior and exterior surfaces by light contact with a cellulosic wipe (Figure 29A). Unlike previous reports where the free liquid layer was removed via rinsing with water (Cai & Pham, 2022; Lavielle *et al*., 2021; Wong *et al*., 2020; Scherer, 1989), this physical removal treatment was intended to deplete the surface layer to the point where it would not substantially increase via syneresis, defined as free silicone liquid molecules migrating to the surface of the material, over the duration of the

experiments (< 48 hours), as has been recently reported to occur in infused silicones (Lavielle *et al*., 2021; Scherer, 1989). The results of removing the free liquid layer from the surface were visualized using confocal microscopy with different fluorescent dyes for the solid silicone and liquid silicone (Figure 29B) (Cai *et al*., 2021; Kovalenko *et al*., 2017).

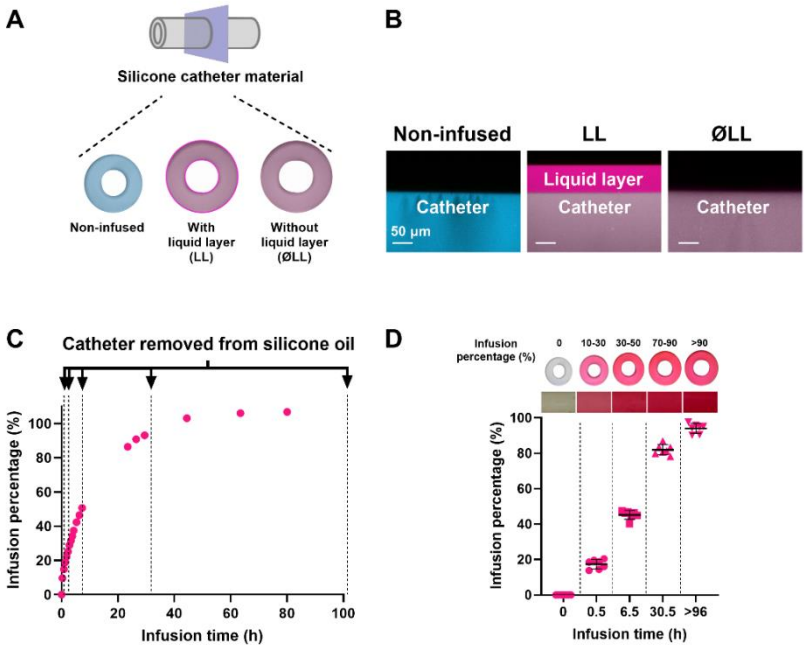

Figure 29. Fabrication of Catheter Samples With and Without Liquid Layer.

(A) Schematic of catheters fabricated with or without a liquid layer (LL; ØLL). **(B)** Confocal image analysis was performed on (from left to right) a non-infused catheter, a catheter with a liquid layer, and a catheter without a liquid layer. **(C)** Various levels of infusion percentage versus infusion time. The arrows denote the timepoint when the catheters were removed from the infusing silicone oil. **(D)** (Top) Images of catheter cross sections in which the infusing silicone oil was dyed for visualization of the distribution throughout the material. Close-up images of the color are shown in boxes underneath.

The images of LL samples showed a layer ~60 µm in thickness, in agreement with previous reports on similar systems (Kovalenko *et al*., 2017). In contrast, ØLL samples showed a marked reduction of the free liquid layer to a value below what could be observed using this technique (≤500nm), confirming the successful removal of nearly all, if not all, the free liquid at the catheter surface.

In our system, partial infusion was achieved by removing the catheter samples at defined points during the infusion process, as shown in Figure 29C, followed by absorbing excess liquid from the surface to prevent further infusion. The result was a series of well-defined groups of samples with

increasingly less free liquid distributed throughout the matrix (Figure 29D). In particular, samples infused for 0.5 hours exhibited a 17.4±0.99 infusion percentage, those infused for 6.5 hours achieved a 45.25±0.94 infusion percentage, and samples infused for 30.5 hours reached an 81.98±1.08 infusion percentage. Samples were considered as fully infused if they were removed from the silicone oil after more than 5 days and exhibited an infusion percentage exceeding 90.0%.

Our approaches outlined here present a replicable method for infusing catheter samples with varying degrees of silicone oil incorporated into the catheter, as well as creating catheter surfaces with or without a liquid overlayer. Previous literature has indicated that in silicone oil-infused silicone materials, lower degrees of infusion can prevent oil leaching behavior, with the silicone oil remaining within the polymer matrix due to a strong affinity between the polymer and the silicone oil (Cai and Pham, 2022; Cai *et al*., 2021). This suggests that catheter materials with lower infusion levels might effectively prevent silicone oil leaching from the polymer matrix into the bladder, thereby increasing safety levels.

As a potential material for catheter use, it is important to understand the properties of the material before practical application. For urinary catheters, the material should not be too stiff, as increased stiffness can lead to urethral injury, nor too soft, as it must maintain mechanical integrity to prevent device breakage (Hendlin *et al*., 2009). It was found that the shear modulus, which indicates the material's rigidity, decreases with increasing infusion: the higher the infusion level, the lower the material's rigidity (Cai and Pham, 2022). This suggests that increased levels of liquid infusion percentage in catheters would result in lower stiffness levels, potentially increasing the comfort of catheter insertion. In three brands of commercially available catheters, it was found in the literature that the coefficient of friction varies from 0.45 to 0.62, while tensile strength varies from 6.6 to 8.0 mPa (Ramesh *et al*., 2001). A lower coefficient of friction is desired as it aids in the

catheterization process and reduces the potential for injury and pain to patients, while higher flexural strength is preferred as it indicates greater mechanical stability. These are factors that have not been tested in this dissertation and will require future exploration to understand how these infusion treatments affect these properties and ensure suitability for real-life application.

3.4 Summary

The presented results highlight the development of our liquid infused catheter as a tool for subsequent experiments. The fabricated catheters were characterized by their physical properties, with higher amounts of silicone oil infused into catheters when lower viscosities of infusing silicone oil were used. This is evident in increased mass, longer length, and larger inner and outer diameters, and vice versa. Crucially, the establishment of standardization through infusion percentage proved valuable for achieving specific material infusion percentages in later experiments. This standardization method is not limited to our infused catheter samples and can be applied to other infusion materials. Additionally, catheters with the removal of free liquid layers were generated through physical removal or partial infusion. The method of physical removal was validated through confocal imaging, which confirmed the effective removal of nearly all, if not all, free liquid from the catheter surface. The method of partial infusion limits the presence of silicone oil in the system, and thereby reduces excess oil migrating to the catheter surface. The creation of these catheter samples allows us to test infused catheters without a free liquid layer for functionality in subsequent experimental sections. Overall, the swelling observed in silicone oil-infused catheters and the resulting length and diameter changes align with existing theories of polymer swelling. Additional mechanical tests, such as flexural strength and friction, are still necessary for these materials. This dissertation will provide an analysis of functionality, as

documented in Chapter 4. This aspect is crucial for understanding the performance of urinary catheters and is an essential consideration in their development and application.

3.5 Acknowledgement

Section 3.3.3 is based on work previously published in medRxiv, doi: 10.1101/2023.09.14.23295548; authors: **ChunKi Fong**, Marissa Jeme Andersen, Emma Kunesh, Evan Leonard, Donovan Durand, Rachel Coombs, Ana Lidia Flores-Mireles, Caitlin Howell.

CHAPTER 4
FUNCTIONALITY OF INFUSED CATHETERS

4.1 Introduction

It is most likely that liquid-infused urinary catheters *in vivo* are frequently subjected to conditions which can disrupt and/or remove any free liquid layer present on the catheter surface. The potential for loss of the free liquid layer from liquid-infused system is well documented (Dutta et al., 2022; Johnson *et al.,* 2006; Rother *et al.,* 1996). Under water, silicone oil infused silicone surface can maintain a low sliding angle under both turbulent flow and laminar flow conditions for a little over an hour before experiencing a significant loss of the free liquid layer (Gadalla *et al*., 2019). However, it is also documented that when a surface with a free liquid layer is exposed to an air/water interface, the amount of liquid lost undergoes a substantial increase of 1–2 orders of magnitude, compared to being placed directly in water under flow (Rother *et al.,* 1996). In addition, it is understood that physical contact of a solid with a free liquid layer can also easily result in layer disruption and removal (National Healthcare Safety Network, 2024). Catheter insertion, which involves the catheter rubbing against urinary tissue, and urine drainage, which exposes the catheter to the air/water interface during the catheterization period, are likely to disrupt or remove the free liquid layer on the infused catheter surface. Yet recent *in vivo* results demonstrate that infused catheters remain highly effective at resisting surface adhesion (Andersen *et al*.,2023), despite the fact that they are unlikely to have a uniform liquid layer at the surface. It is therefore possible that infused catheters may not require full infusion to still provide antifouling functionality.

To gain further insight into the functionality criteria for infused catheters, we developed catheters without a liquid layer on the surface and partially infused catheters (as detailed in Chapter 3) for functionality testing. To provide insights into whether the infused catheters retain hydrophobic

characteristics or fluid repellency after the removal of surface liquid layer, partial infusion, or infusion with different viscosities, we conducted a preliminary slippery surface assessment using a sliding angle test and droplet speed test, as described in Regan *et al*., 2019. To further ensure their ability to prevent foulant adhesion, we also conducted tests on infused catheters with low amount or no free liquid layer against whey proteins and Fb adhesion. Whey proteins contain a mixture of proteins, including immunoglobulins and bovine serum albumin, creating a complex environment that can lead to fouling on material surface (Liu *et al.,* 2022; Madureira *et al*., 2007). The significance of testing Fb lies in its role as a docking site for pathogen adhesion. Within 1-2 hours of catheterization, Fb tends to coat the entire catheter surface (Flores-Mireles *et al*., 2017). Therefore, if our liquid-infused catheter can repel Fb adhesion, it suggests a high likelihood of lower bacteria adhesion levels via reducing their docking site, as supported by existing literature (Andersen *et al.,* 2023; Flores-Mireles *et al*., 2017, 2014). To confirm and investigate whether the infused catheters can repel bacterial adhesion, we conducted immunolabelling tests for *E. faecalis* adhesion, which is one of the most prevalent pathogens found in CAUTIs.

Through sliding angle and droplet speed tests, we observed an inverse relationship between infusion percentages and the slipperiness of materials. Specifically, higher infusion percentages correlated with surfaces being more slippery, potentially indicating higher antifouling capability. This finding is further supported by the results showing that increased infusion percentages led to decreased adhesion levels of whey protein, Fb, and E. faecalis. These results suggest that not only can the adhesion levels of foulants be tuned, but full infusion may not be necessary for antifouling function.

4.2 Materials and Methods

4.2.1 Slippery Surface Characterization

Catheter samples underwent infusion for more than 5 days to ensure complete infusion (Figure 26). For details regarding samples with the free liquid layer removed or partially infused, please refer to Section 3.3.1. All samples, regardless of infusion status, were standardized to a length of 2 cm.

4.2.1.1 Sliding Angle Test

Sections of catheters were placed on a tilt stage at 0°. A digital angle gauge (AccuMASTER 2 in 1 Magnetic Digital Level and Angle Finder, Calculated Industries) was affixed to the tilt stage to measure changes in the angle. Using a pipette, a 20µl crystal violet dye or water droplet was deposited into the catheter's lumen. Immediately after the droplet was deposited, the tilt stage was gradually inclined until the droplet began to move out of the tubing. The minimum angle at which the droplet began to move was recorded.

4.2.1.2 Droplet Speed Test

Sections of the catheters were placed on a tilt stage at 30°. A digital camera (EOS Rebel T5 Digital SLR Camera; Canon; USA) was used to record the sliding of a 20µl water droplet down the lumen. A frame-by-frame analysis was then used to determine the time the droplet took to travel from one end to the other.

4.2.2 Protein Adhesion Characterization

4.2.2.1 Whey Protein Incubation and Analysis

The catheters were infused with various percentages as described in Sections 3.3.1, they were then submerged in whey protein solution (21.5g in 100 ml deionized water) or deionized water (used

as a negative control) for 30 minutes at room temperature. The catheters were then gently rinsed with deionized water to remove unattached protein. Subsequently, they were immersed in a 0.01% crystal violet solution for 10 minutes at room temperature. Post-staining with crystal violet, the catheters were rinsed with deionized water to remove excess crystal violet solution. The resulting samples were then placed on a lightbox to ensure consistent lighting for each photograph. Photos were captured with a digital camera (EOS Rebel T5 Digital SLR Camera; Canon; USA). For analysis, the photos were processed using ImageJ software. In addition, areas stained by crystal violet were manually selected through the color threshold function. This function allows the software to count the number of pixels stained purple, providing a quantitative measure of crystal violet presence on the catheters. The area coverage percentage was determined by dividing the number of purplish pixels by the total pixel count and multiplying the result by 100%.

Following staining, catheter samples were immersed in 3 mL of 70% ethanol for 30 minutes. After vortexing to ensure dissolution of all crystal violet stains on the catheters, the resulting solution was analyzed using a ultra-violet spectrophotometer (Thermo Scientific™ BioMate™ 160 UV-Vis Spectrophotometer; Thermo Fisher; USA) to measure peak absorbance at 590 nm (Ghanadan *et al*., 2019).

4.2.2.2 Fb Incubation and Immunolabelling

The catheters were infused with various percentages or fully infused with physical removal of liquid overlayer as described in Sections 3.3.1. Adhesion testing with human Fb free from plasminogen and von Willebrand factor (Enzyme Research Laboratory #FB3) were conducted using previously published methods (Andersen *et al*., 2022). Briefly, after overnight incubation with Fb in PBS (150μg/mL), the catheters were fixed using 10% neutralized formalin, followed by blocking with PBS with 1.5% bovine serum albumin (BSA). Goat anti-Fg primary antibody

(Sigma) was used in 4ºC overnight staining at a dilution of 1:1000, followed by Donkey anti-Goat IRD800 antibody (Invitrogen; 1:5000) staining at room temperature for 2 hours. The antibodies were diluted with PBS with 0.05% Tween-20 and 0.1% BSA. The images were visualized uwing Odyssey Imaging System (LICOR Biosciences), the fluorescent signals were then analyzed using Image Studio^{TM} software.

4.2.3 Bacteria Adhesion Characterization

Adhesion testing with *E. faecalis* (ATCC 47077) was conducted using previously described methods (Andersen *et al*., 2022). Human urine was collected from 2 female donors between 20 and 40 years of age. The urine was first sterilized with 0.22 μm filter, the pH level of the urine was then adjusted to 6.0 to 6.5 before use. *E. faecalis* were then inoculated and cultured in human urine supplemented with 20 mg/mL BSA overnight at 37ºC. The *E.faecalis* was separated from the urine with centrifugation, then resuspended with sterile PBS. The OD_{600} of the resulting media is adjusted to ~0.5. The catheters sections were then immersed in *E. faecalis* for 2 hours under room temperature. They were then fixed using 10% neutralized formalin, followed by blocking and staining steps. Anti-strep group D rabbit primary antibody (1:1000) was used followed by Donkey anti-Rabbit IRD680 antibody (Invitrogen; 1:5000). The dilution and analyzation method are the same as described in Section 4.2.2.2.

4.3 Results and Discussion

4.3.1 Slippery Surface Characterization of Fully Infused Catheters

To validate that our fully infused catheters exhibit similar antifouling properties as reported in the literature, where a slippery surface effectively repels droplets, we conducted a sliding angle test using crystal violet as a droplet foulant for better visualization (Fang *et al*., 2021; Geraldi *et al*.,

2019; Chen *et al.*, 2017; MacCallum *et al.*, 2015). In the sliding angle test, we measured the critical angle at which a droplet initiates sliding down the sample (Figure 30A*i*). It has been reported that the sliding angle serves as an indicator of the surface's fluid repellency and, consequently, its ability to resist adhesion (Fang *et al.*, 2021; Geraldi *et al.*, 2019; Chen *et al.*, 2017; MacCallum *et al.*, 2015).

The results indicate that non infused catheters have a sliding angle of approximately 53.6 (±1.6) º, while catheters infused with 10, 20, or 50 cSt silicone oil exhibit significantly lower sliding angles of 1.4 (±0.4) º, 1.0 (±0.4) º, and 1.5 (±0.1) º, respectively (Figure 30A*ii*). Additionally, we measured the droplet speed, representing the time taken for a droplet to traverse the length of the catheter (Figure 30B*i*). For non-infused catheters, only one sample was able to complete the course with a time of ~9.4 s, while the remaining samples experienced droplet entrapment within the lumen. In

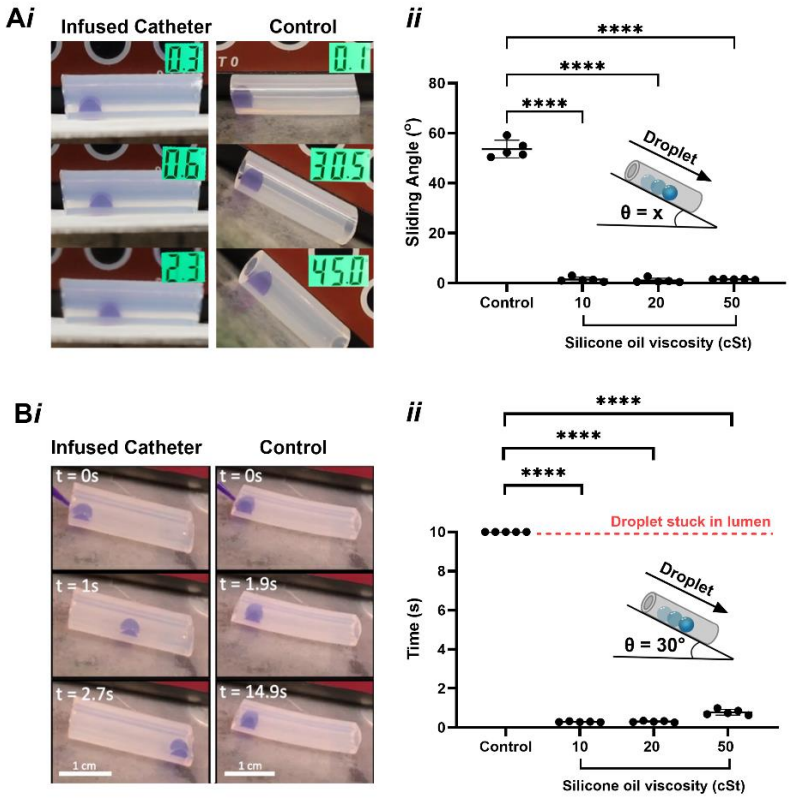

Figure 30. Sliding Angle and Droplet Speed Test on Fully Infused Catheters.

Representative images of **(A*i*)** sliding angle test on 20 cSt silicone oil infused catheters, where the numbers on the right upper corner indicated the angle; and **(B*i*)** droplet speed test on 20 cSt silicone oil infused catheters, where t denotes time in seconds. **(A*ii*)** Results of sliding angle test. **(B*ii*)** Results of droplet speed test. In all graphs presented, the error bars represent the standard error of the mean. Statistical significance between the groups was assessed using ANOVA, **** = P < 0.0001. In all graphs presented, the error bars represent the standard deviation.

contrast, for catheters infused with 10, 20, or 50 cSt silicone oil, the respective times were 0.3 (±0.009) s, 0.3 (±0.02) s, and 0.78 (±0.06) s (Figure 30B*ii*).

Consistent with previously published studies, it is generally expected that samples with low sliding angles and high sliding rates would result in the most effective antifouling surfaces (Kovalenko *et al*., 2017; Sotiri *et al*., 2016; Sunny *et al*., 2014). The combined results from both tests suggest that liquid infusion on catheter material creates a slippery surface indicative of antifouling properties, providing preliminary data for our next stage of testing.

4.3.2 Slippery Surface Characterization of Catheters with Lower Liquid Content

As outlined in Section 3.3.3, the removal or reduction of the free liquid overlayer on catheters can be achieved through physical removal or partial infusion. To assess the impact of such removal or reduction on functionality, we conducted investigations using the sliding angle and droplet speed tests. In this set of experiments, water droplets were employed to ensure that the results were not influenced by electric charge of the droplet, as crystal violet is a positively charged dye. We observed no difference in sliding angle between the LL and ØLL samples (Figure 31A, $P > 0.9999$). Measurements of the droplet sliding velocity, which provide an indication of surface uniformity (Regan *et al.,* 2019), yielded comparable results (Figure 31B). Similar results can also be achieved when charged liquids such as crystal violet (positively charged) and bromophenol blue (negatively charged) dye were used as foulant droplets (Figure A2A*i* and Figure A2B*i*).

Similarly, this is also tested in partially infused catheters with 20 cSt silicone oil. The results of the sliding angle test (Figure 32A) showed that as the infusion percentage increases, (i.e. a higher amount of free silicone liquid is present in the system), the sliding angle gradually decreases. Samples at 30–50% infusion already showed a significant difference in sliding angle compared to non-infused controls ($P = 0.03$). Although samples 70–90% of infusion showed somewhat higher values than fully infused samples (24.71±2.54 compared to 8.41±1.20, respectively), the difference was found to be non-significant ($P > 0.9999$). In the droplet speed test, a similar outcome was observed (Figure 32B). This observed trend, where an increase in infusion percentage results in a more slippery surface, is consistent across various conditions. This includes scenarios where different viscosities of silicone oil were used for infusion (Figure A3), as well as when charged liquids were employed as foulant droplets (Figure A2A*ii* and Figure A2B*ii*).

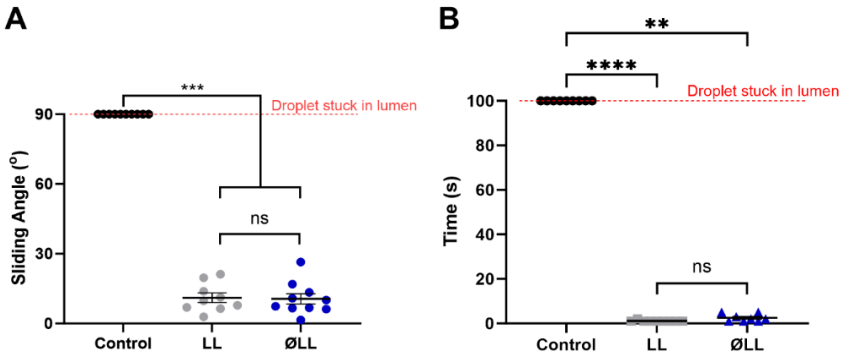

Figure 31. Sliding Angle and Droplet Speed Tests on Catheters Infused with Free Liquid Layer Removed.

(A) Sliding angle test of non-infused catheters, and catheters with (LL) or without liquid layer (ØLL). **(B)** Droplet Speed test results for LL and ØLL catheters. In all graphs presented, the error bars represent the standard error of the mean. Statistical significance between the groups was evaluated using ANOVA test. **= $P < 0.05$; *** = $P < 0.0005$; **** = $P < 0.0001$ and ns = not significant.

4.3.3 Protein Adhesion Characterization

4.3.3.1 Whey Protein Adhesion

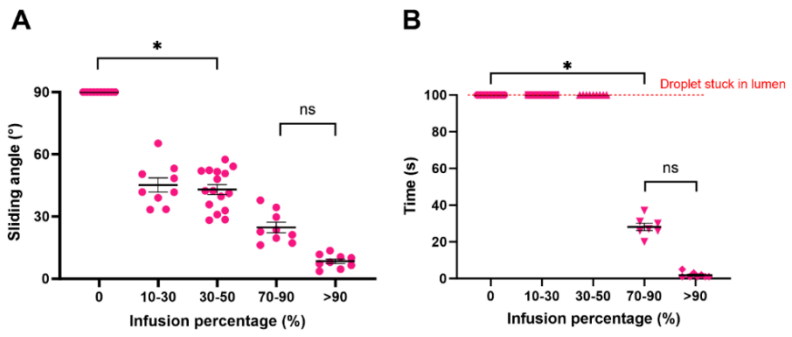

Figure 32. Sliding Angle and Droplet Speed Tests on Catheters Infused into Different Extent.

(A) Sliding angle and **(B)** Droplet Speed (tested with water droplet) results for catheter infused into various infusion percentage. In all graphs presented, the error bars represent the standard error of the mean. Statistical significance between groups was assessed using the ANOVA test. * = P< 0.05 and ns = not significant.

To investigate the antifouling functionality of infused catheters with limited or no free liquid layer on their surfaces, we assessed whey protein adhesion levels on catheters infused at various infusion percentages through image analysis and UV-vis spectrophotometer measurements. As discussed in Section 3.3.3, partially infused catheters incorporate a lower amount of silicone oil into the catheters' polymer network, making the occurrence of syneresis, i.e. the migration of silicone oil molecules onto the surface, unlikely (Cai & Pham, 2022).

Crystal violet served as an indirect method for visualizing the locations where whey protein had attached to the catheter surface. The results indicated that as the infusion percentage increased, the amount of whey protein adhesion observed decreased, as evidenced by lower percentage of crystal violet stained areas (Figures 33A and B). This trend was consistent across catheter samples infused with different viscosities of silicone oil.

However, this method has its limitations. The manual selection of areas for pixel count introduces subjectivity, potentially leading to variations in the chosen areas between researchers. To enable better comparison and ensure an objective quantification approach between samples, a UV spectrophotometer was used to quantify the amount of crystal violet staining on the catheter materials. Similarly, the results showed that higher infusion percentages were associated with lower absorbance levels at 589 nm, indicating reduced crystal violet presence on the samples and suggesting a lower protein adhesion level (Figure 33C). This decreasing trend in absorbance was observed across catheter samples infused using different viscosities of silicone oil, though less prominent in 50 cSt silicone oil infused catheters (Figure A4).

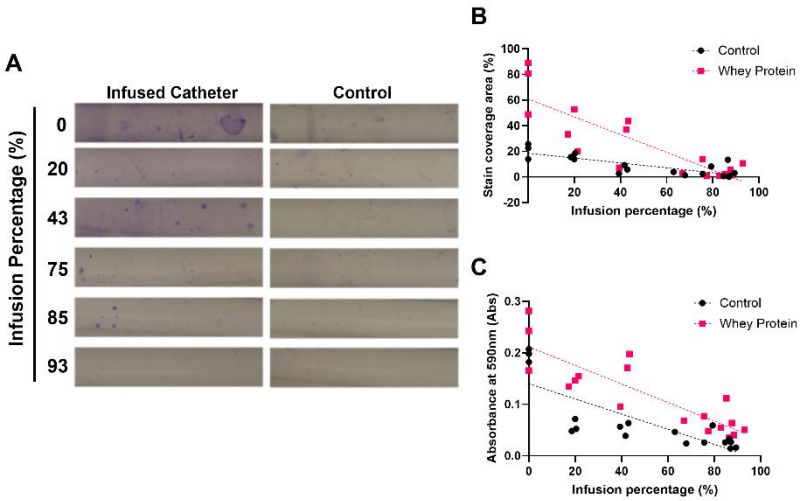

Figure 33. Whey Protein Adhesion Test on Catheters Infused into Different Infusion Percentages.

(A) Crystal violet stains on whey protein incubated catheters. **(B)** Quantification of the areas stained by crystal violet, as a function of infusion percentage (%). **(C)** Crystal violet stains were stripped off with ethanol, absorbance at 590 nm were measured for catheters incubated in whey protein solution. The data has been fit with linear function.

4.3.3.2 Fibrinogen Adhesion

Previous studies on liquid-infused silicone have indicated that a thin and stable free liquid layer is crucial for effective fouling resistance (Kolle *et al.*, 2022; Amini *et al.,* 2017). This layer serves as a physical barrier, reducing the force required to release attached fouling organisms. To evaluate whether the removal of the free liquid layer in our system affects the adherence of relevant CAUTI

foulants to the surface, we incubated fully infused catheters, with (LL) or without a free liquid layer (ØLL), with Fb. The results demonstrated that both fully infused catheters, LL and ØLL, effectively resisted Fb adhesion, exhibiting significantly less surface attachment compared to controls ($P < 0.0001$ and $P = 0.0001$, respectively) (Figures 34A*i* and A*ii*). Additionally, there was no significant difference in Fb adhesion between the samples ($P > 0.9999$), suggesting that removing the free liquid overlayer does not significantly impact the material's ability to resist fouling in terms of Fb adhesion (Figures 34A*i* and A*ii*).

To assess the effectiveness of partially infused silicone catheter material in repelling fouling agents, we again incubated the samples with Fb followed by immunolabeling to assess the levels of adhesion. The results indicate that, as the infusion level increased, the adhesion levels of Fb gradually decreased (Figure 34B*i* and B*ii*). Notably, the first significant difference was observed between non-infused catheters and those infused to the 70–90% of infusion ($P < 0.0001$). In addition, silicone catheter material infused to 70–90% of infusion did not show a significant difference compared to fully infused materials ($P = 0.19$).

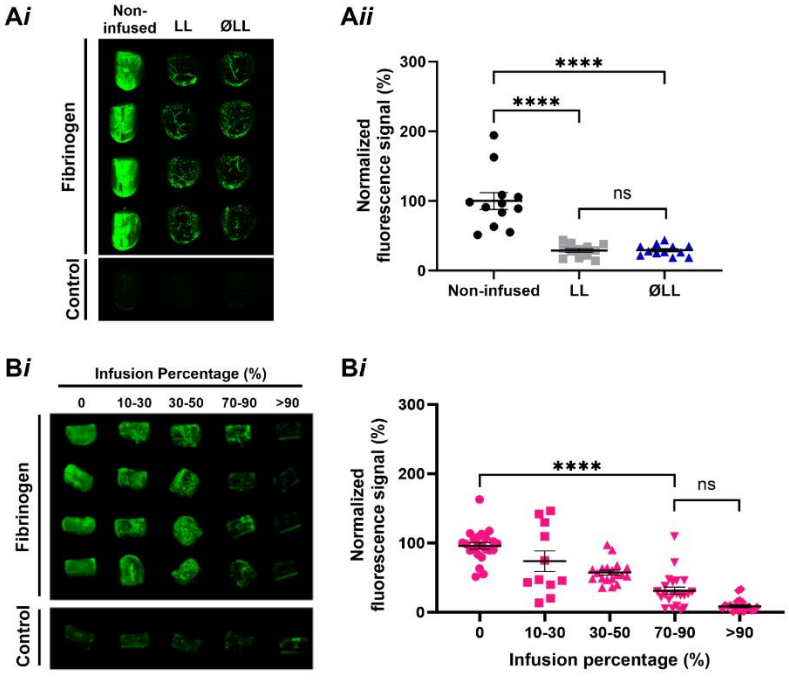

Figure 34. Fb Adhesion on Infused Catheters.

Fb adhesion levels were tested on catheters that are **(A)** non-infused, with (LL), or without (ØLL) a liquid layer, and **(B)** infused into various infusion percentage. The images on the left show the visualization of the samples while the plots on the right show the fluorescence quantification. At least three replicates with n = 4-5 each were conducted. In all graphs presented, the error bars represent the standard error of the mean. Statistical significance between the groups was assessed using ANOVA, with **** = $P < 0.0001$; and ns = not significant.

The results obtained here are consistent with the findings from the sliding angle and droplet speed tests presented in Section 4.3.1. In these tests, both liquid layer (LL) and ØLL demonstrated significantly more slippery surfaces compared to controls, with no significant difference observed between LL and ØLL (Figures 31A and B). This increased slipperiness is reflected in the results for Fb adhesion, where both LL and ØLL exhibited significantly lower Fb adhesion levels compared to non-infused controls (Figures 34A*i* and A*ii*). For partially infused catheters, the sliding angle and droplet speed tests indicated a trend towards increased slipperiness as the infusion percentage increased (Figure 32A and B). This trend was similarly observed in the adhesion of whey protein and Fb, with less protein being attached to the surface as the infusion level increased (Figure 34B*i* and B*ii*).

Current understanding of the mechanism of antifouling action of liquid-infused surfaces relies most heavily on the presence of a free and continuous liquid layer. It is thought that such a layer presents a physical barrier to contaminants and can deceive the mechanosensing mechanism of fouling organisms, preventing the initiation of their adhesive behavior (Amini *et al*., 2017; Kovalenko *et al.*, 2017; Manna *et al*., 2015; Epstein *et al*., 2012). Furthermore, the presence of the free liquid overlayer is thought to contribute to increased slipperiness on the infused surface, reducing the energy required for detaching fouling organisms and facilitating their release (Sotiri *et al*., 2016). The results indicating no significant difference in slippery properties and antifouling functionality between LL and ØLL are therefore surprising to us. Several possibilities could explain this phenomenon: it is possible that the presence of a free and continuous liquid layer is still necessary for optimal functionality, and that ØLL still contains a surface liquid layer, albeit significantly thinner than LL (Figure 29B). Since the characterization of the liquid layer in ØLL was conducted under a confocal microscope, which has a resolution limitation of 500nm, meaning

that any liquid layer below 500nm thickness cannot be visualized. In this case, our results may suggest that a liquid layer below 500nm thickness can still maintain functionality.

However, it is unlikely that this is the case, as adhesion tests on partially infused catheters showed a decrease in adhesion, albeit not significant compared to controls, even at infusion percentages as low as 30-50%. This decrease in adhesion corresponded with increasing infusion percentage. According to literature, the lower concentration of excess liquid in partially infused materials reduces the amount of free liquid available to accumulate at the surface (Cai & Pham, 2022). This suggests that the decrease in adhesion may not be entirely due to the presence of a free continuous liquid layer.

In fact, the understanding that liquid-infused silicone surfaces are more nuanced and dynamic than previously thought has been growing. Hatton *et al.* (2021) reported that when the free liquid layer was removed via washing with water, it would spontaneously regenerate over the following 360 hours (h), increasing linearly from ~50 nm to ~1μm (Lavielle *et al*., 2021). Cai *et al.* (2021) demonstrated that free silicone liquid could spontaneously separate from the silicone solid at the edge of a water droplet (Scherer, 1989). Wong *et al.* (2020) also showed that free molecules within the silicone solid could migrate to the surface in response to the presence of a water drop, but, importantly, also showed that they could return to the bulk after the droplet was removed (Wong *et al*., 2020). These studies point to infused silicone surfaces as able to dynamically respond to changes in conditions, which might explain our results. Understanding how free molecules in the silicone polymer matrix respond to protein foulants attaching to the surface, and whether the liquid layer dynamically reacts to protein foulants similarly to what has been reported in the literature, still requires further investigation.

4.3.4 Bacteria Adhesion Characterization

To directly visualize the attachment of pathogens relevant to CAUTI on infused catheter surface with a minimal amount of free liquid layer on the surface, we incubated both LL and ØLL samples with the bacterium *E. faecalis*. The results (Figures 35A*i* and A*ii*) showed that both LL and ØLL catheters effectively resisted *E. faecalis* adhesion, showing significantly less surface attachment compared to controls ($P < 0.0001$ and $P = 0.009$, respectively). Moreover, the results showed no significant difference in *E. faecalis* adhesion between LL and ØLL samples ($P = 0.25$), suggesting that removing the free liquid overlayer does not have a significant impact on the material's ability to resist fouling in terms of *E. faecalis* adhesion. These results, similar to protein adhesion, also align with the findings from sliding angle and droplet speed tests, where a more slippery surface in LL and ØLL corresponded to significantly lower bacteria adhesion.

Similarly, we again incubated the samples with *E. faecalis* followed by immunolabeling to assess the levels of adhesion on partially infused catheters (Figures 35B*i* and B*ii*). The results indicate that, as the infusion level increased, the adhesion levels of *E.*

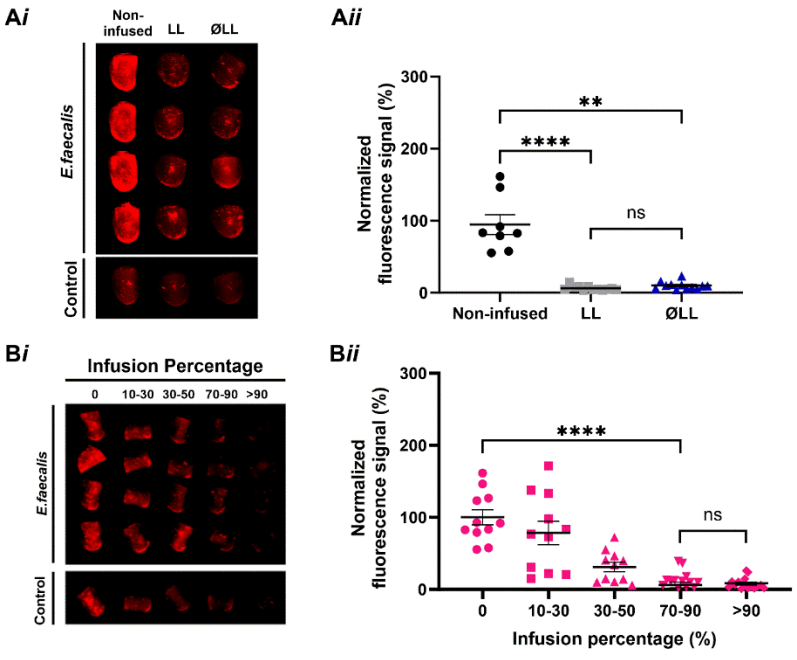

Figure 35. *E. faecalis* Adhesion on Infused Catheters.

E. faecalis adhesion levels on catheters that are **(A)** non-infused, with (LL), or without (ØLL) a liquid layer; or **(B)** infused into different infusion percentages. The images on the left show the visualization of the samples while the plots on the right show the fluorescence quantification. At least three replicates with n = 4–5 each were conducted. In all graphs presented, the error bars represent the standard error of the mean. Statistical significance between groups was assessed using ANOVA. **** = $P < 0.0001$; and ns = not significant.

faecalis gradually decreased. Notably, the first significant difference was observed between non-infused catheters and those infused to the 70–90% of infusion percentage ($P < 0.0001$ *E. faecalis*). In addition, catheters infused to 70–90% of infusion percentage did not show a significant difference compared to fully infused materials ($P > 0.9999$ for *E. faecalis*). Once more, this finding is reflected with the results from sliding angle and droplet speed tests, where an increase in slippery properties on catheters with increasing infusion percentage led to a decrease in bacteria adhesion.

In addition to potential factors such as the interaction between the fouling substrate and the catheter surface, as discussed in Section 4.3.2.2, other factors may also contribute to our results when it comes to the adhesion of living organisms. Previous studies have suggested that in silicone oil-infused silicone material, bacterial flagella, such as those found in *E. coli* and *P. aeruginosa*, interact with the liquid layer (Kovalenko *et al*., 2016). It has been demonstrated that biofilm-forming signals are triggered when bacterial flagella come into contact with a solid material (Belas, 2013). The interaction between bacterial flagella and the liquid layer may enable some degree of flagellar movement, thereby reducing the likelihood of initiating such signals and consequently lowering adhesion. Recent RNA sequencing research has also revealed that the introduction of silicone liquid to silicone solids leads to an upregulation of 10 distinct genes in *P. aeruginosa* while simultaneously downregulating a gene that may impede initial adhesion, although the precise mechanism behind this phenomenon remains unknown (Shen *et al*., 2023). Furthermore, factors such as the stiffness of material might also impact adhesion levels of bacteria. Research on non-infused dry silicone materials with varying degrees of stiffness has revealed that *E. coli* and *P. aeruginosa* attach more readily to softer silicone surfaces than to harder ones (Straub *et al*., 2019). This phenomenon is unlikely to be solely attributed to the presence of flagella, as the researchers have found similar results when testing the same silicone surfaces with mutants lacking flagella

and abiotic carboxylated-modified polystyrene beads. As it has been observed that stiffness levels correspond to the extent of infusion (Cai and Pham, 2022), the alteration in stiffness level may also be a contributing factor affecting bacterial adhesion on infused materials. All these studies suggest that the adhesion of bacteria in our infused catheter material involves numerous complex interactions and is influenced by various factors. It cannot be explained solely by one factor, highlighting the multifaceted nature of bacterial adhesion on infused materials.

4.4 Summary

Our results collectively demonstrate that catheters with minimal or absent free liquid layers maintained their antifouling properties effectively. This is evidenced by the lack of significant differences in sliding angle, droplet speed, protein adhesion, and bacterial adhesion between fully infused catheters with and without the removal of liquid layers. Furthermore, we investigated catheters with varying infusion percentages, revealing a positive correlation between infusion percentage and antifouling ability. Importantly, achieving a significant difference from non-infused controls may not require complete infusion; it can be accomplished with an infusion percentage ranging from 70% to 90%. However, this may vary depending on the type of foulant tested or the bacterial species involved. These findings highlight two key points: first, the ability to adjust foulant levels on infused materials by controlling infusion levels, and second, the potential to reduce the amount of infusing liquid while maintaining functionality that is comparable to materials fully saturated with infusion liquid.

4.5 Acknowledgement

Chapter 4 is based on work previously published in medRxiv, doi: 10.1101/2023.09.14.23295548; authors: **ChunKi Fong**, Marissa Jeme Andersen, Emma Kunesh, Evan Leonard, Donovan Durand, Rachel Coombs, Ana Lidia Flores-Mireles, Caitlin Howell.

CHAPTER 5
DETECTING INFUSING LIQUID LOSS OF INFUSED CATHETERS

5.1 Introduction

From our experiments detailed in Chapter 3 and 4, we have observed that infused catheters, whether with the surface free liquid layer removed or with a lower infusion of liquid into the material, still exhibit antifouling properties comparable to catheters fully saturated with infusing liquid. As highlighted in Section 1.2.7, it is important to minimize the loss of infusing silicone liquid from the catheters into the environment, as silicone oil droplets may trigger immune responses (Melo *et al*., 2021; Cheng *et al*., 2020; Krayukhina *et al*., 2019; Chisholm *et al*., 2015).

As discussed in Section 1.2.4.1, characterizing the thickness of infused materials presents significant challenges due to the minimal volume of liquid and the constraints imposed by analysis protocols. This challenge is further compounded when attempting to measure the loss of infusing liquid from our catheters, as the volume becomes even smaller. As shown in Figure 25B, the maximum amount of silicone oil present in fully infused catheter is less than 30 μL/mm. While highly sensitive instruments do exist, they often come with a significant price tag, such as flow cytometers, which can range from $80,000 to $150,000 for a single unit and require extensive training to operate. In light of these considerations, the development of our protocol to detect liquid loss from infused catheters in water prioritizes the use of instruments readily available on the University of Maine campus or with our collaborators, and aims to establish a method that is quick, easy to implement, and widely applicable across laboratories. By doing so, we hope to enable future researchers to detect small amounts of infusing liquid loss with our developed protocol without the need for substantial financial investment, thereby preserving resources for other areas of research.

Previous studies have demonstrated the visualization of silicone oil droplets in distilled water under microscopes (Melo *et al*., 2021). Researchers observed these droplets by filling silicone oil-lubricated syringes with water and agitating them. Literature has also demonstrated the detectability of silicone in biological liquid samples using Inductively coupled plasma – optical emission spectrometry (ICP-OES; Hauptkorn *et al*., 2001). In this analytical technique, samples are typically dissolved in hot acidic solutions, allowing elemental components to remain in solution. Subsequently, the ICP-OES instrument analyzes and quantifies the elemental composition of the sample. Within the instrument, argon plasma generates high heat, enabling the absorption of energy by the sample's atoms and ions. This energy causes electrons to transition from their ground state to an excited state. Upon returning to lower energy levels, specific wavelengths corresponding to the elements present are emitted. The instrument detects the intensity of light emitted, allowing the quantification of trace elements in a sample. Moreover, previous studies have demonstrated the detection and quantification of oil-in-water emulsions using UV-Vis spectrophotometry (Banan Khorshid *et al*., 2021). The underlying hypothesis is that an oil-in-water emulsion would render the solution more turbid compared to water with lower concentration of silicone oil. This increased turbidity is expected to generate a distinct absorbance profile contingent upon the concentration of silicone oil present (Banan Khorshid *et al*., 2021). Dynamic Light Scattering was used in past studies to study small molecule, such as protein-protein or protein-nucleic acid interactions (Stetefeld *et al*., 2016), although not commonly used in studying silicone oil in water. This instrument operates by passing a laser through a 1 mL liquid sample, with scattered light detected by a photon detector. Different particle sizes suspended in the liquid sample scatter light uniquely, allowing the instrument to provide information on particle

number and size distribution, a principle potentially applicable to detecting oil droplets suspended in water.

Building upon previous literature and taking advantage of the availability of these instruments on campus or from collaborators, we investigated the potential use of light microscopy, dynamic light scattering instruments, ICP-OES, and UV-Vis instruments for detecting oil loss in infused catheters. By experimenting with various protocols, we successfully developed a method using UV-Vis to detect silicone oil content as low as 0.004 μL in 10 ml of water. With this successful protocol, we quantify the potential loss of silicone oil from our infused catheter material into the environment.

5.2 Materials and Methods

5.2.1 Microscopy

Standards were first established to assess whether small amounts of silicone oil droplets could be visualized. 0.1% (v/v) and 0.2% (v/v) of 10 cSt silicone oil was pipetted respectively into 1 mL of deionized water. After vortexing, 100 μL from each resulting solution was quickly transferred onto a glass slide, and the samples were visualized under a light microscope at 100X magnification.

To begin testing this protocol with infused catheter samples, fully infused catheters were cut into 2 cm sections and subjected to full submersion into 1 mL of deionized water and removal for a 20 or 40 cycles. Following this, the resulting solution was vortexed, and similarly, 100 μL of the solution was quickly transferred onto a glass slide for visualization under light microscopy at 100X magnification. We opted for a small volume of solution for dipping to increase the likelihood of extracting water containing oil for visualization.

5.2.2 Dynamic Light Scattering

To assess the suitability of Dynamic Light Scattering (Zetasizer Nano ZS, Malvern Panalytical, US) in detecting oil loss, standards of silicone oil were created by spiking silicone oil into deionized water at concentrations of 0.1% (v/v) and 0.2% (v/v). After vortexing, 1 mL of samples were pipetted into a glass cuvette and measured with DLS for approximately 5 minutes. To mitigate low counts from the measurements, the same procedure was followed, except that the standards were allowed to settle for 15 and 30 minutes after vortexing, respectively, before measurement. Additionally, 2 cm fully infused catheters were submerged and removed from 1 mL of deionized water for 20 cycles and tested using the same protocol as the standards. Various modifications were also attempted to decrease polydispersity and allow droplets to coalesce for a more uniform suspension, including (1) increased measurement times to 1 or 3 hours, (2) settling periods for at least 30 minutes, and (3) filtration through a Nylon filter to eliminate dust particles. Furthermore, 25% infused catheters, representing samples with the lowest infusion percentage of interest, were also tested using the same protocol.

5.2.3 Inductively Coupled Plasma Optical Emission spectroscopy (ICP-OES)

Mouse models were catheterized for 24 hours with mouse catheters fully infused with 20 cSt silicone oil, as described in Section 1.2.6. Subsequently, 10 bladders of the catheterized mice were carefully extracted using aseptic techniques (Andersen *et al*., 2023). Four bladders from non-catheterized mice were also extracted as negative control; and two 15 mg standard soil samples were used as positive control. All samples were then digested with hydrofluoric acid and nitric acid using a microwave digester. The digested liquid was then measured with ICP-OES (from Dartmouth College) for silicone detection.

5.2.4 Ultraviolet-visible spectrophotometry

5.2.4.1 Turbidity Method

A known amount of 10 cSt silicone oil was pipetted into 10 mL deionized water to create standard suspensions of 0%; 20%; 40%; 60%; 80% and 100% silicone oil (v/v for all percentages). The standard solution was then subjected to vortexing for one minute. 1 mL of the solution was quickly transferred to a glass cuvette for absorbance measurement in the UV-Vis spectrophotometer. The vortexing aimed to temporarily create a water-in-oil emulsion for measurement (Wang *et al*., 2022). Another refined methodology was also performed the same way as above, except that a surfactant, 40 µL of Tween-20, was pipetted into the 10 mL water solution before vortexing.

To assess silicone oil loss in catheters, 10 cm segments of fully infused catheters (infused for at least 5 days) were fully submerged and removed from 10 mL of deionized water for a designated number of cycles. Similarly, 40 µL of Tween-20 was added into the water. After the water was vortexed, 1 mL of the sample was immediately transferred into a glass cuvette for absorbance measurement with UV-Vis spectrophotometry. An alternate method involved cutting fully infused 2 cm catheters into quarters, then conducted the full submersion and removal of catheters from a glass cuvette filled with 1 ml of deionized water. 4 µL of Tween-20 were then pipetted into the glass cuvette, and subjected to UV-Vis measurements.

5.2.4.2 Homogenization Method

For every 9.5 mL of 20 cSt silicone oil, 0.5 mL of oil dye (LF2001, Leak Detection Dye, Leak Finder) was added to create a silicone oil/dye mixture. A known amount of silicone oil/dye mixture was then pipetted into 10 mL deionized water to create standard solutions of 0.1%; 0.5% and 1% silicone oil (v/v). Next, 40 µL of Novec™ 7100 engineered fluid (3M™), an agent that has some level of solubility in water and can dissolve silicone oil, was introduced into the mixture to attempt

the creation of a homogenized solution with uniform color. After vortexing for 1 minute, 1 mL of the total liquid was transferred to a cuvette for UV-vis detection.

5.2.4.3 Water Evaporation Method

Approximately 9 mg of pyrromethene (05971, Pyrromethene 597-8C9, Exciton, USA) was added to every 100 mL of silicone oil and thoroughly mixed. Pyrromethene was selected for its better documented characteristics in absorption and emission wavelengths compared to the commercial oil dye referenced in Section 4.2.4.2, facilitating easier characterization. The solution was then filtered through a 0.45 μm filter to remove any particulates.

Standard solutions were created by pipetting a known quantity of the silicone oil/pyrromethene mixture into a 10 mL water. Subsequently, employing a heat plate, water content was evaporated. Due to the absence of precise temperature control on our heat plate, adjustments were made to achieve intermittent boiling of water, indicative of a fluctuating temperature around 100°C. After water evaporation, 1 mL of toluene was then introduced into the container to dissolve all remaining silicone oil/pyrromethene, allowing sufficient volume to be transferred into the glass cuvette for UV-VIS measurement.

5.2.4.4 Extraction Method

5.2.4.4.1 Standard Curve Development

A standard curve of the silicone oil/pyrromethene mixture in 18.2MΩ-cm water (Millipore Milli-Q Direct 8 Water Purification System; 18.2MΩ-cm) was created by adding a fixed percentage of dyed silicone oil in 10 mL of MilliQ water. Afterward, 1 mL of toluene (108-883, Toluene anhydrous, Alfa Aesar, USA) was pipetted into the MilliQ water, and the mixture was manually shaken for 10 seconds and left to settle for at least a minute to separate into upper and bottom

layers. The top layer was then carefully extracted and placed in a glass cuvette for UV-Vis (840-277000, GENESYS™ 30 Visible Spectrophotometer, Thermo Fisher, USA) measurement. The absorbance of the samples was measured at 2nm intervals within the 350–650 nm range.

5.2.4.4.2 Sample Preparation

To prepare the dyed silicone oil for infusion, approximately 9 mg of pyrromethene (05971, Pyrromethene 597-8C9, Exciton, USA) was added to every 100 mL of silicone oil and thoroughly mixed. The solution was filtered through a 0.45 μm filter to remove any particulates. The fabrication process for catheters with a liquid layer (LL), those with no liquid layer (ØLL), and partially infused catheters remains consistent with the method described in Section 3.3.1, but with dyed silicone oil used as the infusing liquid.

5.2.4.4.3 Silicone Oil Loss from Infused Catheters

The assessment of silicone oil removal from infused catheters infused with dyed silicone oil followed a consistent procedure as the standard curve development protocol. Instead of dispensing a fixed volume of liquid into 18.2MΩ-cm water, we immersed catheters, prepared using the aforementioned infusion method, into 10 mL of 18.2MΩ-cm water. This immersion-withdrawal cycle was repeated ten times. Subsequently, the absorbance readings from UV-Vis Spectrophotometer were compared against the standard curve to quantify the amount of silicone oil extracted.

5.3 Results and Discussion

5.3.1 Microscopy

To initiate testing the visualization of small amounts of silicone oil in water, we used a microscope at 100X magnification to observe whether we could visualize 0.1% and 0.2% concentrations of

silicone oil in 100 µL of deionized water. Results indicated that we could indeed visualize silicone oil droplets in the samples (Figure 36A). We selected areas occupied by the oil droplets and counted the number of pixels of oil droplets using ImageJ. Samples containing 0.2% silicone oil exhibited roughly double the number of relative pixel area (~3803) compared to those with 0.1% silicone oil (~9962), providing an indirect method of quantifying oil present in water samples, which might be applicable to catheters subjected to water stripping cycles (Figure 36B).

Having achieved success in visualization, we proceeded to test this protocol with infused catheter samples. Results

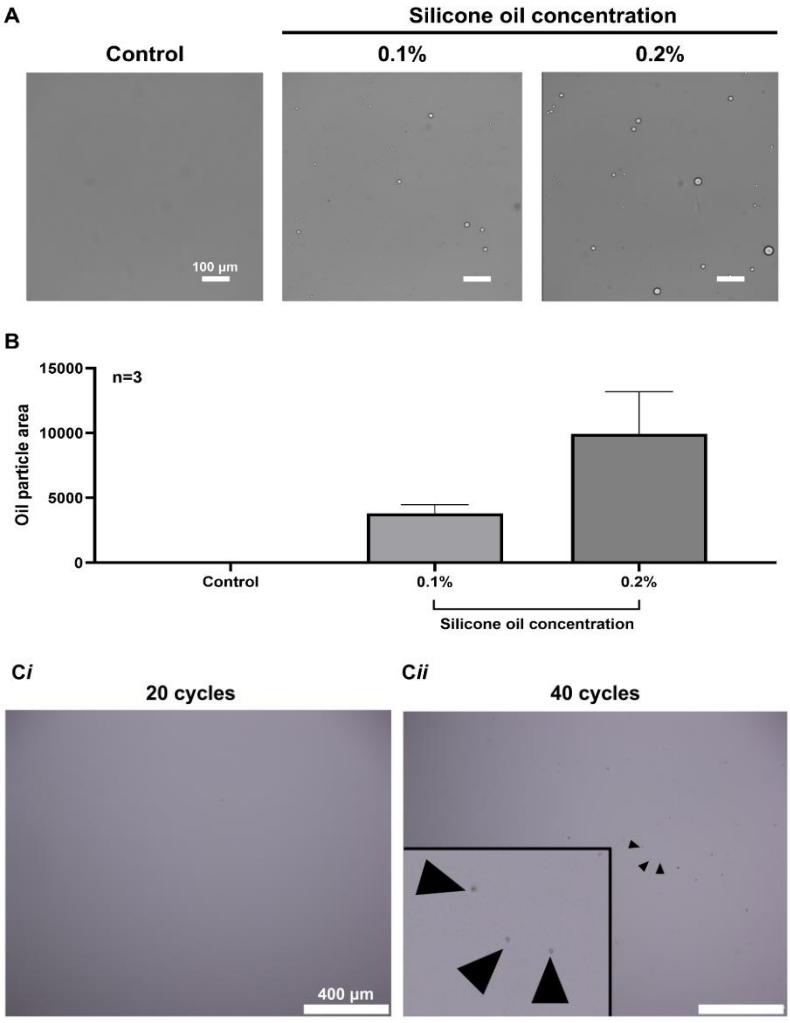

Figure 36. ImageJ Analysis of Silicone Oil in Water.

(A) Microscopic images depict water samples containing trace amounts of silicone oil. From left to right: deionized water control, 0.1% silicone oil in deionized water, and 0.2% silicone oil in deionized water, respectively. **(B)** Quantification of the area occupied by oil particles, analyzed using Image J. Error bars represent the standard error of the mean. n=3. The catheters were fully submerged in water and subsequently removed for either **(C*i*)** 20 cycles or **(C*ii*)** 40 cycles. The resulting water sample was then visualized under a microscope to detect silicone oil droplets. Arrows indicate the location of several, but not all, silicone oil droplets. In **(C*ii*),** a zoomed-in image of the figure is displayed in the lower left corner.

revealed the presence of silicone oil droplets in the water, but the particles were too minuscule for quantification (Figure 36C). This shows a limitation of the method, wherein with a small volume of solution, only a limited surface area of fully infused catheters may come into contact with the water body. Consequently, this could potentially reduce the amount of oil that could be stripped off and detected. Nonetheless, this observation confirms the loss of some amount of silicone oil from fully infused samples. We chose not to proceed with partially infused samples due to their even lower silicone oil content, rendering them unlikely to be visualized under light microscopy.

5.3.2 Dynamic Light Scattering

To assess the suitability of Dynamic Light Scattering (DLS) for measuring oil loss, 0.1% (v/v) and 0.2% (v/v) silicone oil standards in deionized water were measured with DLS for ~5 minutes. However, detection results showed significant variations in count rate indicating sample instability, likely caused by active coalescence of silicone oil droplets during measurement (Bera *et al*., 2021). The DLS instrument therefore was not able to provide a proper size or count measurement of oil droplets suspended in the deionized water.

The coalescence rate of silicone oil is influenced by various factors, including the size and distance of oil droplets (Li *et al*., 2024). To obtain preliminary data and assess the reliability of results, we followed the same procedure used for measuring silicone oil standards. However, in this case, the standards were allowed to settle for 15 and 30 minutes after vortexing before measurement. Although signals were detected this time (Figures 37A and B), the DLS instrument produced count rates with extremely low data quality, as reported by the DLS instrument software. The ineffectiveness of the DLS measurements can be attributed to the high polydispersity of the silicone oil droplets in the water sample (Danaei *et al.*, 2018). Polydispersity refers to the non-uniformity in the size distribution of oil particles within the sample. Given that DLS relies on

measuring fluctuations in scattered light intensity from a collection of particles, excessively polydisperse samples can lead to inaccurate results (Danaei *et al.*, 2018). This is because different distributions in particle size may produce similar outcomes, compromising the reliability of the DLS measurements. The same results were also observed when using deionized water to remove silicone oil from 2 cm fully infused catheters (Figures 37C and D).

Various modifications were attempted to decrease polydispersity and allow droplets to coalesce, including (1) increased measurement times to 1 or 3 hours, (2) settling periods for at least 30 minutes, and (3) filtration through a Nylon filter to eliminate dust particles. However, these efforts yielded similarly low-quality data profiles. Furthermore, 25%

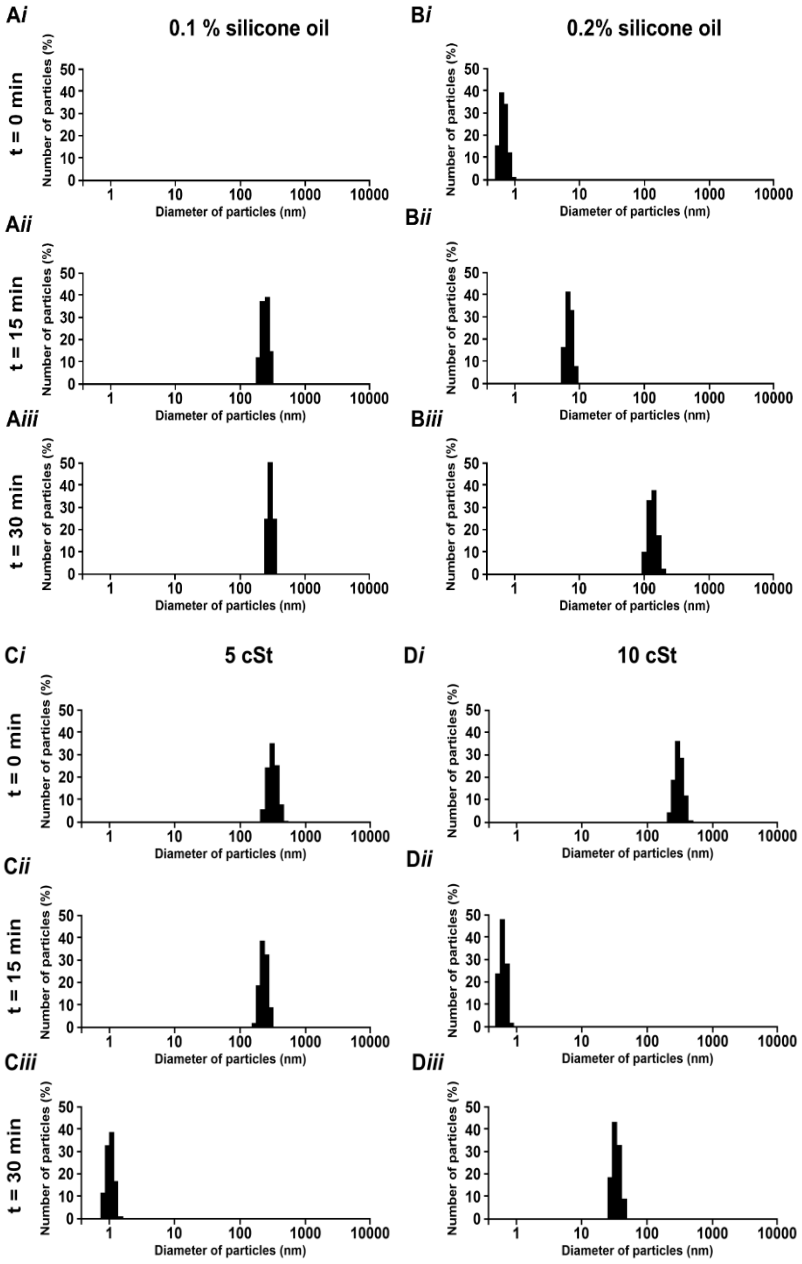

Figure 37. DLS Measurement of Silicone Oil in Deionized Water.

Deionized water with trace amount of silicone oil was prepared via spiking with **(A)** 0.1% or **(B)** 0.2% silicone oil or dipping with catheters infused with **(C)** 5 cSt or **(D)** 10 cSt silicone oil. Subsequently, the samples were allowed to settle for **(A*i*, B*i*, C*i*, D*i*)** 0 min; **(A*ii*, B*ii*, C*ii*, D*ii*)** 15 min; or **(A*iii*, B*iii*, C*iii*, D*iii*)** 30 min after vortexing before DLS measurement.

infused catheters, representing samples with the lowest infusion percentage of interest, were tested using the same protocol. Even after evaporating the deionized water, then pooling 3 samples to increase oil content, results remained unsatisfactory, with samples exhibiting count signals too low for detection. In conclusion, despite extensive attempts to optimize the protocol, the DLS instrument proved ineffective for accurately measuring silicone oil content in water samples due to the oil droplets being too polydisperse in deionized water.

5.3.3 Inductively Coupled Plasma Optical Emission spectroscopy (ICP-OES)

In order to explore the use of ICP-OES in detecting silicone oil loss in catheter samples, mouse bladders were extracted from mice that had been catheterized with fully infused catheters. These extracted bladders were then subjected to digestion for subsequent measurement in Dartmouth College using ICP-OES. Our previous experimental data suggested that if all silicone oil were lost from the mouse catheter to the bladder, only approximately 1.08 µL of silicone oil would be lost (Figure A1) which is below the literature's detection limit (Hauptkorn *et al*., 2001). However, since each mouse bladder weighs more than 100 mg (~0.15 - 0.7g), there is a possibility that some signals could still be detected, we therefore proceeded with the analysis. The results indicated very low silicon recovery with only 25-30%, as referenced with a soil positive control (4-5 mg of silicon present). Among the 10 bladders obtained from catheterized mice and subjected to testing, silicone signals were detected in only 2 bladder samples. (19292 and 48706 ng silicon/mL). Additionally, 3 out of 4 bladders without catheterization exhibited silicon signals (5935; 57326; 16595 ng silicon/mL respectively). Since silicon can naturally occur in mammalian connective tissues (Jugdaohsingh *et al*., 2015), the silicon signals detected in the non-catheterized mouse bladders are likely attributed to the presence of silicon within the animal tissue itself. Since most sample signals were below the detection limit for fully infused catheters, detecting silicon signals is even

less likely with lower oil amounts, in the case of partially infused catheters. The findings suggest that the current method may not be optimal for our purposes, primarily due to the minimal amount of silicone oil content. In literature, it was also reported that silicone's low solubility in acid and high volatility could also exacerbate its loss during sample preparation (Hornung & Krivan, 1997; Van Dyck et al., 1997). This could potentially further diminish the amount of detectable silicone oil in our samples, rendering this method non-effective for our purposes.

5.3.4 Ultraviolet- visible (UV-Vis) spectrophotometry

5.3.4.1 Turbidity Method

To investigate the application of UV-Vis spectrophotometry in detecting silicone oil, standard solutions with varying concentrations of silicone oil in deionized water were prepared. These solutions were quickly vortexed before being measured. Results revealed differences in absorbance across wavelength ranges; however, these differences did not correlate with the concentration of silicone oil in the samples and exhibited inconsistency (Figure 38A). This outcome was somewhat anticipated, as vortexing creates the suspension of various sizes of silicone oil droplets in water, this unstable emulsion of silicone oil would also migrate to the surface during absorbance measurements in the spectrophotometer.

To refine our methodology, we follow the same protocol, but introduced Tween-20 as a surfactant in an attempt to establish a more stable and uniform emulsion suitable for absorbance measurements. This adjustment yielded improved results, although typical absorbance peaks were

not observed (Figures 38B and 38C). Nonetheless, the variations in overall absorbance across wavelengths appeared to somewhat correlate with the percentage concentration of silicone oil in the water. For 100% silicone oil, it is a uniform solution without any observable turbidity, we expected the resulting absorbance profile to resemble that of 0% silicone oil, as was indeed demonstrated in our results. Anticipating the need for detection of minute liquid volumes when we test our catheters, we further reduced the percentage of oil in water for UV-Vis measurement and the results somewhat show a linear relationship between absorbance and concentration of silicone oil present in the water (Figure 39).

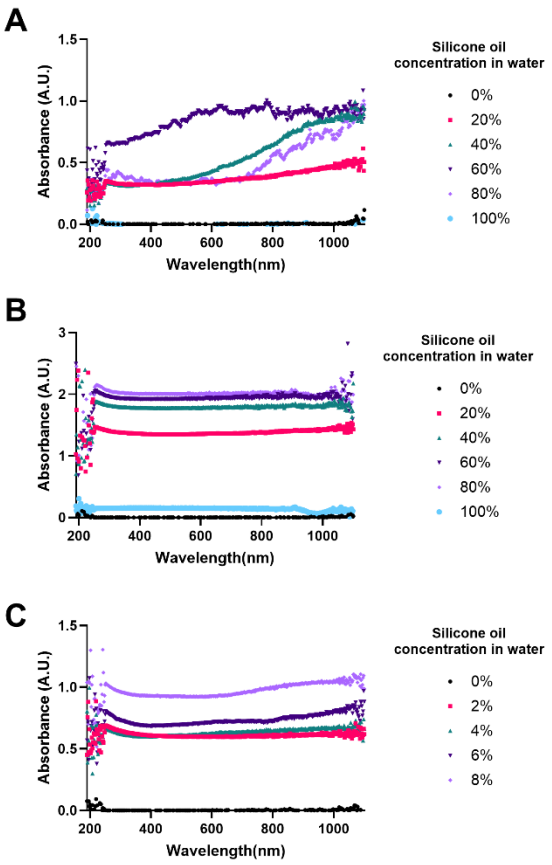

Figure 38. Absorbance Measurement for Silicone Oil in Water.

Absorbance from 190-1100 nm wavelength was plotted for **(A)** 0-100% of silicone oil in water; **(B)** 0-100% of silicone oil in water + 4% Tween-20; and **(C)** 0-8% of silicone oil in water + 4% Tween-20.

With promising initial results, we proceeded to investigate the removal of silicone oil from fully infused catheters. We chose to test this protocol on fully infused catheters, as they contain the highest amount of oil integrated into the polymer. Therefore, theoretically, the potential for silicone oil removal from these catheters should be the highest. If successful in detecting silicone oil loss from fully infused catheters, there would be a greater likelihood of detecting oil loss from catheters with lower infusion percentages. Resulting signals did not exhibit any significant difference compared to negative controls, suggesting that this method lacks the sensitivity required to detect

the desired amount of silicone oil (Figures 40A*i*, B*i* and C*i*). Another potential explanation is the absence of silicone oil removal through water stripping, which is unlikely since it was reported that repeated exposure to an air/water interface as an effective means of removing the free liquid layer from infused systems (Sotiri *et al*., 2018). A possible flaw in this protocol is the risk of losing silicone oil samples during the transfer process of 1 mL of solution from the bulk water solution, which could lead to the under detection of silicone oil signals, especially given the minute amounts of oil present. To address this flaw, we eliminated the transfer process and instead cut fully infused 2 cm catheters into quarters to conduct silicone oil removal and surfactant addition directly in the glass cuvette. This modification ensured that all oil content removed remained in the container for measurement. However, despite these adjustments, the results remained similar, with no significant signals detected (Figures 40A*ii*, B*ii* and C*ii*). The challenge with these protocols lies in the smaller size of the infused catheter samples, resulting in

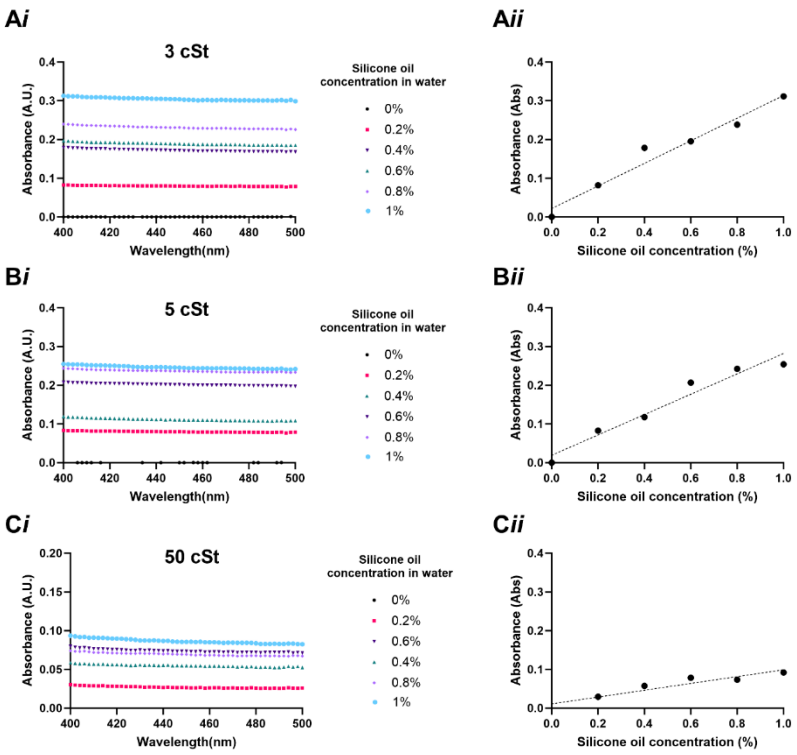

Figure 39. Absorbance Measurement for Small Concentration of Silicone Oil in 4% Tween-20 with Water.

Absorbance values within the range of 400-500 nm were graphed for difference viscosities of silicone oil: **(A*i*)** 3 cSt, **(B*i*)** 5 cSt, and **(C*i*)** 50 cSt. On the right panel, standard curves were generated with five randomly selected points between 400-500 nm: **(A*ii*)** for 3 cSt, **(B*ii*)** for 5 cSt, and **(C*ii*)** for 50 cSt silicone oil.

a reduced amount of oil that could potentially be lost. Alternatively, using a larger sample size would require a larger volume of water, making the transfer of solution into the cuvette inevitable and risking the exclusion of oil content during detection.

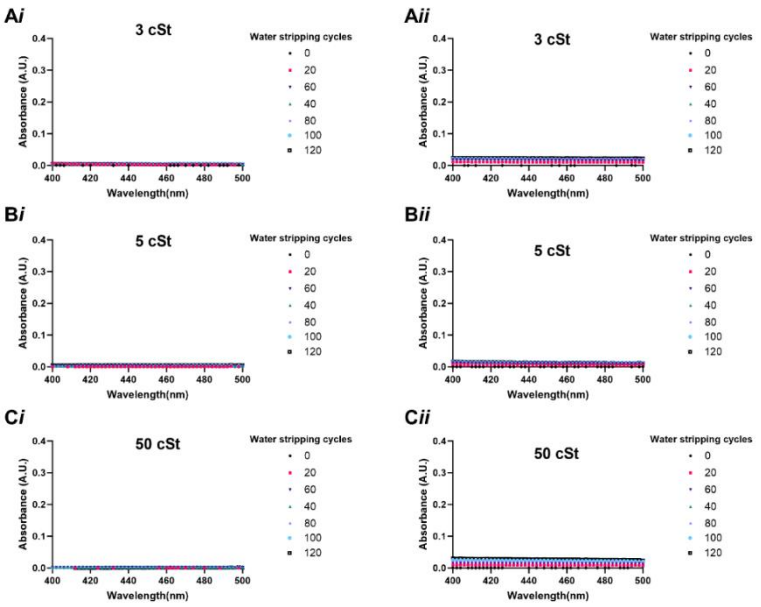

Figure 40. Absorbance Measurement for Fully Infused Catheter Samples.

Absorbance values within the range of 400-500 nm were graphed for catheters fully infused with different viscosities of silicone oil: **(A)** 3 cSt, **(B)** 5 cSt, and **(C)** 50 cSt. The left panel **(i)** displays absorbance when samples were generated by dipping catheters in a larger volume of deionized water and then transferred to a cuvette. On the right panel **(ii)**, samples were generated by directly dipping catheters into the cuvette used in UV-Vis for absorbance measurement.

5.3.4.2 Homogenization Method

From our exploration in Section 5.3.4.1, we have uncovered some limitations. First of all, given that we are essentially creating a solution comprising oil suspended in water, the transfer of this solution into the cuvette may not accurately represent the total oil loss, as there is a risk of excluding some oil content during the transfer process. To address this, our upcoming protocol integrates a silicone oil emulsifier into the water, thereby facilitating the creation of a homogenized solution. By emulsifying the silicone oil into a uniform solution, regardless of which portion of the solution is being transferred into the cuvette for measurement, the results should remain relatively consistent. The second limitation arises from the fact that we are dealing with minute quantities of silicone oil, resulting in very small signals for measurement. In response to this challenge, we also introduced a dye to the silicone oil to enhance signal detection using UV-VIS spectrophotometry.

In order to assess the effectiveness of these approaches, we prepared standard solutions containing known concentrations of silicone oil/oil dye mixture in deionized water. With the inclusion of silicone oil dye and emulsifier, we have noted a significant change. In samples containing lower percentages of silicone oil, unlike in previous protocols where we observed varying levels of flat absorbances (Figure 39), we now detected a distinct peak corresponding to the color of the silicone oil/oil dye mixture. (Figure 41A). The increase in absorbance corresponds to the amount of silicone oil/oil dye mixture added to the water sample (Figure 41B). However, before further testing of catheter samples with this protocol, we observed that although relatively stable emulsions seemed to form at lower percentages (Figure 41C), at 5% silicone oil/dye in water, the silicone oil/dye mixture floated to the top after 2-3 minutes (Figure 41D). This indicates that we may have overlooked this phenomenon at the lower percentages' standard samples due to their significantly smaller volume. A significant portion of the oil could have floated to the top, and not have been visible to the naked eye, potentially interfering with the results.

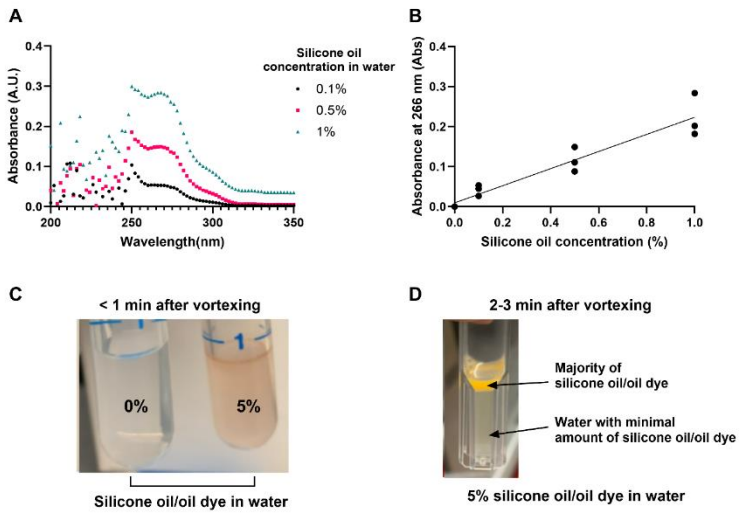

Figure 41. Absorbance Measurement of Silicone Oil/Oil Dye.

(A) Absorbance values within the range of 200-350 nm were graphed for water solution with 0.1%; 0.5%; and 1% of silicone oil/oil dye mixture respectively. **(B)** Absorbance values at 266 nm were plotted against silicone oil concentration. **(C)** Appearance of silicone oil/oil dye mixture in water less than a minute after vortexing. Water without any silicone oil/oil dye mixture is showed on the left, labelled as 0%; water with 5% of silicone oil/oil dye mixture is showed on the right, labelled as 5%. **(D)** Appearance of 5% silicone oil/oil dye mixture in water 2-3 minutes after vortexing.

5.3.4.3 Water Evaporation Method

From the results presented in Sections 5.3.4.1 and 5.3.4.2, it becomes evident that achieving a uniform oil/water emulsion is a challenging endeavor with our existing tools. To address this, we

explore the possibility of isolating the oil layer from the water for measurement. We hypothesized that following the creation of a silicone oil/pyrromethene (silicone oil dye) mixture in water, we can isolate silicone oil/pyrromethene by evaporating all water content on a heat plate. To enhance the volume of the remaining trace amount of silicone/pyrromethene, toluene was subsequently introduced to dissolve all silicone oil. This process aimed to generate a liquid volume of at least 1mL, facilitating measurement with a UV-Vis spectrophotometer. Prior to testing the protocol, we conducted preliminary tests on known quantities of silicone/pyrromethene dye in 1 mL toluene. The resultant solutions exhibit a consistent and uniform coloration throughout, devoid of any discernible phase separation after >30 minutes, where higher concentrations of silicone oil/pyrromethene in toluene result in a more pronounced pinkish hue (Figure 42A). UV-Vis measurements show that these solutions yield detectable peaks that correspond to silicone oil/pyrromethene concentration (Figure 42B). This indicates that silicone oil/pyrromethene in toluene is a stable homogenized mixture that allows analysis with the UV-Vis spectrophotometer.

To assess the efficacy of our newly devised protocol, we prepared a silicone oil/pyrromethene mixture as previously outlined, and then introduced a known quantity of this mixture into deionized water. Subsequently, we evaporated the water and added toluene to yield enough volume for UV-Vis measurement. Results revealed a loss of silicone oil samples during the heating process, evident in discrepancies between the expected and observed peaks of the silicone oil/pyrromethene mixture (Figure 42C). For instance, in the standard solution depicted in Figure 42A, the peak absorbance of 0.5% silicone oil/pyrromethene in toluene at 528nm is approximately 0.17. However, when measuring the same concentration of silicone oil/pyrromethene under the water

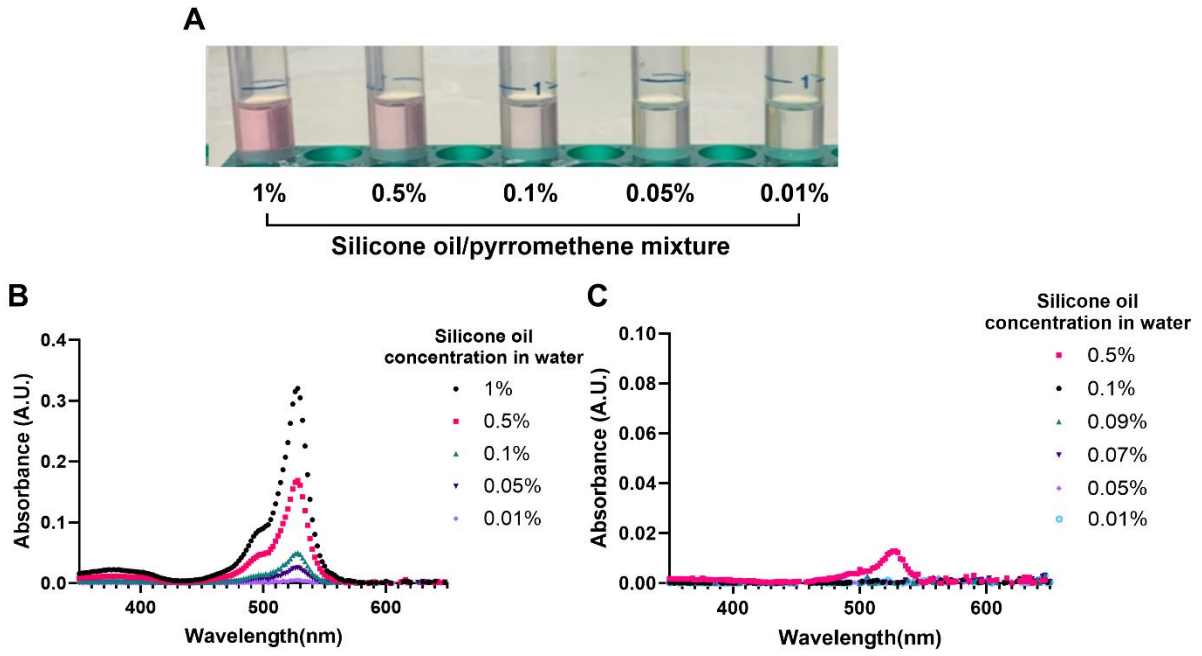

Figure 42. Absorbance Measurement of Silicone Oil/ Pyrromethene in Toluene.

(A) Appearance of silicone oil/pyrromethene mixture in toluene 30 minutes after vortexing. From left to right, the toluene solution contains concentrations of 1%, 0.5%, 0.1%, 0.05%, and 0.01% of silicone oil/pyrromethene. **(B)** Absorbance values within the range of 350-650 nm were graphed for 0.01%, 0.05%, 0.1%, 0.5%, and 1% of silicone oil/pyrromethene mixture in toluene respectively. **(C)** After water evaporation treatment, Absorbance values within the range of 350-650 nm were graphed for 0.01%, 0.05%, 0.1%, 0.5%, and 1% of silicone oil/pyrromethene mixture in toluene respectively.

evaporation protocol, a notable decrease in absorbance is observed, dropping to approximately 0.013. Due to the lack of precise temperature control on our heat plate, we could only adjust the temperature knobs to the extent where intermittent boiling of water was observed. Consequently, it is plausible that the temperature fluctuated, possibly exceeding 100°C, which might have led to the unintentional removal of some silicone oil.

5.3.4.4 Extraction Method

Section 5.3.4.3 has demonstrated that the silicone oil/pyrromethene mixture in toluene remains stable, enabling UV-Vis analysis to quantify trace amounts of silicone oil. However, it was

observed that using our existing heat plate led to the loss of silicone oil, likely due to the lack of precise temperature control. An alternative protocol was devised to isolate silicone oil/pyrromethene from water without risking the loss of silicone oil.

In this protocol, silicone oil/pyrromethene was added into deionized water. Subsequently, toluene was added directly into the mixture and mixed gently. Due to the fact that both toluene and the silicone oil/pyrromethene mixture are less dense than water, the resulting solution exhibited a gradual separation into two distinct phases (Figure 43A). The upper layer, characterized by its pink hue, consisted of silicone oil/pyrromethene dissolved in toluene, while the lower layer comprised water. With this clear separation, we can pipette only the top layer, which contains the silicone oil/pyrromethene in toluene, for UV-Vis measurement.

To establish a standard curve for quantifying infused catheter silicone oil loss in subsequent experimental sections, silicone oil/pyrromethene standards were extracted from deionized water using the discussed method. The resulting standard curve exhibited a positive linear correlation between the concentration of silicone oil/pyrromethene mixture and absorbance at 528 nm (Figure

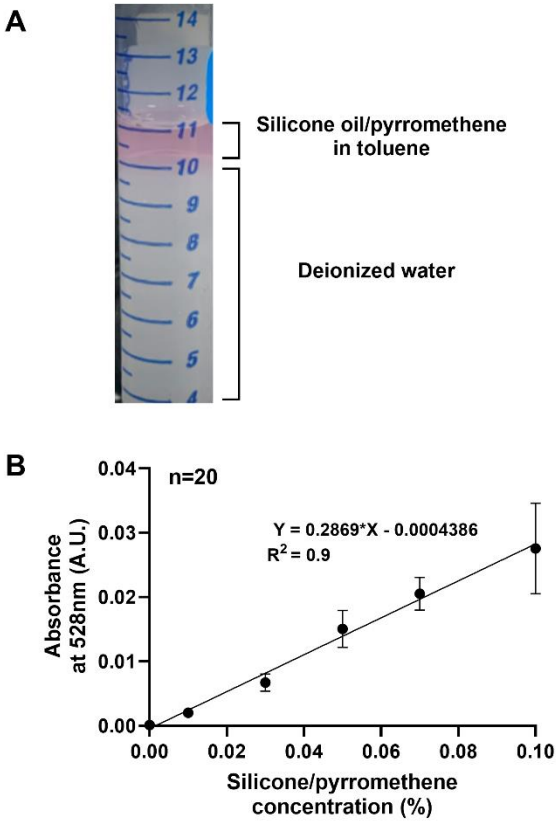

Figure 43. Absorbance of Silicone Oil/ Pyrromethene in Toluene at 528 nm.

(A) Appearance of silicone oil/pyrromethene in toluene extracted from deionized water; **(B)** Absorbance at 528 nm is plotted against the concentration of silicone/pyrromethene. The error bars represent the standard deviation. n=20.

43B). We tested 20 samples per standard concentration of silicone oil, aligning with recommendations from prior literature to ensure robust results. Following guidelines from the Clinical and Laboratory Standards Institute (Armbruster and Pry, 2008), we calculated the limit of detection to be 0.0012% (v/v). This ensured our ability to accurately measure silicone oil content in subsequent experiments, facilitating the generation of reliable data.

To compare the quantity of silicone oil that could be lost into the environment in infused catheters with a free liquid layer (LL) versus without free liquid layer (ØLL), the catheters underwent repeated passage through air-water interface to strip away the surface layer. In LL, 0.05± 0.01 µL of silicone liquid/mm of sample length were lost from the infused catheter, while ØLL samples lost significantly less, 0.02 ± 0.006 µL of liquid/mm (P = 0.038; Figure 36A).

To investigate the silicone oil loss levels of partially infused silicone catheter materials, the samples were again repeatedly exposed to an air-water interface to strip away surface liquid (Figure 44B). Fully infused samples were found to lose 0.025±0.004 µL of liquid, while

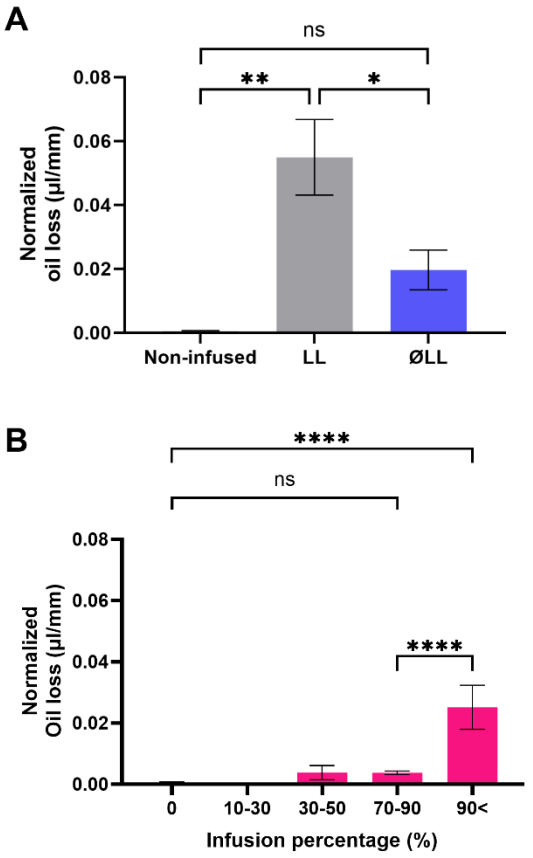

Figure 44. Silicone Oil Loss of Infused Catheter Samples

(A) Liquid loss comparison between non-infused silicone catheter samples; silicone catheter samples with (LL) and without liquid layer (ØLL) **(B)** Amount of liquid loss per mm of sample's length is plotted against catheters infused into different infusion percentage (%). The error bars represent the standard error of the mean. Statistical significance between the groups was evaluated using ANOVA test. * = P < 0.05; ** = P < 0.01; **** = P < 0.0001 and ns = not significant.

samples at 70–90% infusion lost significantly less at 0.004±0.0004 μL ($P < 0.0001$). Samples at 30–50% infusion lost 0.004 ±0.0013 μL of liquid, which was not significantly different from samples at 70–90% infusion ($P > 0.9999$). Neither samples at 30–50% nor 70–90% of infusion were found to be significantly different from non-infused controls ($P = 0.50$ and 0.52, respectively), unlike fully infused samples, which were significantly higher ($P < 0.0001$).

Various absorption routes for silicone oil were tested in animal models in past literatures, including oral ingestion, intraperitoneal, intramuscular, intravenous injections, and subcutaneous administration (Hao *et al*., 2022; The Danish Environmental Protection Agency, 2014; Franklin, 1967; McGregor, 1961). The absorption into body tissues depends on factors like polymerization degree and molecular weight, with silicone oil above a certain polymerization degree (>15, equivalent to >10 cSt viscosity) unable to directly penetrate membrane systems (Hao *et al*., 2022). In mouse models, oral administration of up to 1000 mg/kg of 10 cSt silicone oil over a year showed no toxic reactions (Hao *et al*., 2022). Similarly, injections of 1-500 mL of silicone oil intraperitoneally, subcutaneously, or intramuscularly in various animal species such as monkeys, guinea pigs, rats, and mice did not result in toxicity responses (The Danish Environmental Protection Agency, 2014; Franklin, 1967; McGregor, 1961). The permitted daily exposure of inorganic silicon varies depending on the administration route: 18,919 μg/day for oral administration, 93 μg/day for parenteral exposure, and 224 μg/day for inhalation route. (Hao *et al*., 2022). In the context of liquid-infused catheters, removal of the free liquid layer in 40 cm (typical longest catheter length) fully infused catheters would result in an estimated silicone oil loss of ~8 μL (0.02 μL/mm x 400 mm; Figure 44A), i.e. ~7600 μg (0.008 mL x 0.95 g/mL). For catheters infused to 70-90%, this loss could decrease further to an estimated of ~1.6 μL (0.004 μL/mm x 400 mm; Figure 44B), i.e. 1520 μg (0.0016 mL x 0.95 g/mL). In both scenarios, potential

silicone oil loss remains below reported dosages that could cause health impacts via oral administration, but above permitted daily exposure for parenteral and inhalation route. Further testing is therefore essential to assess the safety implications of the detected amount of silicone oil loss in urinary tissue.

5.4 Summary

We have successfully developed a protocol relying on the UV-VIS instrument for detecting silicone oil loss in liquid-infused catheters after exploring various methodologies, including microscopy, dynamic light scattering, ICP-OES, and UV-VIS instruments (Table 1). Together with the results from Chapters 3 and 4, we observe that fully infused silicone catheter materials, devoid of a free surface liquid layer, not only maintain their efficacy in repelling CAUTI-related pathogens but also significantly reduce silicone oil loss into the environment. This enhancement elevates the safety profile and usability of liquid-infused catheters in medical settings. Furthermore, similar benefits are observed when catheters are infused to 70-90%, further diminishing the silicone oil content within the catheter. Our reported liquid loss of infused catheters (7600 μg; if all silicone oil content was removed in 40 cm fully infused catheter) falls below past literature's estimation of conservative permitted daily exposure to silicone oil when administered orally (18919 μg/day), but above permitted daily exposure in parenteral (93 μg/day) and inhalation route (224 μg/day). Further understanding of the safety and impact of liquid-infused urinary catheters is therefore warranted, as the impact of silicone oil on urinary tissue might differ.

Table 1. Protocol for Detecting Minuscule Amounts of Silicone Oil.

Methods	Principle	Limitation
Microscopy	Direct visualization of silicone oil under a microscope enables quantification.	- Transferring liquid from the water body used to strip oil from catheters could potentially result in the loss of silicone oil samples. - A high-resolution microscope is required to visualize minute quantities of silicone oil effectively.
Dynamic light scattering	As a laser passes through the light sample, the suspended molecules in the water scatter light in a distinct manner based on their size, facilitating the quantification of oil droplets.	- The coalescence of silicone oil droplets leads to significant sample instability, resulting in measurement failures. - The high polydispersity of silicone oil droplets in terms of size contributes to inaccurate results.
ICP-OES	Following the digestion of samples into their elemental composition, the argon plasma within the machine energizes the atoms and ions in the sample. The subsequent transition of electrons from an excited to a ground state releases element-specific light, enabling the quantification of silicon.	- Silicone contamination is frequently encountered in containers. - The utilization of highly concentrated acids poses significant dangers and risks. - Silicone's low solubility in acid and high volatility could aggravate the loss of samples, particularly when the silicone being measured is already on the smaller end.
UV-Vis spectrometry	This instrument measures the light absorbance of the liquid sample: - An oil-in-water emulsion might render the solution more turbid compared to water with a lower concentration of silicone oil. - By adding an emulsifier, a homogenized solution containing silicone oil and water can be created, yielding solutions with varying absorbance. - By isolating the water layer from the dyed oil-water mixture, the absorbance of just the oil can be measured.	- The transfer of liquid from the water body used to strip oil from catheters poses a risk of losing silicone oil samples. - The use of a silicone oil dye was necessary to enhance detection signals. - To separate water from silicone oil droplets, precise control of temperature is essential to prevent accidental evaporation of oil samples.

CHAPTER 6
CONCLUSIONS

6.1 Summary of Dissertation Work

Previous studies have demonstrated that fully infused liquid-infused urinary catheters possess the capability to diminish *in vivo* infection by mitigating Fb adhesion (Andersen *et al*., 2022). In this dissertation, we aimed to standardize the production process and provide insights for the future manufacturing of liquid-infused catheters. This also provides information for the manufacturing of liquid infused catheters from existing commercially available catheters. We detailed the development of these catheters, characterizing their physical properties and the infusion duration needed to achieve specific infusion percentages of the materials. Our findings revealed that full liquid infusion significantly increased the mass, length, inner, and outer diameter of the medical device, and that these parameters were dependent on infusion extent, highlighting the importance of manufacturing controls to ensure size appropriateness for patient use when employing liquid infusion in catheters. Given the involvement of silicone oil, a foreign liquid, in these medical devices, we have also devised methods to reduce the amount of free silicone liquid present in liquid infused catheters. We removed the bulk of the free liquid layer from liquid infused catheters by absorbing the liquid, resulting in a decrease in thickness of the liquid layer from ~60 μm to <1 μm; and adjusted the infusion duration to decrease the amount of silicone liquid infused, thereby enabling the creation of infused catheters with varying levels of silicone oil incorporation.

Tests measuring sliding angle and droplet speed suggested that catheters with and without a free liquid layer exhibited comparable slippery surfaces, indicating similar anti-fouling functionality. Subsequent functionality tests demonstrated that both types of catheters performed similarly in repelling protein and bacteria associated with CAUTI. Furthermore, in partially infused samples, tests showed a gradual increase in slippery surface as infusion percentage increased, suggesting a

potential enhancement in anti-fouling properties with higher infusion levels. This was corroborated by testing the adhesion of bacteria and proteins, where both Fb and E. faecalis adhesion decreased with increasing infusion levels.

Furthermore, we have devised a protocol for detecting minuscule amounts of silicone oil (<0.005μL). Employing spectrophotometry testing, we observed that removing bulk amounts of silicone oil through liquid absorption led to a significant reduction in the quantity of liquid lost to the environment. Moreover, we discovered that infused catheters with higher levels of infusion percentage exhibited a gradual decrease in liquid loss to the environment. Combining these results with our functionality tests, this dissertation provides evidence of the potential benefits of incorporating the removal of the free liquid layer into the fabrication process of liquid-infused catheters as a method of both preserving antifouling properties, which may improve the safety of such medical device.

Our findings suggest that lower infusion percentages, particularly within the range of 70-90%, perform comparably to fully infused catheter material. Parameter changes are of lesser extent when infused to a lower percentage, and less oil can be removed from catheters infused to a lower extent. This implies that lower infusion percentages, such as those within the 70-90% range, may be more optimal in manufacturing, as they can help avoid significant size changes while still maintaining functionality and improving safety. Although not essential, as highlighted in Section 1.2.2, introducing surface roughness to the polymer being infused can improve the stability of the liquid on the solid surface via capillary forces (Lv *et al*., 2022; Boveri *et al*., 2021; Cai *et al*., 2021, 2020; Huang and Guo, 2019). However, it's important to acknowledge that if the liquid is gradually depleted over time due to aging or leakage (which necessitates further investigation), there's a possibility that the catheter could experience increased blockage due to increased roughness of the

surface (Lawrence and Turner, 2006a). Moreover, a rougher surface may promote pathogen colonization by providing more surface area for adhesion and attachment compared to a smoother surface (Zheng *et al.*, 2021). Finally, there are several knowledge gaps remaining in this study. These include the need to measure the flexural strength of the catheter material post-infusion, as changes in structural integrity may occur. Furthermore, detailed modeling of the infusion phenomenon could consider different brands of commercially available catheters (that might consist of different crosslink density or other factors that could affect infusion) to enhance generalizability. Additionally, in vivo testing to determine the relationship between oil quantity and catheter oil loss is another important area that requires further investigation.

6.2 Future Directions

While we have successfully characterized the fabrication process and functionality of liquid-infused catheters, transitioning them to clinical trials and eventual market release as medical devices necessitates further investigation in several areas. These include examining the interaction between the silicone oil layer and urine within the bladder, determining the rate of silicone oil release from the catheter into the bladder environment, assessing the material's aging and stability within the bladder. Furthermore, the exploration of the potential incorporation of functional lipids or drugs with the silicone oil layer may further enhance functionality.

Although many investigations of liquid-infused silicones have examined their ability to repel bacterial adhesion (Shen *et al*., 2023; Van Den Berg *et al*., 2023; Lavielle *et al*., 2021; Regan *et al*., 2019; Sotiri *et al*., 2018; Kovalenko *et al*., 2017; Kratochvil *et al*., 2016; Manna *et al*., 2015; MacCallum *et al*., 2015; Howell *et al*., 2014; Epstein *et al*., 2012), notably fewer have examined protein deposition (Andersen *et al*., 2022; Li *et al*., 2022; Amini *et al*., 2017). However, recent work has begun to reveal not only the critical role that proteins play in infection (Flores-Mireles

et al., 2016a, 2016b; Flores-Mireles *et al*., 2014; Sunny *et al*., 2014), but also the ability of liquid-infused silicones to robustly resist their deposition (Andersen *et al*., 2022). In this dissertation, we show that protein deposition on liquid-infused surfaces can be modulated by adjusting the quantity of silicone oil embedded in the polymer network. The ability to precisely modulate surface protein levels could potentially open new doors in a variety of fields, particularly materials engineering. In addition, the mechanism by which liquid-infused surfaces reduce protein deposition will be an important area of investigation going forward and may involve multiple interacting factors including masking of microscale defects and the neutralization of surface charges (Van Den Berg *et al*., 2023; Lavielle *et al*., 2021; Hyltegren *et al*., 2020; Kubiak *et al*., 2015; Lin *et al*., 2005; Jung *et al*., 2003; Marchin & Berrie, 2003).

Overall, the enhanced understanding of liquid-infused systems enables us to manufacture medical devices capable of effectively repelling foulants like proteins and bacteria, which are common causes of infections. With this technological advancement, we can transition away from relying solely on antibiotics, potentially reducing the incidence of CAUTIs. This advancement will be particularly significant for safeguarding our elderly community and offering hope to individuals and families affected by recurrent infections.

6.3 Disclosure

In this thesis, the Chat Generative Pre-Trained Transformer 3.5 was employed as a tool for grammar checks and enhancing language readability. All content generated by the tool underwent thorough manual review and verification to guarantee content accuracy. Modifications were applied as necessary during this process.

REFERENCES

Absulkareem, A., Abusrafa, A.E., Zavahir, S., Habib, S., Sobolčiak, P., Lehocky, M., Pištěková, H., Humpoliček, P., & Popelka, A. (2022). Novel Slippery Liquid-Infused Porous Surfaces (SLIPS) Based on Electrospun Polydimethylsiloxane/Polystyrene Fibrous Structures Infused with Natural Blackseed Oil. *Int. J. Mol. Sci. 23(7).* 3682.

Adamczyk, B., Struwe, W. B., Ercan, A., Nigrovic, P. A., & Rudd, P. M. (2013). Characterization of Fibrinogen Glycosylation and Its Importance for Serum/Plasma *N* -Glycome Analysis. *Journal of Proteome Research*, *12*(1), 444–454. https://doi.org/10.1021/pr300813h

Aharony, S. M., Lam, O., & Corcos, J. (2017). Evaluation of lower urinary tract symptoms in multiple sclerosis patients: Review of the literature and current guidelines. *Canadian Urological Association Journal*, *11*(1–2), 61. https://doi.org/10.5489/cuaj.4058

Akkurt Arslan, M., Brignole-Baudouin, F., Chardonnet, S., Pionneau, C., Blond, F., Baudouin, C., & Kessal, K. (2023). Profiling tear film enzymes reveals major metabolic pathways involved in the homeostasis of the ocular surface. *Scientific Reports*, *13*(1), 15231. https://doi.org/10.1038/s41598-023-42104-2

Akter, M., Sikder, Md. T., Rahman, Md. M., Ullah, A. K. M. A., Hossain, K. F. B., Banik, S., Hosokawa, T., Saito, T., & Kurasaki, M. (2018). A systematic review on silver nanoparticles-induced cytotoxicity: Physicochemical properties and perspectives. *Journal of Advanced Research*, *9*, 1–16. https://doi.org/10.1016/j.jare.2017.10.008

Al Taweel, W., & Seyam, R. (2015). Neurogenic bladder in spinal cord injury patients. *Research and Reports in Urology*, 85. https://doi.org/10.2147/RRU.S29644

Al-Badr, A., & Al-Shaikh, G. (2000). *Recurrent Urinary Tract Infections Management in Women*.

Alcantar, N. A., Aydil, E. S., & Israelachvili, J. N. (2000). Polyethylene glycol-coated biocompatible surfaces. *Journal of Biomedical Materials Research*, *51*(3), 343–351. https://doi.org/10.1002/1097-4636(20000905)51:3<343::AID-JBM7>3.0.CO;2-D

Alshehri, S. M., Aldalbahi, A., Al-hajji, A. B., Chaudhary, A. A., Panhuis, M. I. H., Alhokbany, N., & Ahamad, T. (2016). Development of carboxymethyl cellulose-based hydrogel and nanosilver composite as antimicrobial agents for UTI pathogens. *Carbohydrate Polymers*, *138*, 229–236. https://doi.org/10.1016/j.carbpol.2015.11.004

Amini, S., Kolle, S., Petrone, L., Ahanotu, O., Sunny, S., Sutanto, C.N., Hoon, S., Cohen, L., Weaver, J.C., Aizenberg, J., Vogel, N., & Miserez, A. (2017). Preventing mussel adhesion using lubricant-infused materials. *Science. 357(6352).* 668-673.

Andersen, M. J., & Flores-Mireles, A. L. (2019). Urinary Catheter Coating Modifications: The Race against Catheter-Associated Infections. *Coatings*, *10*(1), 23. https://doi.org/10.3390/coatings10010023

Andersen, M. J., Fong, C., La Bella, A. A., Molina, J. J., Molesan, A., Champion, M. M., Howell, C., & Flores-Mireles, A. L. (2022). Inhibiting host-protein deposition on urinary catheters reduces associated urinary tract infections. *eLife*, *11*, e75798. https://doi.org/10.7554/eLife.75798

Anderson, G.G., Palermo, J.J., Schilling, J.D., Roth, R., Heuser, J., & Hultgren, S.J. (2003). Intracellular Bacterial Biofilm-Like Pods in Urinary Tract Infections. *Science. 301(5629).* 105-107.

Applebee, Z., & Howell C. (2024). Multi-component liquid-infused systems: a new approach to functional coatings. *Industrial Chemistry & Materials.* DOI: 10.1039/d4im00003j

Armbruster, C. E., & Mobley, H. L. T. (2012). Merging mythology and morphology: The multifaceted lifestyle of Proteus mirabilis. *Nature Reviews Microbiology*, *10*(11), 743–754. https://doi.org/10.1038/nrmicro2890

Armbruster, D. A., & Pry, T. (2008). *Limit of Blank, Limit of Detection and Limit of Quantitation*.

Assadi, F. (2018). Strategies for preventing catheter-associated urinary tract infections. *International Journal of Preventive Medicine*, *9*(1), 50. https://doi.org/10.4103/ijpvm.IJPVM_299_17

Badv, M., Alonso-Cantu, C., Shakeri, A., Hosseinidoust, Z., Weitz, J. I., & Didar, T. F. (2019). Biofunctional Lubricant-Infused Vascular Grafts Functionalized with Silanized Bio-Inks Suppress Thrombin Generation and Promote Endothelialization. *ACS Biomaterials Science & Engineering*, *5*(12), 6485–6496. https://doi.org/10.1021/acsbiomaterials.9b01062

Badv, M., Jaffer, I. H., Weitz, J. I., & Didar, T. F. (2017). An omniphobic lubricant-infused coating produced by chemical vapor deposition of hydrophobic organosilanes attenuates clotting on catheter surfaces. *Scientific Reports*, *7*(1), 11639. https://doi.org/10.1038/s41598-017-12149-1

Bagley, K., & Severud, L. (2021). Preventing Catheter-Associated Urinary Tract Infections with Incontinence Management Alternatives. *Nursing Clinics of North America*, *56*(3), 413–425. https://doi.org/10.1016/j.cnur.2021.05.002

Banan Khorshid, Z., Mahdi Doroodmand, M., & Abdollahi, S. (2021). UV–Vis. Spectrophotometric method for oil and grease determination in water, soil and different mediates based on emulsion. *Microchemical Journal*, *160*, 105620. https://doi.org/10.1016/j.microc.2020.105620

Barthlott, W., & Neinhuis, C. (1997). Purity of the sacred lotus, or escape from contamination in biological surfaces. *Planta*, *202*(1), 1–8. https://doi.org/10.1007/s004250050096

Bazyar, H., Lv, P., Wood, J. A., Porada, S., Lohse, D., & Lammertink, R. G. H. (2018). Liquid–liquid displacement in slippery liquid-infused membranes (SLIMs). *Soft Matter*, *14*(10), 1780–1788. https://doi.org/10.1039/C7SM02337E

Becknell, B., Schober, M., Korbel, L., & Spencer, J. D. (2015). The diagnosis, evaluation and treatment of acute and recurrent pediatric urinary tract infections. *Expert Review of Anti-Infective Therapy*, *13*(1), 81–90. https://doi.org/10.1586/14787210.2015.986097

Beek, M.V., Jones, L., & Sheardown, H. (2008). Hyaluronic acid containing hydrogels for the reduction of protein adsorption. *Biomaterials. 29.* 780-789.

Belas, R. (2013). When the swimming gets tough, the tough form a biofilm. *Mol Microbiol. 90(1).* 1-5.

Belfield, P. W. (1988). Everyday Aids and Appliances. *Br Med J (Clin Res Ed). 296(6625)*. 836-837.

Benton, J., Chawla, J., Parry, S., & Stickler, D. (1992). Virulence factors in Escherichia coli from urinary tract infections in patients with spinal injuries. *The Journal of Hospital Infection. 22(2).* 117-127.

Bera, B., Khazal, R., & Schroën, K. (2021). Coalescence dynamics in oil-in-water emulsions at elevated temperatures. *Scientific Reports*, *11*(1), 10990. https://doi.org/10.1038/s41598-021-89919-5

Bergqvist, D., Brönnestam, R., Hedelin, H., & Ståhl, A. (1980). The relevance of urinary sampling methods in patients with indwelling Foley catheters. *Br J Urol. 52(2).* 92-95.

Berka, R. M., & Vasil, M. L. (1982). Phospholipase C (Heat-Labile Hemolysin) of Pseudomonas aeruginosa: Purification and Preliminary Characterization. *J. BACTERIOL.*, *152*.

Bhattacharyya, R. P., Bandyopadhyay, N., Ma, P., Son, S. S., Liu, J., He, L. L., Wu, L., Khafizov, R., Boykin, R., Cerqueira, G. C., Pironti, A., Rudy, R. F., Patel, M. M., Yang, R., Skerry, J., Nazarian, E., Musser, K. A., Taylor, J., Pierce, V. M., … Hung, D. T. (2019). Simultaneous detection of genotype and phenotype enables rapid and accurate antibiotic susceptibility determination. *Nature Medicine*, *25*(12), 1858–1864. https://doi.org/10.1038/s41591-019-0650-9

Bikerman, J. J. (1950). Sliding of drops from surfaces of different roughnesses. *Journal of Colloid Science*, *5*(4), 349–359. https://doi.org/10.1016/0095-8522(50)90059-6

Bjelobrk, N., Girard, H.-L., Bengaluru Subramanyam, S., Kwon, H.-M., Quéré, D., & Varanasi, K. K. (2016). Thermocapillary motion on lubricant-impregnated surfaces. *Physical Review Fluids*, *1*(6), 063902. https://doi.org/10.1103/PhysRevFluids.1.063902

Bocquet, L., & Lauga, E. (2011). A smooth future? *Nature Materials*, *10*(5), 334–337. https://doi.org/10.1038/nmat2994

Bohn, H. F., & Federle, W. (2004). Insect aquaplaning: *Nepenthes* pitcher plants capture prey with the peristome, a fully wettable water-lubricated anisotropic surface. *Proceedings of the National Academy of Sciences*, *101*(39), 14138–14143. https://doi.org/10.1073/pnas.0405885101

Boles, B. R., Thoendel, M., & Singh, P. K. (2004). Self-generated diversity produces “insurance effects” in biofilm communities. *Proceedings of the National Academy of Sciences*, *101*(47), 16630–16635. https://doi.org/10.1073/pnas.0407460101

Bologna, R. A., Tu, L. M., Polansky, M., Fraimow, H. D., Gordon, D. A., & Whitmore, K. E. (1999). Hydrogel/silver ion-coated urinary catheter reduces nosocomial urinary tract infection rates in intensive care unit patients: A multicenter study. *Urology*, *54*(6), 982–987. https://doi.org/10.1016/S0090-4295(99)00318-0

Bonadio, W., & Maida, G. (2014). Urinary Tract Infection in Outpatient Febrile Infants Younger than 30 Days of Age A 10-year Evaluation. *The Pediatric Infectious Disease Journal. 33(4).* 342-344.

Borkow G., & Gabbay, J. (2004). Putting copper into action: copper- impregnated products with potent biocidal activities. *The Faseb Journal.* DOI: https://doi.org/10.1096/fj.04-2029fje

Bossa, L., Kline, K., McDougald, D., Lee, B. B., & Rice, S. A. (2017). Urinary catheter-associated microbiota change in accordance with treatment and infection status. *PLOS ONE*, *12*(6), e0177633. https://doi.org/10.1371/journal.pone.0177633

Boveri, G., Corozzi, A., Veronesi, F., & Raimondo, M. (2021). Different Approaches to Low-Wettable Materials for Freezing Environments: Design, Performance and Durability. *Coatings*, *11*(1), 77. https://doi.org/10.3390/coatings11010077

Brading, A. F. (1999). The physiology of the mammalian urinary outflow tract. *Experimental Physiology*, *84*(1), 215–221. https://doi.org/10.1111/j.1469-445X.1999.tb00084.x

Brown, P.S., & Bhushan, B. (2017). Liquid-impregnated porous polypropylene surfaces for liquid repellency. *Journal of Colloid and Interface Science. 487.* 437-443.

Burkett, E., Carpenter, C. R., Arendts, G., Hullick, C., Paterson, D. L., & Caterino, J. M. (2019). Diagnosis of urinary tract infection in older persons in the emergency department: To pee or not to pee, that is the question. *Emergency Medicine Australasia*, *31*(5), 856–862. https://doi.org/10.1111/1742-6723.13376

Burnham, P., Dadhania, D., Heyang, M., Chen, F., Westblade, L. F., Suthanthiran, M., Lee, J. R., & De Vlaminck, I. (2018). Urinary cell-free DNA is a versatile analyte for monitoring infections of the urinary tract. *Nature Communications*, *9*(1), 2412. https://doi.org/10.1038/s41467-018-04745-0

Cai, G., Liu, F., & Wu, T. (2021). Slippery liquid-infused porous surfaces with inclined microstructures to enhance durable anti-biofouling performances. *Colloids and Surfaces B: Biointerfaces*, *202*, 111667. https://doi.org/10.1016/j.colsurfb.2021.111667

Cai, G., Zeng, Q., & Wu, T. (2020). Effect of Surface Microstructure on the Long-term Anti-bacterial Performance for Slippery Liquid Infused Porous Surfaces. *2020 IEEE SENSORS*, 1–4. https://doi.org/10.1109/SENSORS47125.2020.9278715

Cai, Z., & Pham, J. T. (2022). How Swelling, Cross-Linking, and Aging Affect Drop Pinning on Lubricant-Infused, Low Modulus Elastomers. *ACS Applied Polymer Materials*, *4*(5), 3013–3022. https://doi.org/10.1021/acsapm.1c01455

Cai, Z., Skabeev, A., Morozova, S., & Pham, J. T. (2021). Fluid separation and network deformation in wetting of soft and swollen surfaces. *Communications Materials*, *2*(1), 21. https://doi.org/10.1038/s43246-021-00125-2

Calderon-Margalit, R., Golan, E., Twig, G., Leiba, A., Tzur, D., Afek, A., Skorecki, K., & Vivante, A. (2018). History of Childhood Kidney Disease and Risk of Adult End-Stage Renal Disease. *New England Journal of Medicine*, *378*(5), 428–438. https://doi.org/10.1056/NEJMoa1700993

Campoccia, D., Montanaro, L., & Arciola, C. R. (2013). A review of the biomaterials technologies for infection-resistant surfaces. *Biomaterials*, *34*(34), 8533–8554. https://doi.org/10.1016/j.biomaterials.2013.07.089

Carman, M.L., Estes, T.G., Feinberg, A.W., Schumacher, J.F., Wilerson, W., Wilson, L.H., Callow, M.E., Callow, J.A., & Brennan, A.B. (2005). Engineered antifouling microtopographies – correlating wettability with cell attachment. *Biofouling. 22(1).* 11-21.

Cathcart, G. R. A., Quinn, D., Greer, B., Harriott, P., Lynas, J. F., Gilmore, B. F., & Walker, B. (2011). Novel Inhibitors of the Pseudomonas aeruginosa Virulence Factor LasB: A Potential Therapeutic Approach for the Attenuation of Virulence Mechanisms in Pseudomonal Infection. *Antimicrobial Agents and Chemotherapy*, *55*(6), 2670–2678. https://doi.org/10.1128/AAC.00776-10

CDC. (2019). Antibiotic Resistance Threats in the United States. http://dx.doi.org/10.15620/cdc:82532.

Chamy R., (2013). Antimicrobial Modifications of Polymers Intechopen. https://doi.org/10.5772/52777

Chen, J., Howell, C., Haller, C. A., Patel, M. S., Ayala, P., Moravec, K. A., Dai, E., Liu, L., Sotiri, I., Aizenberg, M., Aizenberg, J., & Chaikof, E. L. (2017). An immobilized liquid interface prevents device associated bacterial infection in vivo. *Biomaterials*, *113*, 80–92. https://doi.org/10.1016/j.biomaterials.2016.09.028

Chene, G., Boulard, G., & Gachie, J.P. (1990). A controlled trial of a new material for coating urinary catheters. *Agressologie: Revue Internationale de Physio-biologie et de Pharmacologie Appliquees aux Effets de L'agression. 31(8).* 499-501.

Cheng, Z., Shurer, C. R., Schmidt, S., Gupta, V. K., Chuang, G., Su, J., Watkins, A. R., Shetty, A., Spector, J. A., Hui, C.-Y., Reesink, H. L., & Paszek, M. J. (2020). The surface stress of biomedical silicones is a stimulant of cellular response. *Science Advances*, *6*(15), eaay0076. https://doi.org/10.1126/sciadv.aay0076

Chisholm, C. F., Nguyen, B. H., Soucie, K. R., Torres, R. M., Carpenter, J. F., & Randolph, T. W. (2015). In Vivo Analysis of the Potency of Silicone Oil Microdroplets as Immunological Adjuvants in Protein Formulations. *Journal of Pharmaceutical Sciences*, *104*(11), 3681–3690. https://doi.org/10.1002/jps.24573

Cho, Y.H., Lee, S.J., Lee, J.Y., Kim, S.W., Kwon, I.C., Chung, S.Y., & Yoon, M.S. (2002). Prophylactic efficacy of a new gentamicin-releasing urethral catheter in short-term catheterized rabbits. *BJU International . 87(1).* 104-109.

Cho, Y.W., Park, J.H., Kim, S.H., Cho, Y., Choi, J.M., Shin, H.J., Bae, Y.H., Chung, H., Jeong, S.Y., & Kwon, I.C. (2003). Gentamicin-releasing urethral catheter for short-term catheterization. *Journal of Biomaterials Science. 14(9).* 963-972.

Choi, J.B., & Min, S.K. (2021). Complicated urinary tract infection in patients with benign prostatic hyperplasia. *Journal of Infection and Chemotherapy. 27(9).* 1284-1287.

Cole, S. J., & Lee, V. T. (2016). Cyclic Di-GMP Signaling Contributes to Pseudomonas aeruginosa-Mediated Catheter-Associated Urinary Tract Infection. *Journal of Bacteriology*, *198*(1), 91–97. https://doi.org/10.1128/JB.00410-15

Cole, S. J., Hall, C. L., Schniederberend, M., Farrow Iii, J. M., Goodson, J. R., Pesci, E. C., Kazmierczak, B. I., & Lee, V. T. (2018). Host suppression of quorum sensing during catheter-associated urinary tract infections. *Nature Communications*, *9*(1), 4436. https://doi.org/10.1038/s41467-018-06882-y

Cole, S. J., Records, A. R., Orr, M. W., Linden, S. B., & Lee, V. T. (2014). Catheter-Associated Urinary Tract Infection by Pseudomonas aeruginosa Is Mediated by Exopolysaccharide-Independent Biofilms. *Infection and Immunity*, *82*(5), 2048–2058. https://doi.org/10.1128/IAI.01652-14

Colomer-Winter, C., Flores-Mireles, A. L., Baker, S. P., Frank, K. L., Lynch, A. J. L., Hultgren, S. J., Kitten, T., & Lemos, J. A. (2018). Manganese acquisition is essential for virulence of Enterococcus faecalis. *PLOS Pathogens*, *14*(9), e1007102. https://doi.org/10.1371/journal.ppat.1007102

Colomer-Winter, C., Lemos, J.A., & Flores-Mireles, A.L. (2019). Biofilm Assays on Fibrinogen-coated Silicone Catheters and 96-well Polystyrene Plates. *Bio Protoc. 9(6).* E3196.

Colosqui, C. E., Wexler, J. S., Liu, Y., & Stone, H. A. (2016). Crossover from shear-driven to thermally activated drainage of liquid-infused microscale capillaries. *Physical Review Fluids*, *1*(6), 064101. https://doi.org/10.1103/PhysRevFluids.1.064101

Conover, M. S., Hadjifrangiskou, M., Palermo, J. J., Hibbing, M. E., Dodson, K. W., & Hultgren, S. J. (2016). Metabolic Requirements of Escherichia coli in Intracellular Bacterial Communities during Urinary Tract Infection Pathogenesis. *mBio*, *7*(2), e00104-16. https://doi.org/10.1128/mBio.00104-16

Cortes-Penfield, N. W., Trautner, B. W., & Jump, R. L. P. (2017). Urinary Tract Infection and Asymptomatic Bacteriuria in Older Adults. *Infectious Disease Clinics of North America*, *31*(4), 673–688. https://doi.org/10.1016/j.idc.2017.07.002

Costerton, J. W., Irvin, R. T., & Cheng, K. J. (1981). The Bacterial Glycocalyx in Nature and Disease. *Annual Review of Microbiology*, *35*(1), 299–324. https://doi.org/10.1146/annurev.mi.35.100181.001503

COVID-19: U.S. Impact on Antimicrobial Resistance, Special Report 2022. (2022). National Center for Emerging and Zoonotic Infectious Diseases. https://doi.org/10.15620/cdc:117915

Cox, J., & Mann, M. (2008). MaxQuant enables high peptide identification rates, individualized p.p.b.-range mass accuracies and proteome-wide protein quantification. *Nature Biotechnology*, *26*(12), 1367–1372. https://doi.org/10.1038/nbt.1511

Croxall, G., Weston, V., Joseph, S., Manning, G., Cheetham, P., & McNally, A. (2011). Increased human pathogenic potential of Escherichia coli from polymicrobial urinary tract infections in comparison to isolates from monomicrobial culture samples. *Journal of Medical Microbiology*, *60*(1), 102–109. https://doi.org/10.1099/jmm.0.020602-0

Cui, Y., Zhao, Y., Tian, Y., Zhang, W., Lü, X., & Jiang, X. (2012). The molecular mechanism of action of bactericidal gold nanoparticles on Escherichia coli. *Biomaterials*, *33*(7), 2327–2333. https://doi.org/10.1016/j.biomaterials.2011.11.057

Curran, E. M., Tassell, A. H., Judy, B. M., Nowicki, B., Montgomery-Rice, V., Estes, D. M., & Nowicki, S. (2007). Estrogen Increases Menopausal Host Susceptibility to Experimental Ascending Urinary-Tract Infection. *The Journal of Infectious Diseases*, *195*(5), 680–683. https://doi.org/10.1086/511275

D'Incau, S., Atkinson, A., Leitner, L., Kronenberg, A., Kessler, T. M., & Marschall, J. (2023a). Bacterial species and antimicrobial resistance differ between catheter and non–catheter-associated urinary tract infections: Data from a national surveillance network. *Antimicrobial Stewardship & Healthcare Epidemiology*, *3*(1), e55. https://doi.org/10.1017/ash.2022.340

Dai, S., Gao, Y., & Duan, L. (2023). Recent advances in hydrogel coatings for urinary catheters. *Journal of Applied Polymer Science. 140(14).*e53701.

Damle, V. G., Tummala, A., Chandrashekar, S., Kido, C., Roopesh, A., Sun, X., Doudrick, K., Chinn, J., Lee, J. R., Burgin, T. P., & Rykaczewski, K. (2015). "Insensitive" to Touch: Fabric-Supported Lubricant-Swollen Polymeric Films for Omniphobic Personal Protective Gear. *ACS Applied Materials & Interfaces*, *7*(7), 4224–4232. https://doi.org/10.1021/am5085226

Danaei, M., Dehghankhold, M., Ataei, S., Hasanzadeh Davarani, F., Javanmard, R., Dokhani, A., Khorasani, S., & Mozafari, M. (2018). Impact of Particle Size and Polydispersity Index on the Clinical Applications of Lipidic Nanocarrier Systems. *Pharmaceutics*, *10*(2), 57. https://doi.org/10.3390/pharmaceutics10020057

Daniels, K. R., Lee, G. C., & Frei, C. R. (2014). Trends in catheter-associated urinary tract infections among a national cohort of hospitalized adults, 2001-2010. *American Journal of Infection Control*, *42*(1), 17–22. https://doi.org/10.1016/j.ajic.2013.06.026

Danish Ministry of the Environment. (2014). Siloxanes (D3, D4,D5, D6, HMDS) Evaluation of health hazards and proposal of a health-based quality criterion for ambient air. *The Danish Environmental Protection Agency.* https://www2.mst.dk/Udgiv/publications/2013/08/978-87-93026-34-6.pdf

Darouiche, R. O., & Hull, R. A. (2012). Bacterial Interference for Prevention of Urinary Tract Infection. *Clinical Infectious Diseases*, *55*(10), 1400–1407. https://doi.org/10.1093/cid/cis639

Darouiche, R. O., Mansouri, M. D., Gawande, P. V., & Madhyastha, S. (2008). Efficacy of combination of chlorhexidine and protamine sulphate against device-associated pathogens. *Journal of Antimicrobial Chemotherapy*, *61*(3), 651–657. https://doi.org/10.1093/jac/dkn006

Davies, D.G., Parsek, M.R., Pearson, J.P., Iglewski, B.H., Costerton, J.W., & Greenberg, E.P. (1998). The Involvement of Cell-to-Cell Signals in the Development of a Bacterial Biofilm. *Science. 280(5361).* 295-298.

Delnay, K.M., Stonehill, W.H., Goldman, H., Jukkola, A.F., & Dmochowski, R.R. (1999). Bladder histological changes associated with chronic indwelling urinary catheter. *The Journal of Urology 161:1106–1108.*

Di Benedetto, A., Arena, S., Nicotina, P. A., Mucciardi, G., Galì, A., & Magno, C. (2013). Pacemakers in the upper urinary tract. *Neurourology and Urodynamics*, *32*(4), 349–353. https://doi.org/10.1002/nau.22310

Di Venanzio, G., Flores-Mireles, A. L., Calix, J. J., Haurat, M. F., Scott, N. E., Palmer, L. D., Potter, R. F., Hibbing, M. E., Friedman, L., Wang, B., Dantas, G., Skaar, E. P., Hultgren, S. J., & Feldman, M. F. (2019). Urinary tract colonization is enhanced by a plasmid that regulates uropathogenic Acinetobacter baumannii chromosomal genes. *Nature Communications*, *10*(1), 2763. https://doi.org/10.1038/s41467-019-10706-y

Díaz Pollán, B., Guedez López, G. V., García Clemente, P. M., Jiménez González, M., García Bujalance, S., & Gómez-Gil Mirá, M. R. (2022). Urinary Tract Infections in Hospitalized COVID-19 Patients, What's Up, Doc? *Journal of Clinical Medicine*, *11*(7), 1815. https://doi.org/10.3390/jcm11071815

DiCarlo-Meacham, A., Dengler, K., Welch, E.K., Hamade, S., Olsen, C., Horbach, N., Jeffrey, W., Mazloomdoost, D., & von Pechmann, W. (2022). Suprapubic Versus Transurethral Catheterization: Perioperative Outcomes After Colpocleisis. *Female Pelvic Medicine & Reconstructive Surgery. 28(3).* 149-152.

Doll, K., Fadeeva, E., Schaeske, J., Ehmke, T., Winkel, A., Heisterkamp, A., Chichkov, B. N., Stiesch, M., & Stumpp, N. S. (2017). Development of Laser-Structured Liquid-Infused Titanium with Strong Biofilm-Repellent Properties. *ACS Applied Materials & Interfaces*, *9*(11), 9359–9368. https://doi.org/10.1021/acsami.6b16159

Drewa, T., Wolski, Z., Galazka, P., Wozniak, A., Olszewska-Stonina, D., Sir, J. (2004). Silicone and latex urinary catheters cytotoxicity on primary cultured rabbit urothelial cells. *Pol Merkur Lekarski. 16(93).* 228-231.

Durán, N., Durán, M., De Jesus, M. B., Seabra, A. B., Fávaro, W. J., & Nakazato, G. (2016). Silver nanoparticles: A new view on mechanistic aspects on antimicrobial activity. *Nanomedicine: Nanotechnology, Biology and Medicine*, *12*(3), 789–799. https://doi.org/10.1016/j.nano.2015.11.016

Dutta, C., Pasha, K., Paul, S., Abbas, M. S., Nassar, S. T., Tasha, T., Desai, A., Bajgain, A., Ali, A., & Mohammed, L. (2022). Urinary Tract Infection Induced Delirium in Elderly Patients: A Systematic Review. *Cureus*. https://doi.org/10.7759/cureus.32321

Efstathiou, S.P., Pefanis, A.V., Tsioulos, D.I., Zacharos, I.D., Tsiakou, A.G., Mitromaras, A.G., Mastorantonakis, S.E., Kanavaki, S.B., & Mountokalakis, T.D. (2003). Acute Pyelonephritis in AdultsPrediction of Mortality and Failure of Treatment. *Arch Intern Med. 163(10).* 1206-1212.

Eisenbach, M. (2001). Bacterial Chemotaxis. *Encyclopedia of Life Sciences.*

Ejrnæs, K., Stegger, M., Reisner, A., Ferry, S., Monsen, T., Holm, S. E., Lundgren, B., & Frimodt-Møller, N. (2011). Characteristics of *Escherichia coli* causing persistence or relapse of urinary tract infections: Phylogenetic groups, virulence factors and biofilm formation. *Virulence*, *2*(6), 528–537. https://doi.org/10.4161/viru.2.6.18189

Eldridge, G. R., Hughey, H., Rosenberger, L., Martin, S. M., Shapiro, A. M., D'Antonio, E., Krejci, K. G., Shore, N., Peterson, J., Lukes, A. S., & Starks, C. M. (2021). Safety and immunogenicity of an adjuvanted *Escherichia coli* adhesin vaccine in healthy women with and without histories of recurrent urinary tract infections: Results from a first-in-human phase 1 study. *Human Vaccines & Immunotherapeutics*, *17*(5), 1262–1270. https://doi.org/10.1080/21645515.2020.1834807

Elliott, A. D. (2020). Confocal Microscopy: Principles and Modern Practices. *Current Protocols in Cytometry*, *92*(1), e68. https://doi.org/10.1002/cpcy.68

Epstein, A. K., Wong, T.-S., Belisle, R. A., Boggs, E. M., & Aizenberg, J. (2012). Liquid-infused structured surfaces with exceptional anti-biofouling performance. *Proceedings of the National Academy of Sciences*, *109*(33), 13182–13187. https://doi.org/10.1073/pnas.1201973109

Eriksen, J. R., Munk-Madsen, P., Kehlet, H., & Gögenur, I. (2019). Postoperative Urinary Retention After Laparoscopic Colorectal Resection with Early Catheter Removal: A Prospective Observational Study. *World Journal of Surgery*, *43*(8), 2090–2098. https://doi.org/10.1007/s00268-019-05010-1

Eto, D. S., Jones, T. A., Sundsbak, J. L., & Mulvey, M. A. (2007). Integrin-Mediated Host Cell Invasion by Type 1–Piliated Uropathogenic Escherichia coli. *PLoS Pathogens*, *3*(7), e100. https://doi.org/10.1371/journal.ppat.0030100

Fang, X., Liu, Y., Lei, S., & Ou, J. (2021). Slippery liquid-infused porous surface based on MOFs with excellent stability. *Chemical Physics Letters*, *771*, 138470. https://doi.org/10.1016/j.cplett.2021.138470

Fang, Z., Cheng, Y., Yang, Q., Lu, Y., Zhang, C., Li, M., Du, B., Hou, X., & Chen, F. (2022). Design of Metal-Based Slippery Liquid-Infused Porous Surfaces (SLIPSs) with Effective Liquid Repellency Achieved with a Femtosecond Laser. *Micromachines*, *13*(8), 1160. https://doi.org/10.3390/mi13081160

Faustino, C. M. C., Lemos, S. M. C., Monge, N., & Ribeiro, I. A. C. (2020). A scope at antifouling strategies to prevent catheter-associated infections. *Advances in Colloid and Interface Science*, *284*, 102230. https://doi.org/10.1016/j.cis.2020.102230

Feneley, R. C. L., Hopley, I. B., & Wells, P. N. T. (2015). Urinary catheters: History, current status, adverse events and research agenda. *Journal of Medical Engineering & Technology*, *39*(8), 459–470. https://doi.org/10.3109/03091902.2015.1085600

Flores-Mireles, A. L., Pinkner, J. S., Caparon, M. G., & Hultgren, S. J. (2014). EbpA vaccine antibodies block binding of *Enterococcus faecalis* to fibrinogen to prevent catheter-associated bladder infection in mice. *Science Translational Medicine*, *6*(254). https://doi.org/10.1126/scitranslmed.3009384

Flores-Mireles, A. L., Walker, J. N., Bauman, T. M., Potretzke, A. M., Schreiber, H. L., Park, A. M., Pinkner, J. S., Caparon, M. G., Hultgren, S. J., & Desai, A. (2016). Fibrinogen Release and Deposition on Urinary Catheters Placed during Urological Procedures. *Journal of Urology*, *196*(2), 416–421. https://doi.org/10.1016/j.juro.2016.01.100

Flores-Mireles, A. L., Walker, J. N., Caparon, M., & Hultgren, S. J. (2015). Urinary tract infections: Epidemiology, mechanisms of infection and treatment options. *Nature Reviews Microbiology*, *13*(5), 269–284. https://doi.org/10.1038/nrmicro3432

Flores-Mireles, A., Hreha, T. N., & Hunstad, D. A. (2019). Pathophysiology, Treatment, and Prevention of Catheter-Associated Urinary Tract Infection. *Topics in Spinal Cord Injury Rehabilitation*, *25*(3), 228–240. https://doi.org/10.1310/sci2503-228

Flory, P.J. (1950). Statistical Mechanics of Swelling of Network Structures. *J.Chem. 18(1).* 108-111.

Flory, P.J., & Rehner, J.Jr. (1943). Statistical mechanics of cross-linked polymer networks. II. Swelling. *Journal of Chemical Physics. 11(11).* 521-526

Flum, A. S., Firmiss, P. R., Bowen, D. K., Kukulka, N., Delos Santos, G. B., Dettman, R. W., & Gong, E. M. (2017). Testosterone Modifies Alterations to Detrusor Muscle after Partial Bladder Outlet Obstruction in Juvenile Mice. *Frontiers in Pediatrics*, *5*, 132. https://doi.org/10.3389/fped.2017.00132

Foxman, B. (2010). The epidemiology of urinary tract infection. *Nature Reviews Urology*, *7*(12), 653–660. https://doi.org/10.1038/nrurol.2010.190

Foxman, B. (2014). Urinary Tract Infection Syndromes: Occurrence, Recurrence, Bacteriology, Risk Factors, and Disease Burden. *Infectious Disease Clinics of North America. 28(1).* 1-13.

Foxman, B., Klemstine, K. L., & Brown, P. D. (2003). Acute Pyelonephritis in US Hospitals in 1997: Hospitalization and In-hospital Mortality. *Ann Epidemiol.13*(2).

Foxman, B., Zhang, L., Tallman, P., Palin, K., Rode, C., Bloch, C., Gillespie, B., Marrs, C.F. (1995). Virulence Characteristics of Escherichia coli Causing First Urinary Tract Infection Predict Risk of Second Infection. *The Journal of Infectious Diseases. 172(6).* 1536-1541.

Franklin, A., Silas, B., Thomas, R., Dicran, G., & Donald, B. (1967). The Present Status of Silicone Fluid in Soft Tissue Augmentation. *Plastic and Reconstructive Surgery. 39(4).* 411-420.

Gadalla, A. A. H., Friberg, I. M., Kift-Morgan, A., Zhang, J., Eberl, M., Topley, N., Weeks, I., Cuff, S., Wootton, M., Gal, M., Parekh, G., Davis, P., Gregory, C., Hood, K., Hughes, K., Butler, C., & Francis, N. A. (2019). Identification of clinical and urine biomarkers for uncomplicated urinary tract infection using machine learning algorithms. *Scientific Reports*, *9*(1), 19694. https://doi.org/10.1038/s41598-019-55523-x

Gambello, M. J., & Iglewski, B. H. (1991). Cloning and characterization of the Pseudomonas aeruginosa lasR gene, a transcriptional activator of elastase expression. *Journal of Bacteriology*, *173*(9), 3000–3009. https://doi.org/10.1128/jb.173.9.3000-3009.1991

Gaston, J. R., Andersen, M. J., Johnson, A. O., Bair, K. L., Sullivan, C. M., Guterman, L. B., White, A. N., Brauer, A. L., Learman, B. S., Flores-Mireles, A. L., & Armbruster, C. E. (2020). Enterococcus faecalis Polymicrobial Interactions Facilitate Biofilm Formation, Antibiotic Recalcitrance, and Persistent Colonization of the Catheterized Urinary Tract. *Pathogens*, *9*(10), 835. https://doi.org/10.3390/pathogens9100835

Gedde, U.W., Hellebuych, A., & Hedenqvist, M. (1996). Sorption of Low Molar Mass Silicones in Silicone Elastomers. *Polymer Engineering and Science. 36(16).* 2077-2082.

Geraldi, N. R., Guan, J. H., Dodd, L. E., Maiello, P., Xu, B. B., Wood, D., Newton, M. I., Wells, G. G., & McHale, G. (2019). Double-sided slippery liquid-infused porous materials using conformable mesh. *Scientific Reports*, *9*(1), 13280. https://doi.org/10.1038/s41598-019-49887-3

Gerstel, U., Latendorf, T., Bartels, J., Becker, A., Tholey, A., & Schröder, J. (2018). Hornerin contains a Linked Series of Ribosome-Targeting Peptide Antibiotics. *Scientific Reports. 2018 (8).* 16158.

Ghanadan, H., Hoseini, M., Sazgarnia, A., & Sharifi. S. (2019). Effect of Ion Pairs on Nonlinear Optical Properties of CrystalbViolet: Surfactants, Nano-droplets, and In Vitro Culture Conditions. *Journal of Electronic Materials.* DOI: 10.1007/s11664-019-07516-9

Gibney, L.E., (2016). Blocked urinary catheters: can they be better managed?. *British Journal of Nursing. 25(15).*

Gibson, K. E., Neill, S., Tuma, E., Meddings, J., & Mody, L. (2019). Indwelling urethral versus suprapubic catheters in nursing home residents: Determining the safest option for long-term use. *Journal of Hospital Infection*, *102*(2), 219–225. https://doi.org/10.1016/j.jhin.2018.07.027

Gilbert, P., Evans, D.J., Duguid, I.G., & Brown, M.R.W. (1991). Surface characteristics and adhesion of Escherichia coli and Staphylococcus epidermidis. *Journal of Applied Bacteriology. 71.* 72-77.

Ginsburg, C.M., & McCracken, G.H. (1982). Urinary Tract Infections in Young Infants. *Journal of Urology. 128(3).* 655.

Gjødsbøl, K., Christensen, J. J., Karlsmark, T., Jørgensen, B., Klein, B. M., & Krogfelt, K. A. (2006). Multiple bacterial species reside in chronic wounds: A longitudinal study. *International Wound Journal*, *3*(3), 225–231. https://doi.org/10.1111/j.1742-481X.2006.00159.x

Glahn, B.E., Braendstrup, O., & Olesen, H.P. (1988). Influence of drainage conditions on mucosal bladder damage by indwelling catheters. II. Histological study. *Scandinavian Journal of Urology and Nephrology 22:93–99.*

Glavan, A.C., Martinez, R.V., Subramaniam, A.B., Yoon, H.Y., Lange, H., Thuo, M.M., & Whitesides, G.M. (2014). Omniphobic "rF paper" produced by silanization of paper with fluoroalkyltrichlorosilanes. *Advanced Functional Materials. 24(1).* 60-70.

Goble, N.M., Clarke, T., & Hammonds, J.C. (1989). Histological Changes in the Urinary Bladder Secondary to Urethral Catheterisation. *British Journal of Urology. 63(4).* 354-357.

Golji, H. (1981). Complications of external condom drainage. *Spinal Cord*, *19*(3), 189–197. https://doi.org/10.1038/sc.1981.40

Goodband, S. J., Armstrong, S., Kusumaatmaja, H., & Voïtchovsky, K. (2020). Effect of Ageing on the Structure and Properties of Model Liquid-Infused Surfaces. *Langmuir*, *36*(13), 3461–3470. https://doi.org/10.1021/acs.langmuir.0c00059

Gould, C. V., Umscheid, C. A., Agarwal, R. K., Kuntz, G., & Pegues, D. A. (2009). *Guideline for Prevention of Catheter-Associated Urinary Tract Infections (2009).*

Gould, C.V., Umscheid, C.A., Agarwal, R.K., Kuntz, G., Pegues, D.A. & Healthcare Infection Control Practices Advisory Committee. (2015). Guideline for Prevention of Catheter-Associated Urinary Tract Infections. *Cambridge University Press. 31(4).*

Grahn, D., Norman, D. C., White, M. L., Cantrell, M., & Yoshikawa, T. T. (1985). *Validity of Urinary Catheter Specimen for Diagnosis of Urinary Tract Infection in the Elderly*.

Gribble, M. J., McCallum, N. M., & Schechter, M. T. (1988). Evaluation of diagnostic criteria for bacteriuria in acutely spinal cord injured patients undergoing intermittent catheterization. *Diagnostic Microbiology and Infectious Disease*, *9*(4), 197–206. https://doi.org/10.1016/0732-8893(88)90109-5

Guan, Q., Xia, C., & Li, W. (2019). Bio-friendly controllable synthesis of silver nanoparticles and their enhanced antibacterial property. *Catalysis Today*, *327*, 196–202. https://doi.org/10.1016/j.cattod.2018.05.004

Guiton, P. S., Cusumano, C. K., Kline, K. A., Dodson, K. W., Han, Z., Janetka, J. W., Henderson, J. P., Caparon, M. G., & Hultgren, S. J. (2012). Combinatorial Small-Molecule Therapy Prevents Uropathogenic Escherichia coli Catheter-Associated Urinary Tract Infections in Mice. *Antimicrobial Agents and Chemotherapy*, *56*(9), 4738–4745. https://doi.org/10.1128/AAC.00447-12

Guiton, P.S., Hannan, T.J., Ford, B., Caparon, M.G., Hultgren, S.J. (2013). Enterococcus faecalis Overcomes Foreign Body-Mediated Inflammation To Establish Urinary Tract Infections. *Infect Immun. 81(1).* 329-339.

Gunnarsson, A. K., Gunningberg, L., Larsson, S., & Jonsson, K. B. (2017). Cranberry juice concentrate does not significantly decrease the incidence of acquired bacteriuria in female hip fracture patients receiving urine catheter: A double-blind randomized trial. *Clinical Interventions in Aging*, *Volume 12*, 137–143. https://doi.org/10.2147/CIA.S113597

Gupta, K., Chou, M. Y., Howell, A., Wobbe, C., Grady, R., & Stapleton, A. E. (2007). Cranberry Products Inhibit Adherence of P-Fimbriated Escherichia Coli to Primary Cultured Bladder and Vaginal Epithelial Cells. *Journal of Urology*, *177*(6), 2357–2360. https://doi.org/10.1016/j.juro.2007.01.114

Gyftopoulos, K. (2018). The aberrant urethral meatus as a possible aetiological factor of recurrent post-coital urinary infections in young women. *Medical Hypotheses*, *113*, 6–8. https://doi.org/10.1016/j.mehy.2018.02.005

Ha, U.-S., & Cho, Y.-H. (2006). Catheter-associated urinary tract infections: New aspects of novel urinary catheters. *International Journal of Antimicrobial Agents*, *28*(6), 485–490. https://doi.org/10.1016/j.ijantimicag.2006.08.020

Hacker, J. & Kaper, J.B. (2000). Pathogenicity Islands and the Evolution of Microbes. *Annual Review of Microbiology. 54.* 641-679.

Hahn, F., & Sarre, S. (1969). Mechanism of Action of Gentamicin. *The Journal of Infectious Diseases. 119(4/5).*364-369.

Han, J. H., Kim, M. S., Lee, M. Y., Kim, T. H., Lee, M.-K., Kim, H. R., & Myung, S. C. (2010). Modulation of human β-defensin-2 expression by 17β-estradiol and progesterone in vaginal epithelial cells. *Cytokine*, *49*(2), 209–214. https://doi.org/10.1016/j.cyto.2009.09.005

Hang, T., Chen, H.-J., Yang, C., Xiao, S., Liu, G., Lin, D., Tao, J., Wu, J., Yang, B., & Xie, X. (2017). Slippery surface based on lubricant infused hierarchical silicon nanowire film. *RSC Advances*, *7*(88), 55812–55818. https://doi.org/10.1039/C7RA10460J

Hannan, T. J., Mysorekar, I. U., Hung, C. S., Isaacson-Schmid, M. L., & Hultgren, S. J. (2010). Early Severe Inflammatory Responses to Uropathogenic E. coli Predispose to Chronic and Recurrent Urinary Tract Infection. *PLoS Pathogens*, *6*(8), e1001042. https://doi.org/10.1371/journal.ppat.1001042

Hannan, T. J., Totsika, M., Mansfield, K. J., Moore, K. H., Schembri, M. A., & Hultgren, S. J. (2012). Host–pathogen checkpoints and population bottlenecks in persistent and intracellular uropathogenic *Escherichia coli* bladder infection. *FEMS Microbiology Reviews*, *36*(3), 616–648. https://doi.org/10.1111/j.1574-6976.2012.00339.x

Hao, P., Wang, Y., Sun, X., Wang, J., & Zhang, L. W. (2022). Derivation of the toxicological threshold of silicon element in the extractables and leachables from the pharmaceutical packaging and process components. *Toxicology and Industrial Health*, *38*(12), 819–834. https://doi.org/10.1177/07482337221123368

Haraldsson, B., & Sörensson, J. (2004). Why Do We Not All Have Proteinuria? An Update of Our Current Understanding of the Glomerular Barrier. *Physiology*, *19*(1), 7–10. https://doi.org/10.1152/nips.01461.2003

Hardy., C.C., Ramasamy, R., Rosenberg, D.A., Kuchel, G.A., Yan, R., Hu, X., & Smith, P.P. (2022). Alzheimer's disease amyloidogenesis is linked to altered lower urinary tract physiology. *Neurourology and Urodynamics. 41 (6)*, 1344-1354.

Harris, J.M., & Chess, R.B. (2003). Effect of pegylation on pharmaceuticals. *Nature Reviews Drug Discovery. 2.* 214-221.

Hashitani, H., & Lang, R. J. (Eds.). (2019). *Smooth Muscle Spontaneous Activity: Physiological and Pathological Modulation* (Vol. 1124). Springer Singapore. https://doi.org/10.1007/978-981-13-5895-1

Hauptkorn, S., Pavel, J., & Seltner, H. (2001). Determination of silicon in biological samples by ICP-OES after non-oxidative decomposition under alkaline conditions. *Fresenius' Journal of Analytical Chemistry*, *370*(2–3), 246–250. https://doi.org/10.1007/s002160100759

He, M., Gao, K., Zhou, L., Jiao, Z., Wu, M., Cao, J., You, X., Cai, Z., Su, Y., & Jiang, Z. (2016). Zwitterionic materials for antifouling membrane surface construction. *Acta Biomaterialia*, *40*, 142–152. https://doi.org/10.1016/j.actbio.2016.03.038

Hendlin, K., Meyers, J., & Monga, M. (2009). Foley Catheter Characteristics: Predicting Problems. *Journal of Endourology. 23(1).* DOI:. https://doi.org/10.1089/end.2008.0503

Herath, M., Hosie, S., Bornstein, J. C., Franks, A. E., & Hill-Yardin, E. L. (2020). The Role of the Gastrointestinal Mucus System in Intestinal Homeostasis: Implications for Neurological Disorders. *Frontiers in Cellular and Infection Microbiology*, *10*, 248. https://doi.org/10.3389/fcimb.2020.00248

Hillebrand, U., & Schmitt, R. (2022). Purple Urine in the Catheter Bag. *Dtsch Arztebl Int. 119(45).* 764.

Hiraku, Y., Sekine, A., Nabeshi, H., Midorikawa, K., Murata, M., Kumagai, Y., & Kawanishi, S. (2004). Mechanism of carcinogenesis induced by a veterinary antimicrobial drug, nitrofurazone, via oxidative DNA damage and cell proliferation. *Cancer Letters*, *215*(2), 141–150. https://doi.org/10.1016/j.canlet.2004.05.016

Homeyer, K. H., Goudie, M. J., Singha, P., & Handa, H. (2019). Liquid-Infused Nitric-Oxide-Releasing Silicone Foley Urinary Catheters for Prevention of Catheter-Associated Urinary Tract Infections. *ACS Biomaterials Science & Engineering*, *5*(4), 2021–2029. https://doi.org/10.1021/acsbiomaterials.8b01320

Hooton, T. M., Bradley, S. F., Cardenas, D. D., Colgan, R., Geerlings, S. E., Rice, J. C., Saint, S., Schaeffer, A. J., Tambayh, P. A., Tenke, P., & Nicolle, L. E. (2010). Diagnosis, Prevention, and Treatment of Catheter-Associated Urinary Tract Infection in Adults: 2009 International Clinical Practice Guidelines from the Infectious Diseases Society of America. *Clinical Infectious Diseases*, *50*(5), 625–663. https://doi.org/10.1086/650482

Hooton, T.M. (2012). Clinical practice. Uncomplicated urinary tract infection. *N Engl J Med. 366(11).* 1028-1037.

Hornung, M., & Krivan, V. (1997). *Determination of Silicon in Biological Tissue by Electrothermal Atomic Absorption Spectrometry Using Slurry Sampling of Original and Pre-ashed Samples*.

Horváth. (2012). Fluorous Chemistry. Topics in Current Chemistry.

Horwitz, D., McCue, T., Mapes, A. C., Ajami, N. J., Petrosino, J. F., Ramig, R. F., & Trautner, B. W. (2015). Decreased microbiota diversity associated with urinary tract infection in a trial of bacterial interference. *Journal of Infection*, *71*(3), 358–367. https://doi.org/10.1016/j.jinf.2015.05.014

Hosseinpour, M., Noori, S., Amir-Beigi, M., Pourfakharan, M., Ehteram, H., & Hamsayeh, M. (2014). Safety of latex urinary catheters for the short time drainage. *Urology Annals*, *6*(3), 198. https://doi.org/10.4103/0974-7796.134257

Howell, C., Grinthal, A., Sunny, S., Aizenberg, M., & Aizenberg, J. (2018). Designing Liquid-Infused Surfaces for Medical Applications: A Review. *Advanced Materials*, *30*(50), 1802724. https://doi.org/10.1002/adma.201802724

Howell, C., Vu, T. L., Johnson, C. P., Hou, X., Ahanotu, O., Alvarenga, J., Leslie, D. C., Uzun, O., Waterhouse, A., Kim, P., Super, M., Aizenberg, M., Ingber, D. E., & Aizenberg, J. (2015). Stability of Surface-Immobilized Lubricant Interfaces under Flow. *Chemistry of Materials*, *27*(5), 1792–1800. https://doi.org/10.1021/cm504652g

Howell, C., Vu, T. L., Lin, J. J., Kolle, S., Juthani, N., Watson, E., Weaver, J. C., Alvarenga, J., & Aizenberg, J. (2014). Self-Replenishing Vascularized Fouling-Release Surfaces. *ACS Applied Materials & Interfaces*, *6*(15), 13299–13307. https://doi.org/10.1021/am503150y

Hoyer, L. L., & Cota, E. (2016). Candida albicans Agglutinin-Like Sequence (Als) Family Vignettes: A Review of Als Protein Structure and Function. *Frontiers in Microbiology*, *7*. https://doi.org/10.3389/fmicb.2016.00280

Hsu, L.C., Fang, J., Borca-Tasciuc, D.A.B., Worobo, R.W., & Moraru, C.I. (2013). Effect of Micro- and Nanoscale Topography on the Adhesion of Bacterial Cells to Solid Surfaces. *Applied and Environmental Microbiology.* DOI: https://doi.org/10.1128/AEM.03436-12

Huang, C., & Guo, Z. (2019). Fabrications and Applications of Slippery Liquid-infused Porous Surfaces Inspired from Nature: A Review. *Journal of Bionic Engineering. 16.* 769-793.

Huang, W., Wei, L., Ji, Y., Xu, D., & Mo, J. (2005). Effect of silicon and latex urinary catheters: a comparative study. *Di Yi Jun Yi Da Xue Xue Bao. 25(8).* 1026-1028.

Humphreys, B. D. (2018). Mechanisms of Renal Fibrosis. *Annual Review of Physiology*, *80*(1), 309–326. https://doi.org/10.1146/annurev-physiol-022516-034227

Hunt, B. C., Brix, V., Vath, J., Guterman, B. L., Taddei, S. M., Learman, B. S., Brauer, A. L., Shen, S., Qu, J., & Armbruster, C. E. (2023). *Metabolic interplay between* Proteus mirabilis *and* Enterococcus faecalis *facilitates polymicrobial biofilm formation and invasive disease* [Preprint]. Microbiology. https://doi.org/10.1101/2023.03.17.533237

Inge, L.D. (2010). Management of Catheter-Associated Urinary Tract Infections. *US Pharm. 35(8).* 6-10.

Ismaili, K., Lolin, K., Damry, N., Alexander, M., Lepage, P., & Hall, M. (2010). Febrile Urinary Tract Infections in 0- to 3-Month-Old Infants: A Prospective Follow-Up Study. *The Journal of Pediatrics. 158(1).* 91-94.

Ivanova, E. P., Hasan, J., Webb, H. K., Gervinskas, G., Juodkazis, S., Truong, V. K., Wu, A. H. F., Lamb, R. N., Baulin, V. A., Watson, G. S., Watson, J. A., Mainwaring, D. E., & Crawford, R. J.

(2013). Bactericidal activity of black silicon. *Nature Communications*, *4*(1), 2838. https://doi.org/10.1038/ncomms3838

Jacobsen, S. M., & Shirtliff, M. E. (2011). *Proteus mirabilis* biofilms and catheter-associated urinary tract infections. *Virulence*, *2*(5), 460–465. https://doi.org/10.4161/viru.2.5.17783

Jacobsen, S. M., Stickler, D. J., Mobley, H. L. T., & Shirtliff, M. E. (2008). Complicated Catheter-Associated Urinary Tract Infections Due to *Escherichia coli* and *Proteus mirabilis*. *Clinical Microbiology Reviews*, *21*(1), 26–59. https://doi.org/10.1128/CMR.00019-07

Jamil, M. I., Song, L., Zhu, J., Ahmed, N., Zhan, X., Chen, F., Cheng, D., & Zhang, Q. (2020). Facile approach to design a stable, damage resistant, slippery, and omniphobic surface. *RSC Advances*, *10*(33), 19157–19168. https://doi.org/10.1039/D0RA01786H

Jarrell, A., Wood, G.C., Ponnapula, S., Magnotti, L.J., Croce, M.A., Swanson, J.M., Boucher, B.A., & Fabian, T.C. (2015). Short-duration treatment for catheter-associated urinary tract infections in critically ill trauma patients. *Journal of Trauma and Acute Care Surgery. 79(4).* 649-653.

Jennewein, C., Tran, N., Paulus, P., Ellinghaus, P., Eble, J. A., & Zacharowski, K. (2011). Novel Aspects of Fibrin(ogen) Fragments during Inflammation. *Molecular Medicine*, *17*(5–6), 568–573. https://doi.org/10.2119/molmed.2010.00146

Johansson, K., Greis, G., Johansson, B., Grundtmann, A., Pahlby, Y., Törn, S., Axelberg, H., & Carlsson, P. (2013). Evaluation of a new PVC-free catheter material for intermittent catheterization: A prospective, randomized, crossover study. *Scandinavian Journal of Urology*, *47*(1), 33–37. https://doi.org/10.3109/00365599.2012.696136

Johnson, D. E., Lockatell, C. V., Russell, R. G., Hebel, J. R., Island, M. D., Stapleton, A., Stamm, W. E., & Warren, J. W. (1998). Comparison of Escherichia coli Strains Recovered from Human Cystitis and Pyelonephritis Infections in Transurethrally Challenged Mice. *INFECT. IMMUN.*, *66*.

Johnson, J. R., Berggren, T., & Conway, A. J. (1993). Activity of a nitrofurazone matrix urinary catheter against catheter-associated uropathogens. *Antimicrobial Agents and Chemotherapy*, *37*(9), 2033–2036. https://doi.org/10.1128/AAC.37.9.2033

Johnson, J. R., Delavari, P., & Azar, M. (1999). Activities of a Nitrofurazone-Containing Urinary Catheter and a Silver Hydrogel Catheter against Multidrug-Resistant Bacteria Characteristic of Catheter-Associated Urinary Tract Infection. *Antimicrobial Agents and Chemotherapy*, *43*(12), 2990–2995. https://doi.org/10.1128/AAC.43.12.2990

Johnson, J.R., & Russo, T. A. (2018). Acute Pyelonephritis in Adults. *N Engl J Med. 378.* 48-59.

Johnson, J.R., Kuskowski, M.A., & Wilt, T.J. (2006). Systematic Review: Antimicrobial Urinary Catheters To Prevent Catheter-Associated Urinary Tract Infection in Hospitalized Patients. *Annals of Internal Medicine.* https://doi.org/10.7326/0003-4819-144-2-200601170-00009

Jugdaohsingh, R., Watson, A.I.E., Pedro, L.D., & Powell, J.J. (2015). The decrease in silicon concentration of the connective tissues with age in rats is a marker of connective tissue turnover. *Bone. 75.* 40-48.

Juthani, N., Howell, C., Ledoux, H., Sotiri, I., Kelso, S., Kovalenko, Y., Tajik, A., Vu. T.L., Lin, J.J., Sutton, A., & Aizenberg, J. (2016). Infused polymers for cell sheet release. *Scientific Reports*. 6. 206109.

Kakaria, B. A., K., A., & Tushar, R. (2018). Study of incidence and risk factors of urinary tract infection in catheterised patients admitted at tertiary care. *International Journal of Research in Medical Sciences*, *6*(5), 1730. https://doi.org/10.18203/2320-6012.ijrms20181768

Kanamaru, S., Kurazono, H., Ishitoya, S., Terai, A., Habuchi, T., Nakano, M., Ogawa, O., & Yamamoto, S. (2003). Distribution and Genetic Association of Putative Uropathogenic Virulence Factors Iron, iha, kpsMT, ompT and usp in Escherichia Coli Isolated From Urinary Tract Infections in Japan. *Journal of Urology. 170(6).* 2490-2493.

Kanellopoulos, T. A., Salakos, C., Spiliopoulou, I., Ellina, A., Nikolakopoulou, N. M., & Papanastasiou, D. A. (2006). First urinary tract infection in neonates, infants and young children: A comparative study. *Pediatric Nephrology*, *21*(8), 1131–1137. https://doi.org/10.1007/s00467-006-0158-7

Kanjilal, S., Oberst, M., Boominathan, S., Zhou, H., Hooper, D. C., & Sontag, D. (2020). A decision algorithm to promote outpatient antimicrobial stewardship for uncomplicated urinary tract infection. *Science Translational Medicine*, *12*(568), eaay5067. https://doi.org/10.1126/scitranslmed.aay5067

Karchmer, T.B., Giannetta, E.T., Muto, C.A., Strain, B.A., & Farr, B.A. (2000). A Randomized Crossover Study of Silver-Coated Urinary Catheters in Hospitalized Patients. *Arch Intern Med. 160(21).* 3294-3298.

Kasapgil, E., Erbil, H. Y., & Anac Sakir, I. (2022). Multi-liquid repellent, fluorine-free, heat stable SLIPS via layer-by-layer assembly. *Colloids and Surfaces A: Physicochemical and Engineering Aspects*, *654*, 130076. https://doi.org/10.1016/j.colsurfa.2022.130076

Kashi, S., Varley, R., Souza, M.D., Al-Assafi, S., Pietro, A.D., Lavigne, C.D., & Fox, B. (2018). Mechanical, Thermal, and Morphological Behavior of Silicone Rubber during Accelerated Aging. *Polymer-plastics Technology and Engineering.* https://doi.org/10.1080/03602559.2017.1419487

Kaur, R., & Kaur, R. (2021). Symptoms, risk factors, diagnosis and treatment of urinary tract infections. *Postgraduate Medical Journal*, *97*(1154), 803–812. https://doi.org/10.1136/postgradmedj-2020-139090

Kazmierska, K. A., Thompson, R., Morris, N., Long, A., & Ciach, T. (2010). In Vitro Multicompartmental Bladder Model for Assessing Blockage of Urinary Catheters: Effect of Hydrogel Coating on Dynamics of Proteus mirabilis Growth. *Urology*, *76*(2), 515.e15-515.e20. https://doi.org/10.1016/j.urology.2010.04.039

Kertes, P.J., Wafapoor, H., Peyman, G.A., Calixto, N., Thompson, H., & Vitreon Collaborative Study Group. (1997). The Management of Giant Retinal Tears Using Perfluoroperhydrophenanthrene A Multicenter Case Series. *Ophthalmology. 104(7).* 1159-1165.

Khandelwal, P., Abraham, S.N., & Apodaca, G. (2009). Cell biology and physiology of the uroepithelium. *Am J Physiol Renal Physiol. 297(6).* F1477-F1501.

Ki, M. (2004). The Epidemiology of Acute Pyelonephritis in South Korea, 1997-1999. *American Journal of Epidemiology*, *160*(10), 985–993. https://doi.org/10.1093/aje/kwh308

Kilonzo, M., Vale, L., Pickard, R., Lam, T., & N'Dow, J. (2014). Cost Effectiveness of Antimicrobial Catheters for Adults Requiring Short-term Catheterisation in Hospital. *European Urology*, *66*(4), 615–618. https://doi.org/10.1016/j.eururo.2014.05.035

Kim, P., Wong, T.-S., Alvarenga, J., Kreder, M. J., Adorno-Martinez, W. E., & Aizenberg, J. (2012). Liquid-Infused Nanostructured Surfaces with Extreme Anti-Ice and Anti-Frost Performance. *ACS Nano*, *6*(8), 6569–6577. https://doi.org/10.1021/nn302310q

Klein, R. D., & Hultgren, S. J. (2020). Urinary tract infections: Microbial pathogenesis, host–pathogen interactions and new treatment strategies. *Nature Reviews Microbiology*, *18*(4), 211–226. https://doi.org/10.1038/s41579-020-0324-0

Kline, K. A., & Lewis, A. L. (2016). Gram-Positive Uropathogens, Polymicrobial Urinary Tract Infection, and the Emerging Microbiota of the Urinary Tract. *Microbiology Spectrum*, *4*(2), 4.2.04. https://doi.org/10.1128/microbiolspec.UTI-0012-2012

Kolle, S., Ahanotu, O., Meeks, A., Stafslien, S., Kreder, M., Vanderwal, L., Cohen, L., Waltz, G., Lim, C. S., Slocum, D., Greene, E. M., Hunsucker, K., Swain, G., Wendt, D., Teo, S. L.-M., & Aizenberg, J. (2022). On the mechanism of marine fouling-prevention performance of oil-containing silicone elastomers. *Scientific Reports*, *12*(1), 11799. https://doi.org/10.1038/s41598-022-15553-4

Kostakioti, M., Hadjifrangiskou, M., & Hultgren, S. J. (2013). Bacterial Biofilms: Development, Dispersal, and Therapeutic Strategies in the Dawn of the Postantibiotic Era. *Cold Spring Harbor Perspectives in Medicine*, *3*(4), a010306–a010306. https://doi.org/10.1101/cshperspect.a010306

Kovalenko, Y., Sotiri, I., Timonen, J. V. I., Overton, J. C., Holmes, G., Aizenberg, J., & Howell, C. (2017). Bacterial Interactions with Immobilized Liquid Layers. *Advanced Healthcare Materials*, *6*(15), 1600948. https://doi.org/10.1002/adhm.201600948

Krause, K. M., Serio, A. W., Kane, T. R., & Connolly, L. E. (2016). Aminoglycosides: An Overview. *Cold Spring Harbor Perspectives in Medicine*, *6*(6), a027029. https://doi.org/10.1101/cshperspect.a027029

Krayukhina, E., Yokoyama, M., Hayashihara, K. K., Maruno, T., Noda, M., Watanabe, H., Uchihashi, T., & Uchiyama, S. (2019). An Assessment of the Ability of Submicron- and Micron-Size Silicone Oil Droplets in Dropped Prefillable Syringes to Invoke Early- and Late-Stage Immune Responses.

Journal of Pharmaceutical Sciences, *108*(7), 2278–2287. https://doi.org/10.1016/j.xphs.2019.02.002

Kucheria, R., Dasgupta, P., Sacks, S. H., Khan, M. S., & Sheerin, N. S. (2005). Urinary tract infections: New insights into a common problem. *Postgraduate Medical Journal*, *81*(952), 83–86. https://doi.org/10.1136/pgmj.2004.023036

Kumar, S., Bandyopadhyay, M., Chatterjee, M., Mukhopadhyay, P., Pal, S., Poddar, S., & Banerjee, P. (2013). Red discoloration of urine caused by Serratia rubidae: A rare case. *Avicenna Journal of Medicine*, *03*(01), 20–22. https://doi.org/10.4103/2231-0770.112790

Kunin, C.M., Chin, Q.F., & Chambers, S. (1987). Formation of Encrustations on Indwelling Urinary Catheters in the Elderly: A Comparison of Different types of Catheter Materials in "Blockers" and "Nonblockers". *The Journal of Urology. 138(4):1,* 899-902.

Lam, T. B., Omar, M. I., Fisher, E., Gillies, K., & MacLennan, S. (2014). Types of indwelling urethral catheters for short-term catheterisation in hospitalised adults. *Cochrane Database of Systematic Reviews*. https://doi.org/10.1002/14651858.CD004013.pub4

Langermann, S., Möllby, R., Burlein, J. E., Palaszynski, S. R., Auguste, C. G., DeFusco, A., Strouse, R., Schenerman, M. A., Hultgren, S. J., Pinkner, J. S., Winberg, J., Guldevall, L., Söderhäll, M., Ishikawa, K., Normark, S., & Koenig, S. (2000). Vaccination with FimH Adhesin Protects Cynomolgus Monkeys from Colonization and Infection by Uropathogenic *Escherichia coli*. *The Journal of Infectious Diseases*, *181*(2), 774–778. https://doi.org/10.1086/315258

Langermann, S., Palaszynski, S., Barnhaart, M., Auguste, G., Pinkner, J.S., Burlein, J., Barren, P., Koenig, S., Leath, S., Jones, C.H., & Hultgren, S.J. (1997). Prevention of Mucosal Escherichia coli Infection by FimH-Adhesin-Based Systemic Vaccination. *Science. 276 (5312).* 607-611.

Lapides, J., Diokno, A.C., Silber, S.J., & Lowe, B.S. (1972). Clean, Intermittent Self-Catheterization in the Treatment of Urinary Tract Disease. *Journal of Urology. 107(3).* 458-461.

Lavielle, N., Asker, D., & Hatton, B. D. (2021). Lubrication dynamics of swollen silicones to limit long term fouling and microbial biofilms. *Soft Matter*, *17*(4), 936–946. https://doi.org/10.1039/D0SM01039A

Lawrence, E.L., & Turner, I.G. (2006a). Characterisation of the internal and external surfaces of four types of Foley catheter using SEM and profilometry. *Journal of Materials Science: Materials in Medicine. 17.* 1421-1431.

Lawrence, E.L., & Turner, I.G. (2006a). Kink, flow and retention properties of urinary catheters part 1: Conventional foley catheters. *Journal of Materials Science: Materials in Medicine. 17.* 147-152.

Lederer, J. W., Jarvis, W. R., Thomas, L., & Ritter, J. (2014). Multicenter Cohort Study to Assess the Impact of a Silver-Alloy and Hydrogel-Coated Urinary Catheter on Symptomatic Catheter-Associated Urinary Tract Infections. *Journal of Wound, Ostomy & Continence Nursing*, *41*(5), 473–480. https://doi.org/10.1097/WON.0000000000000056

Lee, G. (2011). Uroplakins in the Lower Urinary Tract. *International Neurourology Journal*, *15*(1), 4. https://doi.org/10.5213/inj.2011.15.1.4

Lee, S.-J., Kim, S. W., Cho, Y.-H., Shin, W.-S., Lee, S. E., Kim, C.-S., Hong, S. J., Chung, B. H., Kim, J. J., & Yoon, M. S. (2004). A comparative multicentre study on the incidence of catheter-associated urinary tract infection between nitrofurazone-coated and silicone catheters. *International Journal of Antimicrobial Agents*, *24*, 65–69. https://doi.org/10.1016/j.ijantimicag.2004.02.013

Leslie, D. C., Waterhouse, A., Berthet, J. B., Valentin, T. M., Watters, A. L., Jain, A., Kim, P., Hatton, B. D., Nedder, A., Donovan, K., Super, E. H., Howell, C., Johnson, C. P., Vu, T. L., Bolgen, D. E., Rifai, S., Hansen, A. R., Aizenberg, M., Super, M., Aizenberg, J., & Ingber, D. E. (2014). A bioinspired omniphobic surface coating on medical devices prevents thrombosis and biofouling. *Nature Biotechnology*, *32*(11), 1134–1140. https://doi.org/10.1038/nbt.3020

Levine, A.R., Tran, M., Shepherd, J., & Naut, E. (2018). Utility of initial procalcitonin values to predict urinary tract infection. *The American Journal of Emergency Medicine. 36 (11).* 1993-1997.

Levison, M.E., & Kaye, D. (2013). Treatment of Complicated Urinary Tract Infections With an Emphasis on Drug-Resistant Gram-Negative Uropathogens. *Genitourinary Infections (J Sobel, Section Editor). 15.* 109-115.

Levkin, P. A., Svec, F., & Fréchet, J. M. J. (2009). Porous Polymer Coatings: A Versatile Approach to Superhydrophobic Surfaces. *Advanced Functional Materials*, *19*(12), 1993–1998. https://doi.org/10.1002/adfm.200801916

Li, J., Kleintschek, T., Rieder, A., Cheng, Y., Baumbach, T., Obst, U., Schwartz, T., & Levkin, P. A. (2013). Hydrophobic Liquid-Infused Porous Polymer Surfaces for Antibacterial Applications. *ACS Applied Materials & Interfaces*, *5*(14), 6704–6711. https://doi.org/10.1021/am401532z

Li, Z., Huang, X., Xu, X., Bai, Y., & Zou, C. (2024). Unstable Coalescence Mechanism and Influencing Factors of Heterogeneous Oil Droplets. *29(7). 1582.*

Lichtenberger, P., & Hooton, T.M. (2008). Complicated urinary tract infections. *Current Infectious Disease Reports. 10*. 499-504.

Lin, W.-H., Wang, M.-C., Liu, P.-Y., Chen, P.-S., Wen, L.-L., Teng, C.-H., & Kao, C.-Y. (2022). Escherichia coli urinary tract infections: Host age-related differences in bacterial virulence factors and antimicrobial susceptibility. *Journal of Microbiology, Immunology and Infection*, *55*(2), 249–256. https://doi.org/10.1016/j.jmii.2021.04.001

Liu, M., Li, M.-T., Xu, S., Yang, H., & Sun, H.-B. (2020). Bioinspired Superhydrophobic Surfaces via Laser-Structuring. *Frontiers in Chemistry*, *8*, 835. https://doi.org/10.3389/fchem.2020.00835

Liu, R., Chi, Z., Cao, L., Weng, Z., Wang, L., Li, L., Saeed, S., Lian, Z., & Wang, Z. (2020). Fabrication of biomimetic superhydrophobic and anti-icing Ti6Al4V alloy surfaces by direct laser interference lithography and hydrothermal treatment. *Applied Surface Science*, *534*, 147576. https://doi.org/10.1016/j.apsusc.2020.147576

Liu, W., Chen, X., Jeantet, R., André C., & Delaplace, G. (2022). Role of casein micelle on the whey protein fouling in a bench-scale fouling device. *Heat Exchanger Fouling and Cleaning.*

Lorenzo-GÃ³mez, M. F., Padilla-FernÃ¡ndez, B., GarcÃa-Cenador, M. B., Virseda-RodrÃguez, Ã. J., MartÃn-GarcÃa, I., SÃ¡nchez-Escudero, A., Vicente-Arroyo, M. J., & MirÃ³n-Canelo, J. A. (2015). Comparison of sublingual therapeutic vaccine with antibiotics for the prophylaxis of recurrent urinary tract infections. *Frontiers in Cellular and Infection Microbiology*, *5*. https://doi.org/10.3389/fcimb.2015.00050

Lüthje, P., Brauner, H., Ramos, N.L., Övregaard, A., Gläser, R., Hirschberg, A.L., Aspenström, P., & Brauner, A. (2013). Estrogen Supports Urothelial Defense Mechanisms. *Science Translational Medicine. 190(5)*.

Lv, S., Zhang, X., Yang, X., Liu, Q., Liu, X., Yang, Z., & Zhai, Y. (2022). Slippery surface with honeycomb structures for enhancing chemical durability of aluminum. *Colloids and Surfaces A: Physicochemical and Engineering Aspects*, *648*, 129187. https://doi.org/10.1016/j.colsurfa.2022.129187

Lyczak, J. B., Cannon, C. L., & Pier, G. B. (2000). Establishment of Pseudomonas aeruginosa infection: Lessons from a versatile opportunist. *Microbes and Infection*.

MacCallum, N., Howell, C., Kim, P., Sun, D., Friedlander, R., Ranisau, J., Ahanotu, O., Lin, J. J., Vena, A., Hatton, B., Wong, T.-S., & Aizenberg, J. (2015). Liquid-Infused Silicone As a Biofouling-Free Medical Material. *ACS Biomaterials Science & Engineering*, *1*(1), 43–51. https://doi.org/10.1021/ab5000578

Madureira, A.R., Pereira, C.I., Gomes, A.M.P., Pintado, M.E., & Malcata, F.X. (2007). Bovine whey proteins – Overview on their main biological properties. *Food Res Int. 40(10).* 1197-1211.

Magistro, G., & Stief, C.G. (2018). Vaccine Development for Urinary Tract Infections: Where Do We Stand?. *European Urology. 5(1).* 39-41.

Maki, D. G., & Tambyah, P. A. (2001). Engineering Out the Risk for Infection with Urinary Catheters. *Emerging Infectious Diseases*, *7*(2).

Manabe, K., Kyung, K.-H., & Shiratori, S. (2015). Biocompatible Slippery Fluid-Infused Films Composed of Chitosan and Alginate via Layer-by-Layer Self-Assembly and Their Antithrombogenicity. *ACS Applied Materials & Interfaces*, *7*(8), 4763–4771. https://doi.org/10.1021/am508393n

Manna, U., & Lynn, D.M. (2015). Fabrication of Liquid-Infused Surfaces Using Reactive Polymer Multilayers: Principles for Manipulating the Behaviors and Mobilities of Aqueous Fluids on Slippery Liquid Interfaces. *Advanced Materials. 27(19).* 3007-3012.

Mazaheri, M. (2021). Serum Interleukin-6 and Interleukin-8 are Sensitive Markers for Early Detection of Pyelonephritis and Its Prevention to Progression to Chronic Kidney Disease. *Int J Prev Med. 12(2).* 2.

McCloskey, A., Gilmore, B., & Laverty, G. (2014). Evolution of Antimicrobial Peptides to Self-Assembled Peptides for Biomaterial Applications. *Pathogens*, *3*(4), 791–821. https://doi.org/10.3390/pathogens3040791

McGregor, R.R. (1961). Toxicology of the Silicones. *Journal of Occupational and Environmental Medicine. 3(7).* 360.

McLellan, L. K., & Hunstad, D. A. (2016). Urinary Tract Infection: Pathogenesis and Outlook. *Trends in Molecular Medicine*, *22*(11), 946–957. https://doi.org/10.1016/j.molmed.2016.09.003

Meddings, J., Rogers, M. A. M., Krein, S. L., Fakih, M. G., Olmsted, R. N., & Saint, S. (2014). Reducing unnecessary urinary catheter use and other strategies to prevent catheter-associated urinary tract infection: An integrative review. *BMJ Quality & Safety*, *23*(4), 277–289. https://doi.org/10.1136/bmjqs-2012-001774

Melo, G. B., Cruz, N. F. S. D., Emerson, G. G., Rezende, F. A., Meyer, C. H., Uchiyama, S., Carpenter, J., Shiroma, H. F., Farah, M. E., Maia, M., & Rodrigues, E. B. (2021). Critical analysis of techniques and materials used in devices, syringes, and needles used for intravitreal injections. *Progress in Retinal and Eye Research*, *80*, 100862. https://doi.org/10.1016/j.preteyeres.2020.100862

Melo, G. B., Dias Junior, C. D. S., Carvalho, M. R., Cardoso, A. L., Morais, F. B., Figueira, A. C. M., Lima Filho, A. A. S., Emerson, G. G., & Maia, M. (2019). Release of silicone oil droplets from syringes. *International Journal of Retina and Vitreous*, *5*(1), 1. https://doi.org/10.1186/s40942-018-0153-8

Metze F.K., Sant, S., Meng, Z., Klok, H., & Kaur, K. (2023). Swelling-Activated, Soft Mechanochemistry in Polymer Materials. *Langmuir. 39(10).* 3546-3557.

Meyers, D. J., Palmer, K. C., Bale, L. A., Kernacki, K., Preston, M., Brown, T., & Berk, R. S. (1992). In vivo and in vitro toxicity of phospholipase C from Pseudomonas aeruginosa. *Toxicon*, *30*(2), 161–169. https://doi.org/10.1016/0041-0101(92)90469-L

Michalska, M., & Wolf, P. (2015). Pseudomonas Exotoxin A: Optimized by evolution for effective killing. *Frontiers in Microbiology*, *6*. https://doi.org/10.3389/fmicb.2015.00963

Mihut, D. M., Afshar, A., Lackey, L. W., & Le, K. N. (2019). Antibacterial effectiveness of metallic nanoparticles deposited on water filter paper by magnetron sputtering. *Surface and Coatings Technology*, *368*, 59–66. https://doi.org/10.1016/j.surfcoat.2019.04.039

Mikkelsen, H., Hui, K., Barraud, N., & Filloux, A. (2013). The pathogenicity island encoded PvrSR / RcsCB regulatory network controls biofilm formation and dispersal in *P seudomonas aeruginosa* PA 14. *Molecular Microbiology*, *89*(3), 450–463. https://doi.org/10.1111/mmi.12287

Mittal, R., Aggarwal, S., Sharma, S., Chhibber, S., & Harjai, K. (2009). Urinary tract infections caused by Pseudomonas aeruginosa: A minireview. *Journal of Infection and Public Health*, *2*(3), 101–111. https://doi.org/10.1016/j.jiph.2009.08.003

Mittal, R., Khandwaha, R.K., Gupta, V., Mittal, P.K., & Harjai, K. (2006). Phenotypic characters of urinary isolates of Pseudomonas aeruginosa & their association with mouse renal colonization. *Indian J Med Res. 123(1).* 67-72.

Mittal, R., Sharma, S., Chhibber, S., & Harjai, K. (2006). Effect of macrophage secretory products on elaboration of virulence factors by planktonic and biofilm cells of Pseudomonas aeruginosa. *Comparative Immunology, Microbiology and Infectious Diseases*, *29*(1), 12–26. https://doi.org/10.1016/j.cimid.2005.11.002

Mittal, R., Sharma, S., Chhibber, S., & Harjai, K. (2008). Contribution of free radicals to Pseudomonas aeruginosa induced acute pyelonephritis. *Microbial Pathogenesis*, *45*(5–6), 323–330. https://doi.org/10.1016/j.micpath.2008.08.003

Mittal, R., Sharma, S., Chhibber, S., & Harjai, K. (2008). Iron dictates the virulence of Pseudomonas aeruginosa in urinary tract infections. *Journal of Biomedical Science. 15*, 731-741.

Miwa, M., Nakajima, A., Fujishima, A., Hashimoto, K., & Watanabe, T. (2000). Effects of the Surface Roughness on Sliding Angles of Water Droplets on Superhydrophobic Surfaces. *Langmuir*, *16*(13), 5754–5760. https://doi.org/10.1021/la991660o

Mobley, H. L., Chippendale, G. R., Tenney, J. H., Hull, R. A., & Warren, J. W. (1987). Expression of type 1 fimbriae may be required for persistence of Escherichia coli in the catheterized urinary tract. *Journal of Clinical Microbiology*, *25*(12), 2253–2257. https://doi.org/10.1128/jcm.25.12.2253-2257.1987

Mohr, K.I. (2016). History of Antibiotics Research. *Current Topics in Microbiology and Immunology. Volume 398.* https://doi.org/10.1007/822016499.

Mojsiewicz-Pieńkowska, K. (2012). Size exclusion chromatography with evaporative light scattering detection as a method for speciation analysis of polydimethylsiloxanes. III. Identification and determination of dimeticone and simeticone in pharmaceutical formulations. *Journal of Pharmaceutical and Biomedical Analysis. 58. 200-207.*

Morgenstein, R. M., & Rather, P. N. (2012). Role of the Umo Proteins and the Rcs Phosphorelay in the Swarming Motility of the Wild Type and an O-Antigen (*waaL*) Mutant of Proteus mirabilis. *Journal of Bacteriology*, *194*(3), 669–676. https://doi.org/10.1128/JB.06047-11

Murakami, S., Igarashi, T., Tanaka, M., Tobe, T., & Mikami, K. (1993). Adherence of bacteria to various urethral catheters and occurrence of catheter-induced urethritis. *Acta Urologica Japonica. 39(1).* 107-111.

Naber, K. G., Cho, Y.-H., Matsumoto, T., & Schaeffer, A. J. (2009). Immunoactive prophylaxis of recurrent urinary tract infections: A meta-analysis. *International Journal of Antimicrobial Agents*, *33*(2), 111–119. https://doi.org/10.1016/j.ijantimicag.2008.08.011

Narins, R., & Beer, K. (2006). Liquid Injectable Silicone: A Review of Its History, Immunology, Technical Considerations, Complications, and Potential. *Plastic and Reconstructive Surgery. 118 (3S).* 77S-84S.

Nasr, Ahmed. (2010). State of the Globe: Catheterizations Continue to Cultivate Urinary Infections. *Journal of Global Infectious Diseases. 2(2).*

National Healthcare Safety Network (2024). Urinary Tract Infection (Catheter-Associated Urinary Tract Infection [CAUTI] and Non-Catheter-Associated Urinary Tract Infection [UTI]) Events. https://www.cdc.gov/nhsn/pdfs/pscmanual/7psccauticurrent.pdf

National Institute on Disability and Rehabilitation Research. (2016). The Prevention and Management of Urinary Tract Infections Among People With Spinal Cord Injuries. https://doi.org/10.1080/01952307.1992.11735873

Newman, J. W., Floyd, R. V., & Fothergill, J. L. (2017). The contribution of Pseudomonas aeruginosa virulence factors and host factors in the establishment of urinary tract infections. *FEMS Microbiology Letters*, *364*(15). https://doi.org/10.1093/femsle/fnx124

Nickel, J. C., Lorenzo-Gómez, M. F., Foley, S., & Saz-Leal, P. (2021). A Novel Sublingual Vaccine Will Dramatically Alter The Clinical Management of Recurrent Urinary Tract Infections in Women. *Journal of Urology*, *206*(Supplement 3). https://doi.org/10.1097/JU.0000000000002150.02

Nicolle, L. E. (2014). Catheter associated urinary tract infections. *Antimicrob Resist Infect Control. 25(3).* 23.

Nicolle, L. E., Friesen, D., Harding, G. K. M., & Roos, L. L. (1996). Hospitalization for Acute Pyelonephritis in Manitoba, Canada, During the Period from 1989 to 1992: Impact of Diabetes, Pregnancy, and Aboriginal Origin. *Clinical Infectious Diseases*, *22*(6), 1051–1056. https://doi.org/10.1093/clinids/22.6.1051

Nielsen, H. V., Flores-Mireles, A. L., Kau, A. L., Kline, K. A., Pinkner, J. S., Neiers, F., Normark, S., Henriques-Normark, B., Caparon, M. G., & Hultgren, S. J. (2013). Pilin and Sortase Residues Critical for Endocarditis- and Biofilm-Associated Pilus Biogenesis in Enterococcus faecalis. *Journal of Bacteriology*, *195*(19), 4484–4495. https://doi.org/10.1128/JB.00451-13

Nielubowicz, G. R., & Mobley, H. L. T. (2010). Host–pathogen interactions in urinary tract infection. *Nature Reviews Urology*, *7*(8), 430–441. https://doi.org/10.1038/nrurol.2010.101

Niël-Weise, B.S., van den Broek, P.J., da Silva, E.M.K., & Silva, L.A. (2012). Urinary catheter policies for long-term bladder drainage. *Cochrane Database of Systematic Reviews.*

Nishioka, S., Tenjimbayashi, M., Manabe, K., Matsubayashi, T., Suwabe, K., Tsukada, K., & Shiratori, S. (2016). Facile design of plant-oil-infused fine surface asperity for transparent blood-repelling endoscope lens. *RSC Advances*, *6*(53), 47579–47587. https://doi.org/10.1039/C6RA08390K

Nongnual, T., Kaewpirom, S., Damnong, N., Srimongkol, S., & Benjalersyarnon, T. (2022). A Simple and Precise Estimation of Water Sliding Angle by Monitoring Image Brightness: A Case Study of the Fluid Repellency of Commercial Face Masks. *ACS Omega*, *7*(15), 13178–13188. https://doi.org/10.1021/acsomega.2c00628

Nowrouzian, F. L., Adlerberth, I., & Wold, A. E. (2006). Enhanced persistence in the colonic microbiota of Escherichia coli strains belonging to phylogenetic group B2: Role of virulence factors and adherence to colonic cells. *Microbes and Infection*, *8*(3), 834–840. https://doi.org/10.1016/j.micinf.2005.10.011

O'Brien, V. P., Hannan, T. J., Nielsen, H. V., & Hultgren, S. J. (2016). Drug and Vaccine Development for the Treatment and Prevention of Urinary Tract Infections. *Microbiology Spectrum*, *4*(1), 4.1.07. https://doi.org/10.1128/microbiolspec.UTI-0013-2012

Ochsner, U. A., & Reiser, J. (1995). Autoinducer-mediated regulation of rhamnolipid biosurfactant synthesis in Pseudomonas aeruginosa. *Proceedings of the National Academy of Sciences*, *92*(14), 6424–6428. https://doi.org/10.1073/pnas.92.14.6424

Okkeh, M., Bloise, N., Restivo, E., De Vita, L., Pallavicini, P., & Visai, L. (2021). Gold Nanoparticles: Can They Be the Next Magic Bullet for Multidrug-Resistant Bacteria? *Nanomaterials*, *11*(2), 312. https://doi.org/10.3390/nano11020312

Okumura, R. and Takeda, K. (2018). Maintenance of intestinal homeostasis by mucosal barriers. *Inflammation and Regeneration. 38(5).*

Olson, P. D., Hruska, K. A., & Hunstad, D. A. (2016). Androgens Enhance Male Urinary Tract Infection Severity in a New Model. *Journal of the American Society of Nephrology*, *27*(6), 1625–1634. https://doi.org/10.1681/ASN.2015030327

Ouslander, J. G., Greengold, B., & Chen, S. (1987). External Catheter Use and Urinary Tract Infections Among Incontinent Male Nursing Home Patients. *Journal of the American Geriatrics Society*, *35*(12), 1063–1070. https://doi.org/10.1111/j.1532-5415.1987.tb04922.x

Pamp, S. J., & Tolker-Nielsen, T. (2007). Multiple Roles of Biosurfactants in Structural Biofilm Development by *Pseudomonas aeruginosa*. *Journal of Bacteriology*, *189*(6), 2531–2539. https://doi.org/10.1128/JB.01515-06

Pariente, J.L., Bordenave, L., Jacob, F., Bareille, R., Baquey, C., & Le Guillou, M. (2000). Cytotoxicity Assessment of Latex Urinary Catheters on Cultured Human Urothelial Cells. *European Urology. 38(5).* 640-643.

Park, K. D., Kim, Y. S., Han, D. K., Kim, Y. H., Lee, E. H. B., Suh, H., & Choi, K. S. (1998). Bacterial adhesion on PEG modified polyurethane surfaces. *Biomaterials*, *19*(7–9), 851–859. https://doi.org/10.1016/S0142-9612(97)00245-7

Park, S., Han, J., & Kim, K. S. (2011). Risk Factors for Recurrent Urinary Tract Infection in Infants With Vesicoureteral Reflux During Prophylactic Treatment: Effect of Delayed Contrast Passage on Voiding Cystourethrogram. *Pediatric Urology. 78(1).* 170-173.

Parker, D., Callan, L., Harwood, J., Thompson, D.L., Wilde, M., & Gray, M. (2009). Nursing Interventions to Reduce the Risk of Catheter-Associated Urinary Tract Infection Part 1: Catheter Selection. *Journal of Wound, Ostomy and Continence Nursing. 36(1).* 23-34.

Pearson, J. P., Gray, K. M., Passador, L., Tucker, K. D., Eberhard, A., Iglewski, B. H., & Greenberg, E. P. (1994). Structure of the autoinducer required for expression of Pseudomonas aeruginosa virulence genes. *Proceedings of the National Academy of Sciences*, *91*(1), 197–201. https://doi.org/10.1073/pnas.91.1.197

Pearson, J. P., Passador, L., Iglewski, B. H., & Greenberg, E. P. (1995). A second N-acylhomoserine lactone signal produced by Pseudomonas aeruginosa. *Proceedings of the National Academy of Sciences*, *92*(5), 1490–1494. https://doi.org/10.1073/pnas.92.5.1490

Peppou-Chapman, S., Hong, J. K., Waterhouse, A., & Neto, C. (2020). Life and death of liquid-infused surfaces: A review on the choice, analysis and fate of the infused liquid layer. *Chemical Society Reviews*, *49*(11), 3688–3715. https://doi.org/10.1039/D0CS00036A

Perrotta, C., Aznar, M., Mejia, R., Albert, X., & Ng, C.W. (2008). Oestrogens for preventing recurrent urinary tract infection in postmenopausal women. *Cochrane Database of Systematic Reviews.*

Peychl, L., & Zalud, R. (2008). Changes in the urinary bladder caused by short-term permanent catheter insertion. *Casopis Lekaru Ceskych 147:325–329.*

Pfefferkorn, U., Sanlav, L., Moldenhauer, J., Peterli, R., von Flüe, M., & Ackermann, C. (2009). Antibiotic Prophylaxis at Urinary Catheter Removal Prevents Urinary Tract Infections A Prospective Randomized Trial. *Annals of Surgery. 249(4).* 573-575.

Piatti, G., Mannini, A., Balistreri, M., & Schito, A. M. (2008). Virulence Factors in Urinary *Escherichia coli* Strains: Phylogenetic Background and Quinolone and Fluoroquinolone Resistance. *Journal of Clinical Microbiology*, *46*(2), 480–487. https://doi.org/10.1128/JCM.01488-07

Piljić, D., Piljić, D., Ahmetagić, S., Ljuca, F., & Porobić-Jahić, H. (2010). Clinical and Laboratory Characteristics of Acute Community-Acquired Urinary Tract Infection in Adult Hospitalized Patients. *Bosn J Basic Med Sci. 10(1).* 49-53.

Podschun, R., & Ullmann, U. (1998). *Klebsiella* spp. as Nosocomial Pathogens: Epidemiology, Taxonomy, Typing Methods, and Pathogenicity Factors. *Clinical Microbiology Reviews*, *11*(4), 589–603. https://doi.org/10.1128/CMR.11.4.589

Popoola, M., & Hillier, M. (2022). Purple Urine Bag Syndrome as the Primary Presenting Feature of a Urinary Tract Infection. *Cureus*. https://doi.org/10.7759/cureus.23970

Prasad, A., Cevallos, M. E., Riosa, S., Darouiche, R. O., & Trautner, B. W. (2009). A bacterial interference strategy for prevention of UTI in persons practicing intermittent catheterization. *Spinal Cord*, *47*(7), 565–569. https://doi.org/10.1038/sc.2008.166

Prieto, J. A., Murphy, C. L., Stewart, F., & Fader, M. (2021). Intermittent catheter techniques, strategies and designs for managing long-term bladder conditions. *Cochrane Database of Systematic Reviews*, *2023*(3). https://doi.org/10.1002/14651858.CD006008.pub5

Quéré, D. (2005). Non-sticking drops. *Materials Science, Physics.* DOI:10.1088/0034-4885/68/11/R01

Rafienia, M., Zarinmehr, B., Poursamar, S. A., Bonakdar, S., Ghavami, M., & Janmaleki, M. (2013). Coated urinary catheter by PEG/PVA/gentamicin with drug delivery capability against hospital infection. *Iranian Polymer Journal*, *22*(2), 75–83. https://doi.org/10.1007/s13726-012-0105-3

Ramakrishnan, K. (2005). *Diagnosis and Management of Acute Pyelonephritis in Adults*. *71*(5).

Ramesh, P., Joseph, R., & Sunny, M.C. (2001). A Comparative Evaluation of Coefficient of Friction and Mechanical Properties of Commercially Available Foley Catheters. Journal of Biomaterials Applications. *15*. DOI: 10.1106/NCRR-MDV5-FQFG-L7PG

Ramos, Y., Rocha, J., Hael, A.L., Gestel, J.V., Vlamakis, H., Cywes-Bentley, C., Cubillos-Ruiz, J.R., Pier, G.B., Gilmore, M.S., Kolter, R., & Morales, D.K. (2019). PolyGlcNAc-containing exopolymers enable surface penetration by non-motile Enterococcus faecalis. *PLoS Pathog. 15(2).* E1007571.

Rao, N. (2018). Diagnosing catheter-associated urinary tract infection in critically Ill patients: Do the guidelines help? *Indian Journal of Critical Care Medicine*, *22*(5), 357–360. https://doi.org/10.4103/ijccm.IJCCM_434_17

Razatos, A., Ong, Y.-L., Boulay, F., Elbert, D. L., Hubbell, J. A., Sharma, M. M., & Georgiou, G. (2000). Force Measurements between Bacteria and Poly(ethylene glycol)-Coated Surfaces. *Langmuir*, *16*(24), 9155–9158. https://doi.org/10.1021/la000818y

Reed, D., & Kemmerly, S. A. (2009). *Infection Control and Prevention: A Review of Hospital-Acquired Infections and the Economic Implications*. *9*(1).

Regan, D.P., Lilly, C., Weigang, A., White, L.R., LeClair, M.J., Collins, A., & Howell, C. (2019). Combining the geometry of folded paper with liquid-infused polymer surfaces to concentrate and localize bacterial solutions. *Biointerphases. 14.* 041005.

Reid, G., Sharma, S., Advikolanu, K., Tieszer, C., Martin, R. A., & Bruce, A. W. (1994). Effects of ciprofloxacin, norfloxacin, and ofloxacin on in vitro adhesion and survival of Pseudomonas aeruginosa AK1 on urinary catheters. *Antimicrobial Agents and Chemotherapy*, *38*(7), 1490–1495. https://doi.org/10.1128/AAC.38.7.1490

Rijavec, M., Erjavec, M. S., Avguštin, J. A., Reissbrodt, R., Fruth, A., Križan-Hergouth, V., & Žgur-Bertok, D. (2006). High Prevalence of Multidrug Resistance and Random Distribution of Mobile Genetic Elements Among Uropathogenic Escherichia coli (UPEC) of the Four Major Phylogenetic Groups. *Current Microbiology*, *53*(2), 158–162. https://doi.org/10.1007/s00284-005-0501-4

Rocha, C. L., Coburn, J., Rucks, E. A., & Olson, J. C. (2003). Characterization of *Pseudomonas aeruginosa* Exoenzyme S as a Bifunctional Enzyme in J774A.1 Macrophages. *Infection and Immunity*, *71*(9), 5296–5305. https://doi.org/10.1128/IAI.71.9.5296-5305.2003

Rodney, M.D. (2002). Biofilms: Microbial Life on Surfaces. *Emerg Infect Dis. 8(9).* 881-890.

Roe, D., Karandikar, B., Bonn-Savage, N., Gibbins, B., & Roullet, J.-B. (2008). Antimicrobial surface functionalization of plastic catheters by silver nanoparticles. *Journal of Antimicrobial Chemotherapy*, *61*(4), 869–876. https://doi.org/10.1093/jac/dkn034

Rose, G., & Pyle-Eilola, A. L. (2021). The Effect of Urine Collection with a Novel External Catheter Device on Common Urine Chemistry and Urinalysis Results. *The Journal of Applied Laboratory Medicine*, *6*(6), 1618–1622. https://doi.org/10.1093/jalm/jfab054

Rother, P., Löffler, S., Dorschner, W., Reibiger, I., & Bengs, T. (1996). Anatomic basis of micturition and urinary continence. Muscle systems in urinary bladder neck during ageing. *Surg Radiol Anat. 18(3)*, 173-177.

Rtimi, S., Sanjines, R., Pulgarin, C., & Kiwi, J. (2016). Quasi-Instantaneous Bacterial Inactivation on Cu–Ag Nanoparticulate 3D Catheters in the Dark and Under Light: Mechanism and Dynamics. *ACS Applied Materials & Interfaces*, *8*(1), 47–55. https://doi.org/10.1021/acsami.5b09730

Rubi, H., Mudey, G., & Kunjalwar, R. (2022). Catheter-Associated Urinary Tract Infection (CAUTI). *Cureus.14(10).* E30385. https://doi.org/10.7759/cureus.30385

Ruutu, M., Alfthan, O., Talja, M., & Andersson, L.C. (1985). Cytotoxicity of Latex Urinary Catheters. *British Journal of Urology. 57(1).* 82-87.

Saini, H., Chhibber, S., & Harjai, K. (2016). Antimicrobial and antifouling efficacy of urinary catheters impregnated with a combination of macrolide and fluoroquinolone antibiotics against *Pseudomonas aeruginosa*. *Biofouling*, *32*(5), 511–522. https://doi.org/10.1080/08927014.2016.1155564

Saint, S., Greene, M. T., Krein, S. L., Rogers, M. A. M., Ratz, D., Fowler, K. E., Edson, B. S., Watson, S. R., Meyer-Lucas, B., Masuga, M., Faulkner, K., Gould, C. V., Battles, J., & Fakih, M. G. (2016). A Program to Prevent Catheter-Associated Urinary Tract Infection in Acute Care. *New England Journal of Medicine*, *374*(22), 2111–2119. https://doi.org/10.1056/NEJMoa1504906

Saint, S., Wiese, J., Amory, J.K., Bernstein, M.L., Patel, U.S., Zemencuk, J.K., Bernstein, S.J., Lipsky, B.A., & Hofer, T.P. (2000). Are physicians aware of which of their patients have indwelling urinary catheters?. *Am J Med, 109(6),* 476-480.

Sanchez, K. G., Ferrell, M. J., Chirakos, A. E., Nicholson, K. R., Abramovitch, R. B., Champion, M. M., & Champion, P. A. (2020). EspM Is a Conserved Transcription Factor That Regulates Gene Expression in Response to the ESX-1 System. *mBio*, *11*(1), e02807-19. https://doi.org/10.1128/mBio.02807-19

Sasaki, K., Tenjimbayashi, M., Manabe, K., & Shiratori, S. (2016). Asymmetric Superhydrophobic/Superhydrophilic Cotton Fabrics Designed by Spraying Polymer and Nanoparticles. *ACS Applied Materials & Interfaces*, *8*(1), 651–659. https://doi.org/10.1021/acsami.5b09782

Scalerandi, M. V., Peinetti, N., Leimgruber, C., Cuello Rubio, M. M., Nicola, J. P., Menezes, G. B., Maldonado, C. A., & Quintar, A. A. (2018). Inefficient N2-Like Neutrophils Are Promoted by

Androgens During Infection. *Frontiers in Immunology*, *9*, 1980. https://doi.org/10.3389/fimmu.2018.01980

Schaeffer, A. J., Amundsen, S. K., & Jones, J. M. (1980). Effect of Carbohydrates on Adherence of Escherichia coli to Human Urinary Tract Epithelial Cells. *INFECT. IMMUN.*, *30*.

Schallom, M., Prentice, D., Sona, C., Vyers, K., Arroyo, C., Wessman, B., & Ablordeppey, E. (2020). Accuracy of Measuring Bladder Volumes With Ultrasound and Bladder Scanning. *American Journal of Critical Care*, *29*(6), 458–467. https://doi.org/10.4037/ajcc2020741

Scherer, G. W. (1989). Mechanics of syneresis I. Theory. *Journal of Non-Crystalline Solids*, *108*(1), 18–27. https://doi.org/10.1016/0022-3093(89)90328-1

Schreiber, H. L., Conover, M. S., Chou, W.-C., Hibbing, M. E., Manson, A. L., Dodson, K. W., Hannan, T. J., Roberts, P. L., Stapleton, A. E., Hooton, T. M., Livny, J., Earl, A. M., & Hultgren, S. J. (2017). Bacterial virulence phenotypes of *Escherichia coli* and host susceptibility determine risk for urinary tract infections. *Science Translational Medicine*, *9*(382), eaaf1283. https://doi.org/10.1126/scitranslmed.aaf1283

Schwartz, D. S., & Barone, J. E. (2006). Correlation of urinalysis and dipstick results with catheter-associated urinary tract infections in surgical ICU patients. *Intensive Care Medicine*, *32*(11), 1797–1801. https://doi.org/10.1007/s00134-006-0365-5

Scotland, K. B., Kung, S. H., Chew, B. H., & Lange, D. (2020). Uropathogens Preferrentially Interact with Conditioning Film Components on the Surface of Indwelling Ureteral Stents Rather than Stent Material. *Pathogens*, *9*(9), 764. https://doi.org/10.3390/pathogens9090764

Semprebon, C., McHale, G., & Kusumaatmaja, H. (2017). Apparent contact angle and contact angle hysteresis on liquid infused surfaces. *Soft Matter*. 13 (101).

Sen, A., Iyer, J., Boddu, S., Kaul, A., & Kaul, R. (2019). Estrogen receptor alpha differentially modulates host immunity in the bladder and kidney in response to urinary tract infection. *Am J Clin Exp Urol. 7(3).* 110-122.

Sergeant, G.P., Hollywood, M.A., & Thornbury, K.D. (2019). Spontaneous Activity in Urethral Smooth Muscle. *Adv Exp Med Biol.* 2019 (1124), 149-167.

Shah, R. M., Cihanoğlu, A., Hardcastle, J., Howell, C., & Schiffman, J. D. (2022). Liquid-Infused Membranes Exhibit Stable Flux and Fouling Resistance. *ACS Applied Materials & Interfaces*, *14*(4), 6148–6156. https://doi.org/10.1021/acsami.1c20674

Shaikh, N., Morone, N., Bost, J.E., & Farrel, M.H. (2008). Prevalence of Urinary Tract Infection in Childhood A Meta-Analysis. *The Pediatric Infectious Disease Journal. 27(4).* 302-308.

Sharma, D., Misba, L., & Khan, A. U. (2019). Antibiotics versus biofilm: An emerging battleground in microbial communities. *Antimicrobial Resistance & Infection Control*, *8*(1), 76. https://doi.org/10.1186/s13756-019-0533-3

She, P., Wang, Y., Li, Y., Zhou, L., Li, S., Zeng, X., Liu, Y., Xu, L., & Wu, Y. (2021). Drug Repurposing: In vitro and in vivo Antimicrobial and Antibiofilm Effects of Bithionol Against Enterococcus faecalis and Enterococcus faecium. *Front. Microbiol. 12.* 579806.

Shen, Y., Sun, Y., Wang, P., & Zhang, D. (2023). Why does SLIPS inhibit P.aeruginosa initial adhesion in static condition? *Journal of Industrial and Engineering Chemistry*, *124*, 532–538. https://doi.org/10.1016/j.jiec.2023.05.008

Shillingford, C., Maccallum, N., Wong, T., Kim, P., & Aizenberg, J. (2013). Fabrics coated with lubricated nanostructures display robust omniphobicity. *Nanotechnology. 25(1).* 14-19.

Singha, P., Locklin, J., & Handa, H. (2017). A review of the recent advances in antimicrobial coatings for urinary catheters. *Acta Biomaterialia*, *50*, 20–40. https://doi.org/10.1016/j.actbio.2016.11.070
Singha, P., Locklin, J., & Handa, H. (2017). A review of the recent advances in antimicrobial coatings for urinary catheters. *Acta Biomaterialia*, *50*, 20–40. https://doi.org/10.1016/j.actbio.2016.11.070

Sinha, A. K., Kumar, N., Kumar, A., & Singh, S. (2018). Condom catheter induced penile skin erosion. *Journal of Surgical Case Reports*, *2018*(10). https://doi.org/10.1093/jscr/rjy275

Skafle, I., Nordahl-Hansen, A., Quintana, D.S., Wynn, R., & Gabarron, E. (2022). Misinformation About COVID-19 Vaccines on Social Media: Rapid Review. *J Med Internet Res. 24(8).* E37367.

Skelton-Dudley, F., Doan, J., Suda, K., Holmes, S. A., Evans, C., & Trautner, B. (2019). Spinal Cord Injury Creates Unique Challenges in Diagnosis and Management of Catheter-Associated Urinary Tract Infection. *Topics in Spinal Cord Injury Rehabilitation*, *25*(4), 331–339. https://doi.org/10.1310/sci2504-331

Skjøt-Rasmussen, L., Hammerum, A. M., Jakobsen, L., Lester, C. H., Larsen, P., & Frimodt-Møller, N. (2011). Persisting clones of Escherichia coli isolates from recurrent urinary tract infection in men and women. *Journal of Medical Microbiology*, *60*(4), 550–554. https://doi.org/10.1099/jmm.0.026963-0

Smith, J. D., Dhiman, R., Anand, S., Reza-Garduno, E., Cohen, R. E., McKinley, G. H., & Varanasi, K. K. (2013). Droplet mobility on lubricant-impregnated surfaces. *Soft Matter*, *9*(6), 1772–1780. https://doi.org/10.1039/C2SM27032C

Snopkova, K., Dufkova, K., Klimesova, P., Vanerkova, M., Ruzicka, F., & Hola, V. (2020). Prevalence of bacteriocins and their co-association with virulence factors within Pseudomonas aeruginosa catheter isolates. *International Journal of Medical Microbiology*, *310*(8), 151454. https://doi.org/10.1016/j.ijmm.2020.151454

Song, C., & Rutledge, G. C. (2023). Three-Dimensional Imaging of Emulsion Separation through Liquid-Infused Membranes Using Confocal Laser Scanning Microscopy. *Langmuir*, *39*(32), 11468–11480. https://doi.org/10.1021/acs.langmuir.3c01477

Sonnex, C. (1998). Influence of ovarian hormones on urogenital infection. *Sexually Transmitted Infections*, *74*(1), 11–19. https://doi.org/10.1136/sti.74.1.11

Sotiri, I., Overton, J. C., Waterhouse, A., & Howell, C. (2016). Immobilized liquid layers: A new approach to anti-adhesion surfaces for medical applications. *Experimental Biology and Medicine*, *241*(9), 909–918. https://doi.org/10.1177/1535370216640942

Sotiri, I., Tajik, A., Lai, Y., Zhang, C. T., Kovalenko, Y., Nemr, C. R., Ledoux, H., Alvarenga, J., Johnson, E., Patanwala, H. S., Timonen, J. V. I., Hu, Y., Aizenberg, J., & Howell, C. (2018). Tunability of liquid-infused silicone materials for biointerfaces. *Biointerphases*, *13*(6), 06D401. https://doi.org/10.1116/1.5039514

Spurbeck, R.R., Stapleton, A.E., Johnson, J.R., Walk, S.T., Hooton, T.M., & Mobley, H.L.T. (2011). Fimbrial Profiles Predict Virulence of Uropathogenic Escherichia coli Strains: Contribution of Ygi and Yad Fimbriae. *Infect Immun. 79(12).* 4753-4763.

Starčič Erjavec, M., Rijavec, M., Križan-Hergouth, V., Fruth, A., & Žgur-Bertok, D. (2007). Chloramphenicol- and tetracycline-resistant uropathogenic Escherichia coli (UPEC) exhibit reduced virulence potential. *International Journal of Antimicrobial Agents*, *30*(5), 436–442. https://doi.org/10.1016/j.ijantimicag.2007.06.025

Steel, D.H.W., Wong, D., & Sakamoto, T. (2021). Silicone oils compared and found wanting. *259:11-12.*

Steward, D.K., Wood, G.L., Cohen, R.L., Smith, J.W., Mackowiak, P.A. (1985). Failure of the urinalysis and quantitative urine culture in diagnosing symptomatic urinary tract infections in patients with long-term urinary catheters. *American Journal of Infection Control. 13(4).* 154-160.

Stickler, D., Young, R., Jones, G., Sabbuba, N., & Morris, N. (2003). Why are Foley catheters so vulnerable to encrustation and blockage by crystalline bacterial biofilm?. *Urol Res. 31*. 306-311.

Stickler, D.J., & Morgan, S.D. (2008). Observations on the development of the crystalline bacterial biofilms that encrust and block Foley catheters. *Journal of Hospital Infection. 69.* 350-360.

Straub, H., Bigger, C.M., Valentin, J., Abt, D., Qin, X., Eberl, L., Maniura-Weber, K., & Ren, Q. (2019). Bacterial Adhesion on Soft Materials: Passive Physicochemical Interactions or Active Bacterial Mechanosensing?. *Advanced Healthcare Materials. 8(8).* 1801323.

Sunny, S., Cheng, G., Daniel, D., Lo, P., Ochoa, S., Howell, C., Vogel, N., Majid, A., & Aizenberg, J. (2016). Transparent antifouling material for improved operative field visibility in endoscopy. *Proceedings of the National Academy of Sciences*, *113*(42), 11676–11681. https://doi.org/10.1073/pnas.1605272113

Sunny, S., Vogel, N., Howell, C., Vu, T.L., Aizenberg, J. (2014). Lubricant-Infused Nanoparticulate Coatings Assembled by Layer-by-Layer Deposition. *Advanced Functional Materials. 24(42).*

Sutradhar, I., Kalyan, P., Chukwu, K., Abia, A.L.K., Mbanga, J., Essack, S., Hamer, D.H., & Zaman, M.H. (2023). *bioRxiv*. DOI: 10.1101/2023.06.16.545339

Talja, M., Korpela, A., & Järvi, K. (1990). Comparison of Urethral Reaction to Full Silicone, Hydrogen-coated and Siliconised Latex Catheters. *British Journal of Urology. 66(6).* 652-657.

Tambyah, P., & Oon, J. (2012). Catheter-associated urinary tract infection. *Current Opinion in Infectious Diseases. 25(4).* 365-370.

Tambyah, P.A., & Maki, D.G. (2000). Catheter-Associated Urinary Tract Infection Is Rarely Symptomatic- A Prospective Study of 1497 Catheterized Patients. *Arch Intern Med. 160(5)*. 678-682.

Tambyah, P.A., Knasinski, V., Maki, D.G. (2002). The direct costs of nosocomial catheter-associated urinary tract infection in the era of managed care. *Infect Control Hosp Epidemiol. 23(1).* 27-31.

Tamer, T. M. (2013). Hyaluronan and synovial joint: Function, distribution and healing. *Interdisciplinary Toxicology*, *6*(3), 111–125. https://doi.org/10.2478/intox-2013-0019

Tangy, F., Moukkadem, M., Vindimian, E., Capmau, M., & Le Goffic, F. (1985). Mechanism of action of gentamicin components: Characteristics of their binding to *Escherichia coli* ribosomes. *European Journal of Biochemistry*, *147*(2), 381–386. https://doi.org/10.1111/j.1432-1033.1985.tb08761.x

Tenke, P., Kovacs, B., Bjerklund Johansen, T. E., Matsumoto, T., Tambyah, P. A., & Naber, K. G. (2008). European and Asian guidelines on management and prevention of catheter-associated urinary tract infections. *International Journal of Antimicrobial Agents*, *31*, 68–78. https://doi.org/10.1016/j.ijantimicag.2007.07.033

Tenke, P., Köves, B., & Johansen, T. (2014). An update on prevention and treatment of catheter-associated urinary tract infections. *Current Opinion in Infectious Diseases. 27(1).* 102-107.

Tenney, J.H., & Warren, J.W. (1988). Bacteriuria in Women with Long-Term Catheters: Paired Comparison of Indwelling and Replacement Catheters. *The Journal of Infectious Diseases. 157(1).* 199-202.

Tesler, A. B., Kim, P., Kolle, S., Howell, C., Ahanotu, O., & Aizenberg, J. (2015). Extremely durable biofouling-resistant metallic surfaces based on electrodeposited nanoporous tungstite films on steel. *Nature Communications*, *6*(1), 8649. https://doi.org/10.1038/ncomms9649

Thibon, P., Le Coutour, X., Leroyer, R., & Fabry, J. (2000). Randomized multi-centre trial of the effects of a catheter coated with hydrogel and silver salts on the incidence of hospital-acquired urinary tract infections. *Journal of Hospital Infection*, *45*(2), 117–124. https://doi.org/10.1053/jhin.1999.0715

Thomas, D., Rutman, M., Cooper, K., Abrams, A., Finkelstein, J., & Chughtai, B. (2017). Does cranberry have a role in catheter-associated urinary tract infections? *Canadian Urological Association Journal*, *11*(11), E421-4. https://doi.org/10.5489/cuaj.4472

Thumbikat, P., Berry, R.E., Zhou, G., Billips, B.K., Yaggie, R.E., Zaichuck, T., Sun, T., Schaeffer, A.J., & Klumpp, D.J. (2009). Bacteria-Induced Uroplakin Signaling Mediates Bladder Response to Infection. *PLoS Pathog. 5(5).* E1000415.

Tien, B. Y. Q., Goh, H. M. S., Chong, K. K. L., Bhaduri-Tagore, S., Holec, S., Dress, R., Ginhoux, F., Ingersoll, M. A., Williams, R. B. H., & Kline, K. A. (2017). Enterococcus faecalis Promotes Innate Immune Suppression and Polymicrobial Catheter-Associated Urinary Tract Infection. *Infection and Immunity*, *85*(12).

Togasawa, R., Tenjimbayashi, M., Matsubayashi, T., Moriya, T., Manabe, K., & Shiratori, S. (2018). A Fluorine-free Slippery Surface with Hot Water Repellency and Improved Stability against Boiling. *ACS Applied Materials & Interfaces*, *10*(4), 4198–4205. https://doi.org/10.1021/acsami.7b15689

Toh, S.-L., Lee, B. B., Ryan, S., Simpson, J. M., Clezy, K., Bossa, L., Rice, S. A., Marial, O., Weber, G. H., Kaur, J., Boswell-Ruys, C. L., Goodall, S., Middleton, J. W., Tuderhope, M., & Kotsiou, G. (2019). Probiotics [LGG-BB12 or RC14-GR1] versus placebo as prophylaxis for urinary tract infection in persons with spinal cord injury [ProSCIUTTU]: A randomised controlled trial. *Spinal Cord*, *57*(7), 550–561. https://doi.org/10.1038/s41393-019-0251-y

Tolani, M. A., Suleiman, A., Awaisu, M., Abdulaziz, M. M., Lawal, A. T., & Bello, A. (2020). Acute urinary tract infection in patients with underlying benign prostatic hyperplasia and prostate cancer. *Pan African Medical Journal*, *36*. https://doi.org/10.11604/pamj.2020.36.169.21038

Toomey, R., Freidank, D., & Rühe, J. (2003). Swelling Behavior of Thin, Surface-Attached Polymer Networks. *Macromolecules. 37.* 882-887.

Tractenberg, R. E., Frost, J. K., Yumoto, F., Rounds, A. K., Ljungberg, I. H., & Groah, S. L. (2021). Reliability of the Urinary Symptom Questionnaires for people with neurogenic bladder (USQNB) who void or use indwelling catheters. *Spinal Cord*, *59*(9), 939–947. https://doi.org/10.1038/s41393-021-00665-x

Trautner, B. W., & Darouiche, R. O. (2004a). Catheter-Associated Infections: Pathogenesis Affects Prevention. *Archives of Internal Medicine*, *164*(8), 842. https://doi.org/10.1001/archinte.164.8.842

Trautner, B. W., & Darouiche, R. O. (2004b). Role of biofilm in catheter-associated urinary tract infection☆. *American Journal of Infection Control*, *32*(3), 177–183. https://doi.org/10.1016/j.ajic.2003.08.005

Tryggvason, K., & Wartiovaara, J. (2005). How Does the Kidney Filter Plasma? *Physiology*, *20*(2), 96–101. https://doi.org/10.1152/physiol.00045.2004

Tsuchimori, N., Hayashi, R., Shino, A., Yamazaki, T., & Okonogi, K. (1994). Enterococcus faecalis aggravates pyelonephritis caused by Pseudomonas aeruginosa in experimental ascending mixed urinary tract infection in mice. *Infection and Immunity*, *62*(10), 4534–4541. https://doi.org/10.1128/iai.62.10.4534-4541.1994

Tunney, M.M., & Gorman, S.P. (2002). Evaluation of a poly(vinyl pyrollidone)-coated biomaterial for urological use. *Biomaterials. 23 (2002).* 4601-4608.

Urinary Tract Infection. (2024). *Urinary Tract Infection*.

Van Dyck, K., Robberecht, H., Van Cauwenbergh, R., Deelstra, H., Arnaud, J., Willemyns, L., Benijts, F., Centeno, J. A., Taylor, H., Soares, M. E., Bastos, M. L., Ferreira, M. A., D'Haese, P. C., Lamberts, L. V., Hoenig, M., Knapp, G., Lugowski, S. J., Moens, L., Riondato, J., … Uytterhoeven, M. (2000). Spectrometric determination of silicon in food and biological samples: An interlaboratory trial. *Journal of Analytical Atomic Spectrometry*, *15*(6), 735–741. https://doi.org/10.1039/b000572j

Vance, R. E., Rietsch, A., & Mekalanos, J. J. (2005). Role of the Type III Secreted Exoenzymes S, T, and Y in Systemic Spread of *Pseudomonas aeruginosa* PAO1 In Vivo. *Infection and Immunity*, *73*(3), 1706–1713. https://doi.org/10.1128/IAI.73.3.1706-1713.2005

Vejborg, R. M., Hancock, V., Schembri, M. A., & Klemm, P. (2011). Comparative Genomics of Escherichia coli Strains Causing Urinary Tract Infections. *Applied and Environmental Microbiology*, *77*(10), 3268–3278. https://doi.org/10.1128/AEM.02970-10

Veronesi, F., Guarini, G., Corozzi, A., & Raimondo, M. (2021). Evaluation of the Durability of Slippery, Liquid-Infused Porous Surfaces in Different Aggressive Environments: Influence of the Chemical-Physical Properties of Lubricants. *Coatings*, *11*(10), 1170. https://doi.org/10.3390/coatings11101170

Villanueva, C., Hossain, S.G.M., & Nelson, C.A. (2011). Silicone Catheters May Be Superior to Latex Catheters in Difficult Urethral Catheterization After Urethral Dilation. *Journal of Endourology. 25(5).* 841-844.

Villegas, M., Zhang, Y., Abu Jarad, N., Soleymani, L., & Didar, T. F. (2019). Liquid-Infused Surfaces: A Review of Theory, Design, and Applications. *ACS Nano*, *13*(8), 8517–8536. https://doi.org/10.1021/acsnano.9b04129

Vogel, N., Belisle, R. A., Hatton, B., Wong, T.-S., & Aizenberg, J. (2013). Transparency and damage tolerance of patternable omniphobic lubricated surfaces based on inverse colloidal monolayers. *Nature Communications*, *4*(1), 2176. https://doi.org/10.1038/ncomms3176

Waites, K. B., Canupp, K. C., Roper, J. F., Camp, S. M., & Chen, Y. (2006). Evaluation of 3 Methods of Bladder Irrigation to Treat Bacteriuria in Persons With Neurogenic Bladder. *The Journal of Spinal Cord Medicine*, *29*(3), 217–226. https://doi.org/10.1080/10790268.2006.11753877

Walker, J. N., Flores-Mireles, A. L., Pinkner, C. L., Schreiber, H. L., Joens, M. S., Park, A. M., Potretzke, A. M., Bauman, T. M., Pinkner, J. S., Fitzpatrick, J. A. J., Desai, A., Caparon, M. G., & Hultgren, S. J. (2017). Catheterization alters bladder ecology to potentiate *Staphylococcus aureus* infection of the urinary tract. *Proceedings of the National Academy of Sciences*, *114*(41). https://doi.org/10.1073/pnas.1707572114

Wang, C., Symington, J.W., Ma, E., Cao, B., & Mysorekar, I.U. (2013). Estrogenic Modulation of Uropathogenic Escherichia coli Infection Pathogenesis in a Murine Menopause Model. https://doi.org/10.1128/iai.01234-12

Wang, H., Min, G., Glockshubber, R., Sun, T. & Kong, X. (2009). Uropathogenic E. coli adhesin-induced host cell receptor conformational changes: implications in transmembrane signaling transduction. *J Mol Bio. 392(2).* 352-361.

Wang, J., Hahn, S., Amstad, E., & Vogel, N. (2022). Tailored Double Emulsions Made Simple. *Advanced Materials*, *34*(5), 2107338. https://doi.org/10.1002/adma.202107338

Wang, L., Zhang, S., Keatch, R., Corner, G., Nabi, G., Murdoch, S., Davidson, F., & Zhao, Q. (2019). In-vitro antibacterial and anti-encrustation performance of silver-polytetrafluoroethylene nanocomposite coated urinary catheters. *Journal of Hospital Infection*, *103*(1), 55–63. https://doi.org/10.1016/j.jhin.2019.02.012

Wang, P., Zhang, D., Sun, S., Li, T., & Sun, Y. (2017). Fabrication of Slippery Lubricant-Infused Porous Surface with High Underwater Transparency for the Control of Marine Biofouling. *ACS Applied Materials & Interfaces*, *9*(1), 972–982. https://doi.org/10.1021/acsami.6b09117

Ware, C. S., Smith-Palmer, T., Peppou-Chapman, S., Scarratt, L. R. J., Humphries, E. M., Balzer, D., & Neto, C. (2018). Marine Antifouling Behavior of Lubricant-Infused Nanowrinkled Polymeric Surfaces. *ACS Applied Materials & Interfaces*, *10*(4), 4173–4182. https://doi.org/10.1021/acsami.7b14736

Wargo, M. J., Gross, M. J., Rajamani, S., Allard, J. L., Lundblad, L. K. A., Allen, G. B., Vasil, M. L., Leclair, L. W., & Hogan, D. A. (2011). Hemolytic Phospholipase C Inhibition Protects Lung Function during *Pseudomonas aeruginosa* Infection. *American Journal of Respiratory and Critical Care Medicine*, *184*(3), 345–354. https://doi.org/10.1164/rccm.201103-0374OC

Warren, C., Fosnacht, J.D., Tremblay, E.E. (2021). Implementation of an external female urinary catheter as an alternative to an indwelling urinary catheter. *Am J Infect Control. 49(6).* 764-768.

Warren, J.W. (1997). Catheter-associated urinary tract infection. *Infectious Disease Clinics of North America. 11(3).* 609-622.

Warren, J.W., MuncieJr, H.L., & Hall-Craggs, M. (1988). Acute Pyelonephritis Associated with Bacteriuria During Long-Term Catheterization: A Prospective Clinicopathological Study. *The The Journal of Infectious Diseases. 158(6).* 1341-1346.

Warren, J.W., Platt, R., Thomas, R.J., Rosner, B., & Kass, E.H. (1978). Antibiotic Irrigation and Catheter-Associated Urinary-Tract Infections. *N Engl J Med. 299.* 570-573.

Wazait, H.D., Patel, H.R., van der Meulen, H.P., Ghei, M., Al-Buheissi, S., Kelsey, M., Miller, R.A., & Emberton, M. (2004). A pilot randomized double-blind placebo-controlled trial on the use of antibiotics on urinary catheter removal to reduce the rate of urinary tract infection: the pitfalls of ciprofloxacin. *BJU International. 94(7).* 1048-1050.

Wazait, H.D., van der Meullen, J., Patel, H.R.H., Brown, C.T., Gadgil, S., Miller, R.A., Kelsey, M.C., & Emberton, M. (2004). Antibiotics on urethral catheter withdrawal: a hit and miss affair. *The Journal of Hospital Infection. 58(4).* 297-302.

Webb, R.J., Lawson, A.L., & Neal, D.E. (1990). Clean Intermittent Self-catheterisation in 172 Adults. *British Journal of Urology. 65(1).* 20-23.

Weiner, L. M., Webb, A. K., Limbago, B., Dudeck, M. A., Patel, J., Kallen, A. J., Edwards, J. R., & Sievert, D. M. (2016). Antimicrobial-Resistant Pathogens Associated With Healthcare-Associated Infections: Summary of Data Reported to the National Healthcare Safety Network at the Centers for Disease Control and Prevention, 2011–2014. *Infection Control & Hospital Epidemiology*, *37*(11), 1288–1301. https://doi.org/10.1017/ice.2016.174

Wen, G., Guo, Z., & Liu, W. (2017). Biomimetic polymeric superhydrophobic surfaces and nanostructures: From fabrication to applications. *Nanoscale*, *9*(10), 3338–3366. https://doi.org/10.1039/C7NR00096K

Westfall, C., Flores-Mireles, A. L., Robinson, J. I., Lynch, A. J. L., Hultgren, S., Henderson, J. P., & Levin, P. A. (2019). The Widely Used Antimicrobial Triclosan Induces High Levels of Antibiotic Tolerance *In Vitro* and Reduces Antibiotic Efficacy up to 100-Fold *In Vivo*. *Antimicrobial Agents and Chemotherapy*, *63*(5), e02312-18. https://doi.org/10.1128/AAC.02312-18

Wettergren, B., Jodal, U., & Jonasson, G. (1985). Epidemiology of Bacteriuria during the First Year of Life. *Acta Paediatrica. 74(6).* 925-933.

Willcox, M.D. (2019). Tear film, contact lenses and tear biomarkers. *Clin Exp Optom. 102(4).* 350-363.

Willson, M., Wilde, M., Webb, M., Thompson, D., Parker, D., Harwood, J., Callan, L., & Gray, M. (2009). Nursing Interventions to Reduce the Risk of Catheter-Associated Urinary Tract Infection Part 2 Staff Education, Monitoring, and Care Techniques. *Journal of Wound, Ostomy and Continence Nursing. 36(2).* 137-154.

Winberg, J., Ander, H.J., Bergström, T., Jacobsson, B., Larson, H., & Lincoln, K. (1974). Epidemiology of Symptomatic Urinary Tract Infection in Childhood. *Acta Paediatrica. 63(25).* 1-20.

Winson, M. K., Camara, M., Latifi, A., Foglino, M., Chhabra, S. R., Daykin, M., Bally, M., Chapon, V., Salmond, G. P., & Bycroft, B. W. (1995). Multiple N-acyl-L-homoserine lactone signal molecules regulate production of virulence determinants and secondary metabolites in Pseudomonas aeruginosa. *Proceedings of the National Academy of Sciences*, *92*(20), 9427–9431. https://doi.org/10.1073/pnas.92.20.9427

Wisplinghoff, H., Bischoff, T., Tallent, S. M., Seifert, H., Wenzel, R. P., & Edmond, M. B. (2004). Nosocomial Bloodstream Infections in US Hospitals: Analysis of 24,179 Cases from a Prospective Nationwide Surveillance Study. *Clin Infect Dis. 39(3).* 309-317.

Wong, S.-N., Tse, N. K.-C., Lee, K.-P., Yuen, S.-F., Leung, L. C.-K., Pau, B. C.-K., Chan, W. K.-Y., Lee, K.-W., Cheung, H.-M., Chim, S., & Yip, C. M.-S. (2010). Evaluating different imaging strategies in children after first febrile urinary tract infection. *Pediatric Nephrology*, *25*(10), 2083–2091. https://doi.org/10.1007/s00467-010-1569-z

Wong, T.-S., Kang, S. H., Tang, S. K. Y., Smythe, E. J., Hatton, B. D., Grinthal, A., & Aizenberg, J. (2011). Bioinspired self-repairing slippery surfaces with pressure-stable omniphobicity. *Nature*, *477*(7365), 443–447. https://doi.org/10.1038/nature10447

Wong, W. S. Y., Hauer, L., Naga, A., Kaltbeitzel, A., Baumli, P., Berger, R., D'Acunzi, M., Vollmer, D., & Butt, H.-J. (2020). Adaptive Wetting of Polydimethylsiloxane. *Langmuir*, *36*(26), 7236–7245. https://doi.org/10.1021/acs.langmuir.0c00538

Woods, D. E., Schaffer, M. S., Rabin, H. R., Campbell, G. D., & Sokol, P. A. (1986). Phenotypic comparison of Pseudomonas aeruginosa strains isolated from a variety of clinical sites. *Journal of Clinical Microbiology*, *24*(2), 260–264. https://doi.org/10.1128/jcm.24.2.260-264.1986

Woods, D.E., Lam, J.S., Paranchych, W., Speert, D.P., Campbell, M. & Godfrey, A.J. (1997). Correlation of Pseudomonas aeruginosa virulence factors from clinical and environmental isolates with pathogenicity in the neutropenic mouse. *Canadian Journal of Microbiology. https://doi.org/10.1139/m97-077*

Wu, D., Ma, L., Liu, B., Zhang, D., Minhas, B., Qian, H., Terryn, H. A., & Mol, J. M. C. (2021). Long-term deterioration of lubricant-infused nanoporous anodic aluminium oxide surface immersed in NaCl solution. *Journal of Materials Science & Technology*, *64*, 57–65. https://doi.org/10.1016/j.jmst.2019.12.008

Wu, S., Zhang, B., Liu, Y., Suo, X., & Li, H. (2018). Influence of surface topography on bacterial adhesion: A review (Review). *Biointerphases. 13.* 060801.

Wylie, M.P., Bell, S.E.J., Nockermann, P., Bell, R., & McCoy, C.P. (2020). Phosphonium Ionic Liquid-Infused Poly(vinyl chloride) Surfaces Possessing Potent Antifouling Properties. *ACS Omega. 5(14).* 7771-7781.

Xiao, L., Li, J., Mieszkin, S., Di Fino, A., Clare, A. S., Callow, M. E., Callow, J. A., Grunze, M., Rosenhahn, A., & Levkin, P. A. (2013). Slippery Liquid-Infused Porous Surfaces Showing Marine Antibiofouling Properties. *ACS Applied Materials & Interfaces*, *5*(20), 10074–10080. https://doi.org/10.1021/am402635p

Xu, W., Flores-Mireles, A. L., Cusumano, Z. T., Takagi, E., Hultgren, S. J., & Caparon, M. G. (2017). Host and bacterial proteases influence biofilm formation and virulence in a murine model of enterococcal catheter-associated urinary tract infection. *Npj Biofilms and Microbiomes*, *3*(1), 28. https://doi.org/10.1038/s41522-017-0036-z

Yan, W., Xue, S., Bin Xiang, Zhao, X., Zhang, W., Mu, P., & Li, J. (2023). Recent advances of slippery liquid-infused porous surfaces with anti-corrosion. *Chemical Communications*, *59*(16), 2182–2198. https://doi.org/10.1039/D2CC06688B

Yang, B., & Foley, S. (2017). First experience in the UK of treating women with recurrent urinary tract infections with the bacterial vaccine Uromune®. *BJU International. 121(2).* 289-292.

Yao, W., Wu, L., Sun, L., Jiang, B., & Pan, F. (2022). Recent developments in slippery liquid-infused porous surface. *Progress in Organic Coatings*, *166*, 106806. https://doi.org/10.1016/j.porgcoat.2022.106806

Yin, J., Mei, M. L., Li, Q., Xia, R., Zhang, Z., & Chu, C. H. (2016). Self-cleaning and antibiofouling enamel surface by slippery liquid-infused technique. *Scientific Reports*, *6*(1), 25924. https://doi.org/10.1038/srep25924

Yong, J., Huo, J., Yang, Q., Chen, F., Fang, Y., Wu, X., Liu, L., Lu, X., Zhang, J., & Hou, X. (2018). Femtosecond Laser Direct Writing of Porous Network Microstructures for Fabricating Super-Slippery Surfaces with Excellent Liquid Repellence and Anti-Cell Proliferation. *Advanced Materials Interfaces*, *5*(7), 1701479. https://doi.org/10.1002/admi.201701479

Yu, M., Liu, M., Hou, Y., Fu, S., Zhang, L., Li, M., & Wang, D. (2020). Facile fabrication of biomimetic slippery lubricant-infused transparent and multifunctional omniphobic surfaces. *Journal of Materials Science*, *55*(10), 4225–4237. https://doi.org/10.1007/s10853-019-04243-8

Yu, Z., Zhou, C., Liu, R., Zhang, Q., Gong, J., Tao, D., & Ji, Z. (2020). Fabrication of superhydrophobic surface with enhanced corrosion resistance on H62 brass substrate. *Colloids and Surfaces A: Physicochemical and Engineering Aspects*, *589*, 124475. https://doi.org/10.1016/j.colsurfa.2020.124475

Zafriri, D., Ofek, I., Adar, R., Pocino, M., & Sharon, N. (1989). Inhibitory activity of cranberry juice on adherence of type 1 and type P fimbriated Escherichia coli to eucaryotic cells. *Antimicrobial Agents and Chemotherapy*, *33*(1), 92–98. https://doi.org/10.1128/AAC.33.1.92

Zahller, J., & Stewart, P.S. (2002). Transmission Electron Microscopic Study of Antibiotic Action on Klebsiella pneumoniae Biofilm. *Antimicrob Agents Chemother*. *46(8).* 2679-2683.

Zavodnick, J., Harley, C., Zabriskie, K., & Brahmbhatt, Y. (2020). Effect of a Female External Urinary Catheter on Incidence of Catheter-Associated Urinary Tract Infection. *Cureus*. https://doi.org/10.7759/cureus.11113

Zhang, J., Sheng, X., & Jiang, L. (2009). The Dewetting Properties of Lotus Leaves. *Langmuir*. *25(3).* 1371-1376.

Zhang, M., Chen, P., Li, J., & Wang, G. (2022). Water-repellent and corrosion resistance properties of epoxy-resin-based slippery liquid-infused porous surface. *Progress in Organic Coatings*, *172*, 107152. https://doi.org/10.1016/j.porgcoat.2022.107152

Zhang, P., Chen, H., Zhang, L., Ran, T., & Zhang, D. (2015). Transparent self-cleaning lubricant-infused surfaces made with large-area breath figure patterns. *Applied Surface Science*, *355*, 1083–1090. https://doi.org/10.1016/j.apsusc.2015.07.159

Zheng, K., Setyawati, M. I., Leong, D. T., & Xie, J. (2018). Antimicrobial silver nanomaterials. *Coordination Chemistry Reviews*, *357*, 1–17. https://doi.org/10.1016/j.ccr.2017.11.019

Zheng, S., Bawazir, M., Dhall, A., Kim, H., He, L., Heo, J., & Hwang, G. (2021). Implication of Surface Properties, Bacterial Motility, and Hydrodynamic Conditions on Bacterial Surface Sensing and Their Initial Adhesion. *Front Bioeng Biotechnol. 9:643722.*

Zhou, G., Mo, W.-J., Sebbel, P., Min, G., Neubert, T. A., Glockshuber, R., Wu, X.-R., Sun, T.-T., & Kong, X.-P. (2001). Uroplakin Ia is the urothelial receptor for uropathogenic *Escherichia coli*: Evidence from in vitro FimH binding. *Journal of Cell Science*, *114*(22), 4095–4103. https://doi.org/10.1242/jcs.114.22.4095

Zhou, X., Lee, Y.-Y., Chong, K. S. L., & He, C. (2018). Superhydrophobic and slippery liquid-infused porous surfaces formed by the self-assembly of a hybrid ABC triblock copolymer and their antifouling performance. *Journal of Materials Chemistry B*, *6*(3), 440–448. https://doi.org/10.1039/C7TB02457F

Zhu, G. H., Cho, S.-H., Zhang, H., Zhao, M., & Zacharia, N. S. (2018). Slippery Liquid-Infused Porous Surfaces (SLIPS) Using Layer-by-Layer Polyelectrolyte Assembly in Organic Solvent. *Langmuir*, *34*(16), 4722–4731. https://doi.org/10.1021/acs.langmuir.8b00335

Zhu, Z., Wang, Z., Li, S., & Yuan, X. (2018). Antimicrobial strategies for urinary catheters. *Journal of Biomedical Materials Research Part A. 107(2).* 445-467.

Zougman, A., Selby, P.J., & Banks, R.E. (2014). Suspension trapping (STrap) sample preparation method for bottom-up proteomics analysis. *Proteomics 14:1006.*

APPENDIX

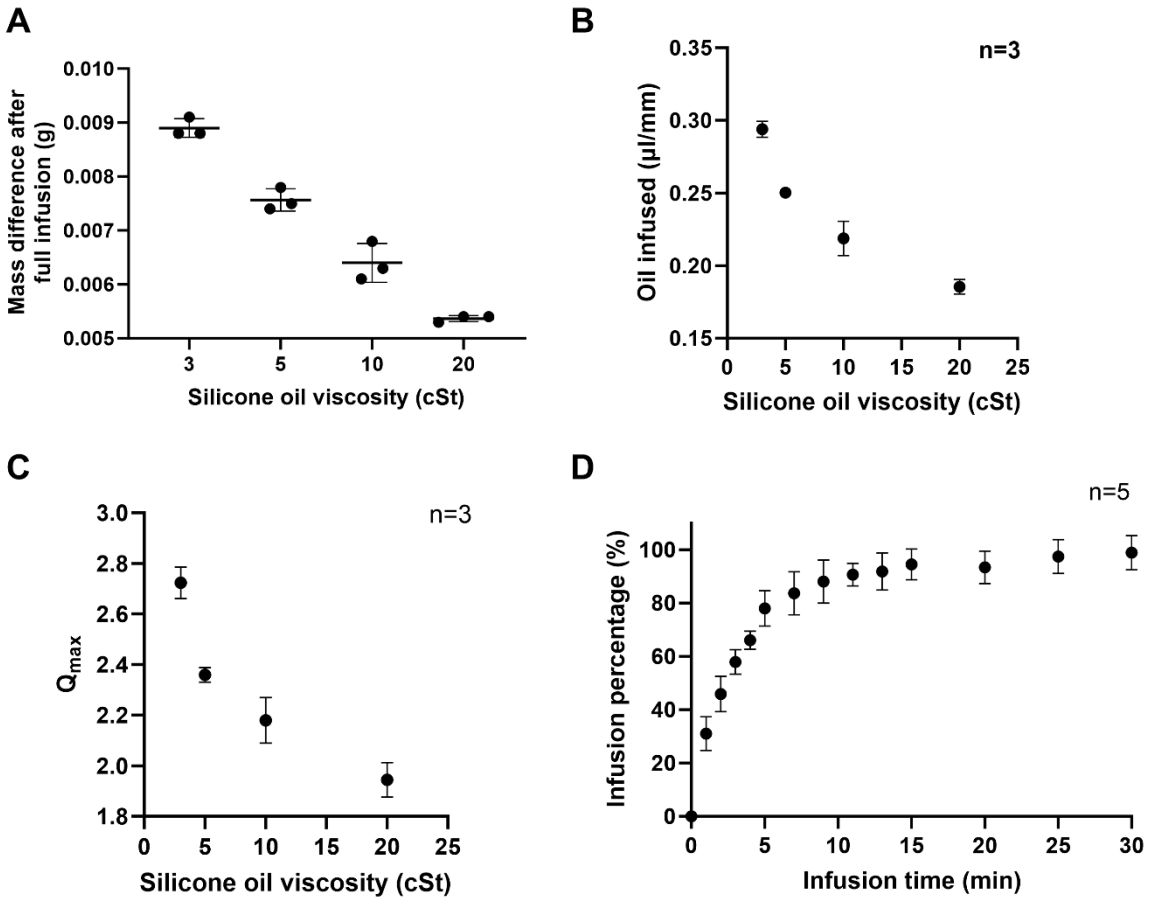

Figure A1. Mouse Catheter Infusion Characterization.

(A) Mass difference after full infusion; **(B)** Silicone oil infused into mouse catheter after full infusion; **(C)** Q_{max} of mouse catheter infused by different viscosities of silicone oil; **(D)** Infusion percentage of mouse catheters overtime. In all graphs presented, the error bars represent the standard deviation.

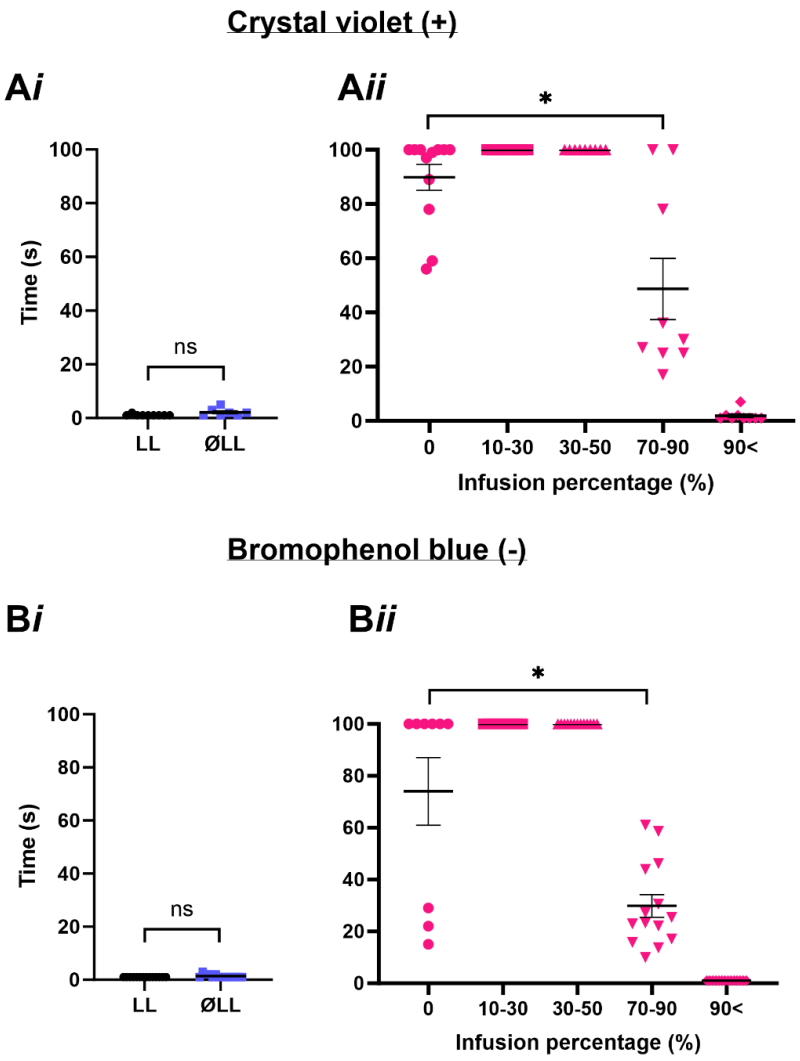

Figure A2. Droplet Speed Tests on Catheters with No Free Liquid Layer.

The Droplet Speed test was performed on catheters with (LL) or without liquid layer (ØLL) using **(Ai)** crystal violet or **(Bi)** bromophenol blue as fouling droplets. Similarly, the same test was conducted on catheters infused with various infusion percentages, employing **(Aii)** crystal violet and **(Bii)** bromophenol blue as fouling droplets. In all graphs presented, the error bars represent the standard error of the mean. Statistical significance between groups was assessed using the ANOVA test. * = P< 0.05 and ns = not significant.

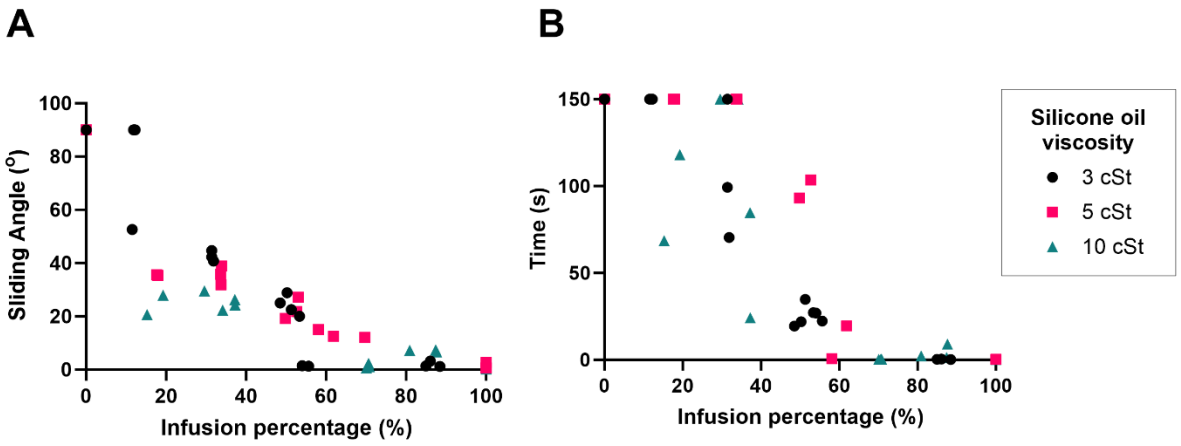

Figure A3. Sliding Angle and Droplet Speed Tests on Catheters Infused into Different Extent.

(A) Sliding angle and **(B)** Droplet Speed test results for catheter infused into various infusion percentage. Crystal violet was used as the tested foulant droplet in this experiment.

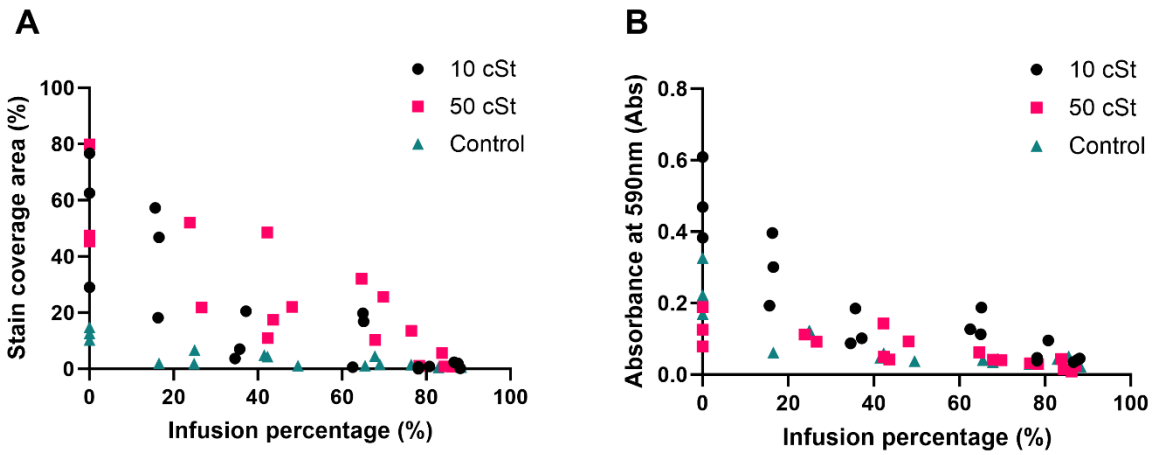

Figure A4. Whey Protein Adhesion Test on Catheters Infused into Different Extents.

(A) Crystal violet-stained area on whey protein-infused catheters were measured. **(B)** Crystal violet stains on whey protein-infused catheters were stripped with ethanol, absorbance at 590 nm was measured.

BIOGRAPHY OF THE AUTHOR

Chun Ki Fong was born and raised in Hong Kong. She graduated from Queen Elizabeth School in 2013. Her academic journey continued as she earned her Bachelor's degree with a major in Biochemistry from the Hong Kong University of Science and Technology in 2017. Following this undergraduate achievement, she pursued her passion for research, obtaining a Master of Philosophy Degree in Life Science from the same institute in 2019, under the guidance of Dr. Andrew Miller and Dr. Sarah Webb. During her MPhil degree, she explored the relationship between the circadian clock and zebrafish embryonic heart development. Driven by her curiosity and dedication to advancing scientific knowledge, she embarked on her doctoral journey. She journeyed to the United States to pursue her Ph.D. at the University of Maine, joining Dr. Caitlin Howell's research group. In her Ph.D. research, she collaborated with Dr. Ana Flores-Mireles' research group at the University of Notre Dame. Together, they are engaged in research on liquid-infused catheter materials aimed at reducing catheter-associated urinary tract infections. Chun Ki is a candidate for the Doctor of Philosophy degree in Biomedical Science and Engineering from the University of Maine in May 2024.